

Soil redistribution impacts on the spatial variation of nutrients, net carbon exchange with the atmosphere and soil respiration rates in highly eroding agricultural fields from the foothills of the Indian Himalaya.

Submitted by SANKAR MARIAPPAN, to the University of Exeter as a thesis for the degree of Doctor of Philosophy in Geography (Physical), June 2016.

This thesis is available for library use on the understanding that it is copyright material and that no quotation from the thesis may be published without proper acknowledgement.

I certify that all material in this thesis which is not my own work has been identified and that no material has previously been submitted and approved for the award of a degree by this or any other university.

.....

Abstract

Using the tracer caesium-137 (^{137}Cs) and experimental approaches this study quantified soil redistribution induced spatial variation of nutrients and soil organic carbon (SOC), net C flux between soil and atmosphere and soil respiration rate at various landscapes positions (eroding to deposition) within agricultural fields from the foot hills of Indian Himalaya. The depth distributions of ^{137}Cs and the spatial patterns of ^{137}Cs inventories were consistent with previous applications of the approach in that low inventories were associated with low concentrations in the cultivation layer and high inventories were reflected in deeper ^{137}Cs profiles indicative of accumulation of labelled soil. This supports the contention that ^{137}Cs is a suitable tracer for use in this environment.

The study found that soil redistribution within fields altered the spatial variation of nutrients and SOC; with significantly lower concentrations of nutrients in the most eroded part of fields (upslope) and significantly higher concentrations of nutrients and SOC in the depositional part of field (downslope). The spatial pattern of nutrients and SOC is reflected in differences in depth distributions between eroded and depositional areas.

The ^{137}Cs and SOC inventory and depth distribution data were used to derive retrospective assessments of net C exchange between soil and atmosphere. The C flux quantification model was used to estimate lateral and vertical soil and SOC redistribution under an assumption of equilibrium conditions and the net exchange of C between soil and atmosphere was derived from the difference between measured and 'equilibrium' SOC inventories. Fluxes were derived for each landscape position within the agricultural fields studies and calculated at field and site scale. High rates of soil loss were measured and the results showed that the majority of eroded sediment and SOC was exported from field with only a small fraction redeposited within the field. The effect of soil and SOC redistribution was to create disequilibrium in SOC dynamics at eroding and deposition positions and this supported the formation of a field scale C sink. The sink strength is highest in the most eroded parts of the fields due to dynamic replacement of eroded C. This is assumed to be due to the high rate of incorporation of SOC-poor subsoil, with a large C-unsaturated surface area, into the cultivation layer. The C sink is smaller than those reported from high nutrient-input mechanised farm lands. Irrespective of the fate of exported SOC, the SOC stocks in the fields appear to be in dynamic equilibrium and, therefore, there is no

evidence of a C source to the atmosphere due to erosion. Also the rate of SOC export from the fields is very high, especially when compared with mechanised fields and, if it is assumed that some portion of exported C is stored in some part of low lying area, the C sink strength would be comparable to mechanised farm lands.

The soil redistribution and C flux study confirmed the existence of spatial variation in C flux at various landscapes position and was consistent with an important role for vertical mixing of soil and SOC in determining net C exchange with the atmosphere. This informed the design of the final element of the research that examined soil respiration differences in soil from shallow and deep layers in eroding and aggrading landscapes position. Respiration was measured over a one year period in samples derived from separate depth layers and in mixtures of soil from different depths at each landscape position. No significant difference was found in C release rate (per unit mass of C) from topsoil of eroding and deposition position but the subsoil of eroding pits exhibited significantly higher C release than the subsoil from deposition positions. This result suggests that topsoil in both locations has almost equal and similar C origin. The relatively high rate of respiration in sub soils from eroding pits may be due to the presence of a larger proportion of SOC formed from recently incorporated plant material (crop roots) at these locations. In buried and deposition locations the reduced mineralisation is consistent with the proposition that burial of top soil can contribute to formation of a C sink. In the samples containing mixed topsoil and subsoil, evidence for priming was seen where the respiration rate in the mixed sample was significantly higher than the expected rate based on the respiration rate seen in the separate depth samples. No priming was evident in mixed soils from eroding locations, suggesting that mixing of subsoil and surface soil does not accelerate loss of old SOC from the subsoil. In contrast, significant priming action was evident in mixed soils from aggrading locations suggesting that buried SOC at depositional locations may be subject to accelerated respiration as long as it is exposed to fresh plant input (as found in surface soils).

In conclusion, despite the low input and low productivity of the farmlands in the Indian Himalaya region studied here, there is consistent evidence that high rates of soil erosion and soil redistribution have induced spatial variation of nutrients and SOC, net C flux and soil respiration rates that combine to create a pattern of SOC stocks that are close to equilibrium and, if some of the exported C is sequestered, to create a net

C sink. This result again confirms that erosion induced redistribution of C does not directly cause a net release of C to the atmosphere. The consistency of these results with previous studies suggests that there is both scope and need for soil erosion induced carbon fluxes to be incorporated into carbon budgets, research frameworks, land management and climate change mitigation strategies at policy-relevant scales.

Acknowledgements

I have been extremely fortunate in having had an excellent advisory team, both at the University of Exeter and Rothamsted Research, North Wyke and would like to thank Timothy A. Quine, Iain Hartley and Jennifer Dungait for their invaluable support. I would like to particularly express gratitude to my lead supervisor Timothy A. Quine for giving me the fantastic opportunity to undertake this project and for his excellent support and guidance throughout. I would also like to specifically thank Iain Hartley for excellent support and guidance for conducting long term respiration experiment. Further I would like to express my sincere thanks to Jennifer Dungait for interacting during project and get exposure on her biogeochemical expertise it was really new to me.

I would like to express thanks to the numerous people and organisations that have helped me in any way throughout the course of this project. Particularly during field work in India helped by ICAR-Indian Institute of soil and water conservation, Dehradun, and during lab work at University of Exeter and Rothamsted Research, North Wyke.

I am also expressing my sincere thanks to funding body for my course by ICAR-International Fellowship and University of Exeter.

Finally, I would also like to thank my family and friends for providing support and allowing me to maintain stability without deviation throughout this project.

Contents	P.No
Abstract	2
Acknowledgements	5
Contents	6
List of Figures	9
List of Tables	14
Abbreviations	17
1. Introduction.....	18
2. Research context.....	21
2.1. Introduction	21
2.2. Spatial variation of SOC / nutrients	24
2.3. Soil erosion induced net C flux between soil and the atmosphere	25
2.4. Need of long-term assessment of Sink/Source strength influenced by Erosion/Deposition process using ¹³⁷ Cs	29
2.5 Hypothesized influence of soil erosion induced redistribution on SOC balance under various landscape positions in within field	29
2.6. Spatial variation of soil respiration/priming effect	32
2.7. SOC pools composition altered by erosion process.....	34
2.8. SOC dynamics / characteristics in top- and sub-soils	38
2.9. Hypothesised mechanism on SOC/soil redistribution process and vertical mixing of SOC-Possible priming effect	40
2.10. Knowledge gaps	43
2.11. Summary.....	44
3. Aim and Objectives	45
3.1. Objective 1:.....	45
3.2. Objective 2 :.....	46
3.3. Objective 3 :.....	46
4. Experimental framework and methods.....	48
4.1. Site location, Soil, climate and Land use description	48
4.2. Methodology for chapter 5	56
4.3. Methodology for chapter 6	60
4.4. Methodology for chapter 7	69
4.5. Soil particles size	72

4.6. Site 3 soil respiration chapter data not included in main text and kept in Appendix 7 Series (included Appendix Figure 7.1- 7.5, Table 7.1 to 7.7 and Appendix Text 7.1).....	73
4.7. Summary.....	73
5. Does soil redistribution affect spatial variation (vertical and lateral) of nutrients (SOC, TN and P) within agricultural fields from Low input and highly eroding region	74
5.1 Introduction	74
5.2 Summary of methods (for full methodology see Chapter 4)	74
5.3 Results	76
5.3.1 Small-scale spatial variation in ¹³⁷ Cs activity and Inventory	76
5.3.2 Vertical and lateral distribution of ¹³⁷ Cs, SOC, N and P at Site 1	77
5.3.3 Vertical and lateral distribution of ¹³⁷ Cs, SOC, N and P at Site 2	87
5.3.4 Vertical and lateral distribution of ¹³⁷ Cs, SOC, N and P at Site 3	99
5.3.5 Relationship between ¹³⁷ Cs, SOC and total N	112
5.3.6 Relationship between ¹³⁷ Cs activity and SOC and total N concentration ...	112
5.3.7 Relationship between ¹³⁷ Cs and P (OP and TP)	112
5.4 Discussion.....	122
5.4.1 Vertical and lateral distribution of ¹³⁷ Cs activity and Inventory	122
5.4.2 Vertical and lateral distribution of SOC concentration and inventory and relationships with ¹³⁷ Cs	124
5.4.3 Vertical and lateral distribution of total N concentration and Inventory and Relationships with ¹³⁷ Cs.....	127
5.4.4 Vertical and lateral distribution of P (total and Organic P) concentration and Inventory and Relationships with ¹³⁷ Cs	128
5.4.5 Vertical and lateral distribution of C:N and C:OP ratio	128
5.5. Conclusion	129
5.6. Key findings	129
6. Effect of soil redistribution on the net flux of C between soil and the atmosphere within the agricultural fields	132
6.1. Introduction	132
6. 2. Result.....	133
6.2.1. Point/profile scale and field scale soil redistribution rates and budgets	133
6.2.2. Point/profile scale CCI (Carbon Concentration Index) and CII (Carbon Inheritance Index) comparison with SR rate	140

6.2.3. Field-scale and Site C budgets	142
6.2.4. Sensitivity analysis	151
6.3. Discussion.....	158
6.3.1. Profile and field scale soil redistribution rates and budget	158
6.3.2. Discussion of net C fluxes.....	159
6. 4. Conclusion	161
6.5. Key Findings	162
7. Erosion as a carbon sink: effects of lateral and vertical carbon redistribution on decomposition rates?.....	163
7. 1. Introduction	163
7. 2. Results	164
7.2.1. Caesium -137 (¹³⁷ Cs) inventory distribution.....	164
7.2.2. Soil and C mixing (lateral and vertical redistribution) at each landscape (eroding and deposition)	164
7.2.3. Soil organic carbon (SOC), Total Nitrogen (TN) and CN ratio.....	165
7.2.4. Soil respiration cumulative pattern over the experimental period	172
7.2.5. Mixed–soils observed Vs expected cumulative respiration	173
7.2.6. Absolute difference between observed vs expected cumulative respiration release in mixed soils.....	177
7.3. Discussion.....	179
7.3.1. ¹³⁷ Cs inventory, SOC and TN concentration and CN ratio	179
7.3.2. Cumulative C release	181
7.4. Conclusion	183
7.5. Key findings	183
8. Conclusion.....	184
8.1 Introduction	184
8.2. Summary of key results for each objective	185
8.3. Areas for further research	188
8.4. Broader Context and Conclusions	189
Appendix from chapter 4 to 7.....	193
References.....	237

List of Figures

- Figure 2.1 Global carbon pools and their interactions. 22
- Figure 2.2 Simulated global distribution of cropland SOC erosion ($\text{Mg C ha}^{-1} \text{ y}^{-1}$) by water and tillage (top). Simulated global distribution of agricultural (crop land, pasture and rangeland) carbon erosion $\text{Mg C ha}^{-1} \text{ y}^{-1}$ (bottom). (Reproduced from Van Oost *et al.*, 2007). 23
- Figure 2.3 Vertical and horizontal changes of SOC due to erosion process at various landscape positions (developed after Van Oost *et al.*, 2007). Notation: + mean C sink; - mean C source 31
- Figure 2.4 Observed respiration rates for top- and subsoil as a function of the geomorphic positions (Reproduced from Doetterl *et al.*, 2012). In figure same letters indicate statistically not significant. 34
- Figure 2.5 SOC store in aggregate form (above arrow) and SOC release during disturbance (bottom arrow side) Source of original graphic: Brady & Weil (2000) after Tisdall and Oades, 1982. 36
- Figure 2.6 (a) SOC pools by CENTURY model (b) stabilization based pools (Sources: Century slides: <http://www.nrel.colostate.edu/projects/century>; Six *et al.*, 2002) 37
- Figure 2.7 Vertical distribution of SOC stock up to 3 m depth in Global soil profile (Developed from Jobbagy and Jackson, 2000) 39
- Figure 2.8 Conceptual model of erosion and deposition induced vertical mixing of soil, the effect on SOC and soil respiration. 42
- Figure 4.1 Location of the three study sites in the foot hills of Indian Himalaya ; 1: Dhulkhot, 2: Pasauli, and 3: Bhatta Gaon. (Source: ArcGIS@ -Online). 50
- Figure 4.2 Topographical transect (line) and pit locations (red square) for all fields. Site 1(a = DKF1, b =DKF2, and c = DKF3), Site 2 (d =PSF1, e =PSF2 and f =PSF3) and Site 3 (g =BGF1, h=BGF2 and I =BGF3) 51
- Figure 4.3 Major land use pattern in Study area and India (SFR, 2009) 55
- Figure 4.4 Fallout of ^{137}Cs and other radionuclides (Zubanc and Mabit, 2010) 58
- Figure 4.5 Study area field shape for Site 1-DKF1 (Figure a), Site 2-PSF3 (Figure b) and Site 3- BGF3 (Figure c). 70
- Figure 5.1 Total Inventory of ^{137}Cs , SOC, and total N to 50 cm soil depth at profiles along a slope transect within field of Site 1 (DKF1:a, b, c , DKF2: d, e, f and DKF3: g,h,i), For each profile $n = 3$ and the error bars reflect standard error. 81

- Figure 5.2 Total Inventory of OP and TP to 50 cm soil depth at profiles along a slope transect within field of Site 1 (DKF1 – a,b, and DKF2- c,d fields), P analysed as a composite sample of each depth layer . 82
- Figure 5.3 Vertical distributions of ^{137}Cs , SOC, total N and C: N in soil profiles along the slope transects within field Site 1 (DKF1- a, b, c, d and DKF2- e, f, g, h). Error bars are \pm SE ($n = 3$). 83
- Figure 5.4 Vertical distributions of ^{137}Cs , SOC, total N and CN ratio in soil profiles along the slope transects within field Site 1 (DKF3-a, b, c, d and DK Ref- e, f, g, h). Error bars are \pm SE ($n = 3$). 84
- Figure 5.5 Vertical distributions of OP , TP and CP ratio in profiles in Site 1 (DKF1- a,b,c, and DKF2- d,e,f). Each depth layer made it into composite and analysed up to 50 cm 85
- Figure 5.6 Field bund structure marked in image 86
- Figure 5.7 Total Inventory of ^{137}Cs , SOC, and total N to 50 cm soil depth at profiles along a slope transect within field of Site 2 (PSF1: a, b, c, PSF2: d, e, f and PSF3: g, h, i). For each profile $n = 3$ and the error bars reflect standard error. 93
- Figure 5.8 Total Inventory of OP and TP to 50 cm soil depth at profiles along a slope transect within field of Site 2 (PSF1-a,b, PSF2-c,d, and PSF3 – e,f). P analysed as a composite sample of each depth layer. 94
- Figure 5.9 Vertical distributions of ^{137}Cs , SOC, total N and C:N in soil profiles along the slope transects within field Site 1 (PSF1- a, b, c, d and PSF2- e, f, g, h). Error bars are \pm SE ($n = 3$). 95
- Figure 5.10 Vertical distributions of ^{137}Cs , SOC, total N and C:N in soil profiles along the slope transects within field Site 1 (PSF3-a, b, c, d and PS Ref- e, f, g, h). Error bars are \pm SE ($n = 3$). 96
- Figure 5.11 Vertical distributions of OP, TP and CP ratio in profiles in Site 2 (PSF1- a,b,c and PSF2- d,e,f). Each depth layer made it into composite and analysed up to 50 cm 97
- Figure 5.12 Vertical distributions of OP, TP and CP ratio in profiles in Site 2 (PSF3- a,b,c, and PS Ref- d,e,f). Each depth layer made it into composite and analysed up to 50 cm 98
- Figure 5.13 Total Inventory of ^{137}Cs , SOC, and total N to 50 cm soil depth at profiles along a slope transect within field of Site 3 (BGF1 –a, b, c, BGF2- d, e, f and BGF3: g, h, i). For each profile $n = 3$ and the error bars reflect standard error. 105

Figure 5.14 Total Inventory of OP and TP to 50 cm soil depth at profiles along a slope transect within field of Site 3 (BGF1 –a,b, BGF2- c,d , and BGF3-e,f). P analysed as a composite sample of each depth layer	106
Figure 5.15 Vertical distributions of ¹³⁷ Cs, SOC, total N and C:N in soil profiles along the slope transects within field Site 1 (BGF1- a, b, c, d and BGF2- e, f, g, h). Error bars are ± SE (<i>n</i> = 3).	107
Figure 5.16 Vertical distributions of ¹³⁷ Cs, SOC, total N and C:N in soil profiles along the slope transects within field Site 1 (BGF3-a, b, c, d and BG Ref- e, f, g, h). Error bars are ± SE (<i>n</i> = 3).	108
Figure 5.17 Vertical distributions of OP, TP and CP ratio in profiles in field Site 3 (BGF1- a,b,c and BGF2- d,e,f). Each depth layer made it into composite and analysed up to 50 cm	109
Figure 5.18 Vertical distributions of OP, TP and CP ratio in profiles in field Site 2 (BGF3-a,b,c, and BG Ref- d,e,f). Each depth layer made it into composite and analysed up to 50 cm.	110
Figure 5.19 Relationship between individual profile face total inventories of ¹³⁷ Cs, SOC and total N within fields of Site 1 (DKF1-a,b and DKF2 –c,d). All inventories to 0.5 m. Linear regression analysis performed and tested significance	114
Figure 5.20 Relationship between individual profile face total inventories of ¹³⁷ Cs, SOC and total N within fields of Site 2 (PSF1-a,b, PSF2- c,d and PSF3- e,f). All inventories to 0.5 m. linear regression analysis performed and tested significance	115
Figure 5.21 Relationship between individual profile face total inventories of ¹³⁷ Cs, SOC and total N within fields of Site 3 (BGF1- a,b, BGF2- c,d and BGF3- e,f) . All inventories to 0.5 m. Linear regression analysis performed and tested significance	116
Figure 5.22 Relationship between individual depths profile face activity of ¹³⁷ Cs, concentration of SOC and total N within fields of Site 1 (DKF1-a,b and DKF2 – c,d) . All activity and concentration to 0.5 m.	117
Figure 5.23 Relationship between individual depths profile face activity of ¹³⁷ Cs, concentration of SOC and total N within fields of Site 2 (PSF1-a,b, PSF2- c,d and PSF3- e,f). All activity and concentration to 0.5 m.	118

- Figure 5.24 Relationship between individual depths profile face activity of ^{137}Cs , concentration of SOC and total N within fields of Site 3 (BGF1- a,b, BGF2- c,d and BGF3- e,f). All activity and concentration to 0.5 m. 119
- Figure 5.25 Relationship between total inventory of ^{137}Cs , OP and TP for Site 1 (a,b), Site 2 (c,d) and Site 3(e,f) . 120
- Figure 5.26 Depth wise ^{137}Cs and C reflect possible mechanism on C dynamic based on redistribution process 126
- Figure 6.1 Profile /point scale wise relationship between SR rate, CCI and CII (top: a-DKF1, b-DKF2 and c-DKF3) and net C flux (bottom: d-DKF1, e-DKF2 and f-DKF3) for different field of Site 1 Dhulkhot (DK). Mean values \pm SE ($n = 3$) are presented. 144
- Figure 6.2 Profile / point scale wise relationship between SR rate, CCI and CII (Top: a-PSF1, b-PSF2 and c-PSF3) and net C flux (Bottom: d-PSF1, e-PSF2 and f-PSF3) for different field of Site 2 Pasauli (PS). Mean values \pm SE ($n=3$) are presented. 145
- Figure 6.3 Profile/point scale wise relationship between SR rate, CCI and CII (Top: a-BGF1, b-BGF2 and c-BGF3) and net C flux (Bottom: d-BGF1, e-BGF2 and f-BGF3) for different field of Site 3 Bhatta Gaon (BG). Mean values \pm SE ($n = 3$) are presented. 146
- Figure 6.4 Profile / point scale wise SR rate, CCI, CII and Net C flux for different fields of Site 2 by using default parameter of ^{137}Cs inventory 1685 Bq m^{-2} , reference C inventory 5.3 kg m^{-2} up to 50 cm and plough depth 0.26 m for where model not predicting at deposition profile (PSF1 and PSF3). Mean values \pm SE ($n = 3$) are presented. 147
- Figure 6.5 Profile /point scale wise relationship between SR rate and net C flux for combined all fields of Site 1(a), Site 2(b), Site 3(c) and all site field(d). 148
- Figure 6.6 Profile/point scale wise relationship between SR rate, CCI and CII for different reference ^{137}Cs ($1300, 1685$ and 2100 Bq m^{-2}) inventory (Top : a-DKF1, b-DKF2 and c-DKF3), different reference C ($3.5, 4.59$ and 5.5 kg m^{-2}) inventory (mid: d-DKF1, e-DKF2 and f-DKF3) and for different ($14, 20$ and 25 cm) plough depth (Bottom: g-DKF1, h-DKF2 and i-DKF3) of fields to Site 1 Dhulkhot. 154
- Figure 6.7 Profile/point scale wise relationship between SR rate , CCI and CII for different reference ^{137}Cs ($1300, 1685$ and 2100 Bq m^{-2}) inventory (top : a-PSF1, b-PSF2 and c-PSF3), different reference C ($3.3, 4.3, 5.3$ and 6.3 kg m^{-2})

inventory (mid: d-PSF1, e-PSF2 and f-PSF3) and for different (14, 20 and 26 cm) plough depth (bottom: g-PSF1, h-PSF2 and i-PSF3) of fields to Site 2 Pasauli (PS). 155

Figure 6.8 Profile/point scale wise relationship between SR rate, CCI and CII for different reference ^{137}Cs (1300, 1685 and 2100 Bq m^{-2}) inventory (Top: a-BGF1, b-BGF2 and c-BGF3), different reference C (4.5, 5.5 and 6.5 kg m^{-2}) inventory (mid: d-BGF1, e-BGF2 and f-BGF3) and for different (14, 20 and 24 cm) plough depth (Bottom: g-BGF1, h-BGF2 and i-BGF3) of fields to Site 3 Bhatta Gaon (BG). 156

Figure 6.9 Profile/point scale wise relationship between SR rate, CCI and CII for different disequilibrium period (td: 40, 50, 70, 100 years) (Top: a-DKF1, b-DKF2 and c-DKF3), (mid: d-PSF1, e-PSF2 and f-PSF3), (Bottom: g-BGF1, h-BGF2 and i-BGF3) for all fields at different sites 157

Figure 7.1 Depth distribution of ^{137}Cs and SOC inventory in profiles from different slope positions at Site 1 -Low Input Acidic (Figure 7.1a and c) and Site 2-Low Input Acidic (Figure 7.1b and d). Mean values $\pm 1\text{SE}$ ($n = 3$) are presented 170

Figure 7.2 Percentages mixing of soils at eroding and deposition positions plough layer for both sites 170

Figure 7.3 Cumulative $\text{CO}_2\text{-C}$ release from the 0-15 cm (a,b) and 45-60 cm (c,d) depths from Site 1 (a,c) and Site 2 (b,d). Mean values $\pm 1\text{SE}$ ($n = 5$) are presented. 174

Figure 7.4 Soil respiration rate from the 0-15 cm (a,b) and 45-60 cm (c,d) depths from Site 1 (a,c) and Site 2 (b,d). Mean values $\pm 1\text{SE}$ ($n = 5$) are presented. 175

Figure 7.5 Cumulative $\text{CO}_2\text{-C}$ release per gram SOC from the 0-15 cm, 45-60 cm depths, observed and expected (mixed soil) incubated different landscape positions from Site 1 (a) and Site 2 (b). Mean values $\pm 1\text{SE}$ ($n = 5$) are presented. 176

Figure 7.6 Absolute cumulative difference of C release between observed vs expected at different time interval of within 364 days for various landscape positions from Site 1 (a) and Site 2 (b). Mean values $\pm 1\text{SE}$ ($n = 5$) are presented 178

List of Tables

Table 2.1 Variation in erosion influenced C Sink /Source estimation	28
Table 4.1 Site 1 (DhulKhot-DK) slope fields and reference fields basic data description . Soil pH and EC measurements represent mean values for whole profile depth. Distance of pits start from upslope (eroding) to downslope (deposition) within each field.	52
Table 4.2 Site 2 (Pasauli-PS) slope fields and reference fields basic data description. Soil pH and EC measurements represent mean values for whole profile depth. Distance of pits start from upslope (eroding) to downslope (deposition) within each field.	53
Table 4.3 Site 3 (Bhatta Gaon-BG) slope fields and reference fields basic data description. Soil pH and EC measurements represent mean values for whole profile depth. Distance of pits start from upslope (eroding) to downslope (deposition) within each field.	54
Table 4.4 Major crops productivity (kg ha ⁻¹) from different region (Madhu and Sharda, 2011)	55
Table 4.6 Measured total reference ¹³⁷ Cs inventory profiles form different sites of study area.	62
Table 4.7 Global fallout of ¹³⁷ Cs at different latitude band.	63
Table 5.1 Total Inventory of ¹³⁷ Cs, SOC, total N, OP and TP to 50 cm soil depth along the slope transects at Site 1 (DKF1, DKF2, DKF3 and DK Ref fields), For each profile $n = 3$, differences in inventories were tested by one way Anova at $p = 0.05$, significant sub-sets are denoted. CV is the coefficient of variation in total inventory of three replicates (soil pit faces). Mean values \pm SE are presented	80
Table 5.2 Total Inventory of ¹³⁷ Cs, SOC, total N, OP and TP to 50 cm soil depth along the slope transects at Site 2 (PSF1, PSF2, PSF3 and PS Ref fields). For each profile $n = 3$, differences in inventories were tested by one way Anova at $p = 0.05$, significant sub-sets are denoted. CV is the coefficient of variation in total inventory of three replicates (soil pit faces). Mean values \pm SE are presented.	92
Table 5.3 Total Inventory of ¹³⁷ Cs, SOC, total N, OP and TP to 50 cm soil depth along the slope transects at Site 3 (BGF1, BGF2, BGF3 and BG Ref fields). For each profile $n = 3$, differences in inventories were tested by one way Anova at $p = 0.05$,	

significant sub-sets are denoted. CV is the coefficient of variation in total inventory of three replicates (soil pit faces). Mean values \pm SE are presented.	104
Table 5.4 Descriptive statistics for total inventory of ^{137}Cs , SOC, and total N to 50cm depth for all three sites slope field.	111
Table 5.5 Linear regression result between ^{137}Cs activity, SOC and total N concentration for three sites field and with depth increment	121
Table 6.1 Profile/point scale wise soil redistribution rate (SR), CCI, CII and Net C flux for different site by using default parameter of ^{137}Cs inventory 1685 Bg m^{-2} , reference C inventory 4.6 kg m^{-2} up to 50 cm and plough depth (PD) 0.14 m. Site 1 DhulKhot =DK. Mean values \pm SE ($n = 3$) are presented.	136
Table 6.2 Profile/point scale wise SR rate, CCI, CII and Net C flux for different site by using default parameter of ^{137}Cs inventory 1685 Bg m^{-2} , reference C inventory 5.3 kg m^{-2} up to 50 cm and plough depth 0.26 m for PSF2. PSF1 used PD 0.19 m. PSF3 used ^{137}Cs inventory 2100 Bg m^{-2} and reference C inventory 6.09 kg m^{-2} up to 50cm. PS = Site 2 Pasauli.	137
Table 6.3 Profile/point scale wise SR rate, CCI, CII and Net C flux for different site by using default parameter of ^{137}Cs inventory 1685 Bg m^{-2} , reference C inventory 5.5 kg m^{-2} up to 50 cm and plough depth 0.24 m. Site 3 Bhatta Gaon= BG. Mean values \pm SE ($n = 3$) are presented.	138
Table 6.4 Soil redistribution budget for all sites based on profiles mean from erosion and deposition area	139
Table 6.5 Soil carbon budget for fields from Dehradun, India Site 1, 2 and 3. E-eroding profile, Dp- deposition profile, Ea –eroding area, Da- deposition area, F – whole field.	149
Table 6.6 Complete Soil redistribution and C flux budget for study area. E-erosion, D-deposition and EX-export	150
Table 7.1 Total ^{137}Cs inventory, soil pH and other properties along the slope transect. Within a site, values labelled with different letters differ significantly ($p < 0.05$). Mean values \pm 1SE ($n = 3$) are presented. Here Site 1 = field DKF1 and Site 2 = field PSF3.	167
Table 7.2 Soil lateral and vertical redistribution ($\text{kg m}^{-2} \text{ y}^{-1}$) budget for India sites based on profile means from Segment (E/D) and field area. Mean values \pm SE ($n=2$ sites value) are presented	168

Table 7.3 C lateral and vertical redistribution ($\text{g C m}^{-2} \text{y}^{-1}$) budgets for the study sites sites based on profile means from erosional and depositional segments and the whole field area. Mean values \pm SE ($n = 2$ sites value) are presented.	169
Table 7.4 SOC, TN and C:N of Site1 and Site 2 by position and depth. Within a site and depth interval, values labelled with different letters differ significantly ($p < 0.05$). Mean values \pm 1SE ($n = 5$) are presented.	171
Table 7.5 SOC and TN inventory up to 70 cm in depth by position. Mean values \pm 1SE ($n = 3$) are presented.	171

Abbreviations

C	Carbon
CH ₃ COOH	Acetic acid
CH ₄	Methane
CO ₂	Carbon dioxide
EDTA	Ethylene diamine tetra acetic acid
H ₀	Null hypothesis
H ₁	Alternate hypothesis
H ₂ O ₂	Hydrogen peroxide
H ₂ SO ₄	Sulfuric acid
H ₃ PO ₄	Orthophosphoric acid
HCl	Hydrochloric acid
HNO ₃	Nitric acid
LOI	Loss on ignition
N	Nitrogen
N ₂ O	Nitrous Oxide
NaHCO ₃	Sodium bi carbonate
NH ₄ F	Ammonium fluoride
NH ₄ NO ₃	Ammonium nitrate
O ₂	Oxygen
OP	Organic Phosphorous
SE	Standard error
IOC	Soil inorganic carbon
SOC	Soil organic carbon
SOM	Soil organic matter
TC	Total carbon
TOC	Total organic carbon
TP	Total Phosphorous

1. Introduction

Soil erosion is the process of displacement of soil from the place of formation by causative agents (water, tillage, wind, gravity etc.) and thereafter deposition either on land or water courses. Erosion affects soil quality (which can be spatially variable) (Lowery *et al.*, 1998; Beuselinck *et al.*, 2000; Steegen and Govers, 2001; Quine and Zhang, 2002; De Gryze *et al.*, 2008; Nosrati *et al.*, 2015), agronomic productivity (Lal *et al.*, 1998) and landscape process (Li *et al.* 2007b), and can also have implications for water quality as a non-point source pollutant (Burwell *et al.*, 1975). In India, out of 328 Million hectares (Mha) total geographical area, near to 147 Mha are undergoing soil degradation, 64% of which is by water erosion (Bhattacharyya *et al.*, 2015). Water erosion rates vary from 5 t ha⁻¹ y⁻¹ in dense forest regions and are highest in the Shiwalik region (> 80 t ha⁻¹ y⁻¹) (Singh *et al.*, 1992). In a comparison of annual estimates of soil erosion with several tropical countries (Swaify *et al.*, 1982), India was observed to have extremely high erosion values. India's average soil loss is 16.4 t ha⁻¹ y⁻¹ of which 29% is lost permanently to the sea, 10% is deposited in reservoirs, and the remaining 61% is deposited on land (Narayana and Ram Babu, 1983). Thirty-nine percent of India is estimated to have erosion rates of more than 10 t ha⁻¹ y⁻¹ (Sharda and Mandal, 2010). India soil loss tolerance limit (SLTL) values range from 2.5 to 12.5 t ha⁻¹ y⁻¹. Fifty-seven percent of India has permissible soil loss of <10 t ha⁻¹ y⁻¹, these soils need to be treated appropriate and responsibly used (Mandal and Sharda, 2011). Annual soil loss from the Himalayan hills is estimated to be 28.2 t ha⁻¹ y⁻¹ (Singh and Gupta, 1982). In North western Indian Himalaya (NWH) and the Shavlik area are considered to be severely eroded (>20 t ha⁻¹ y⁻¹) (Singh *et al.*, 1992). Thirty-nine percent of the Indian Himalayas has a potential erosion rate of > 40 t ha⁻¹ y⁻¹. In NWH, on average 17% can be categorised as very severe with erosion rates exceeding 40 t ha⁻¹ y⁻¹ and 25% has erosion rates of > 10 t ha⁻¹ y⁻¹. The state of Uttarakhand in NWH and Nagaland in North eastern Indian Himalaya (NEH) region have maximum area of 34 and 65.3%, respectively considered to be very severely eroded, with rates in exceeding 40 t ha⁻¹ y⁻¹ (Madhu and Sharda, 2011). The major form of erosion in this area and India is water erosion.

Soil erosion by water and tillage have a first order influence on the distribution of soil organic carbon content (SOC), within field landscapes by removing SOC from eroding sites, redistribution and deposition (Van Oost *et al.*, 2005b; Zhang *et al.*, 2006). This

process creates disequilibrium between SOC content and carbon input at each position of the landscape (Quine and Van Oost, 2007). The recent estimate of global agricultural sediment flux on crop, pasture and range land is 33 Pg (1 Pg = 10^{15} g) y^{-1} . With respect to sediment, total SOC erosion rate from agricultural land is 0.47 to 0.61 Pg y^{-1} (Van Oost *et al.*, 2007). The erosion induced net loss of nutrients/SOC is well studied, however, the influence of erosion induced redistribution and therefore, spatial variation of nutrients, soil carbon and respiration changes at the field-scale are not well reported upon. In particular, there is a research gap in the understanding of whether erosion induced redistribution of soil/SOC is a carbon (C)-source or sink. This study aims to understand the soil redistribution/erosion induced spatial variation of nutrients (C, N and P), C flux between soil and atmosphere, and soil respiration changes at various landscapes positions (e.g., eroding and deposition points) of low input/productivity and highly eroding agricultural field from foothills of Indian Himalaya. To address this research gap I will use ^{137}Cs to trace the soil sediment/SOC redistribution. .

This thesis is presented in 8 chapters. Following this introduction, Chapter 2 conducts a literature review placing this study into context. Firstly, an overview of soil erosion impacts on soil degradation and within field variation of SOC/nutrients is presented. Followed by the proposed drivers and mechanisms for soil erosion induced spatial variation of SOC (Quine and Van Oost, 2007), and finally summarising the soil respiration rates within eroded landscapes, and the vertical soil mixing effects on soil respiration (Quine and Van Oost, 2007).

Based upon the findings of Chapter 2 and in the context of the overall aim of this study; Chapter 3 states the, and provides the rationale for each of the, the specific objectives that this study addresses.

Chapter 4 documents and justifies the methodology used to address the identified objectives and includes: a detailed description of the study sites; description the field, laboratory, and data analysis methods used. The methods are separated into three sections, with the aim of providing the reader with an easy to use resource, detailing the approaches used within each of the results chapters. To address existing research gap fields were selected at three different locations of foot hills of Indian Himalaya. For studying spatial variation of nutrients and SOC ^{137}Cs technique used as important marker to trace the movements of sediments along slope transect within fields. To

study C flux (C Sink or Source) quantified using model developed by Quine and Van Oost (2007). Soil respiration variation was measured in samples collected along slope transects from top and sub soil in isolation and mixed together to quantify priming effects. Respiration was measured over a long term (one year) soil incubation.

This thesis contains three major results chapters. Chapter 5 presents and discusses results pertaining to the assessment of soil redistribution induced spatial variation (vertically and laterally) of nutrients (SOC, total nitrogen - TN - and total and organic phosphorus – TP & OP), and its stoichiometric relationship within agricultural fields using ^{137}Cs as an erosion tracer. Chapter 6 presents results regarding assessment of the effect of soil redistribution on the net flux of C between soil and the atmosphere within the landscape under low input /low productivity farming fields of the Indian Himalaya by using ^{137}Cs fallout and SOC inventories. Chapter 7 seeks to study the effect of soil erosion induced vertical soil/soil organic carbon (SOC) mixing on soil respiration rates/priming effect at various landscape positions. To conclude this thesis, Chapter 8 summarises the key findings of the study in the context of the identified aims and objectives, as well as giving consideration to key areas for further investigation and research.

2. Research context

2.1. Introduction

The last two decades have seen increasing concern about rising concentrations of carbon dioxide (CO₂) in the atmosphere (IPCC, 2007) and consequent interest in the global carbon cycle (Figure 2.1). In 2016, the global atmospheric CO₂ concentration reached 403 ppm (NOAA, 2016), presently increasing at a rate of 2.0 ppm y⁻¹ compared to pre-industrial levels. Although the rise in CO₂ concentrations over the last century is attributed primarily to fossil fuel combustion and land use change. As Figure 2.1 illustrates, there are several important exchanges of carbon between terrestrial pools and the atmosphere. In particular, soils are the third largest pool of carbon in the terrestrial ecosystem and store 2300 Pg (SOC 1550 Pg and soil inorganic carbon (IOC) 750 Pg) of soil carbon to 1 m depth (Eswaran *et al.*, 1995; Batjes, 1996) and exchange many times as much carbon with the atmosphere as fossil fuels (Paustian *et al.*, 2016). Perturbation to carbon exchanges between soils and the atmosphere have a significant potential for either sequestering or releasing carbon (Schlesinger, 1999; Bellamy *et al.*, 2005). There is, therefore, considerable interest both in predicting the future of soil carbon stocks (Smith *et al.*, 2005; Smith *et al.*, 2006; Gottschalk *et al.*, 2012) and in exploring the potential to store more carbon in soils and the terrestrial ecosystems (Lal, 2004). Furthermore, it has been suggested that the latter may yield significant co-benefits for ecosystem service delivery (Millennium Ecosystem Assessment, 2005; UK National Ecosystem Assessment, 2011; Dungait *et al.*, 2012; Paustian *et al.*, 2016).

In response to this interest, there has been significant progress in understanding terrestrial, and specifically, soil carbon dynamics (Heimann and Reichstein, 2008). The vertical exchange of carbon (and net flux to atmosphere) is increasingly well understood; however, there has been less progress in resolving the influence of lateral fluxes of carbon / nutrients on the direction of net vertical fluxes.

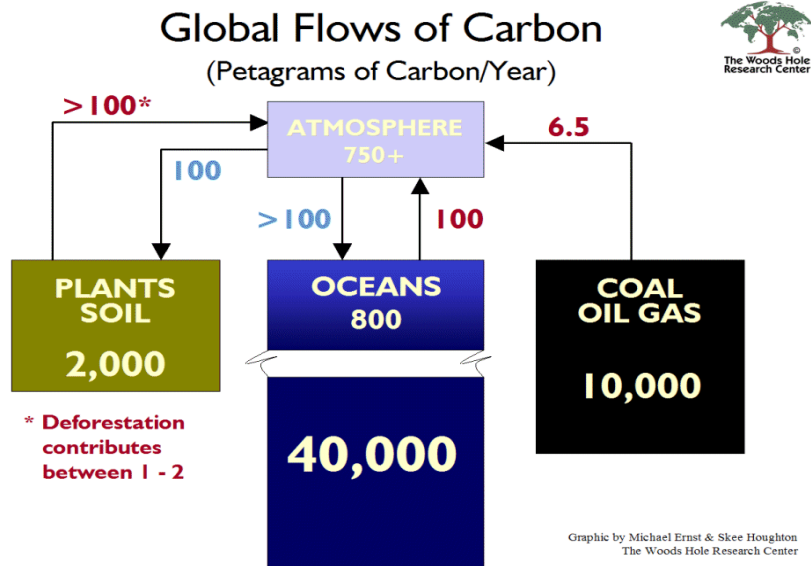


Figure 2.1 Global carbon pools and their interactions.

(source: WHRC <http://www.whrc.org/global/carbon/index.html>)

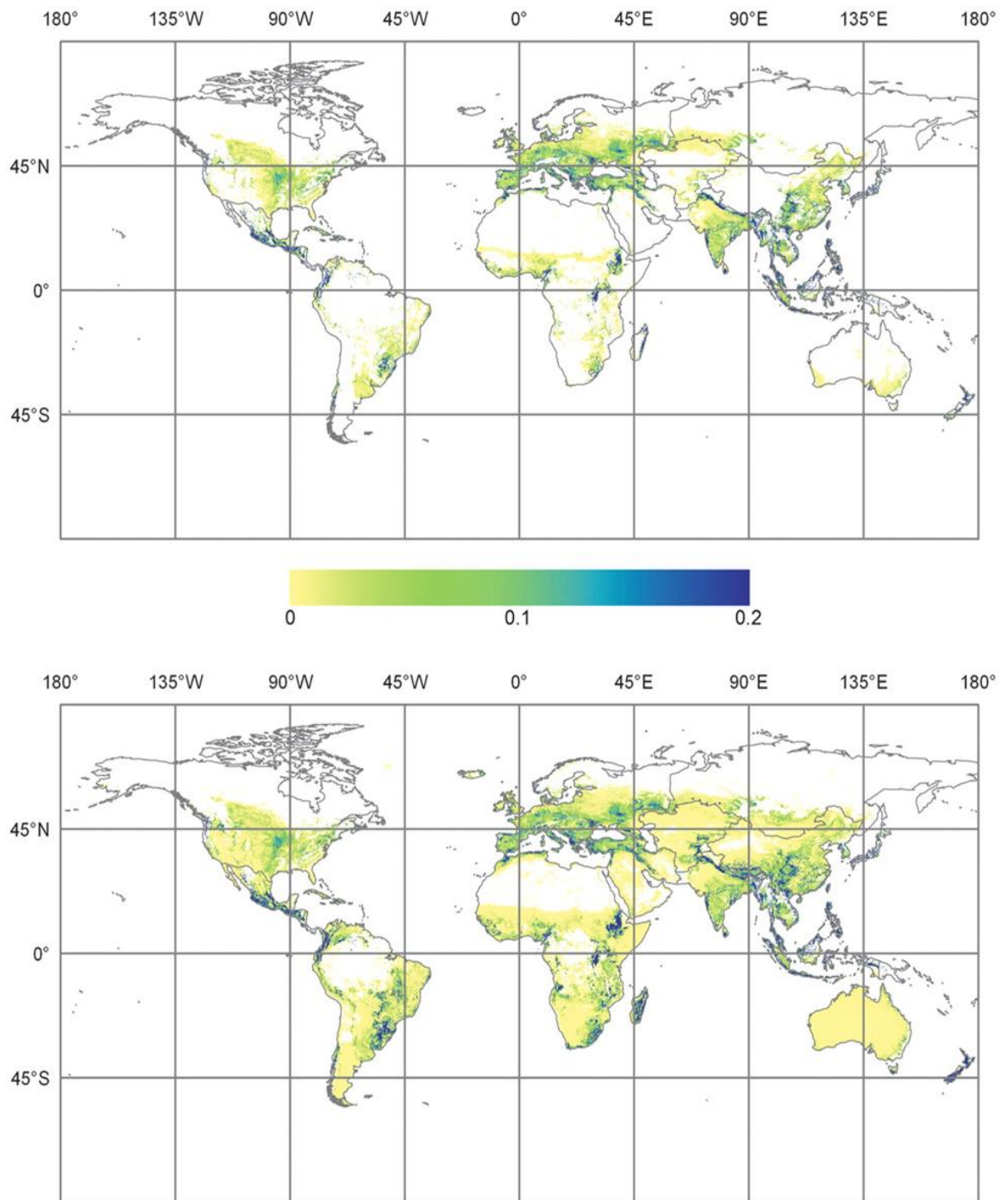


Figure 2.2 Simulated global distribution of cropland SOC erosion ($\text{Mg C ha}^{-1} \text{y}^{-1}$) by water and tillage (top). Simulated global distribution of agricultural (crop land, pasture and rangeland) carbon erosion $\text{Mg C ha}^{-1} \text{y}^{-1}$ (bottom). (Reproduced from Van Oost *et al.*, 2007).

Soil erosion induced redistribution causes spatial variation of SOC and nutrients, it can alter net C flux between soil and atmosphere and also affect soil respiration rates. To improve understanding of erosion induced redistribution impacts on net C flux there is need for an integrated study on spatial variation of SOC/nutrients and soil respiration across a topographic gradient. The importance of this integrated process is reviewed within the next three broader sections and also interlinked work.

1. Spatial variation of SOC / nutrients;
2. Net C flux between the soil and atmosphere;
3. Spatial variation of soil respiration and the potential priming effect.

2.2. Spatial variation of SOC / nutrients

Soils are the terrestrial reservoir of nutrients such as carbon, nitrogen (N), and phosphorous (P). Biogeochemical cycling of C, N and P are strongly interrelated. Soil erosion processes are an important form of land degradation and it has three stages: (1) detachment, (2) transport and (3) deposition. These phases have an impact on SOC, N and P dynamics (Quinton *et al.*, 2010; Berhe *et al.*, 2014). Detachment and removal of soil at the eroding position can remove C, N, and P, and expose these nutrients to further loss via consumption by plants, microbes and leaching. New aggregate formation during the mixing of transported minerals will slow down the nutrient (C, N and P) loss, however, the process of transport itself may break aggregates and expose new surfaces for erosion process to act upon. During deposition, eroded material is deposited at lower landscapes and buries the nutrient rich top soil already present (Berhe *et al.*, 2012; Berhe and Kleber, 2013). In addition, while transport, detachment, deposition, and exposure of buried organic matter (OM) to fresh OM / nutrients may enhance decomposition of buried OM, this is known as priming (Kuzyakov *et al.*, 2000; Fontaine *et al.*, 2007; Kuzyakov, 2010). This entire cycle of erosion and deposition influences the spatial distribution of nutrients (C, N, and P). This erosion induced spatial variation of nutrients will also lead to the spatial variability of crop production/production of new photosynthetic (Quine and Zhang, 2002). Eroded sites are likely to have lower crop productivity than a deposition site (Stallard, 1998; Parfitt *et al.*, 2013). Soil erosion and redistribution has an effect on both rates of input and persistence of soil nutrients in eroded soil system.

Erosion associated with nutrient loss and crop productivity is well studied. Many studies estimate nutrient loss by erosion field level and mainly by water erosion

(Benniston *et al.*, 2014; Gulati and Rai, 2014; Lal and Mishra, 2015). If erosion and deposition occur within a field landscape there is minimal nutrient loss from the field itself as it is redistributed and leads to spatial variability of SOC / nutrients and crop productivity (Beuselinck *et al.*, 2000; Steegen and Govers, 2001; Van Oost *et al.*, 2005a; De Gryze *et al.*, 2008; Li *et al.*, 2012, 2013; Nosrati *et al.*, 2015). Therefore, it's very important to assess erosion induced redistribution of soil nutrient / SOC (Quinton *et al.*, 2010; Berhe *et al.*, 2014; Zhang *et al.*, 2015) and its stoichiometric relationship. There are several studies in this area for mechanised agriculture landscapes (Lobb *et al.*, 1995; Quine and Zhang, 2002; De Alba, 2004; Heckrath *et al.*, 2005; Smith *et al.*, 2005; Li *et al.*, 2007a, b), however, there are few studies that consider low input/less mechanised agriculture farm lands (Quine *et al.*, 1999; Li and Lindstrom, 2001; Thapa *et al.*, 2001). Furthermore, the existing studies on C measurement and modelling of SOC dynamics has been limited to the top 20 cm of soil (Smith *et al.*, 1997), so there is less understanding of deep soil SOC. The restriction to the top 20 cm may lead to misunderstanding of SOC dynamics and potential storage of C (Rumpel and Kogel-Knabner, 2011). Therefore, the impact of soil redistribution on spatial variation (vertical and lateral) of soil nutrients has received limited study especially within low input, non-mechanised, highly erosion susceptible agricultural farm lands. This spatial variation study will enhance the understanding of SOC dynamics and assist in the development of cost effective and environmental protective farming practice (precision farming).

2.3. Soil erosion induced net C flux between soil and the atmosphere

The direct effect of erosion and degradation on productivity (Lal *et al.*, 1998) and the large lateral fluxes of sediment (and associated OM) associated with erosion, prompt the question – what impact does erosion and land degradation have on the terrestrial C cycle? Fundamentally, this is the primary question that this research seeks to address. It is a question that is at the heart of an ongoing debate in the scientific literature (Doetterl *et al.*, 2016) that divides those that consider erosion to cause a source for atmospheric CO₂ (e.g. Lal and Pimentel, 2008) from those who propose that it drives a sink (e.g. Stallard, 1998; Berhe *et al.*, 2007; Van Oost *et al.*, 2007; Li *et al.*, 2015). The following considers both sides of the debate.

Soil erosion as a source for atmospheric CO₂

One proposition is that soil erosion causes a source of 0.8 to 1.2 Pg C y⁻¹ of atmospheric carbon (Lal, 2003; Lal *et al.*, 2004; Lal and Pimentel, 2008). Mechanisms that promote net C loss as a result of erosion have been identified as follows:

1. An increase in breakdown of soil aggregates has been observed to occur during detachment and transport (Raymond and Bauer, 2001) and it is suggested that this exposes protected SOC to microbes and thereby accentuates mineralization and emission of CO₂ (Oskarsson *et al.*, 2004).
2. Where deposition occurs in anaerobic conditions, the rate of aerobic decomposition may be low but SOC mineralisation may be accompanied by efflux of CH₄ and N₂O (Lal and Pimentel, 2008) which have higher global warming potentials than CO₂.
3. The eroded soil is severely SOC depleted (Rhoton *et al.*, 1990) which is preferentially removed by runoff as a result of its low density and concentrates more in the surface layer. Along with SOC, eroded soil lose nutrient and water holding capacity, which causes low productivity, even with additional inputs (Dick and Gregorich, 2004). As a result of low productivity the net return of above and below ground biomass is reduced and the rate of replacement of SOC is low on severely eroded soils (Lal, 2005).
4. The erosional losses of soil C and mixing with sub-soil C may lead to the priming at eroding and at deposition location. Both eroding and deposition location may experience the effects of priming (Fontaine *et al.*, 2007)).

Soil erosion as a sink for atmospheric CO₂

A second proposition is that, human-induced soil erosion causes a global sink of 0.12-1.5 Pg C Y⁻¹ (Stallard, 1998; Harden *et al.*, 1999; Berhe *et al.*, 2007; Van Oost *et al.*, 2007; Li *et al.*, 2015). This is based on:

1. Dynamic partial replacement of SOC at eroding sites with new photosynthate by continuous crop cultivation with proper inputs. At eroded sites subsoil with low SOC content is mixed with plant derived new carbon. The low SOC content implies low saturation of mineral surfaces with SOC and, therefore, a greater potential to store new SOC (Harden *et al.*, 1999; Quine and Van Oost, 2007; Van Oost *et al.*, 2007; Dlugoß, 2011; Doetterl *et al.*, 2012; Dungait *et al.*, 2013; Li *et al.*, 2015; Vandenbygaart *et al.*, 2015; Nie *et al.*, 2016).

2. Removal of SOC from eroding site results in lower SOC stocks at these sites and this may limit the rate of microbial respiration (Li *et al.*, 2015).
3. A significant portion of eroded carbon rich topsoil is buried in different depositional sites and is subject to a reduced rate of decomposition (Doetterl *et al.*, 2012; Vandenbygaart *et al.*, 2012; Wang *et al.*, 2013) and further transported SOC to the distal/ fluvial environment where it may be re aggregated and physically protected and thereafter, conserved in oxygen-limited environments (Stallard, 1998; Van Oost *et al.*, 2007; Li *et al.*, 2015).

The continuing debate

This debate on the influence of erosion on the global C cycle continues (Li *et al.*, 2015; Doetterl *et al.*, 2016) due to the complexity of the controls on fluxes (spatial variability in plant productivity, soil nutrients, hydrology, spatial variability of decomposition, burial and physical protection of C); the lack of clear mechanistic understanding; the underuse of spatially comprehensive methods (Aufdenkampe *et al.*, 2011) and the predominant focus in early studies on short term measurements (Trumbore, 2009). The continuing debate is fuelled by the relatively few datasets available with respect to mineralisation of SOC as affected by erosion process and is reflected in the large variation in estimates of soil erosion caused carbon sink / source (Table 2.1). These reinforce the need for further investigation from diversified regions (Berhe *et al.*, 2007). Most previous empirical studies are from temperate climates and within mechanised agriculture landscapes (Quine and Van Oost, 2007; Van Oost *et al.*, 2007). In particular, there have been very few studies from tropical-subtropical regions with low-input subsistence agriculture landscapes, where the highest sediment and carbon flux are located (Figure 2.2), particularly in South Asia. There is a need to study the impact of erosion process on C flux in different climatic regions and management strategies (Quine and Van Oost, 2007).

Table 2.1 Variation in erosion influenced C Sink /Source estimation

Authors	Sink ($P_g C y^{-1}$)	Authors	Source (%)
Yoo <i>et al.</i> , 2005	0.02	Van Hemelryck <i>et al.</i> , 2010	2.0 – 12.0
Van Oost <i>et al.</i> , 2007	0.12	Lal, 2003a	20.0-30.0
Berhe <i>et al.</i> , 2007	0.72	Polyakov and Lal, 2004	26.0
Smith ., 2001	1.0	Jacinthe <i>et al.</i> , 2004	16.0-42.0
Stallard, 1998	1.5	Beyer <i>et al.</i> , 1993	70.0
Quine and Van Oost, 2007	0.25-0.46	Schlesinger 1990,1995	100.0

2.4. Need of long-term assessment of Sink/Source strength influenced by Erosion/Deposition process using ^{137}Cs

Caesium -137 (^{137}Cs) was produced by thermonuclear weapons testing during 1950s – 1970s and was distributed globally within the stratosphere and deposited as fallout, largely in association with precipitation. Its use as a tracer of erosion is based on assumptions that total fallout was locally uniform and that subsequent lateral redistribution occurred in association with soil/sediment. It has been used as a tracer of erosion and deposition for more than 40 years and, although its reliability and underpinning assumptions have come under scrutiny (Parsons and Foster, 2011; Parsons and Foster, 2013), it remains a valuable tool in assessing long-term erosion rates because of the time period since fallout and the long half-life of ^{137}Cs (30.2 years). Recently many studies used ^{137}Cs as a tracer for the long-term assessment of soil erosion induced redistribution on carbon budgets (Ritchie and McCarty, 2003; Quine and Van Oost, 2007; Ritchie *et al.*, 2007; Van Oost *et al.*, 2007). Earlier studies mainly focus on short term erosional events (1 year to decade) on carbon dynamics. For detailed understanding of erosion influence of sink / source strength, this needs to be studied by long-term measurement. Long-term observation is essential because carbon dynamics at eroding and depositional sites occurs over long processing time in terms of decomposition loss, new plant input, reaggregation at burial site and enhancement of stabilization. Therefore, ^{137}Cs is a valuable tracer in the quantification of sink/source strength through long-term measurements. The application in this study will account for the recent critique of Parsons and Foster (2011) and ensure that sufficient account is taken of sources of local variability.

2.5 Hypothesized influence of soil erosion induced redistribution on SOC balance under various landscape positions in within field

Change in SOC stocks at various landscape positions is controlled by the magnitude of two opposing vertical carbon fluxes, SOC formation (Atmosphere C – Plant C- Humus) and decomposition (SOC-release C to atmosphere; Figure 2.3). When SOC stocks are at equilibrium state, the fluxes balance and formation gains equal decomposition losses. When erosion / deposition occurs, it directly alters the local SOC stocks by removing (or redistributing) or adding SOC. This lateral SOC flux results in SOC redistribution within field or watershed and change in the spatial distribution of SOC storage. This need not directly result in change in soil-atmosphere

exchange. However, erosion and deposition indirectly affect soil atmospheric exchange by causing disequilibrium of SOC content and C input at each position and this is expected to change the relative magnitude of SOC formation and decomposition (Figure 2.3). At eroding sites, the soil profile becomes depleted in SOC, due to erosional export and disequilibrium favours the potential to create an atmospheric sink through reduced mineralisation (Li *et al.*, 2015) as a result of lower SOC stocks and increased SOC stabilisation (Harden *et al.*, 1999; Quine and Van Oost, 2007) through plant input adsorption on new mineral surfaces with low SOC content associated with soil material advected upwards to replace that lost through erosion (Van Oost *et al.*, 2005a). At deposition sites, the soil profile exhibits elevated SOC contents at greater depths than at stable sites as surface accretion leads to burial of SOC to deeper layers. The latter process may inhibit decomposition due to burial of C under deep layer which is less favourable condition for decomposition (Doetterl *et al.*, 2012) or SOC stocks exceed equilibrium levels for C input and disequilibrium may favour continuous C loss through mineralisation even buried C also get continues loss (Van Oost *et al.*, 2005a; Van Oost *et al.*, 2012; Wang *et al.*, 2015). During and after transport, breakdown of aggregates and mixing of SOC (Old SOC with fresh SOC cause Priming –Kuzyakov *et al.*, 2000; Fontaine *et al.*, 2007) can result in net loss of C to atmospheric CO₂. Priming action is also possible at eroding and deposition location by mixing of top and sub soil C. At mid-slope positions where net soil loss and gain from upslope will be there. SOC formation and decomposition fall between range of upslope and downslope condition. The extent to which this drives a source or sink will be dependent on lateral transport rates, the degree to which soil mineral surfaces are saturated with carbon, and the presence or absence of equilibrium between SOC stocks and inputs. Other than within field C flux study need further attention about fate of exported C from the field because highly eroding field mainly through water erosion export maximum eroded C to outside the field.

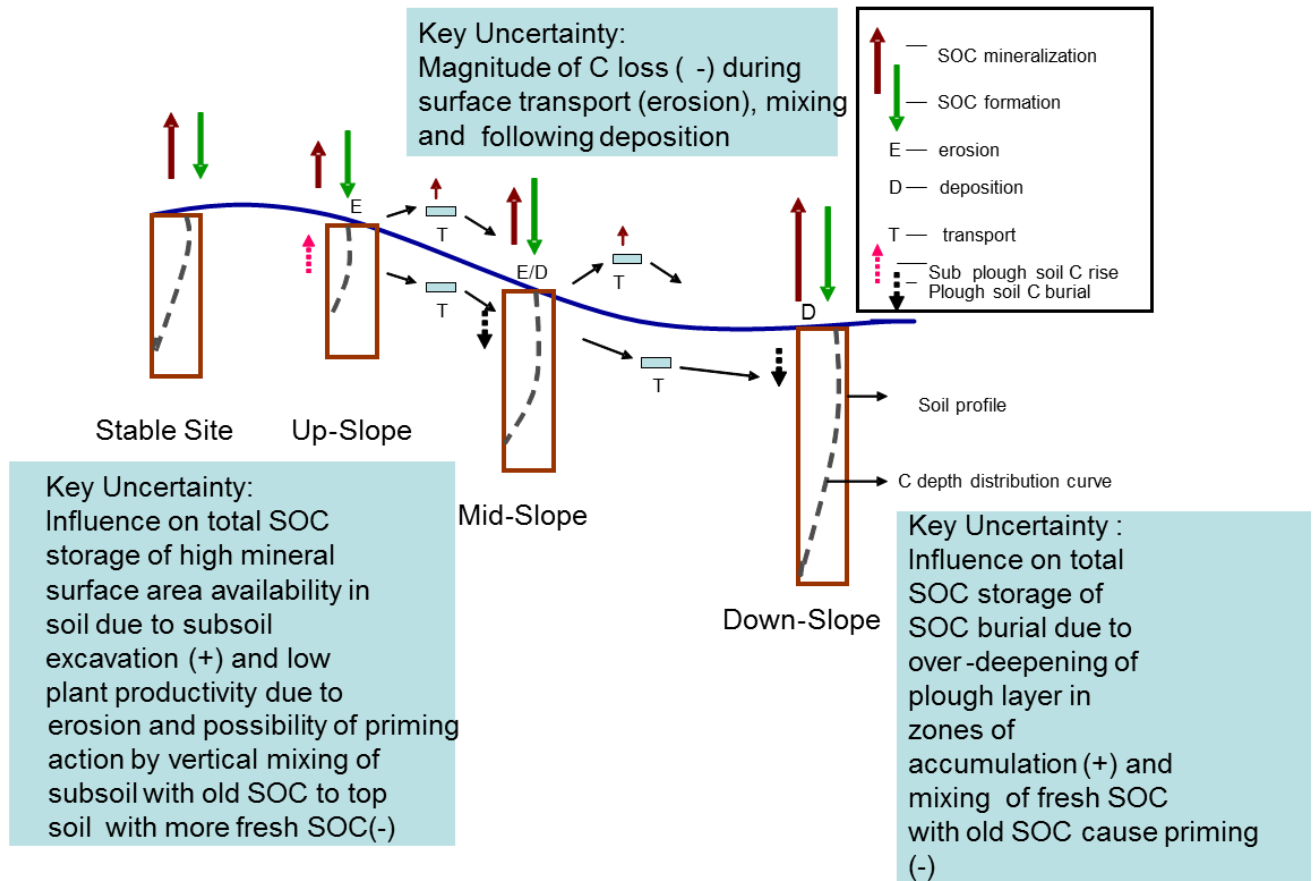


Figure 2.3 Vertical and horizontal changes of SOC due to erosion process at various landscape positions (developed after Van Oost *et al.*, 2007). Notation: + mean C sink; - mean C source

2.6. Spatial variation of soil respiration/priming effect

Soil respiration changes by erosion/deposition process

Atmospheric CO₂ levels have increased steadily over the last century and the current level is 403 ppm (NOAA, 2016). One significant area of uncertainty in prediction of future CO₂ levels is the future trend in soil respiration because small changes in soil respiration rate can cause significant alteration in atmospheric CO₂ level (Meir *et al.*, 2006). Soil respiration is highly variable in space and time because it is controlled by many factors. Temperature and soil moisture are the most important factors that control soil respiration (Kang *et al.*, 2003; Herbst *et al.*, 2009). Other factors that directly or indirectly control soil respiration include: SOC stocks (Li *et al.*, 2015), SOC pools composition along landscape with various depth (Doetterl *et al.*, 2012), nutrient content (Hartley *et al.*, 2010), soil texture and porosity (Papiernik *et al.*, 2007). These factors are modified by soil erosion induced redistribution and can be expected to vary with landscape position as a result.

Soil respiration results from eroded and deposited landscapes reported by different researchers to answer source or sink for atmospheric CO₂

C sink by short term incubation study for soil respiration: Doetterl *et al.*, 2012a studied short term incubation study by keeping top and sub soils from eroding, deposition and non-eroded positions from agricultural fields and measured soil respiration found no significant difference of C release from top soils of eroding and deposition (Figure 2.4). This no difference due to dynamic C replacement from plant inputs equal at both positions. Subsoil respiration from eroding and deposition position indicated high respiration from eroding subsoils than deposition. This may be due to high plant derived fresh inputs deposited at deep soil of eroded position and deposited position less mineralisation due to physical protection by reaggregation. Over all they found soil respiration result from eroded agricultural fields found C sink. Similar short term study also done by other researchers (Wang *et al.*, 2013; Vandenbygaart *et al.*, 2015) and found eroding location high respiration than deposition this due to dynamic replacement fresh C high at eroding position and less respiration at deposition location due to burial of C and formed reaggregation caused physical protection of C (Berhe *et al.*, 2008). Here they found burial and dynamic replacement of C at deposition and eroding landscapes facilitate C sink. Wang *et al.*, 2015 found similar result but warned that buried C may loss continuously and more vulnerable to human disturbance.

C sink/source by insitu measurement study for soil respiration (Interpretation differ): Insitu measurement of soil respiration in croplands at eroding and deposition positions studied (Wiaux *et al.*, 2014; Li *et al.*, 2015) and found that reduced respiration at eroding landscapes and high mineralisation at deposition this due to eroding position less C available than deposited position with more C. This reduced respiration C release at eroded landscapes and dynamic replacement support C sink (Li *et al.*, 2015). Similar at high respiration due to breakdown of aggregates (Van Hemelryck *et al.*, 2010) and more C available to respire due to deposition cause loss of C but continuous burial of C at deposition with considering over all proportion of eroding and deposition area if eroded area less than C loss over all support C sink. This buried C more vulnerable to future changing climate and agricultural practice (Wiaux *et al.*, 2014). The researchers view and interpretation on soil respiration differ but overall support C sink at eroding and deposition landscapes.

No landscapes level variation of C flux Some researchers studied soil respiration at eroding and deposition landscapes position by insitu measurement and found no significant difference of C release (Bhajracharya *et al.*, 2000; Fiener *et al.*, 2012).

Though few studies exist on this contested topic but up to now there is no study conducted on effect of soil erosion induced vertical soil organic carbon (SOC) mixing (redistribution) on soil respiration rates/priming effect at various landscape positions; to answer Source or sink for atmospheric CO₂. Still this uncertain view and debate continuing and existing study mostly lost in short duration of incubation so need further study to address existing research gaps and better understanding of mechanisms involves.

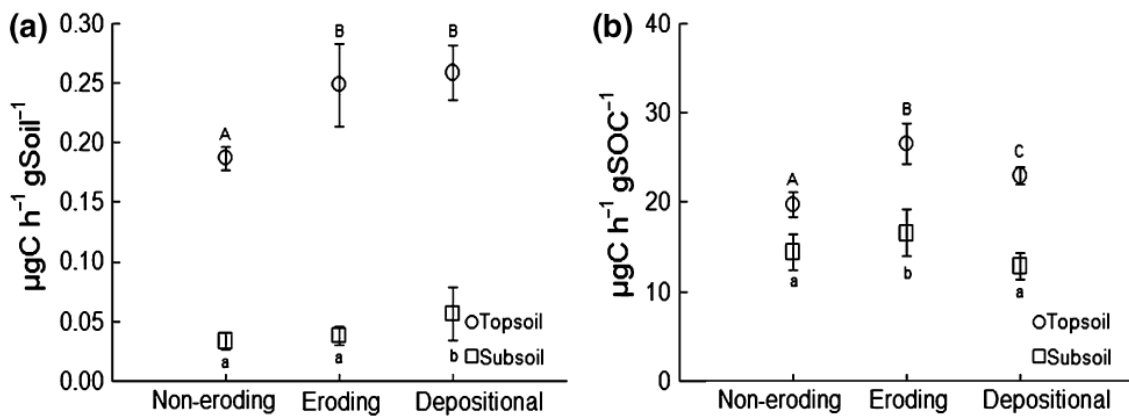


Figure 2.4 Observed respiration rates for top- and subsoil as a function of the geomorphic positions (Reproduced from Doetterl *et al.*, 2012). In figure same letters indicate statistically not significant.

2.7. SOC pools composition altered by erosion process

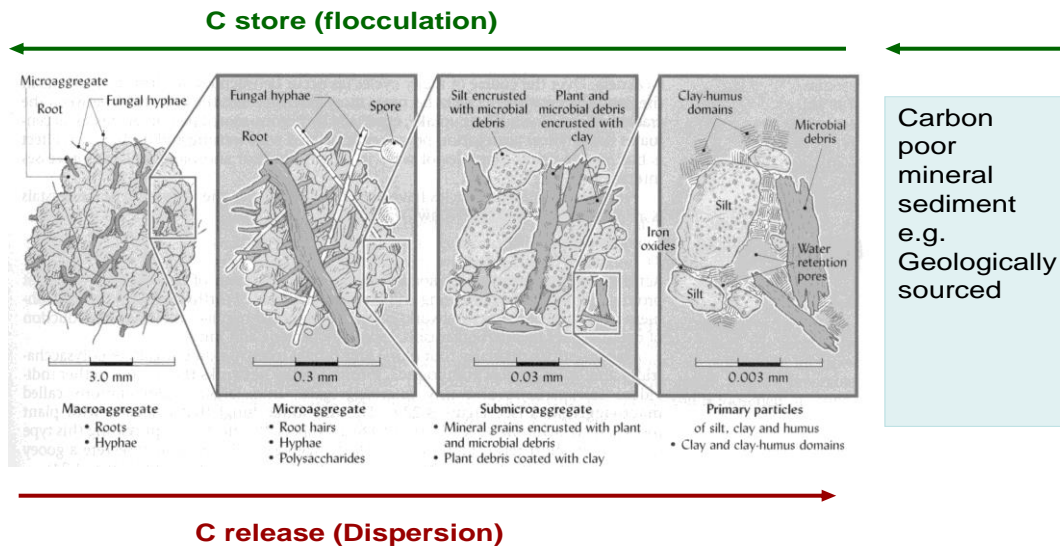
The most abundant element in soil organic matter (SOM) is carbon, followed by Nitrogen, Phosphorus and Sulphur. SOM is derived from fresh to progressively decaying plants, soil microbial decomposition products, soil faunal debris and root exudates. The SOM (& SOC) may be adsorbed and stabilised and contributes to the formation of aggregates (Tisdall and Oades, 1982) as is illustrated in Figure 2.5. These are relevant in the consideration of the mechanisms for SOC stabilisation (Six *et al.*, 2002). In this context, SOC is often conceptualised as existing in pools mainly based on stabilizing mechanism (Six *et al.*, 2002) and decomposition / turnover rate. In dynamic SOC (numerical) models, pool division is typically based on turnover (Figure 2.6a) (Jenkinson and Rayner, 1977; Paustian *et al.*, 1992). The turnover rate of these pools varies due to complex interaction of biological, chemical and physical process in soil (Christensen, 1992; Trumbore, 2009). The active pool is less stable with mean residence time (MRT) of less than one year, slow pool with MRT of few decades and passive pool with long MRT. In the context of SOC characterisation and measurement, pools are often grouped based on their stabilization mechanisms. For example, Six *et al.* (2002) grouped SOC into four measurement pools (Figure 2.6b) viz., silt and clay, micro aggregate, biochemically protected pools and unprotected pools. At stable sites where the erosion/deposition have not occurred, it has been observed that SOC

stability changes with depth; labile carbon pools present in surface soils; and more stable carbon pools are found in deeper layers (Rumpel and Kogel-Knabner, 2011). The implications of erosion and deposition for carbon distribution between pools may be identified as follows:

1. Soil redistribution as a result of erosion and deposition alters the soil texture (Quine and Zhang, 2002; Fiener *et al.*, 2008) and can be expected to affect the SOC pools associated with soil primary mineral particles and aggregate (Six *et al.*, 2002).
2. During high energy transport (wind and water erosion) SOC protected in aggregates (Figure 2.5) may be dispersed and exposed to microbial activity and, therefore, subject to enhanced decomposition.

At eroding site, it is expected that stable carbon pools from subsoil layers will be incorporated into surface horizons and mixed with labile carbon pools. This may increase the rate of decomposition of formerly stable subsoil derived carbon due to the priming effect of the labile carbon (Fontaine *et al.*, 2007). At depositional sites, buried topsoil (rich in labile carbon pools) may be physically protected at deeper layer.

Soil aggregate perspective (SOM transformation)

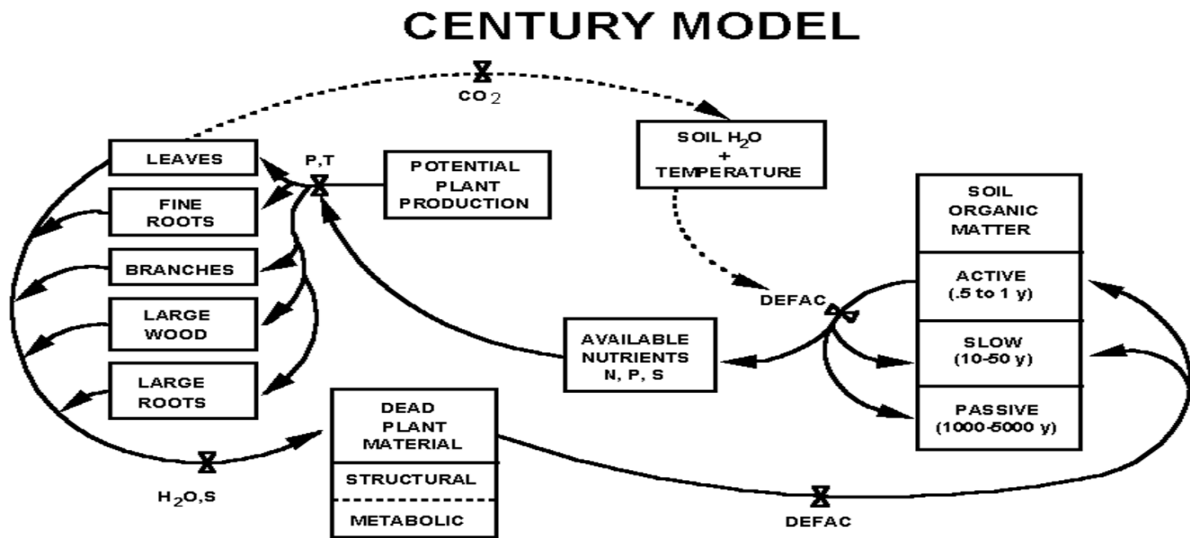


Carbon poor mineral sediment e.g. Geologically sourced

Tisdall & Oades, (1982)

Figure 2.5 SOC store in aggregate form (above arrow) and SOC release during disturbance (bottom arrow side) Source of original graphic: Brady & Weil (2000) after Tisdall and Oades, 1982.

a



b

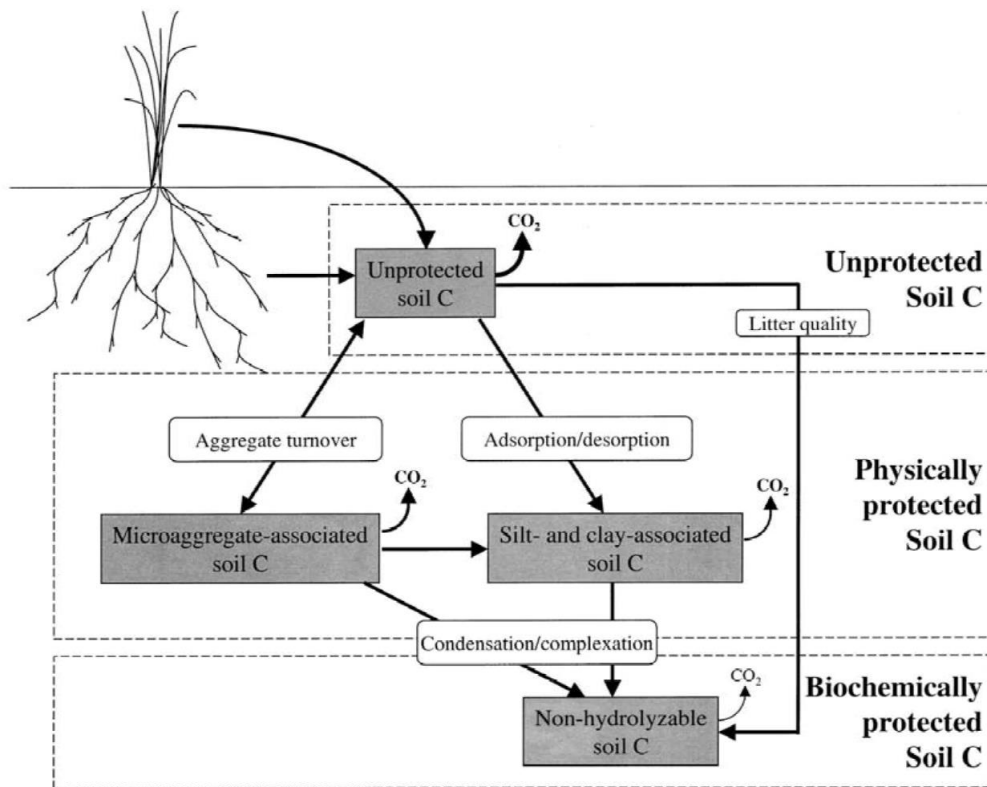


Figure 2.6 (a) SOC pools by CENTURY model (b) stabilization based pools (Sources: Century slides: <http://www.nrel.colostate.edu/projects/century>; Six *et al.*, 2002)

2.8. SOC dynamics / characteristics in top- and sub-soils

Nearly 70% of the total SOC stock (1550 Pg C) is present in the top 1 m of soil profiles (Figure 2.7). In general, SOC contents in soil profiles are highest near the surface and decrease with increasing depth. Pedological, environmental and physicochemical properties, which also influence activity of microorganism/ biological, differ strongly between the top soil (plough layer) and sub soil (sub plough layer). Specifically, top soil SOC is considered to be more labile, highly degradable, highly saturated and be characterised by more microbial activity and lower mean residence time; whereas, sub soil SOC tends to be more passive, less degradable, less saturated, and be characterised by less microbial activity and higher mean residence time. This difference of above important properties in topsoil and subsoil are entirely influence SOC dynamics difference in respective soils layers (Fierer *et al.*, 2003; Fontaine *et al.*, 2007; Salome *et al.*, 2010; Rumpel and Kogel-Knabner, 2011; Wang *et al.*, 2013). Also If erosion and deposition of soil /SOC occur at each landscapes it bring the changes on topsoil and subsoil proportion (eroding position loss the topsoil and subsoil and deposition position gain soils) and ultimately influence SOC dynamics in respective soil layers and landscapes position

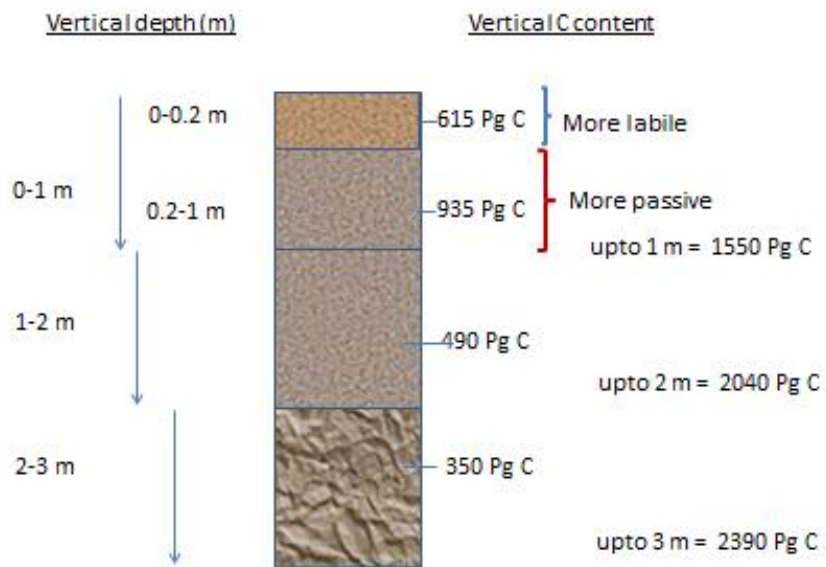


Figure 2.7 Vertical distribution of SOC stock up to 3 m depth in Global soil profile (Developed from Jobbagy and Jackson, 2000)

2.9. Hypothesised mechanism on SOC/soil redistribution process and vertical mixing of SOC-Possible priming effect

Most of landscapes (>60%) are composed of undulating slopes (> 8% slope) (Staub and Rosenzweig, 1992). In world majority of agriculture field under undulating topography and particularly in my study area near foot hills of Indian Himalaya farming practiced in slope fields. In cultivated land, this undulating slope field promotes soil redistribution by water and tillage erosion process within fields (Govers *et al.*, 1999; Quine and Zhang, 2002; Van Oost *et al.*, 2005) and this also alters lateral and vertical distribution of SOC stocks along soil toposequences within rolling fields (Quine and Van Oost , 2007). This within field redistribution of soil/SOC plays an important role in controlling then depth and spatial distribution of SOC. Tillage process in particular act as major conveyors in agricultural fields to move massive soils from eroding convex to depositing concave landscape positions (Van Oost *et al.*, 2005). This redistribution of sediment (with nutrients/SOC) can get mixed with soils (different nutrient/SOC) at various landscape positions (Quinton, *et al.*, 2010) and can be vertically mixed within the profile (Quine and Van Oost, 2007; Van Oost *et al.*, 2012; Vandenbygaart *et al.*, 2012).

In non-eroding stable profile there is no possibility of vertical mixing of top soil SOC with subsoil SOC (Figure 2.8) and both top soil (plough) and sub soil (sub-plough) kept separately. Plough-layer soils and sub plough soils are entirely different in the aspects of nutrients, SOC quality/ quantity, microbial activity and minerals surface (proportion of surface area occupied by minerals and SOC) etc (Salome *et al.*, 2010; Rumpel and Kogel-Knabner, 2011). Normally, in non eroded profiles, plough-layer soils are more fertile and with greater biological activity than sub plough soils when plough and sub plough soils get mixed due to erosion and deposition process, it changes the vertical flux of SOC at each landscape position, and this needs to be quantified. This is my prime aim of the study.

At eroding positions, erosion removes part of the plough layer (maximum), and even some sub plough soil, and redistributes and deposits material in depositional areas within fields, with some export outside of the field. After removal of plough soil at eroding positions, sub plough soil can get exposed at the surface. This soil has less SOC and unsaturated more minerals surface (Harden *et al.*, 1999; Quine and Van Oost, 2007) and gets mixed through cultivation/erosion with remaining plough-layer soil which has high SOC, nutrients and maximum saturated minerals surface (SOC

occupy more minerals surface and left less free minerals surface for further adsorption) than deep soils (Vitousek *et al.*, 2003). This mixing of sub plough soil with plough soil could lead to increased sequestration of new photosynthate due to more availability of non C saturated mineral surface which have more potential to stabilise organic C (Tisdall and Oades, 1982; Six *et al.*, 2002; Berhe *et al.*, 2007; Van Oost *et al.*, 2007) and facilitate C sequestration.

The mixing can potentially result an increase in the rate of organic matter decomposition in soil that was previously below the plough layer through the process of priming. A positive priming effect is the stimulation of soil organic matter mineralisation by the addition of fresh organic matter (Bingeman *et al.*, 1953; Kuzyakov *et al.*, 2000; Fontaine *et al.*, 2007). Priming effects are possible at eroding positions due to the mixing of fresh carbon from plough soil with older carbon in the sub plough soil (Fontaine *et al.*, 2007). In addition, the mixing may further promote sub plough soil organic matter decomposition by exposing the material to higher temperatures or better aerated conditions or greater nutrient availability (Fierer *et al.*, 2003). Whatever the mechanism, any increase in sub plough layer organic matter decomposition could promote C release.

At deposition site eroded plough/sub plough soil deposited and it initially gets mixed with plough soil of depositional site. After that, at deposition site top and subsoil of eroded sediment get buried and mixed along with buried topsoil of depositional site cause complex vertical mixing (Van Oost *et al.*, 2005, 2012; Quine and Van Oost, 2007). This complex vertical mixing of soils may cause priming effects with readily decomposable topsoil organic matter promoting the decomposition of recalcitrant subsoil carbon. Alternatively promote a stronger C sink by burial of eroded carbon / top soil C at depositional site. Buried soil organic matter may become exposed to less favourable conditions for C mineralisation (Less microbial activity, temperature, moisture and oxygen availability) or physically protected by reaggregation which facilitate long-term storage of C (Doetterl *et al.*, 2012; Wang *et al.*, 2013; Wang *et al.*, 2014; Vandenbygaart *et al.*, 2015). Further presence (unsaturated mineral surface) of subsoil at top of depositional site exported from eroding positions has potential to stabilize more C or loss by priming.

Further investigation of these hypothesised mechanisms remains a priority for further study.

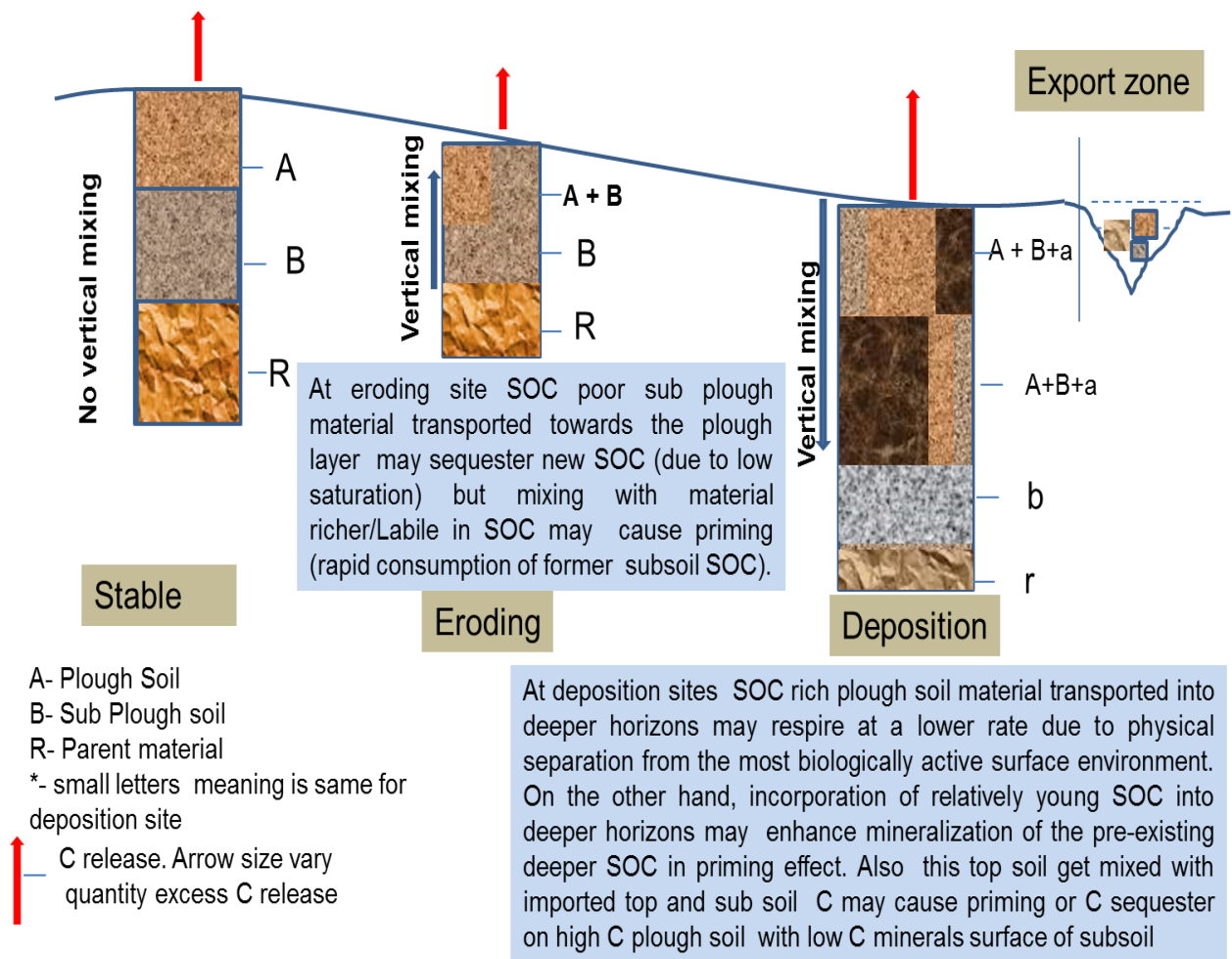


Figure 2.8 Conceptual model of erosion and deposition induced vertical mixing of soil, the effect on SOC and soil respiration.

2.10. Knowledge gaps

Contradictory global estimates of net fluxes and contrasting hypothesized changes in soil SOC stocks, pools composition, respiration and soil profile modification highlight the existence of gaps in knowledge concerning soil erosion induced redistribution process and SOC dynamics. Key areas of uncertainty may be summarised as follows:

- The influence of soil redistribution on spatial variation of SOC stocks is relatively well established (Zhang *et al.*, 2006; Quine and Van Oost, 2007). However there is less known about the effect on the relative distribution of other nutrients with SOC, for better understanding of SOC on sink/source estimates by erosion, need a combined study of spatial variation of nutrients.
- Earlier studies on source/sink strength have used data mainly from high input, mechanized agriculture landscape (Berhe *et al.*, 2007; Quine and Van Oost, 2007; Van Oost *et al.*, 2007; Dlugob, 2011; Van Hemelryck *et al.*, 2011; Doetterl *et al.*, 2012). But few have used data from low input-subsistence farming, low productivity, tropical, sup-tropical climate (Zhang *et al.*, 2006). For thorough sink/source estimates, there is a need for studies from diverse regions, including low input and low productivity regions (Quine and Van Oost, 2007; Van Oost *et al.*, 2007).
- Previous studies inferred C budgets based on control on the soil respiration/ decomposition rates (Quine and Van Oost, 2007; Van Oost *et al.*, 2007). There remains a need to investigate the factors and mechanism that control the observed behaviour.
- Many studies investigated SOC pattern for topsoil layer (Terra *et al.*, 2004; Takata *et al.*, 2007). Spatial pattern of SOC might differ substantially in subsoil layer due to different controls on SOC dynamics compared to topsoil layer (Salome *et al.*, 2010). So there is a need for clear investigation of SOC dynamics in top and subsoil of various landscapes position (Doetterl *et al.*, 2102) separately and mixed layer.

2.11. Summary

This above review has highlighted the need of further research on erosion induced soil redistribution impacts on spatial variation of nutrients, net C flux between soil and atmosphere and soil respiration rates at various landscapes position within agricultural fields.

Soil erosion impacts on net nutrient/SOC loss has been well studied (Ghosh *et al.*, 2012 and 2015) but impacts on within field spatial variability has been less studied and also less linked with SOC dynamics and Crop productivity variability within field. Existing studies on spatial variability of SOC/nutrients have been mainly from mechanised /high productivity farm lands (Quine and Zhang, 2002). There is huge demand of data /study required from where less mechanised/low productivity farm lands where highest erosion occurring.

Studies that have evaluated soil redistribution induced net C flux and found a C sink (Quine and Van Oost, 2007; Van Oost *et al.*, 2007) have been mainly from mechanised farmlands where highest crop productivity exist. It is possible that C sink strength may be lower or there may be no sink in low productivity farm lands because the lower net returns of biomass (Quine and Van Oost., 2007). This need to be tested on lower crop productivity farmland with lower and biomass return to the soil.

Erosion induced spatial variation of soil respiration rate at various landscapes has been relatively less studied and reported results have varied significantly (Doetterl *et al.*, 2012; Li *et al.*, 2015; Vandenbygaart *et al.*, 2015). Also the impact of vertical mixing of SOC (top and subsoil) has not yet studied. Therefore, further research on erosion effects on soil respiration is needed to help better understanding of mechanisms involved in erosion perturbed SOC dynamics.

Based upon the state of current understanding reviewed here; the following chapter outlines the aims and objectives of this study and details how they will further understanding of soil erosion induced redistribution impacts on spatial variation of nutrients, net C flux and soil respiration rates from low input/productivity farm lands.

3. Aim and Objectives

Aim: *To study the effect of erosion induced soil redistribution on spatial variation of nutrients/C, net C flux between soil and atmosphere, and soil respiration rates/ priming*

3.1. Objective 1: *To quantify the impacts of erosion-induced soil redistribution on SOC and nutrients (lateral and vertical) within agricultural fields*

Erosion associated with nutrient loss and crop productivity was well studied. Many studies estimated nutrient loss by erosion field level and mainly by water erosion (Benniston *et al.*, 2014; Gulati and Rai., 2014; Lal and Mishra, 2015) But if erosion and deposition occur within field landscape there is no much nutrient loss out of the field all redistributed within field (Beuselinck *et al.*, 2000; Steegen and Govers, 2001; Van Oost *et al.*, 2005; De Gryze *et al.*, 2008; Li *et al.*, 2012, 2013; Nosrati *et al.*, 2015). This cause within field spatial variability of nutrients/SOC and crop productivity and it will affect SOC dynamics. Therefore it's very important to assess erosion induced redistribution of soil nutrient (Quinton *et al.*, 2010; Berhe *et al.*, 2014; Zhang *et al.*, 2015) and it stoichiometry relationship. Erosion induced redistribution impact on nutrient (C, N and P) spatial variation within field well studied from mainly mechanised agriculture landscape (Quine and Zhang, 2002; De Alba, 2004; Heckrath *et al.*, 2005) and very less from low input/less mechanised agriculture farm lands (Quine *et al.*, 1999; Thapa *et al.*, 2001; Li and Lindstrom, 2001). As per my knowledge no single study studied in highly eroding and low input/crop productivity and less mechanised agriculture field from Indian Himalaya region which is represent large area in the world and more people depended for their subsistence agriculture. **Therefore, the impact of soil redistribution on spatial variation (vertical and lateral) of soil nutrients (C, N, P) needs to be studied well from low input –non mechanised highly erosion susceptible agricultural farm lands where people are highly dependent on farm resource and it will help to better understanding of SOC dynamics and also help to develop cost effective and environmental protective farming practice (Precision farming).** For this I used ¹³⁷Cs tracer technique to understand erosion induced spatial variation of nutrients/SOC.

3.2. Objective 2 : *To quantify erosion-induced soil carbon redistribution on the net effect of carbon exchange between soil and atmosphere in low input/productivity and highly eroding agricultural fields from the foothills of the Indian Himalaya by using ¹³⁷Cs fallout and SOC inventories*

The debate on the influence of erosion on Global C cycle continues (Li *et al.*, 2015; Doetterl *et al.*, 2016) and continuing controversy is fuelled by the relatively few data available with respect to mineralisation of SOC as affected by erosion process and is reflected in the large variation in estimates of soil erosion caused carbon sink /source. These reinforce the need for further investigation from diversified regions (Berhe *et al.*, 2007). Most previous empirical studies are from temperate climates and mechanized agriculture landscape (Quine and Van Oost, 2007; Van Oost *et al.*, 2007). In particular, there have been very few studies from tropical-subtropical region with low-input subsistence agriculture landscape, where the highest sediment and carbon flux is existing, particularly in South Asia. **There is need of study on C flux impact by erosion process from different climate and management region (Quine and Van Oost, 2007) particularly from low input farming fields where net return of biomass will be low to return C input and harm dynamic C replacement (Van Oost *et al.*, 2007; Bhattacharyya *et al.*, 2009).** Based on this existing research gap here this study proposed to investigate the sink/source strength by erosion/deposition process in the Indian –Himalayan region where moderate to severe erosion (Singh and Gupta.,1982; Narayana and Ram Babu, 1983; Kholra and Sastry., 2005; Singh *et al.*, 2016) and low input (Tiwari *et al.*, 2005; Ghosh *et al.*, 2014) and low crop productivity (Madhu and Sharda, 2011; Ghosh *et al.*, 2012; Singh *et al.*, 2016) exist.

3.3. Objective 3 : *To study the effect of erosion- and deposition-induced vertical soil/SOC mixing on soil respiration rates at various landscapes positions.*

Soil erosion-induced redistribution of soil organic carbon (SOC) alters the lateral and vertical distribution of SOC stocks and this has been shown to perturb the net exchange of C between soil and atmosphere (Dungait *et al.*, 2013), although there remains debate concerning the net direction of C exchange. Retrospective studies, using caesium-137 (¹³⁷Cs) and SOC inventories have found that long-term (half-century) erosion-induced SOC redistribution on agricultural land has driven a carbon sink (Van Oost *et al.*, 2007). Furthermore, in a recent study of *in situ* spatial variation in soil respiration in a landscape

subject to sustained high magnitude erosional forcing, Li *et al.*, (2015) demonstrated that SOC stocks in the eroding landscape were in equilibrium and, therefore, that erosion was driving a sink of atmospheric C (assuming that at least some of the eroded C was sequestered elsewhere in the landscape). The lateral redistribution of SOC stocks appeared to be the main control on spatial variation in respiration rates.

Although attention has focussed on lateral redistribution, vertical redistribution of SOC between the plough and sub-plough layer of agricultural soils as a result of erosion and deposition may also have an important effect on respiration rate and SOC 'stability'. At depositional sites, SOC-rich material transported into deeper horizons may respire at a lower rate due to physical separation from the most biologically active surface environment. On the other hand, incorporation of relatively young SOC into deeper horizons may enhance mineralisation of the pre-existing deeper SOC in a priming effect. At erosion sites, SOC-poor material transported towards the surface may sequester new SOC but mixing with material richer in SOC may again see priming and more rapid consumption of formerly buried SOC. This uncertainty defines the objectives of the study. **This will address highly eroding and low input agricultural field from Indian Himalaya region by measuring soil respiration rates in individual layer (plough and sub plough) and mixing both to detect possible priming effect.**

The following chapter outlines the experimental framework, including field, laboratory and analytical techniques used to address the identified objectives.

4. Experimental framework and methods

4.1. Site location, Soil, climate and Land use description

The selected area of study is located in the lower Himalayan region of northern India (Figure 4.1). The Indian Himalayan region covers 53 million hectares (Mha) and it is grouped into North West Himalaya (NWH) and North East Himalaya (NEH). The selected study area falls within the NWH. The NWH occupies major part (about 62%) of the total Himalayan range. The climate is dry and cold in NWH, the mean air temperature varies from 30.0°C in May to 3.5°C in January. Mean annual rainfall is 1600 mm, highest during July-September.

The Himalaya is the youngest mountain system in the world (Burman, 1984). Lower Himalaya rocks provide a source of fresh water deposits that are composed of clays, sandstone, grits and conglomerates. These are products of rising Himalayas and are mobilised by heavy rainfall. Limestone is the major geological rock type, which is highly erodible, particularly in wet and tropical conditions. Lower Himalaya is mostly dominated by loam to sandy loam soil types, which are predominantly slightly acidic to neutral in pH. Major soil orders existing in the study area are Entisol > Inceptisol > Alfisol.

According to State Forest Report (2009), agriculture is the major national land use. However, within the Indian Himalayan region forest cover is the dominant (Figure 4.3). Rice, wheat and maize are the predominant crops grown in Himalaya region and about 70% of population in this area are engaged in agriculture. Comparatively lower productivity of crops in Himalaya region (Table 4.4) is a result of the low application of fertilisers, and the cultivation on steep slopes (Tiwari *et al.*, 2005; Ghosh *et al.*, 2012). Hill and mountain agriculture in the Indian sub-Himalayas has evolved over the centuries with the application of 10-15 t ha⁻¹ Farm yard manure (FYM) along with inorganic NPK fertilizer at lower doses of around 20 kg ha⁻¹ y⁻¹ compared to the national average of 130 kg ha⁻¹ y⁻¹ causing degradation of soil quality in all cropping system (Tiwari *et al.*, 2005). In the Himalaya region after harvesting of crop removal of residues for livestock feed is normal practice and open grazing also affects the net return of biomass to the soil and further accelerates land degradation (Bhattacharyya *et al.*, 2009). Seventy percent of the population depends on agriculture for their livelihood in the NWH region, and small areas of lands were cultivated for subsistence purpose (Ghosh *et al.*, 2012). The major source of water for agricultural purpose is via

rainfall, which can be erratic and insufficient at times, this inevitably leads to low productivity especially within the during the growing season, which coincides with the lowest rainfall period (Ghosh *et al.*, 2012). Drought, intensive tillage, high runoff and soil loss rates are the largest causes of production losses within NWH (Sharda and Singh, 2004).

Site selection

The study was conducted during 2013 in agricultural fields in the foothills of the Indian Himalaya, near Dehradun, Uttarakhand, India. Three sites (Figure 4.1) were selected: Site 1: Dhulkhot (DK)-Low Input Agriculture –Acidic (LIA), Site 2: Pasauli (PS) - Low Input Agriculture- Acidic, and Site 3: Bhatta Gaon (BG)- Low Input Agriculture-Calcareous (LIC). At each site three fields (Figure 4.2 & Appendix Figure 4.1 to 4.3 and Table 4.1 to 4.3) were selected for sampling. Within each field a field slope transect was designated, which was typically ~60m in length. All slope fields were surveyed by using Leica total station survey equipment and pits location and elevation were recorded using GPS (Garmin). The transects extended from eroding upslope to deposition downslope areas at the base. Also, each sites three fields were selected with no apparent erosion and deposition (Appendix Figure 4.1 to 4.3). These were considered as stable areas, and were used to collect reference samples. Due to the lack of stable uncultivated land in the region, cultivated fields were used as reference sites.

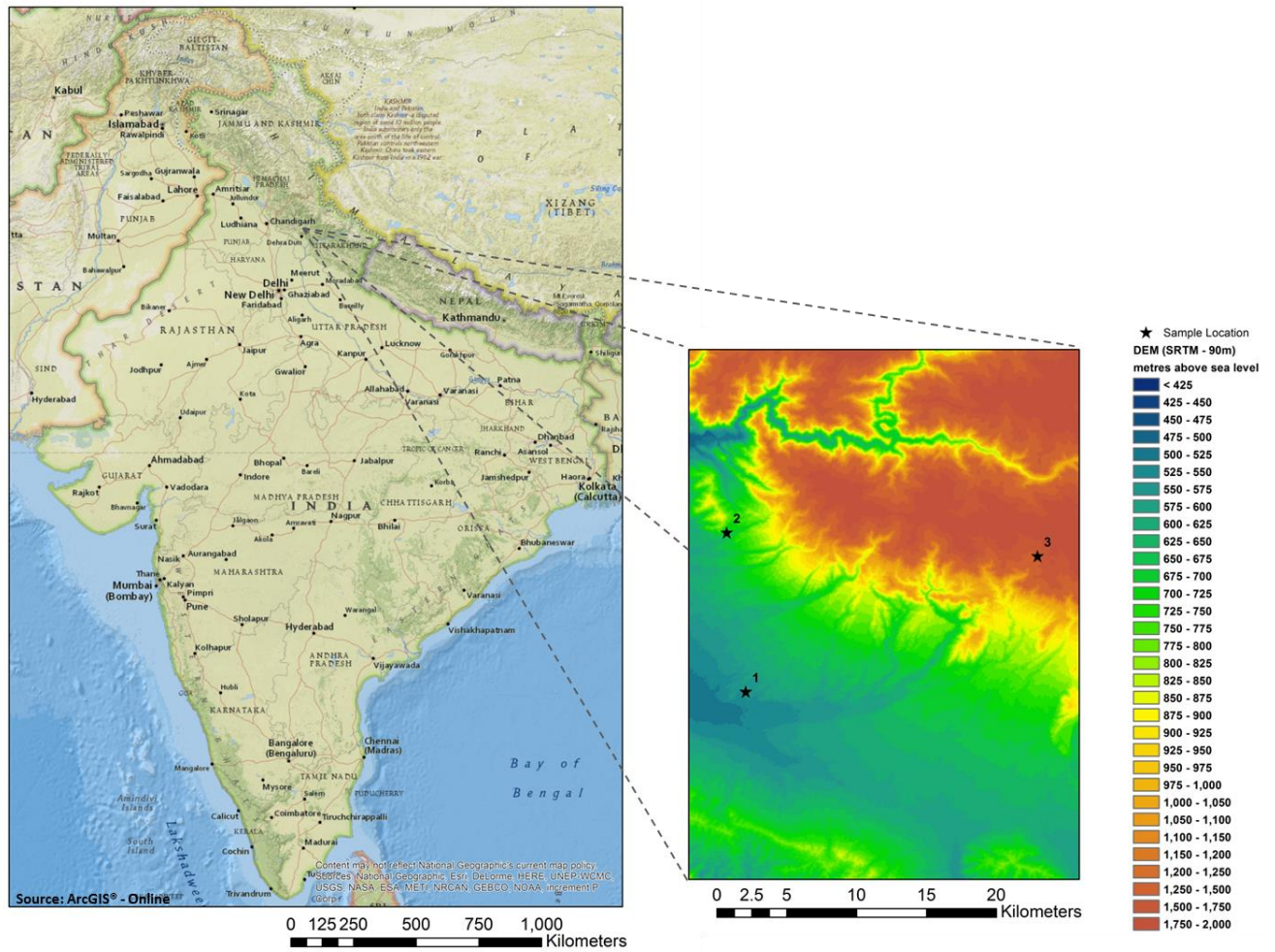


Figure 4.1 Location of the three study sites in the foot hills of Indian Himalaya ; *1: Dhulkhot, *2: Pasauli, and *3: Bhatta Gaon. (Source: ArcGIS® - Online).

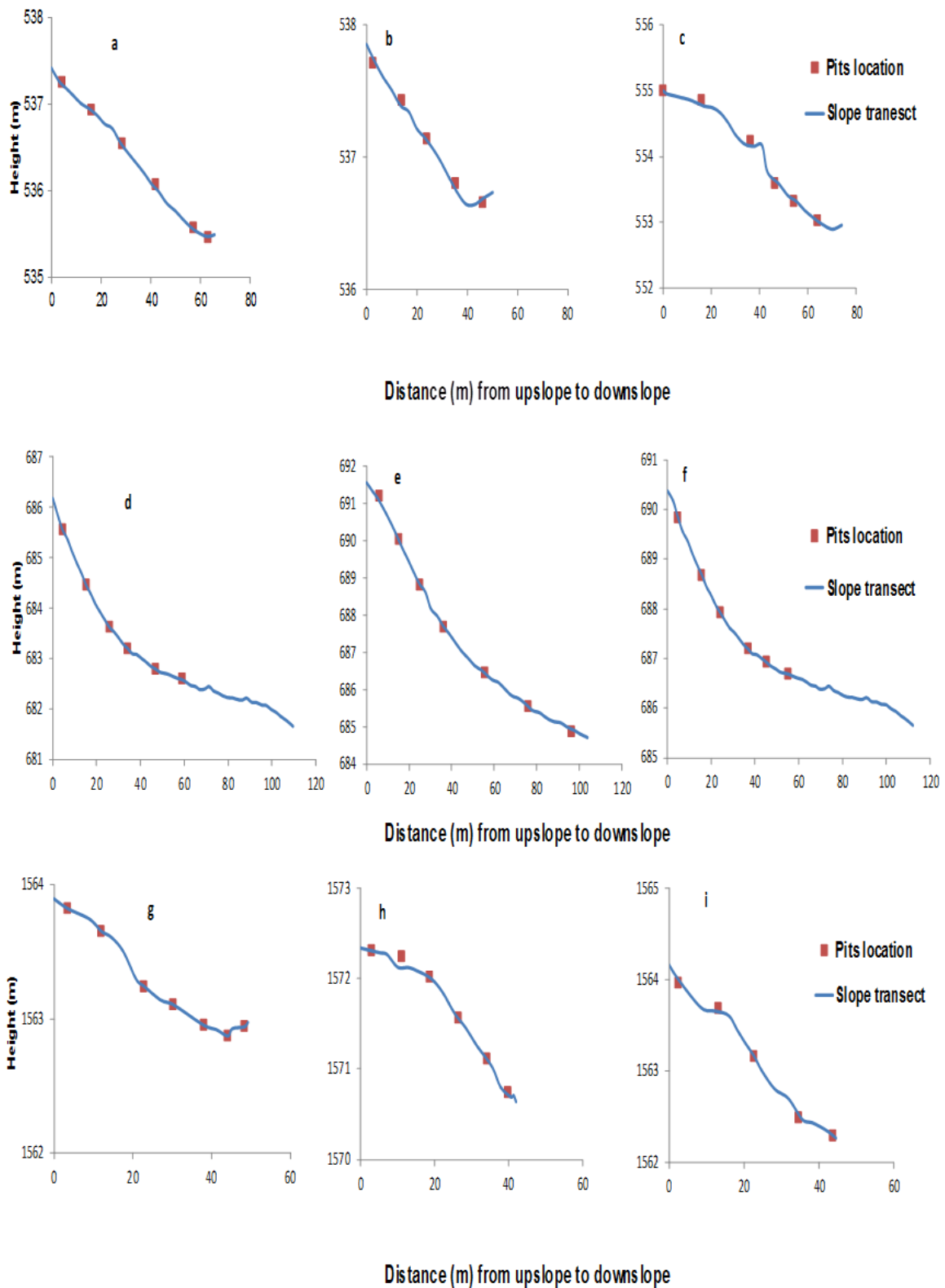


Figure 4.2 Topographical transect (line) and pit locations (red square) for all fields. Site 1(a = DKF1, b =DKF2, and c = DKF3), Site 2 (d =PSF1, e =PSF2 and f =PSF3) and Site 3 (g =BGF1, h=BGF2 and I =BGF3)

Table 4.1 Site 1 (DhulKhot-DK) slope fields and reference fields basic data description . Soil pH and EC measurements represent mean values for whole profile depth. Distance of pits start from upslope (eroding) to downslope (deposition) within each field.

Sites	Fields	Profile	Latitude	Langitude	Elevation (m)	Distance (m)	Soil pH	EC dsm ⁻¹	Depth(cm)
Site 1	DKF1	P1	30°21.052, N	77°53.483, E	537.3	4.2	5.09	0.13	<70
		P2	30°21.062, N	77°53.472, E	536.9	16.1	4.99	0.07	<70
		P3	30°21.062, N	77°53.472, E	536.5	28.6	5.16	0.06	<90
		P4	30°21.067, N	77°53.466, E	536.1	42.0	5.11	0.05	>100
		P5	30°21.073, N	77°53.460, E	535.6	57.2	4.95	0.09	>100
		P6	30°21.076, N	77°53.457, E	535.5	63.0	5.09	0.10	>100
Site 1	DKF2	P1	30°21.065, N	77°53.494, E	537.7	2.5	5.70	0.09	<70
		P2	30°21.069, N	77°53.489, E	537.4	13.9	5.34	0.16	>100
		P3	30°21.073, N	77°53.485, E	537.1	24.1	5.43	0.13	<50
		P4	30°21.077, N	77°53.480, E	536.8	35.3	5.33	0.07	>100
		P5	30°21.082, N	77°53.475, E	536.7	46.4	5.23	0.12	>100
Site 1	DKF3	P1	30°21.087, N	77°53.533, E	555.0	0.0	5.20	0.06	<70
		P2	30°21.096, N	77°53.524, E	554.8	15.9	5.12	0.09	>100
		P3	30°21.101, N	77°53.516, E	554.2	36.3	5.20	0.46	>100
		P4	30°21.104, N	77°53.510, E	553.6	46.4	5.35	0.04	>100
		P5	30°21.107, N	77°53.507, E	553.3	54.1	5.31	0.05	>100
		P6	30°21.111, N	77°53.502, E	553.0	64.0	5.42	0.14	>100
Site 1	DK Ref	Ref1	30°21.011, N	77°53.475, E	550		5.27	0.05	>100
		Ref2	30°21.001, N	77°53.487, E	550		5.29	0.09	>100
		Ref3	30°21.079, N	77°53.541, E	556		5.33	0.06	<70

Table 4.2 Site 2 (Pasauli-PS) slope fields and reference fields basic data description. Soil pH and EC measurements represent mean values for whole profile depth. Distance of pits start from upslope (eroding) to downslope (deposition) within each field.

Sites	Fields	Profile	Lattitude	Langitude	Elevation (m)	Distance (m)	Soil pH	EC dsm ⁻¹	Depth(cm)
Site 2	PSF1	P1	30°27.203, N	77°52.748, E	685.6	4.5	5.64	0.04	>100
		P2	30°27.197, N	77°52.750, E	684.4	15.3	5.38	0.07	>100
		P3	30°27.193, N	77°52.753, E	683.6	25.9	5.53	0.07	>100
		P4	30°27.189, N	77°52.756, E	683.2	34.3	5.33	0.05	<70
		P5	30°27.182, N	77°52.759, E	682.8	46.8	5.35	0.05	>100
		P6	30°27.177, N	77°52.762, E	682.6	58.9	5.33	0.05	>100
Site 2	PSF2	P1	30°27.231, N	77°52.773, E	691.2	5.9	6.05	0.09	>100
		P2	30°27.227, N	77°52.776, E	690.0	15.1	5.25	0.07	>100
		P3	30°27.220, N	77°52.779, E	688.8	25.2	5.24	0.04	>100
		P4	30°27.216, N	77°52.784, E	687.7	36.2	5.24	0.07	>100
		P5	30°27.207, N	77°52.791, E	686.4	55.7	5.07	0.39	>100
		P6	30°27.199, N	77°52.796, E	685.5	75.8	5.34	0.05	>100
		P7	30°27.189, N	77°52.803, E	684.9	96.4	5.24	0.10	>100
Site 2	PSF3	P1	30°27.205, N	77°52.759, E	689.8	4.8	5.17	0.12	<70
		P2	30°27.200, N	77°52.761, E	688.7	15.8	5.22	0.06	>100
		P3	30°27.196, N	77°52.763, E	687.9	24.2	5.07	0.05	>100
		P4	30°27.191, N	77°52.767, E	687.2	36.9	4.99	0.08	>100
		P5	30°27.186, N	77°52.770, E	686.9	45.2	5.21	0.07	>100
		P6	30°27.181, N	77°52.773, E	686.7	55.2	5.00	0.08	>100
Site 2	PS Ref	Ref1	30°27.221, N	77°52.740, E	679		5.70	0.17	>100
		Ref2	30°27.240, N	77°52.776, E	680		7.11	0.11	>100
		Ref3	30°27.224, N	77°52.749, E	679		6.30	0.12	>100

Table 4.3 Site 3 (Bhatta Gaon-BG) slope fields and reference fields basic data description. Soil pH and EC measurements represent mean values for whole profile depth. Distance of pits start from upslope (eroding) to downslope (deposition) within each field.

Sites	Fields	Profile	Latitude	Longitude	Elevation (m)	Distance (m)	Soil pH	EC dsm^{-1}	Depth (cm)
Site 3	BGF1	P1	30°26.310, N	78°04.702, E	1563.8	3.5	7.12	0.20	>100
		P2	30°26.318, N	78°04.703, E	1563.7	12.0	6.86	0.14	>100
		P3	30°26.319, N	78°04.704, E	1563.2	22.9	7.08	0.14	>100
		P4	30°26.326, N	78°04.705, E	1563.1	30.3	7.16	0.22	<90
		P5	30°26.329, N	78°04.709, E	1563.0	38.1	7.35	0.28	<50
		P6	30°26.333, N	78°04.714, E	1562.9	44.1	7.27	0.31	<30
		P7	30°26.329, N	78°04.717, E	1562.9	48.3	7.36	0.26	>100
Site 3	BGF2	P1	30°26.294, N	78°04.726, E	1572.3	4.4	7.20	0.17	>100
		P2	30°26.294, N	78°04.730, E	1572.2	11.9	7.33	0.18	>100
		P3	30°26.296, N	78°04.734, E	1572.0	19.3	7.28	0.17	>100
		P4	30°26.295, N	78°04.738, E	1571.6	27.1	7.19	0.17	>100
		P5	30°26.297, N	78°04.743, E	1571.1	34.6	7.64	0.19	<50
		P6	30°26.301, N	78°04.746, E	1570.7	39.8	7.49	0.31	<30
Site 3	BGF3	P1	30°26.327, N	78°04.698, E	1564.0	2.5	7.36	0.31	<30
		P2	30°26.331, N	78°04.702, E	1563.7	13.1	7.21	0.20	>100
		P3	30°26.334, N	78°04.704, E	1563.2	22.7	7.46	0.22	>100
		P4	30°26.339, N	78°04.704, E	1562.5	34.6	7.45	0.23	>100
		P5	30°26.342, N	78°04.713, E	1562.3	43.7	7.25	0.21	>100
Site 3	BG Ref	Ref1	30°26.267, N	78°04.750, E	1568		7.36	0.31	<50
		Ref2	30°26.251, N	78°04.733, E	1563		7.31	0.19	>100
		Ref3	30°26.273, N	78°04.734, E	1566		7.20	0.22	<90

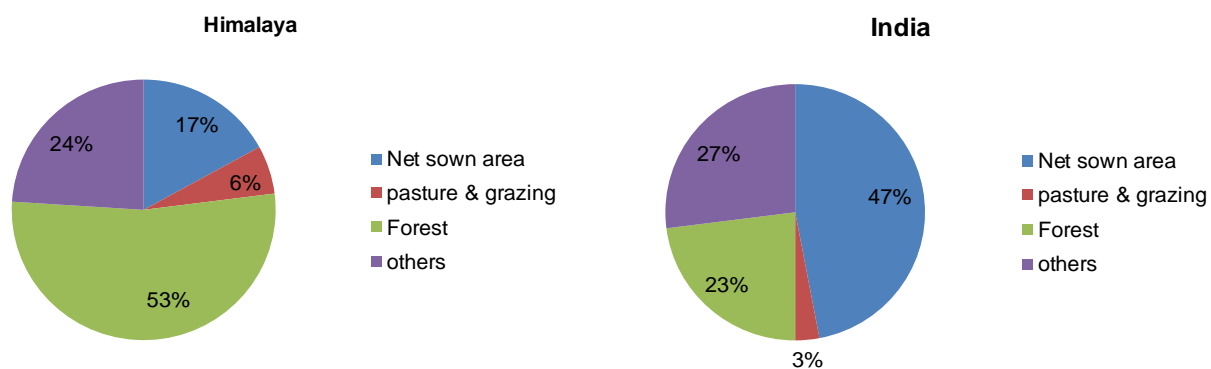


Figure 4.3 Major land use pattern in Study area and India (SFR, 2009)

Table 4.4 Major crops productivity (kg ha^{-1}) from different region (Madhu and Sharda, 2011)

Different region	Maize	Wheat kg ha^{-1}	Rice
NWH	1779	1665	1796
Uttarakhand	1392	1921	1939
Himalaya	1579	1649	1741
India	1998	2715	2051
Developed country (FAO-Stat)	6810	3110	8340

FAO-Stat- Food and Agriculture Organisation -statistics

4.2. Methodology for chapter 5

Chapter 5 address research objective 1: *To quantify the impacts of erosion-induced soil redistribution on SOC and nutrients (lateral and vertical) within agricultural fields*

The statistical data analysis in this chapter assumes the overall null hypothesis:

H₀: Erosion induced redistribution of soils (Top/Subsoil) changes within field spatial variation of soil nutrient stock and its C/N ratio, eroding position has low SOC/nutrient stocks than deposition positions.

Soil sampling design

The effect of soil redistribution on spatial variation (Vertical and Lateral) of ¹³⁷Cs, SOC, TN and P were studied by measuring above parameters in soil samples from eroding to depositional profiles by opening 1 m³ pits along slope transect of each agricultural field and samples were collected from each pits with 3 replication (randomly selected and considered each face of pit as one replicate). The pits were located along slope transect based on slope steepness variation (approximate interval between pit to pit is 10 m) and minimum 5 pits to maximum 7 pits were selected for study in each field. The sample collected in different soil depth increment (0-10, 10-20, 20-30, 30-50, 50-70, 70-100cm) using metal box (dimension 10*10*5cm), collected soil samples were processed (air dried and oven dried at <60°C) and sieved using 2mm sieve and weighed <2 mm and >2 mm mass. This <2 mm particles used for further analysis of ¹³⁷Cs, SOC, TN and P (Walling and Quine, 1991; Quine and Zhang, 2002).

Soil chemical analysis

Soil total Carbon and Nitrogen contents were analysed from the sieved < 2mm soil samples of all replicates using a Flash 2000 Organic elemental analyser (Thermo scientific). Inorganic carbon removed for soils had >6 pH. Inorganic carbon removed by following acid fumigation method (Harris *et al.*, 2001; Walthert *et al.*, 2010) and after IOC removal samples were measured for SOC (review and methods presented in Appendix Text 4.2 and data presented in Appendix Table 4.4 and Appendix Figure 4.4). Total Nitrogen content data used from acid untreated samples because acid treated samples affect total nitrogen concentration.

Soil Phosphorous (Total/ Inorganic P) measured (review and methods presented in Appendix Text 4.3 and Table 4.7) by Saunders and Williams, 1955 method only pits at three

slope positions (eroding, mid and deposition) for each field, soil samples were prepared as a composite of three replicates of each pit up to 50cm depth increment. Soil samples were burnt at 550°C to measure Total P and unburnt for inorganic P and extracted with 0.5M H₂SO₄ solution and P measured in UV-1600 PC spectrophotometer (VWR-Made in China). After measuring Total P and Inorganic P, Organic P calculated based on these two results. Soil pH was measured with Hand held pH meter from a soil slurry of 1:1 ratio by volume of soil to deionised water (complete data in Appendix Table 4.1 to 4.3).

The basic and application of ¹³⁷Cs technique

¹³⁷Cs is an artificial radionuclide present in the environment due to human activity. ¹³⁷Cs fallout was produced as a by-product of atmospheric testing (Figure 4.4) of thermonuclear weapons during the period between 1950 -1970s. The maximum rate of ¹³⁷Cs fallout from the atmosphere occurred in 1963. Another source of ¹³⁷Cs to environment was the accident at the Chernobyl nuclear power station in 1986. ¹³⁷Cs released from Chernobyl is locally important particularly northern Europe and Northern-western Eurasia, but in most parts of the world, the ¹³⁷Cs in environment was derived from weapons testing. This bomb-derived ¹³⁷Cs was distributed globally in the stratosphere and deposited on earth surface by fallout (dry or wet), usually in association with precipitation. After deposition of ¹³⁷Cs on mineral and organo-mineral soils, ¹³⁷Cs fallout was strongly and rapidly adsorbed (Wallbrink *et al.*, 1994; Zhang *et al.*, 2008) and its subsequent redistribution has occurred in association with the erosion and deposition of soil particles by water, tillage and wind (Ritchie and McHenry, 1990; Scott Van Pelt *et al.*, 2007). The Chernobyl derived ¹³⁷Cs is less important for my study area. ¹³⁷Cs has a half-life of 30.17 years and at present day about 40% of original fallout still remains at undisturbed sites. The ¹³⁷Cs distribution at various landscape positions is affected by erosion and different agricultural practices. A sharp decrease in ¹³⁷Cs content with depth is typical of undisturbed areas/stable site are often used to provide a local reference inventory (estimate of fallout input). Where cultivation occurs, ploughing modifies the form of ¹³⁷Cs depth profile, resulting in a relatively uniform distribution over the plough depth. In the absence of soil loss the ¹³⁷Cs inventory is similar to local reference sites. Where soil loss occurs particularly upslope position, ¹³⁷Cs will also be lost leading to reduced ¹³⁷Cs inventory. Conversely wherever soil deposition takes place mainly downslope position, it increases the ¹³⁷Cs inventory. This principle will be applicable to assessment of soil loss and deposition

associated with sheet, rill, and tillage and wind erosion. By using appropriate calibration methods (Walling and Quine, 1991) it is possible to derive quantitative estimates of soil redistribution from ^{137}Cs measurements.

^{137}Cs has been used as a well-established tracer of erosion and deposition for more than 40 years and, although its reliability and underpinning assumptions have come under scrutiny (Parsons and Foster, 2011 and 2013), it remains a valuable tool in assessing long-term erosion rates because of the time period since fallout and the long half-life of ^{137}Cs (30.2 years). The application in this study will account for the critique of Parsons and Foster (2011) and ensured that sufficient account is taken of sources of local variability by collecting high intensity soil samples. ^{137}Cs tracer will help to study redistribution of nutrients under various landscape position –Eroding to Deposition slope - within field and found significant relationship between ^{137}Cs and nutrients (SOC, N and P) (Verity and Anderson, 1990; Pennock, 2000; Quine and Zhang, 2002). This benefit of ^{137}Cs tracer technique was applied in my study.

Few studies only addressed for low input and subsistence agriculture, tropical and subtropical climate. In India, only one study has reported and used ^{137}Cs for soil erosion measurement in arable land (Prokop and Poreba, 2011 and 2012) and no study has used ^{137}Cs for soil erosion/redistribution and nutrients/SOC spatial variation within field. This may be the first study for this highly eroding, important bio diverse Indian Himalayan region

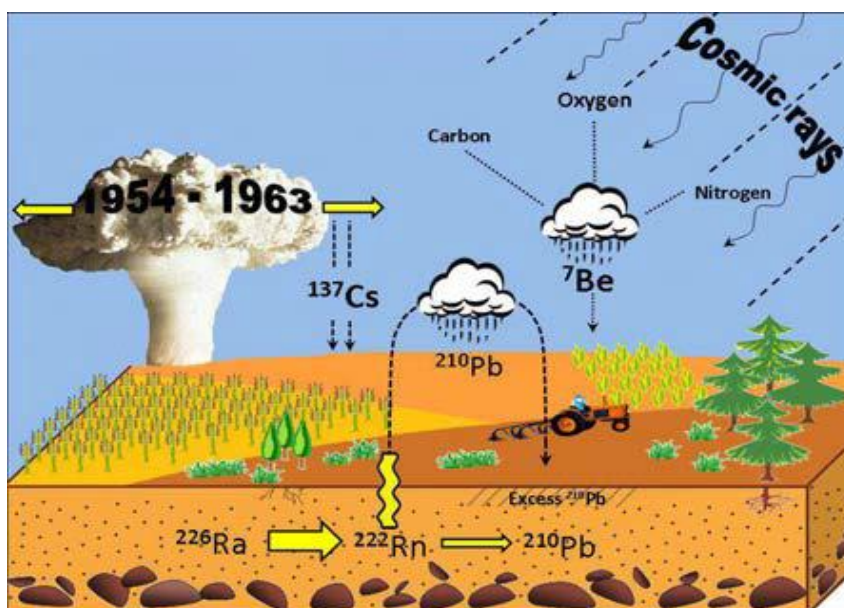


Figure 4.4 Fallout of ^{137}Cs and other radionuclides (Zubanc and Mabit, 2010)

¹³⁷Cs measurement

100 gram of air dried <2mm soil packed in plastic pots and measured the ¹³⁷Cs activity using a high resolution gamma spectrometer (EG & ORTEC, Made in USA). The counting time was at the order of 8, 16 and 24 hrs. ¹³⁷Cs activity was determined by counting the 661.7 keV gamma emissions. As a reference material soil with known ¹³⁷Cs provided by IAEA was used to check the detector working conditions. ¹³⁷Cs activities were expressed in m Bq g⁻¹ or Bqkg⁻¹ and corrected with respect to radioactive decay to sampling time. Total ¹³⁷Cs inventory is defined as a sum of ¹³⁷Cs inventory of each soil layer in soil profile (corrected to unit area of sampling device and <2mm soil mass) and it expressed in Bq m⁻².

Inventory (¹³⁷Cs, SOC, TN or P) estimation formula

$$C_i = \frac{C_a * S_m}{A} \quad (1)$$

C_i= Inventory of ¹³⁷Cs (Bq m⁻²) or SOC or TN or P (kg m⁻²)

C_a= activity of ¹³⁷Cs (m Bq g⁻¹) or concentration of SOC or TN or P (g kg⁻¹)

S_m= soil mass of <2mm soil particles at respective depth layers (g)

A= cross sectional area of sampling device (m²)

Statistical analysis

One-way ANOVA performed to test the mean significance of each slope positions/ pits in slope transect for total inventory of SOC, TN, ¹³⁷Cs and P to 50 cm depth. After Anova analysis adopted test Tukey HSD at $p < 0.05$.

Descriptive statistics performed for Total inventory of ¹³⁷Cs, SOC, and TN to 50 cm depth of all the slope fields.

Linear regression analysis and significance test performed between total ¹³⁷Cs inventory and SOC and TN inventory for all slope fields up to sum of 50 cm depth of each replicate total inventory values. Also Linear regression analysis performed between ¹³⁷Cs activity and SOC and TN concentration for all slope fields up to 50 cm different depth increments.

Linear regression analysis performed between ¹³⁷Cs inventory and OP and TP inventory for all slope fields by combining each site field as a one group of data up to 50 cm depth of

each replicate total inventory values. Each pit all replicate samples made into composite, after analysing the composite sample P concentration used for estimate inventory for each replicate and depth samples.

All statistical analysis executed in R programme 3.1.2 version.

4.3. Methodology for chapter 6

Chapter 6 address research objective 2: *To quantify erosion-induced soil carbon redistribution on the net effect of carbon exchange between soil and atmosphere in low input/productivity and highly eroding agricultural fields from the foothills of the Indian Himalaya by using ^{137}Cs fallout and SOC inventories.*

The statistical data analysis in this chapter assumes the overall null hypothesis:

H₀: Erosion-induced soil redistribution results in a net carbon sink when continuous crop production is maintained, despite low fertiliser inputs, low crop productivity and high biomass removal

To estimate net C flux, SOC and ^{137}Cs data used from chapter 5 up to 50 cm depth of slope fields and up to 100 cm depth of non-slope/ stable fields.

Net C flux estimated based on depth distribution model developed by Quine and Van Oost (2007)

Data of total SOC and ^{137}Cs inventories (mass or activity per unit area) from all soil profile were used in retrospective assessment of erosion-induced perturbation of C dynamics using the approach of Quine and Van Oost (2007). This approach consist different steps as follows

1. Derivation of initial plough layer mass based on initial ^{137}Cs fallout
2. Derivation of Carbon Concentration Index (CCI)
3. Derivation of erosion and deposition rates
4. Simulation of reference C profile shape and it depth distribution based on this derive dynamic equilibrium profile C inventory for eroding and deposition profiles by keeping view no input and C content changed only lateral and vertical redistribution of C within profile.
5. Derive Carbon Inheritance Index (CII)
6. Derive Sink/Source estimation

Reference fallout ¹³⁷Cs Inventories

The approach is based on the fundamental principles of the ¹³⁷Cs technique for erosion assessment and is, therefore, reliant on reliable estimates of fallout reference inventories and robust measurements of point inventories (4.2 above). Reference ¹³⁷Cs inventories are typically based on measurements from undisturbed and uncultivated, uneroded sites nearby to the site under investigation. Due to the intensity of land use in the area, it was not possible to find sites that meet these criteria outside the forest areas, which are unsuitable due to high local variability in precipitation, stemflow and throughfall. Therefore, estimates of fallout reference inventory were initially based on sample collection (same methodology as above) from selected flat/levelled fields, nearby slope /study field, which were not thought to have been subject to erosion and deposition. Naturally, there is some uncertainty in making this assessment and, therefore, for each site three levelled fields within a maximum distance 100 m of the study fields were selected for collection of reference samples. Furthermore, an attempt was made to estimate the fallout reference inventory from global fallout data collected during the period of bomb fallout (Eisenbud, 1987; UNSCEAR, 1982). The measured inventories from the reference fields are presented in Table 4.6 In the light of the relatively small variation in precipitation between sites (approximately 100 mm) and their close geographic proximity, it is surprising that the inventories measured at Site 1 differ as much as they do from Sites 2 and 3. Site 1 is the closest to the urban centre of Dehradun and there is more light industrial activity (including brick-making) in the area. It is, therefore, considered likely that this 'reference' inventory is unreliable and a result of large-scale soil redistribution due to field-levelling since the period of bomb fallout. Sites 2 and 3 are relatively similar; however, it is important to note that they lay in the same agricultural units as the fields under investigation and, while their modest slopes would offer some protection from erosion, they are potentially susceptible to run-on from the surrounding agricultural area, roads and tracks.

In order to estimate the ¹³⁷Cs inventory from global fallout data, the following steps were undertaken:

- Published relationships between ¹³⁷Cs fallout and latitude (Table 4.7) in the northern hemisphere (Eisenbud, 1987; UNSCEAR, 1982) were used to establish the expected ratio, based on latitude alone, between inventories in the Study area and Devon, UK (for which the University of Exeter has good records of fallout

inventories). This was used to estimate expected reference inventory for 900 mm annual precipitation.

- Well-established relationships between precipitation and fallout (e.g. Pálsson et al., 2006) were then used to derive an estimate of reference inventory for 1600 mm precipitation at the latitude of Dehradun (latitude band 30⁰).

This approach yielded an estimate of the reference inventory of 1685 Bq m⁻². While this is of the same order of magnitude as the measured 'reference' inventories at Sites 2 and 3, it is significantly higher. There is, therefore, significant uncertainty in defining the most appropriate reference inventory to use. Taking into account the potential for erosion to have occurred at the fields used to derive reference inventories, the value of 1685 Bq m⁻² based on global patterns was used as the default inventory for the majority of the analysis; however, sensitivity analysis was undertaken to explore the effect on erosion and C exchange calculations of using a range of reference inventories, including a value closer to the observed inventories at the Site 2 and Site 3 reference sites. It is also important to note that in Chapter 5, emphasis is placed on examination of within-field patterns rather than absolute values, recognising the uncertainty with regard to the fallout reference inventory.

Table 4.5 Measured total reference ¹³⁷Cs inventory profiles from different sites of study area.

Ref profile	Site 1	Site 2	Site 3
	(Bq m ⁻²)		
1	430	1346	1257
2	779	1482	1402
3	516	1178	1188
4	787	1228	1069
5	702	1058	1118
6	595	1297	1002
Mean	635	1265	1173
SE	59.6	59.5	58.5

Table 4.6 Global fallout of ^{137}Cs at different latitude band.

Latitude Band (Degrees)	^{137}Cs fallout (derived from ^{90}Sr) (Bq cm⁻²)
70-80N	0.11
60-70N	0.28
50-60N	0.46
40-50N	0.52
30-40N	0.37
20-30N	0.28
10-20N	0.19
0-10N	0.13
0-10S	0.08
10-20S	0.07
20-30S	0.11
30-40S	0.12
40-50S	0.14
50-60S	0.08
60-70S	0.06
70-80S	0.04

Step 1. Derivation of initial plough layer mass

^{137}Cs used as a marker to estimate initial plough layer from 1963. Because 1963 highest ^{137}Cs fallout occurred globally.

$$P_m = P\rho \left(\frac{F_s}{F_n} \right) \quad (1)$$

P_m is the mass of 1963 cultivation layer per unit area (kg m⁻²),

F_s is fallout ^{137}Cs inventory (Bq m⁻²) at slope transect profile (erosion to deposition)

F_n is fallout ^{137}Cs inventory (Bq m⁻²) at non eroding/stable profile (no erosion and deposition)

P the cultivation layer depth (m),

ρ the fine matter bulk density (kg m⁻³) measured without stone mass.

Step 2. Carbon Concentration Index (CCI)-Specific CCI for 1963 plough mass

$$CCI = \frac{C_{mz}}{P_m} \quad (2)$$

CCI is Carbon Concentration Index (kg C kg⁻¹ in initial cultivation layer)

C_{mz} the measured carbon inventory to depth z m (kg C m⁻²)

P_m is the initial cultivation layer (1963) remaining in the profile to depth z m (kg m⁻²)

Step 3. Derive erosion and deposition rates (Walling and Quine, 1991; Quine, 1995; Zhang et al., 1990; Quine and Van Oost, 2007):

Erosion (E , $m\ yr^{-1}$) and deposition (D , $m\ yr^{-1}$) rates for each profile were estimated from the difference between the measured ^{137}Cs inventory (F_s , $Bq\ m^{-2}$) of each profile at erosion and deposition profiles along slope transect and reference ^{137}Cs inventory (F_n , $Bq\ m^{-2}$) at non eroding / stable /reference profile.

$$E = P \left[1 - \left(\frac{F_s}{F_n} \right)^{\frac{1}{tb}} \right] \quad (3)$$

$$F_{ex} = \frac{\sum_{i=1}^{i=n} S_i(F_n - F_{si})}{\sum_{i=1}^{i=n} S_i E_i \rho} \quad (4)$$

$$D = \frac{F_s - F_n}{tb * F_{ex}} \quad (5)$$

P is plough layer depth (m)

tb is time between sampling 1963 to 2013 (50 years)

F_s is fallout ^{137}Cs inventory ($Bq\ m^{-2}$) at slope transect profile (erosion to deposition)

F_n is fallout ^{137}Cs inventory ($Bq\ m^{-2}$) at non eroding/stable profile (no erosion and deposition)

F_{ex} is the fallout ^{137}Cs inventory ($Bq\ m^{-2}$) for exported soil from eroded areas.

S_i the surface area represented by sample i (m^2)

n the number of erosion points

This formula 3 and 5 derive erosion and deposition depth ($m\ yr^{-1}$) for each pits/profile after this converted to mass of soil loss/gain ($kg\ m^{-2}\ yr^{-1}$) by multiplied with bulk density of plough layer. This individual pits/profile soil loss/gain converted represent area of erosion and deposition each fields.

Simulation of Carbon inheritance based on reference C profile shape

Reference /Stable profiles

In order to adopt the approach used by Quine and Van Oost (2007), it is necessary to define the shape and SOC inventory of a stable equilibrium profile. Quine and Van Oost (2007) had access to 50-200 measurements per field and were able to define the reference profile by using those measurement points that appeared, on the basis of ^{137}Cs inventory, to be stable. This is challenging in this study because fewer measurement points are available. The approach employed was, therefore, to use the depth distributions of SOC at the reference sites to tune the shape parameters in the SOC depth distribution model. As in the Quine and Van Oost (2007) study, this assumes that SOC is evenly distributed through the cultivation layer and, below this, declines exponentially with depth towards a minimum value. The total SOC inventory was defined by reference to the soil profile (or profiles) from within each field that had a ^{137}Cs inventory closest to the fallout reference in use. This dual approach is adopted to account for potential differences in SOC inputs (manure) and exports (fuel/biomass) between the reference and study fields.

Although it was possible to ask current land users about the cultivation depth that they employed, it was important to check this against the mixing depth evident in the ^{137}Cs profiles. It was assumed that ^{137}Cs would be evenly mixed through the cultivation layer (mixing depth). Depth increments that appeared to span the base of the mixing layer were identified and the depth of penetration of the mixing layer into the sample was derived using the ratio of ^{137}Cs activity (mBq g^{-1}) in the sample with that in the overlying samples (entirely within the mixing layer). This was undertaken for all samples that had ^{137}Cs inventories lower than the reference inventory and the mean value was used as the cultivation (mixing) depth for the field. Using this approach, the following cultivation depths were derived: Site 1: 0.14m; Site 2: 0.26m and Site 3: 0.24m.

Step 4. Depth distribution model: this depth distribution model will help to simulate shape of reference C profile from cultivation layer to deep layer. This is necessary to simulate carbon inheritance impact by erosion and deposition.

If $z \leq P$

$$C_z = \frac{C_c}{P} \quad (6)$$

If $z \geq P$

$$C_z = C_{\min} + \left(\frac{C_e}{k}\right) e^{-k(z-P)} \quad (7)$$

$$C_e = \left(\frac{C_c}{P}\right) - C_{\min} \quad (8)$$

Where C_z is the carbon concentration at depth z (kg m^{-3}),

C_{\min} is a baseline SOC concentration (kg m^{-3}) at 1m depth with considering 0.9 C_{\min} fraction.

C_c the reference cultivation layer carbon inventory (kg m^{-2})

k depth attenuation co-efficient (m^{-1})

z is depth (m)

P is plough depth (m)

C_0 is SOC concentration (kg m^{-3}) at 0 m depth of sub plough layer starting

After assigning all parameters for depth distribution model to simulate reference C profile shape at end sum of predicted and measured C inventory difference value need to solved by solver programme to get best fit line of measured and predicted C in depth wise.

From this reference profile shape I can extract C_{\min} , k and C_0 values (Appendix Table 6.1) for simulating equilibrium C inventory for eroding and deposition profiles by assuming input and contents were in equilibrium but only allowing lateral redistribution of SOC and vertical redistribution of SOC within profile.

This depth distribution model was applied for eroding and deposition sites and simulated carbon inheritance of each site by assuming with expectation of inputs and C content were in dynamic equilibrium and erosion had no influence on C dynamics

Eroding sites (if measured $^{137}\text{Cs} < \text{reference site } ^{137}\text{Cs}$ inventory);

$$C_{ic} = C_c \left[1 - \frac{E}{P}\right]^{td} + \sum^{t=1,td} \left[\left(C_{\min} + \left(\frac{C_e}{k}\right) \int_{Z=(t-1)E}^{Z=tE} e^{-kz} dz \right) \left(1 - \frac{E}{P}\right)^t \right] \quad (9)$$

$$C_{iz} = C_{ic} + C_{\min}(z_{\max} - P) + \left(\frac{C_e}{k}\right) \int_{Z=tdE}^{Z=z_{\max} + tdE - P} e^{-kz} dz \quad (10)$$

$$C_x = C_c - C_{iz} + C_{\min}(z_{\max} + tdE) + \left(\frac{C_e}{k}\right) \int_{Z=0}^{Z=z_{\max} + tdE - P} e^{-kz} dz \quad (11)$$

C_{ic} is the inherited carbon inventory in the Cultivation layer (kg m^{-2}),

t_d is the time since the onset of disequilibrium (years) and here was set to 50 years on the basis of information from farmers (as there is some uncertainty in this value, the effect of variation in t_d was explored in sensitivity analysis),

C_{iz} is the inherited carbon inventory to depth Z_{\max} (kg m^{-2}),

Z_{\max} is the depth of sampled profile (m),

C_x is the carbon export (kg m^{-2})

Aggrading sites (if measured ^{137}Cs > reference site ^{137}Cs inventory)

Here important is to estimate of inherited carbon content of deposited sediment. An estimate of this for the study area can be derived by dividing total carbon export by the total volume of soil exported.

$$C_{\text{ero}} = \frac{\sum_{i=1,n} C_{xi} S_i}{\sum_{i=1,n} t_d E_i S_i} \quad (12)$$

Where C_{ero} is the carbon export of soil exported from eroded area (kg C m^{-3}),

So C inheritance at cultivation layer and up to profile z depth at depositional sites are,

$$C_{ic} = C_c \left(\frac{P}{P+D} \right)^{t_d} + C_{\text{ero}} D \sum_{t=1,t_d} \left(\frac{P}{P+D} \right)^t, \quad (13)$$

$$C_{iz} = C_c + C_{\text{ero}} t_d D + C_{\min}(Z_{\max} - P - t_d D) + \left(\frac{C_e}{k} \right) \int_{Z=0}^{Z=Z_{\max} - t_d D - P} e^{-kz} dz \quad (14)$$

Step 5. Carbon Inheritance Index (CII)

$$CII = \frac{C_{iz}}{P_m} \quad (15)$$

CCI vs CII provide C flux between atmosphere and soil.

If $CCI > CII$ indicate flux from atmosphere to soil, means C sink

If $CCI < CII$ indicate flux from soil to atmosphere, means C source

Step 6. Sink/Source derivations

$$C_{\text{atm}} = \frac{(C_{\text{mz}} - C_{\text{iz}})}{t_d} \quad (16)$$

If result + sink to atmosphere

If result - source to atmosphere

SOC stock may be changed result of other factors than E/D (e.g. crop yield, management, climatic factors). But based on ref C inventory I could exclude this external force only I can estimate based on erosion and deposition.

After estimating net C flux for each pits/profile of erosion and deposition location were converted to field unit area based of representation of erosion and deposition area.

Notes: Site 2 field 3 PSF3 C flux estimation was not predicted (Figure.6.4) by Model by using normal reference ^{137}Cs inventory (1685 Bq m^{-2}) for study area particularly at deposition pit and need to use higher level of reference ^{137}Cs inventory (2100 Bq m^{-2}) to complete prediction of C flux in field. This may be due to higher accumulation of ^{137}Cs at deposition profiles.

4.4. Methodology for chapter 7

Chapter 7 address research objective: *To study the effect of erosion- and deposition-induced vertical soil/SOC mixing on soil respiration rates at various landscapes positions.*

The statistical data analysis in this chapter assumes the overall null hypothesis H_0 :

1) H_0 In eroded position, mixing topsoil with organic matter-poor subsoil will reduce decomposition rates as organic matter from topsoils may become bound onto unsaturated soil particles in the subsoil.

2) H_0 In depositional areas, mixing fresh organic matter from top soils into organic matter-rich subsoils will promote C release through a positive priming effect.

Site description for soil respiration experiment

Same site description, from there each site one fields were selected for soil respiration measurement (Figure 4.5). In result and discussion text described Site 1, Site 2 and Site 3 which means to represent each site fields of DKF1, PSF3 and BGF3, respectively.

Soil sampling for soil respiration

The effect of vertical mixing was studied by measuring soil respiration in soil samples from eroding, mid-slope and depositional profiles by opening 1 m³ pits and samples were collected from near surface (0-15 cm) and at depth (45-60 cm) in isolation with five replicates and as 1:1 mixtures, each replication represent each face of pits (profile) and fifth replication randomly chosen any side of pits. Collected soil samples were stored in cold storage up to experiment setup.

Another set of soil samples were collected in same pits with 3 replication. The sample collected in different soil depth increment (0-10, 10-20, 20-30, 30-50, 50-70, 70-100cm) with box dimension (10*10*5cm) collected soil samples were processed (air dried and oven dried at <60°C) and sieved using 2mm sieve and weighed <2 mm and >2 mm mass. This <2 mm particles used for further analysis of ¹³⁷Cs (Walling and Quine, 1991) and pH.

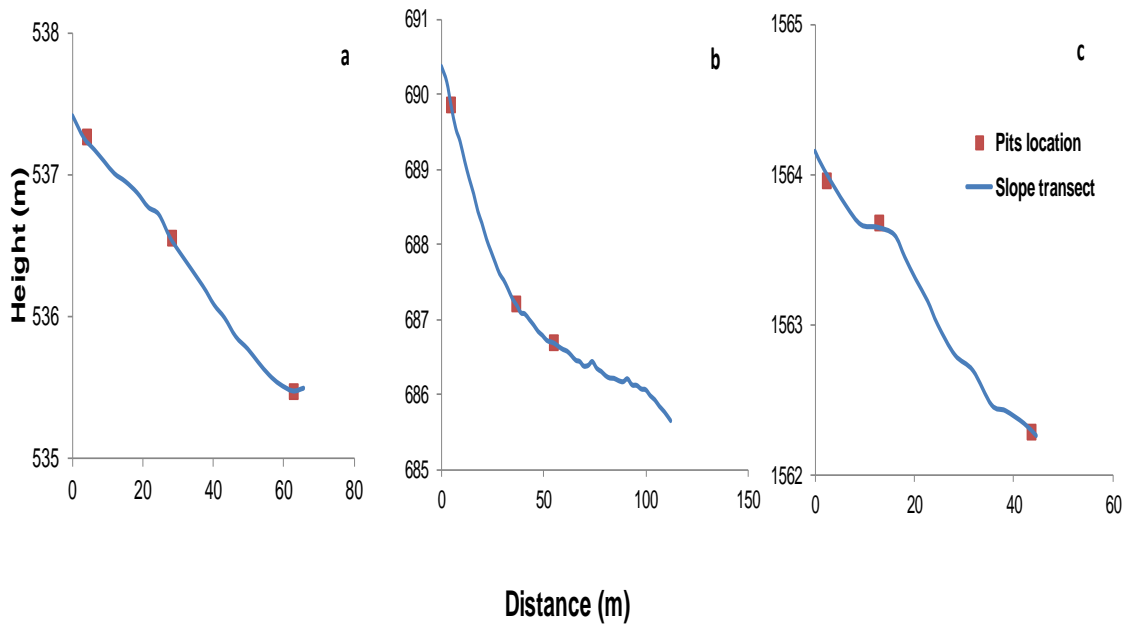


Figure 4.5 Study area field shape for Site 1-DKF1 (Figure a), Site 2-PSF3 (Figure b) and Site 3- BGF3 (Figure c).

Incubation experimental setup

Fresh soil samples were coarsely sieved through 9.5mm sieve to minimise disturbance and obtain homogenise samples and removed large stones and visible roots. Soil moisture content was measured by drying soil samples at 105°C for 24 hrs. The soil water holding capacity (WHC) was determined by wetting soil for 2 hrs followed by draining through filter papers (Fisher brand, QT 270, Code FB59295, size 125 mm). The water content of soil at 100% WHC measured gravimetrically by drying a subsample at 105°C for 24 hrs, and then fixed the WHC 60% for all soil samples. The soil samples kept incubation at 20°C (this is MAT of study area). The soils were prepared by maintaining 60%WHC as optimal water content for microbial activity. 100g fresh soil was placed inside the plastic pots (100ml), these plastic pots had three holes on lids that facilitate gas exchange but minimise drying. Soil pots were placed inside incubators (Sanyo Incubator, MIR-154) with temperature adjusted to 20° C. The samples of five replicates of each depth soil is kept randomly within 3 incubators to ensure that allow soil types and horizons were presented in each incubator to avoid temperature fluctuation variation. Soil moisture was maintained at optimum of 60 % water holding capacity by regularly (weekly) weighing the soil pots and adding deionised water to compensate for moisture loss.

CO₂ Flux measurement

Soil respiration measurement were made over one year, initially weekly (to week 8), biweekly (from weeks 10 to 16), 4 weekly (weeks 20 and 24), 6 weekly (weeks 30 and 36) and 8 weeks (weeks 44 and 52). In one-year period 19 measurement including 0-day measurement. Measurement was conducted (Karhu *et al.*, 2014) by placing soil plastic pots without lids inside a larger airtight 700 ml cylindrical plastic container. This incubation set up (soil pots with large plastic pots) was connected to an infrared gas analyser- EGM-4 (Environmental gas monitor; PP System, version 4.17) in a closed loop configuration. The first CO₂ measurement was measured at 1 hr after closing containers and second measurement of CO₂ concentration was recorded after 24 hrs. The individual fluxes rate were expressed per gram of initial SOC (mg CO₂- C g⁻¹ SOC h⁻¹) and finally calculated cumulative total C release for one year period (mg CO₂- C g⁻¹ SOC).

Vertical mixing of SOC / priming estimation

The effect of vertical mixing on respiration rate was determined by comparing the measured rate of respiration from the mixed samples here after called Observed with an rate of activity based on the measurements made on individual depths here after called Expected (average respiration rates of 0-15cm and 45-60cm samples with respective proportion of SOC in each layers). When comparing Observed with Expected respiration for each slope positions if observed exceed expected then there is positive priming activity and if go less then there is negative priming activity.

Soil chemical analysis

Soil total Carbon and Nitrogen contents were analysed from the sieved <2mm soil samples of all replicates using a flash 2000 elemental analyser (thermos scientific). Inorganic carbon removed for soils had >6 pH. Inorganic carbon removed by following acid fumigation method (Harris *et al.*, 2001; Walthert *et al.*, 2010) and after IOC removal samples were measured for SOC. Soil pH was measured with Hand held pH meter from a soil slurry of 1:1 ratio by volume of soil to deionised water.

¹³⁷Cs measurement

100 gram of air dried <2 mm soil packed in plastic pots and measured the ¹³⁷Cs activity using a high resolution gamma spectrometer (EG & ORTEC, USA). The counting time was at the order of 8, 16 and 24 hrs. ¹³⁷Cs activity was determined by counting the 661.7 keV gamma emissions. As a reference material soil provided by IAEA was used to check the detector working conditions. ¹³⁷Cs activities were expressed in m Bq g⁻¹ or Bq kg⁻¹ and corrected with respect to radioactive decay to sampling time. Total ¹³⁷Cs inventory is defined as a sum of ¹³⁷Cs activity of each soil layer in soil profile (corrected to unit area of sampling device and < 2mm soil mass) and it expressed in Bq m⁻².

Soil erosion and deposition and quantity of vertical soil/C mixing at each landscape positions estimated based on model developed by Quine and Van Oost (2007). Detailed formula presented in earlier chapter 5 methods.

Statistical analysis

One way anova performed to test the mean significance of each slope positions in transect for cumulative C release , soil respiration rate , SOC, TN, ¹³⁷Cs of top and sub soils. After Anova analysis adopted test Tukey HSD at 0.05. For each landscape position (erosion, mid slope and deposition), repeated measures two way ANOVAs were performed with Observed vs Expected as the within-subject factor and site as the between subject factor. To test priming effect at each slope positions pairs Observed vs Expected adopted Paired t.test. Paired t test also executed for top and subsoil of each profiles to test significance difference of C release, SOC, TN, and CN ratio.

All statistical analysis executed in R programme 3.1.2 version. Cumulative C release estimated and plotted in Microsoft Excel 2010.

4.5. Soil particle size distribution

Two methods were used to quantify the particle size distribution of soil samples. First, dry sieving was used to separate into broadly size fractions samples along the slope transect from field BGF1 of Site 3. The method is described in Appendix 4.1 and the results are presented in Appendix Table 4.5 and Appendix Figure 4.5.

Second, the International pipette method was used to measure particle size distributions in greater detail for selected samples from one field at each site (DKF1, PSF3 and BGF2). Surface (0-10 cm) and subsurface (30-50 cm) samples from upslope (P1) and downslope (P6) locations were analysed. Soil texture was classified

based on ISSS (International Soil Science Society) and all soils were found to be loams except Site 2 pit PSF3 P1 (upslope) that was classified as sandy loam texture. Full results are presented in Appendix Table 4.6 and are used to derive enrichment ratios for each particle size at each site and these are presented in Appendix Table 4.6.

4.6. Site 3 soil respiration chapter data not included in main text and kept in Appendix 7 Series (included Appendix Figure 7.1- 7.5, Table 7.1 to 7.7 and Appendix Text 7.1)

Site 3 ^{137}Cs inventory pattern no clear and not significantly different at each slope position when compare with stable profile. Also this Site 3 had inorganic carbon/carbonate in all positions so it was not possible to interpret the CO_2 flux data solely in the context of the organic C cycle. Due to this difficulty Site 3 omitted from result and discussion and only Site 1 and 2 interpreted.

Also measured soil respiration from non-eroded field from all sites kept in Appendix Table 7.5. Measured SOC from fractionated samples kept in Appendix Table 7.6 and Appendix Text 7.1 describes review of methods for SOM fractionation by dry sieving. Appendix Table 7.7 describes soil moisture content and Water holding capacity of soils from various landscapes positions (soils used for respiration)

4.7. Summary

This chapter has provided an overview of the study sites and field/laboratory methods used to enable the testing of the hypothesis stated. The following results chapters will present and discuss the results in the context of the proposed null hypotheses.

5. Does soil redistribution affect spatial variation (vertical and lateral) of nutrients (SOC, TN and P) within agricultural fields from Low input and highly eroding region

5.1 Introduction

The spatial variation of nutrients caused by soil redistribution in agricultural fields under mechanised tillage is well studied (Quine and Zhang, 2002; Heckrath *et al.*, 2005; De Alba, 2004), but less so in low input farming systems (Quine *et al.*, 1999; Thapa *et al.*, 2001; Li and Lindstrom, 2001). It is within these low input agriculture lands that the highest soil erosion rates are observed. Furthermore, no study has focussed on the Indian Himalaya region (Singh *et al.*, 2016; Ghosh *et al.*, 2012). This chapter addresses this existing research gap and seeks to quantify the impacts of erosion-induced soil redistribution on SOC and nutrients (lateral and vertical) within agricultural fields. The following null hypothesis is considered:

H₀: Erosion-induced redistribution of soils (top- / sub-soil) changes within field spatial variation of soil nutrient stocks and stoichiometry (C:N:P ratio), so that eroded sites will have lower SOC and nutrient stocks than sites of deposition.

5.2 Summary of methods (for full methodology see Chapter 4)

To address the objective stated above, three fields at each site were selected based on the status of erosion and deposition within the agricultural field and three fields from with low slopes that were expected to suffer from little or no erosion. In each eroding field, samples were taken along a topographic gradient, which represented a transition from eroding to deposition phases. Three pits were also opened in the level areas (i.e., no slope). After identifying sampling locations, 1m² pits were opened at each to a maximum depth of 1 m (or less if rock was met) and soil samples were collected at 0-10, 10-20, 20-30, 30-50, 50-70, 70-100 cm depth increments. All collected soil samples were air-dried and ground to pass a 2 mm sieve mesh.

All soil samples for each depth increment was analysed for ^{137}Cs activity (gamma spectrometer), total C and total N (Thermos Scientific Flash 2000 elemental analyser). One of the three sites had a significant carbonate component, which was removed by acid fumigation methods (Harris *et al.*, 2001; Walthert *et al.*, 2010). Soil phosphorous (Total and Inorganic P) were measured using the Saunders and Williams (1955) method. With respect to site P only three slope positions were considered (1) eroding, (2) midslope and (3) depositional for each transect.

One-way ANOVA was performed to determine whether there was a difference between slope positions (pits) in nutrients, SOC and ^{137}Cs activity ($n = 3$). Linear regression analysis was completed to determine the relationship between ^{137}Cs tracer and other nutrients (SOC, total N and P).

Notes : result presentation format

The results were grouped and presented by site and field:

At Site 1, Dhulkhot, the three sloping fields are named DKF1, DKF2, and DKF3 and the three low-slope fields: DK Ref1, DK Ref2 and DK Ref3. This site was at the lowest elevation (550 m) and closest to Dehradun (Figure 4.1).

At Site 2, Pasauli, the three sloping fields are named: PSF1, PSF2 and PSF3 and three low-slope fields: PS Ref1, PS Ref2 and PS Ref3. This site was at intermediate elevation (685 m) and on one flank of a long low gradient ridge between 2 incised valleys (Figure 4.1).

At Site 3, Bhatta Gaon, the three sloping fields are named: BGF1, BGF2 and BGF3 and three low-slope fields: BG Ref1, BG Ref2 and BG Ref3. This site was at the highest elevation (1570 m) on a steep slope below a small village (Figure 4.1); the soils had a $\text{pH} > 6$.

On each slope, the pits are numbered from upslope to downslope (P1 to P5 or P6 or P7). Three profiles were collected and analysed from each pit.

5.3 Results

5.3.1 Small-scale spatial variation in ^{137}Cs activity and Inventory

This is one of the first applications of the ^{137}Cs technique in India and it is the first in the study region. Therefore, it was important to establish whether ^{137}Cs behaviour in this area was similar to that seen in other applications of the technique over the last 3 decades. This was evaluated by application of a robust and detailed sampling framework in which small-scale variation ($n=3$ within pit) was addressed as well as variation with depth, in space (along transects) and between fields ($n=3$ sloping fields at each site). In presenting results here, therefore, the first section addresses the small-scale variability observed within pits and within layers within pits. Patterns within fields are and within profiles are then briefly considered for each site. In this chapter comparisons are made between patterns of ^{137}Cs variation (lateral and vertical) and patterns of C, N and P variation. This minimises the reliance on assumptions regarding the conversion of ^{137}Cs inventories into erosion rates. The latter are not considered here but are derived in Chapter 6.

Within-pit variability

The ^{137}Cs results presented in Tables 5.1 to 5.3 and Appendix Table 5.1 to 5.6 include measures mean inventory (activity per unit surface area), activity per unit mass and, the standard error based on the three independent measures from the same pit (or same layer within the same pit). This allows evaluation of the significance of small-scale variation for using ^{137}Cs as an erosion tracer in this environment. The coefficient of variation (CV) in whole profile inventories for individual pits is in most cases between 5% and 20 % and it is of a similar magnitude to the CV of total C and total N. The variation is smallest in near surface layers of the profiles where ^{137}Cs activities are highest, while higher levels of between sample variations are seen lower in the profiles as activity levels decline towards the detectable limit.

5.3.2 Vertical and lateral distribution of ^{137}Cs , SOC, N and P at Site 1

^{137}Cs

In fields DKF1 and DKF2 ^{137}Cs activities (per unit mass) were lower at upslope sampling points and maximum activity was observed up to 30 cm. However, at downslope sample points the profile showed maximum activity up to 50 cm depth (Figure 5.3a and e), which is consistent with deposition at these sites. In field DKF1, ^{137}Cs inventories (per unit area) along the slope transect start from a minimum at pit 1, rise to pit 3 and drop suddenly to pit 4. This seems consistent with the presence, in the past at least, of a barrier to soil redistribution between pits 3 and 4. This was most likely a temporary or semi-permanent bund that are widely used in the region to divide fields (Figure 5.6). Overall the ^{137}Cs inventory within field eroding profiles located in upslope position was significantly lower ($p < 0.05$) than in the deposition soil profiles (Figure 5.1a, d and Table 5.1).

In field DKF3, the pattern of ^{137}Cs inventories is quite different, with relatively high inventories in the first 3 pits followed by a sharp drop to pit 4. While at first view this appears unusual, it is consistent with the field topography (Figure 4.2) that shows the upper part of the field has a low slope angle, whereas, profile 4 occurs on a steep section just below what may have been another former bund. There is no evidence of significant deposition in this field (Figure 5.4a). As discussed in section 4.3, the ^{137}Cs inventories observed in the reference fields of Site 1 are low compared to the value predicted based on rainfall and latitude (1685 Bq m^{-2}) for this study region. The ^{137}Cs activity profiles (Figure 5.4e and Table 5.1) show rapid decline with depth and very low activities. Therefore, it seems likely that, although level, these fields may have subject to disturbance through human activity since the period of maximum fallout. This may have been associated with deliberate levelling for cultivation.

SOC

In DKF1, although the broad pattern of SOC variation is similar to ^{137}Cs variation, it is noticeable that absolute variation in SOC is lower (maximum is twice minimum) compared to ^{137}Cs (maximum is 4 times minimum). Furthermore, the differences in ^{137}Cs between pits 3 and 4, which were attributed to the former presence of a bund, are not reflected in SOC inventories (Table 5.1 and Figure 5.1b,e and h). The SOC

concentration was lower at the upslope sampling points (P1, P2, P3, P4 and P5), concentrated in the top 30 cm with a sharp decline with depth thereafter. In the deposition slope samples (P6) SOC was abundant in the top 30 cm, however, in this instance there was no sharp decline in SOC with increasing depth (Figure 5.3b). In DKF2, the clear differences between P5 and P1-4 in ^{137}Cs activity in the upper 30 cm is not seen in SOC concentrations, although the SOC inventory in the 0-10 cm increment in P5 is 50% larger than in P1-4 (Figure 5.3f). In field DKF3 the distinctive pattern of ^{137}Cs inventories is not reflected in the SOC inventories, which show relatively little variation along the slope (Figure 5.4.b and Table 5.1). Although the reference fields of Site 1 are clearly depleted in ^{137}Cs , their SOC concentrations and inventories are similar to those seen on the eroded sites (Figure 5.4f and Table 5.1).

Total N

In general, the patterns of lateral variation in total N are similar to those seen in total C and, therefore, the relationships with soil redistribution are similar. In field DKF1 total N concentrations were lower at the eroding profiles (P1-P5) of upslope positions and more concentrated in the top soil increments up to 30 cm. At depths below 30 cm in eroding positions there was a decline in concentration, compared to downslope deposition profile (P6) that had relatively high concentrations up to 50 cm depth with no sharp decline in increments below 50 cm depth (Figure 5.3c). However, in field DKF2, the total N concentration of eroding (P1-P4) and deposition (P5) profiles showed no clear difference (Figure 5.3g). In field DKF1, total N inventories in eroding upslope profiles were significantly lower ($p < 0.05$) than in the deposition downslope profile P6 (Figure 5.1c and Table 5.1). In DKF2, no clear decline in total N inventories along the slope transect was observed (Figure 5.1f and Table 5.1). In field DKF3 there is relatively little variation in total N inventories along the slope with only P3, just upslope of the steep section, having an elevated inventory (Figure 5.1i and Table 5.1). The N depth profiles in the reference fields are fairly consistent and similar to those seen in the other fields, despite the suggestion that these fields may have been disturbed total N (Table 5.1 and Figure 5.4g).

C:N ratio

In fields DKF1, the C:N ratio of the soil for highly eroding upslope profile P1 was higher than all other profiles (P2-P6) over the entire depth (Figure 5.3d). At all other profiles

(P2-P6) no clear difference were observed. In Field DKF3, higher C:N ratios were also evident in the upper depth increments of the eroding profiles (P1-P2). In contrast, in field DKF2 almost the opposite pattern was observed, with eroding upslope profiles (P1-P4) having a narrower C:N ratio than down slope deposition profile (P5) in the entire soil depth (Figure 5.3h). In the three profiles from the reference fields of Site 1, the C:N ratio is very similar over the upper 30 cm (Figure 5.4h) although the profiles diverge below this.

Total and Organic P (and C:OP ratio)

In field DKF1, OP concentrations (Figure 5.5a) were lower at the midslope profile (P3), but in this field highly eroding upslope profile (P1) and deposition downslope profile (P6) had similar OP concentrations in top increment, but deeper depth increments at the deposition profile (P6) had relatively increased OP concentration. The OP inventories in at erosion profiles (P1 and P3) were significantly lower ($p < 0.05$) than at the deposition profile (P6) (Figure 5.2a and Table 5.1). P3 was located at the mid slope position, but was poor in nutrients compared to upslope highly eroding profiles. In fields DKF1, TP concentrations (Figure 5.5b) were lower at eroding profiles (P3) of mid slope position but in this field highly eroding profile (P1) and deposition profile (P6) were similar in TP concentrations over the entire depth of the profiles. TP inventories (Figure 5.2b and Table 5.1) in erosion profiles (P1 and P3) was significantly lower ($p < 0.05$) than in the deposition profile (P6). In field DKF1, C:OP ratio (Figure 5.5c) was less at eroding profile (P1) than deposition profile (P6) in the top 20 cm depth increment, but below that all profiles had similar C:OP ratios. Particularly at top layer of P3 looks very wider C:OP ratio.

In fields DKF2, OP concentrations (Figure 5.5d) were lower at the upslope profile (P1) compared with the mid slope (P3) and deposition profile (P5) which were similar in significantly lower. In fields DKF2 TP concentration (Figure 5.5e) were lower at eroding profile (P1) and deposition profile (P6) which were similar at the entire soil depth, compared to the mid slope profile (P3) that contained more TP. OP and TP inventories in erosion profiles (P1 and P3) were significantly lower ($p < 0.05$) than respective inventories in the deposition profile (P5) (Figure 5.2c, d and Table 5.1). In field DKF2 C:OP ratio (Figure 5.5f) was similar in the top 10 cm increment of all profiles, but after that P1 and P5 were similar and P3 had wider C:OP ratio

Table 5.1 Total Inventory of ^{137}Cs , SOC, total N, OP and TP to 50 cm soil depth along the slope transects at Site 1 (DKF1, DKF2, DKF3 and DK Ref fields), For each profile $n = 3$, differences in inventories were tested by one way Anova at $p = 0.05$, significant sub-sets are denoted. CV is the coefficient of variation in total inventory of three replicates (soil pit faces). Mean values \pm SE are presented

Pits of DKF1	^{137}Cs Inventory (Bq m ⁻²)	CV %	SOC Inventory (kg m ⁻²)	CV %	TN Inventory (kg m ⁻²)	CV %	OP Inventory (kg m ⁻²)	TP Inventory (kg m ⁻²)
P1	562 \pm 23a	7.0	3.01 \pm 0.06a	3.0	0.22 \pm 0.01a	6.0	0.074b	0.130a
P2	923 \pm 23b	4.0	3.75 \pm 0.01b	0.3	0.34 \pm 0.01b	7.0		
P3	1352 \pm 63c	8.0	3.51 \pm 0.06ab	3.0	0.31 \pm 0.01b	4.0	0.066a	0.106b
P4	514 \pm 21a	7.0	3.65 \pm 0.10b	5.0	0.32 \pm 0.00b	2.0		
P5	561 \pm 19a	6.0	4.57 \pm 0.16c	6.0	0.39 \pm 0.01bc	6.0		
P6	2065 \pm 117d	10.0	5.39 \pm 0.21d	7.0	0.46 \pm 0.02c	8.0	0.111c	0.173c

Pits of DKF2	^{137}Cs Inventory (Bq m ⁻²)	CV %	SOC Inventory (kg m ⁻²)	CV %	TN Inventory (kg m ⁻²)	CV %	OP Inventory (kg m ⁻²)	TP Inventory (kg m ⁻²)
P1	265 \pm 49a	32	2.86 \pm 0.22a	13	0.34 \pm 0.03a	13	0.05a	0.11a
P2	613 \pm 56a	16	4.17 \pm 0.08b	3	0.41 \pm 0.01ab	6		
P3	668 \pm 125a	32	2.20 \pm 0.28a	22	0.24 \pm 0.02a	17	0.03a	0.09a
P4	641 \pm 80a	22	3.70 \pm 0.20ab	9	0.41 \pm 0.07ab	29		
P5	1794 \pm 150b	15	4.51 \pm 0.16b	6	0.39 \pm 0.02ab	10	0.09b	0.15b

Pits of DKF3	^{137}Cs Inventory (Bq m ⁻²)	CV %	SOC Inventory (kg m ⁻²)	CV %	TN Inventory (kg m ⁻²)	CV %
P1	1274 \pm 285	39.0	3.75 \pm 0.10	5.0	0.33 \pm 0.005	2.0
P2	966 \pm 81	15.0	4.09 \pm 0.13	5.0	0.34 \pm 0.008	4.0
P3	906 \pm 54	10.0	4.12 \pm 0.33	14.0	0.44 \pm 0.082	32.0
P4	173 \pm 45	45.0	3.57 \pm 0.13	6.0	0.38 \pm 0.006	2.0
P5	311 \pm 93	52.0	3.61 \pm 0.05	2.0	0.37 \pm 0.013	6.0
P6	579 \pm 72	21.0	2.93 \pm 0.08	4.0	0.36 \pm 0.013	6.0

Pits of DK Ref	^{137}Cs Inventory (Bq m ⁻²)	CV %	SOC Inventory (kg m ⁻²)	CV %	TN Inventory (kg m ⁻²)	CV %
Ref 1	306 \pm 58	32.0	3.37 \pm 0.11	5.0	0.33 \pm 0.010	5.0
Ref 2	575 \pm 105	32.0	3.71 \pm 0.22	10.0	0.38 \pm 0.043	19.0
Ref 3	695 \pm 56	14.0	3.71 \pm 0.10	5.0	0.39 \pm 0.058	26.0

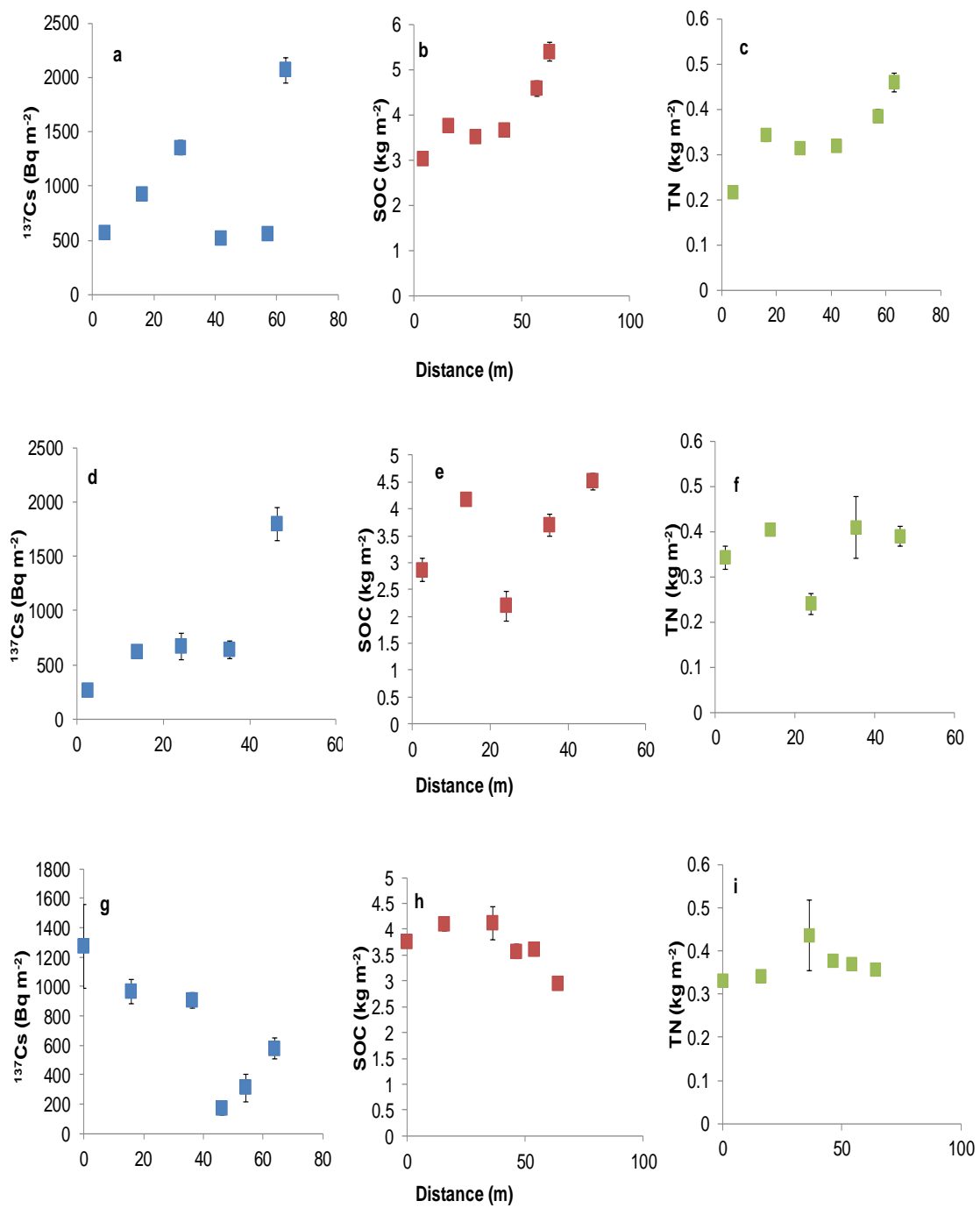


Figure 5.1 Total Inventory of ^{137}Cs , SOC, and total N to 50 cm soil depth at profiles along a slope transect within field of Site 1 (DKF1:a-c , DKF2: d-f and DKF3: g-i), For each profile $n = 3$ and the error bars reflect standard error.

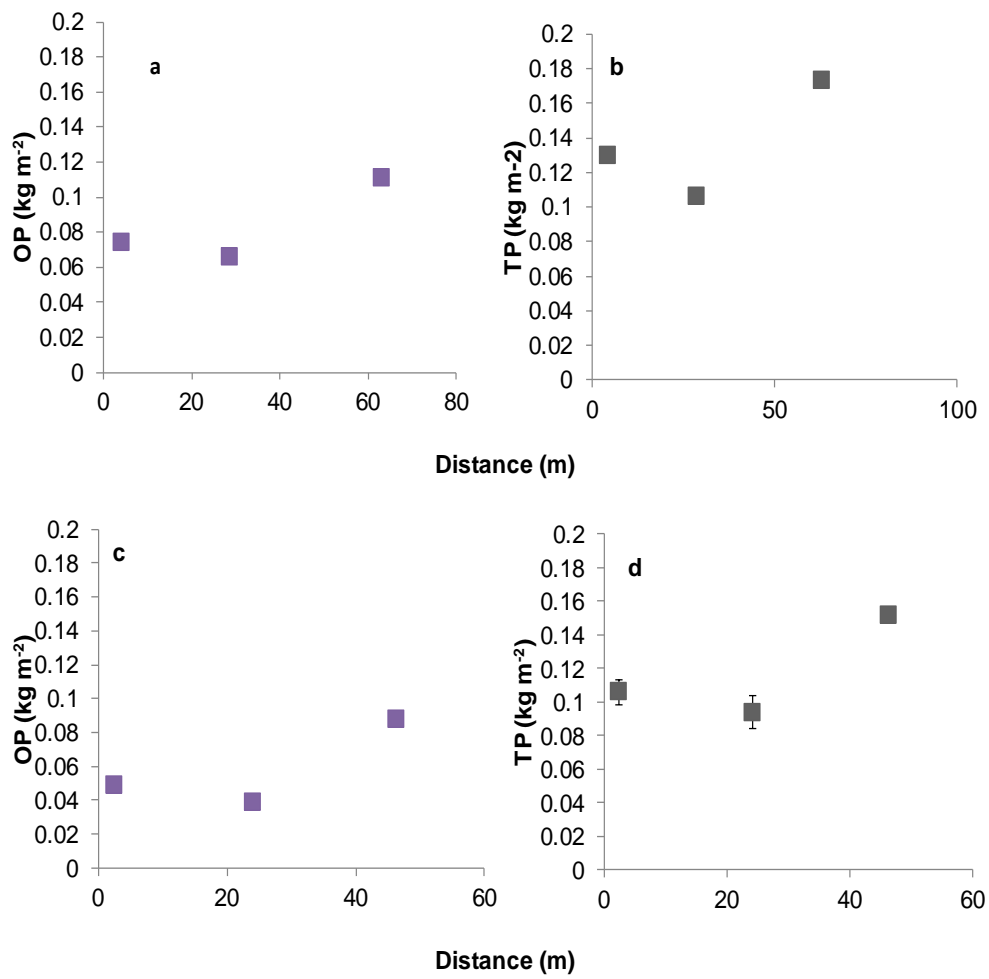


Figure 5.2 Total Inventory of OP and TP to 50 cm soil depth at profiles along a slope transect within field of Site 1 (DKF1: a-b, and DKF2: c-d), P analysed as a composite sample of each depth layer.

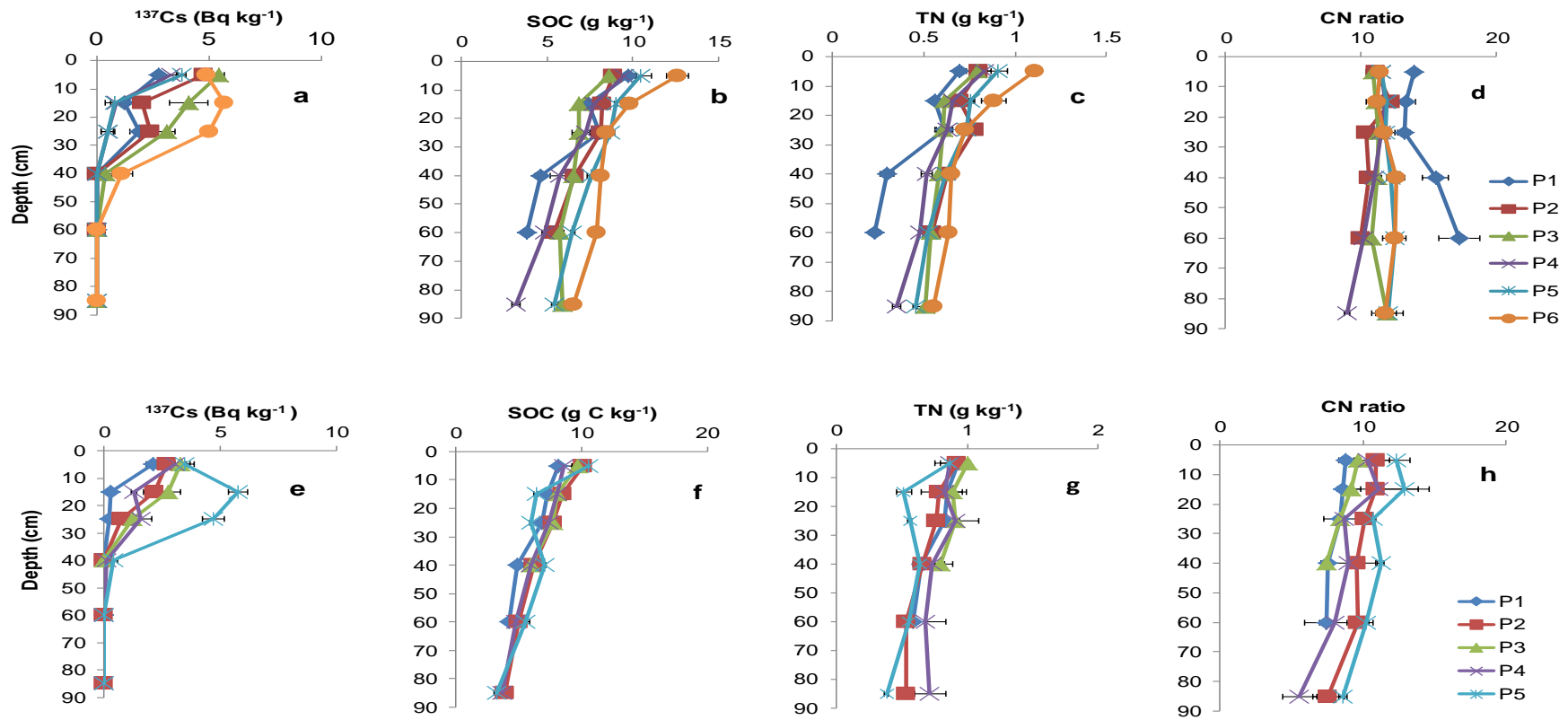


Figure 5.3 Vertical distributions of ^{137}Cs , SOC, total N and C: N in soil profiles along the slope transects within field Site 1 (DKF1: a-d, and DKF2: e-h). Error bars are \pm SE ($n = 3$).

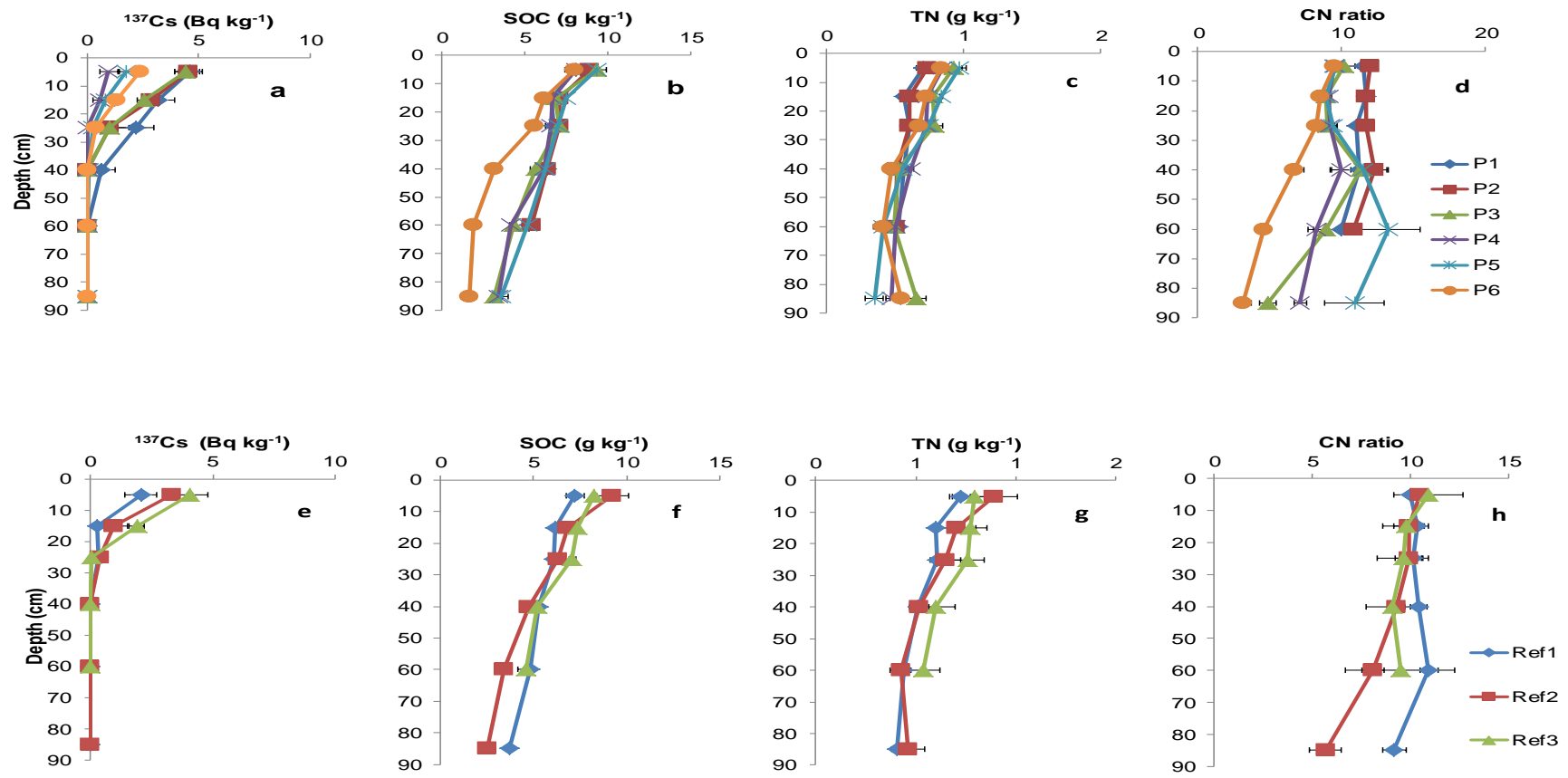


Figure 5.4 Vertical distributions of ^{137}Cs , SOC, total N and CN ratio in soil profiles along the slope transects within field Site 1 (DKF3: a-d, and DK Ref: e-h). Error bars are \pm SE ($n = 3$).

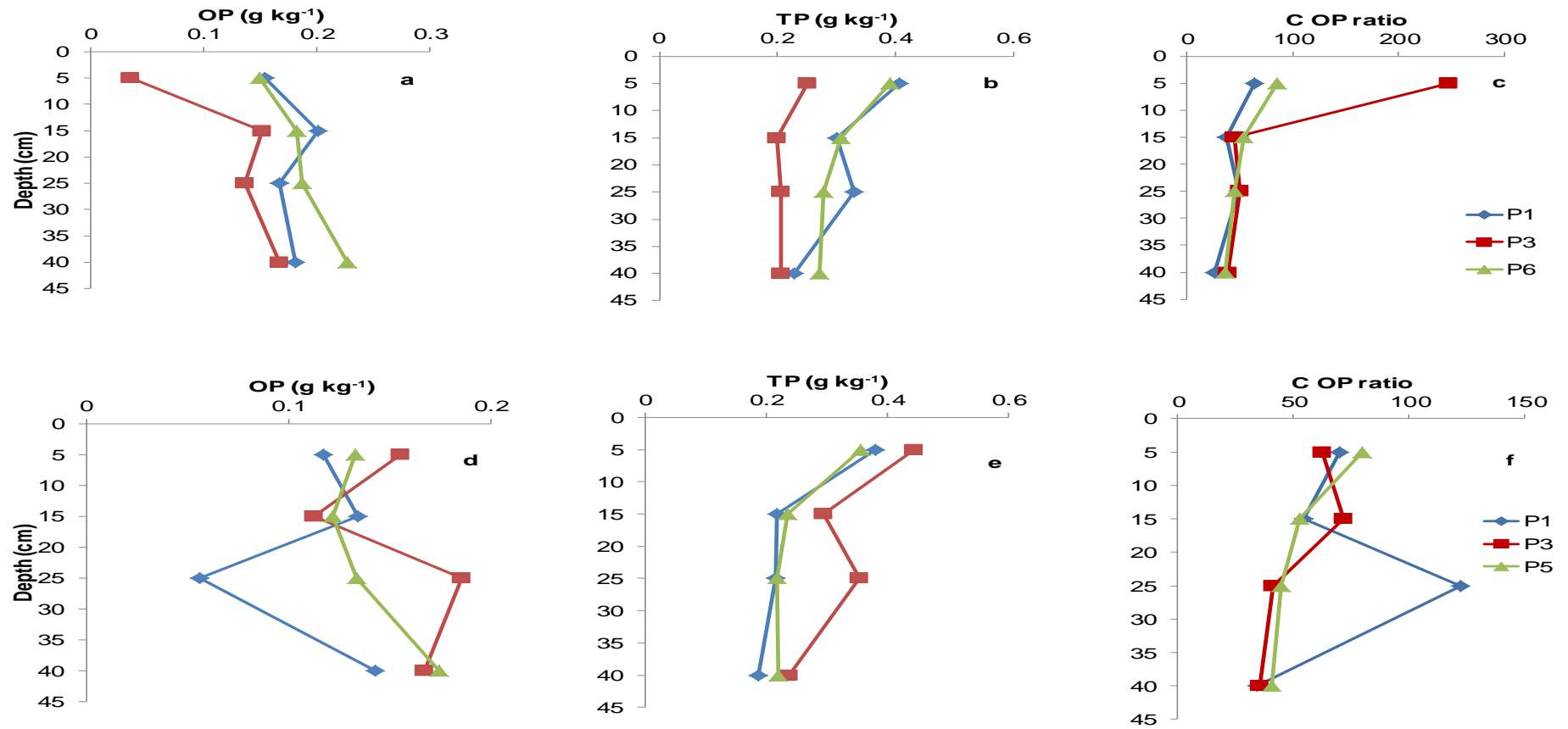


Figure 5.5 Vertical distributions of OP, TP and CP ratio in profiles in Site 1 (DKF1: a-c, and DKF2: d-f). Each depth layer made it into composite and analysed up to 50 cm



Figure 5.6 Field bund structure marked in image

5.3.3 Vertical and lateral distribution of ^{137}Cs , SOC, N and P at Site 2

^{137}Cs

At Site 2, fields PSF2 and PSF3 show similar patterns of ^{137}Cs inventories to DKF1 at Site 1. As in the latter field, the patterns suggest that there may have been a bund or other barrier between pits 3 and 4 in the past. Field PSF1 has a different pattern with only 1 pit with a low inventory and 4 pits showing high inventories consistent with net deposition. It is important to note that this field lies at a lower elevation on the ridge, where Site 2 is located, and may receive soil eroded from fields upslope (including PSF2 and PSF3). There was lower level of activity and lower depth penetration at the upslope low inventory profiles, with maximum activity found up to 30 cm. Whereas in the high inventory downslope profiles (especially pit 6 in PSF2 and pits 2-6 in PSF1), the maximum activity was evident up to 50 cm depth (Figure 5.9a, e and 5.10a and Table 5.2), confirming the redistribution of eroded material to the lower slopes within the study area. Overall the ^{137}Cs inventories within the site showed clear statistically significant differences ($p < 0.05$) between topographic locations significantly lower (Figure 5.7a,d, g and Table 5.2). The inventories and depth distributions from the reference sampling locations show that Ref 2 is unlike Ref 1 and Ref 3. Ref 2 is depleted in ^{137}Cs throughout the profile and cannot be considered to be a reliable reference profile (Figure 5.10e and Table 5.1). In contrast, Ref 1 and Ref 3 have similar profiles and inventories up to 50 cm depth ($1335 \pm 88 \text{ Bq m}^{-2}$ and $1194 \pm 71 \text{ Bq m}^{-2}$, respectively) and although these inventories are lower than the expected predicted fallout for the area (1685 Bq m^{-2}) they appear to be relatively stable sites. This has informed the choice of reference inventories used in the sensitivity analysis (section 6.2.4).

SOC

In contrast to the limited relationship between SOC and ^{137}Cs seen at Site 1 (DK), at Site 2 the broad trends in ^{137}Cs inventories are seen in all fields in the SOC inventories, with a strong tendency for SOC to increase down-field. In field PSF1, SOC concentrations were lower at the eroding profile (P1) of upslope position and more concentrated in the top layer up to 10 cm. Below 10 cm there was a sharp decline in concentration, compared to the downslope slope profile (P2-P6) (Figure 5.9b) where SOC concentrations were increased up to 30 cm depth with no sharp decline in SOC

concentration in deeper soil increments. In this field the top 0-10 cm had similar SOC concentrations along the slope transect at all profiles from eroding to deposition but deeper soil increments had higher SOC concentrations in deposition profiles. SOC inventory along slope (Figure 5.7b and Table 5.2) showed that the upslope profile (P1) had significantly lower SOC inventories ($P < 0.05$) than the other profiles (P2-P6).

In field PSF2, the SOC concentration of the top 10 cm increment at eroding upslope profiles (P1-P2) was similar to that seen in deposition mid and downslope (P3-P7) profiles. Deeper soil increments of eroding profiles had less SOC concentrations than deposition profiles (Figure 5.9f). Profile 5 located downslope is clearly differentiated by SOC concentration compared with the eroding profiles upslope. SOC concentrations increased in deposition profiles indicates the redistribution of eroded material redeposited at bottom and lower slope position within the field. SOC inventories along the slope (Figure 5.7e and Table 5.2) transect within field showed that highly eroding upslope profiles (P1-P2) had significantly lower SOC ($p < 0.05$) than deposition (mid and downslope) profiles (P3-P7).

As in the other fields at this site, in field PSF3 SOC concentration in the top 10 cm increment of the upslope (P1), mid and downslope (P3-P6) profiles were similar, with deeper depths of the eroding upslope profile containing less SOC than the downslope deposition profile (Figure 5.10b). SOC concentration is increased in deposition profiles indicating redistribution of eroded material redeposited at bottom and lower slope position of within field. The SOC inventories along (Figure 5.7h and Table 5.2) the slope transect, again show eroding upslope profiles (P1-P2) to be significantly lower depleted in SOC ($p < 0.05$) compared to deposition, mid and downslope profiles (P3-P6). For Site 2, the ^{137}Cs profiles from Ref 1 and Ref 3 are very similar but Ref 2 appeared to have been disturbed (Figure 5.10f). The total SOC inventory (Table 5.2) up to 50 cm depth in Ref 1 was $3.90 \pm 0.20 \text{ kg m}^{-2}$, Ref 2 was $5.47 \pm 0.68 \text{ kg m}^{-2}$ for Ref 3 was $3.49 \pm 0.43 \text{ kg m}^{-2}$.

Total N

As at Site 1, the patterns of lateral variation in total N are similar to those seen in total C and, therefore, the relationships with soil redistribution are similar. In field PSF1, profiles P1 and P2 differ markedly from profiles P3-P6, which are all similar. The total N concentrations were lower at the eroding profile (P1) at the upslope position and more concentrated top soil increment up to 10 cm followed by a sharp decline of

concentration at lower depth increments. Although P2 was at a depositional location, based on the high ^{137}Cs inventory there and the deep ^{137}Cs penetration, it has low total N concentrations, comparable to P1 over the upper 30 cm. The remaining the depositional profiles (P3-P6) have higher total N concentrations up to 30 cm depth and no sharp decline in total N concentration below that (Figure 5.9c). Total N inventories in eroding P1 and depositional P2 were not significantly different from each other but are both significantly lower ($p < 0.05$) than the inventories in the other profiles (P3-P6). In field PSF2, total N concentrations in the top 30 cm increments of eroding upslope P1-P2 and downslope depositional P3-P7 profiles were similar, but at depths below that the total N concentration at eroding profiles was lower than in the deposition profiles (Figure 5.9g). P5 located at the depositional site was clearly differentiated based on its total N concentration compared with eroding profiles. The total N inventories (Figure 5.7f and Table 5.2) of the eroding upslope profiles (P1-P2) were significantly lower ($p < 0.05$) than those in the deposition profiles (P3-P7).

In field PSF3, total N concentration (Figure 5.10c) was similar from eroding to deposition profiles but was slightly enriched at deposition profiles (P6). Total N inventories (Figure 5.7i and Table 5.2) within erosion profiles (P1-P4) were significantly lower ($p < 0.05$) than in deposition downslope slope profiles (P5-P6). For Site 2 the reference field total N concentration (Figure 5.10g) total N inventories (Table 5.2) up to 50 cm depth were: Ref 1 ($0.30 \pm 0.008 \text{ kg m}^{-2}$), Ref 2 ($0.41 \pm 0.050 \text{ kg m}^{-2}$) and Ref 3 ($0.27 \pm 0.022 \text{ kg m}^{-2}$).

C:N ratio

In field PSF1, the C:N ratio (Figure 5.9d) for highly eroding profile P1 was higher than all other profiles (P2-P6) in the entire soil depth and the absolute values are very high. In profile P2, the C:N ratio is wider than in the other depositional profiles (P3-P6) and is more similar to eroding profile P1. For all other depositional profiles (P3-P6), no clear differences were observed. In field PSF2 (Figure 5.9h) almost opposite pattern was observed, with highly eroding profiles (P1) found to have narrower C:N ratios than other profiles (P2-P7) in entire soil depth along slope transect. In PSF3, the C:N ratio showed a similar pattern to PSF2 (Figure 5.10d). Eroding profiles (P1 and P2) were found to have narrower C:N ratios than other profiles in entire depth profile along slope transect. Site 2 reference profiles looks similar C:N ratio for Ref 1 and Ref 3 but Ref 2 looks abnormal (Figure 5.10h).

Total and Organic P (and C:OP ratio)

In field PSF1, OP concentrations (Figure 5.11a) were lower at eroding upslope profile (P1) than midslope (P3) and downslope profiles (P6). The OP inventory in erosion profile (P1) was significantly lower ($p < 0.05$) than in downslope profile (P6) and equal to mid slope P3 (Figure 5.8a and Table 5.2). In field PSF1 TP concentrations (Figure 5.11b) were lower at eroding upslope profiles (P1) than mid slope (P3) and deposition profile (P6). The TP inventory in erosion profile (P1) was significantly lower ($p < 0.05$) than mid-slope (P3) and deposition profiles (P6) (Figure 5.8b and Table 5.2). In field PSF1, the C:OP ratio (Figure 5.11c) was lower at eroding profiles (P1) than mid (P3) and deposition profiles (P6) below 10 cm depth, but the top 10 cm depth increment of all profiles had similar C:OP ratios.

In field PSF2 OP concentrations (Figure 5.11d) were lower at the eroding upslope profile (P1) than the mid slope (P3) and deposition profiles (P7). However, the mid slope profile had increased OP concentrations compared to other profiles. The OP inventory in erosion profile (P1) was significantly lower ($p < 0.05$) than mid and deposition profile (P7) (Figure 5.8c and Table 5.2). In field PSF2, TP concentrations (Figure 5.11e) were lower at mid slope profile (P3) than eroding slope (P1) and deposition profiles (P7). Though eroding profile P1 and deposition (P7) profile TP concentrations were similar for the top 20 cm increment, soil below that increment in the deposition profile contained more TP than others. The TP inventory in erosion profile (P1) was significantly lower ($p < 0.05$) than mid (P3) and deposition profiles (P7) (Figure 5.8d and Table 5.2). In field PSF2, the C:OP ratio (Figure 5.11f) was less at mid (P3) and deposition profiles (P7) than eroding (P1) profile. Eroding profile seems to have wider C: OP ratio than other profiles.

In field PSF3, OP concentrations (Figure 5.12a) were lower at eroding upslope profile (P1) than mid slope (P4) and deposition profiles (P6). The OP inventory in erosion profile (P1) was significantly lower ($p < 0.05$) than in deposition profile (P6) but equal to mid slope profile P4 (Figure 5.8e and Table 5.2). In field PSF3 TP concentrations (Figure 5.12b) were lower at eroding (P1) and mid slope profiles (P4) than deposition profile (P6). The TP concentration over the whole depth of the deposition profile was higher than seen in other profiles. The TP inventory in erosion profiles (P1) was significantly lower ($p < 0.05$) than in the deposition profile (P6) but equal to the mid

slope profile (Figure 5.8f and Table 5.2). In field PSF3, the C:OP ratio (Figure 5.12c) was similar in the top 10 cm increment of all profiles but after that the ratio was lower in the eroding profile than in the deposition and mid slope profiles.

Site 2 reference OP inventory (Table 5.2) for Ref 1 is 0.06 and Ref 3 is 0.08 (kg m^{-2}) and TP inventory Ref 1 is 0.15 and Ref 3 is 0.20 kg m^{-2} . The OP and TP concentrations and C:OP ratio for reference profile from Site 2 are presented in Figure 5.12d,e and f.

Table 5.2 Total Inventory of ^{137}Cs , SOC, total N, OP and TP to 50 cm soil depth along the slope transects at Site 2 (PSF1, PSF2, PSF3 and PS Ref fields). For each profile $n = 3$, differences in inventories were tested by one way Anova at $p = 0.05$, significant sub-sets are denoted. CV is the coefficient of variation in total inventory of three replicates (soil pit faces). Mean values \pm SE are presented.

Pits of PSF1	^{137}Cs Inventory (Bq m ⁻²)	CV %	SOC Inventory (kg m ⁻²)	CV %	TN Inventory (kg m ⁻²)	CV %	OP Inventory (kg m ⁻²)	TP Inventory (kg m ⁻²)
P1	260 \pm 48a	32.0	3.54 \pm 0.25a	12.0	0.19 \pm 0.02a	19.0	0.10a	0.19a
P2	2038 \pm 36b	3.0	5.13 \pm 0.13b	4.0	0.29 \pm 0.06a	35.0		
P3	2447 \pm 126c	9.0	5.45 \pm 0.22b	7.0	0.45 \pm 0.02b	10.0	0.12ab	0.24b
P4	2146 \pm 109bc	9.0	7.39 \pm 0.19c	4.0	0.54 \pm 0.01b	5.0		
P5	1999 \pm 63b	5.0	7.61 \pm 0.16c	3.0	0.56 \pm 0.03b	9.0		
P6	2127 \pm 16bc	1.0	7.99 \pm 0.35c	8.0	0.62 \pm 0.02bc	4.0	0.20b	0.36c

Pits of PSF2	^{137}Cs Inventory (Bq m ⁻²)	CV %	SOC Inventory (kg m ⁻²)	CV %	TN Inventory (kg m ⁻²)	CV %	OP Inventory (kg m ⁻²)	TP Inventory (kg m ⁻²)
P1	674 \pm 68 a	18.0	1.88 \pm 0.10a	9.0	0.19 \pm 0.009a	8.0	0.03a	0.10a
P2	1061 \pm 44ab	7.0	2.57 \pm 0.13a	8.0	0.22 \pm 0.012a	10.0		
P3	1316 \pm 171b	22.0	3.54 \pm 0.02b	1.0	0.28 \pm 0.011ab	7.0	0.10b	0.16b
P4	1922 \pm 41c	4.0	5.07 \pm 0.14c	5.0	0.36 \pm 0.007c	3.0		
P5	1483 \pm 112bc	13.0	7.19 \pm 0.06e	1.0	0.54 \pm 0.018e	6.0		
P6	1803 \pm 27bc	3.0	5.91 \pm 0.13d	4.0	0.48 \pm 0.010ed	3.0		
P7	2067 \pm 215c	18.0	5.76 \pm 0.36cd	11.0	0.46 \pm 0.027d	10.0	0.12c	0.30c

Pits of PSF3	^{137}Cs Inventory (Bq m ⁻²)	CV %	SOC Inventory (kg m ⁻²)	CV %	TN Inventory (kg m ⁻²)	CV %	OP Inventory (kg m ⁻²)	TP Inventory (kg m ⁻²)
P1	416 \pm 62a	26.0	2.84 \pm 0.74a	4.0	0.25 \pm 0.002a	2.0	0.08a	0.15a
P2	990 \pm 173a	30.0	4.08 \pm 0.14a	6.0	0.32 \pm 0.002a	1.0		
P3	1751 \pm 141b	14.0	4.53 \pm 0.29ab	11.0	0.32 \pm 0.014a	8.0	0.11a	0.20ab
P4	1409 \pm 54ab	7.0	4.74 \pm 0.43ab	16.0	0.31 \pm 0.027a	15.0		
P5	1614 \pm 60ab	6.0	5.55 \pm 0.37bc	11.0	0.35 \pm 0.021ab	10.0		
P6	2707 \pm 248c	16.0	5.85 \pm 0.25bc	7.0	0.41 \pm 0.027ab	11.0	0.17b	0.31b

Pits of PS Ref	^{137}Cs Inventory (Bq m ⁻²)	CV %	SOC Inventory (kg m ⁻²)	CV %	TN Inventory (kg m ⁻²)	CV %	OP Inventory (kg m ⁻²)	TP Inventory (kg m ⁻²)
Ref 1	1335 \pm 88	11.0	3.90 \pm 0.20	9.0	0.30 \pm 0.008	5.0	0.06	0.15
Ref 2	625 \pm 232	64.0	5.47 \pm 0.68	21.0	0.41 \pm 0.050	21.0		
Ref 3	1194 \pm 71	10.0	3.49 \pm 0.43	21.0	0.27 \pm 0.022	14.0	0.08	0.20

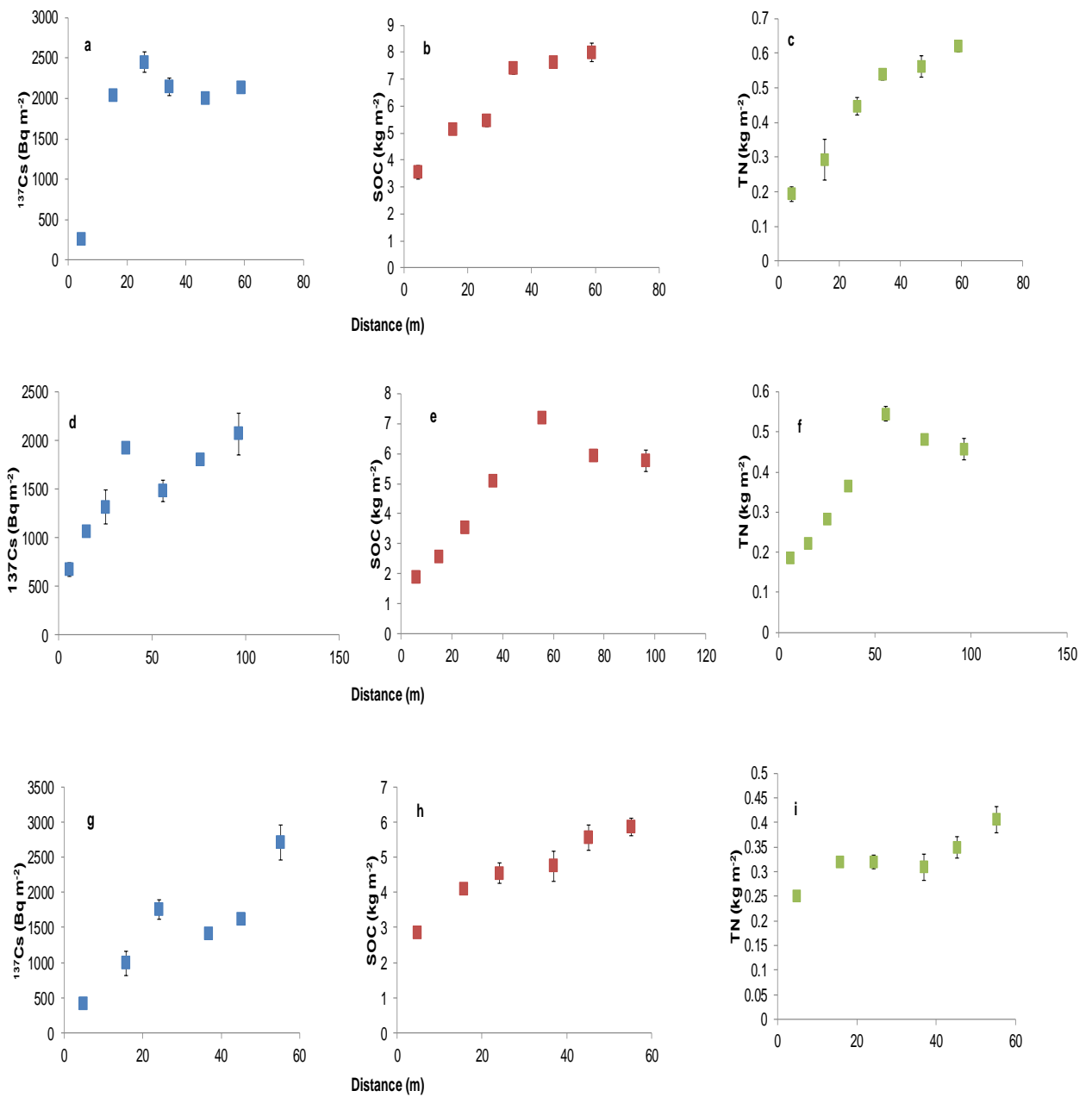


Figure 5.7 Total Inventory of ^{137}Cs , SOC, and total N to 50 cm soil depth at profiles along a slope transect within field of Site 2 (PSF1: a-c, PSF2: d-f, and PSF3: g-i). For each profile $n = 3$ and the error bars reflect standard error.

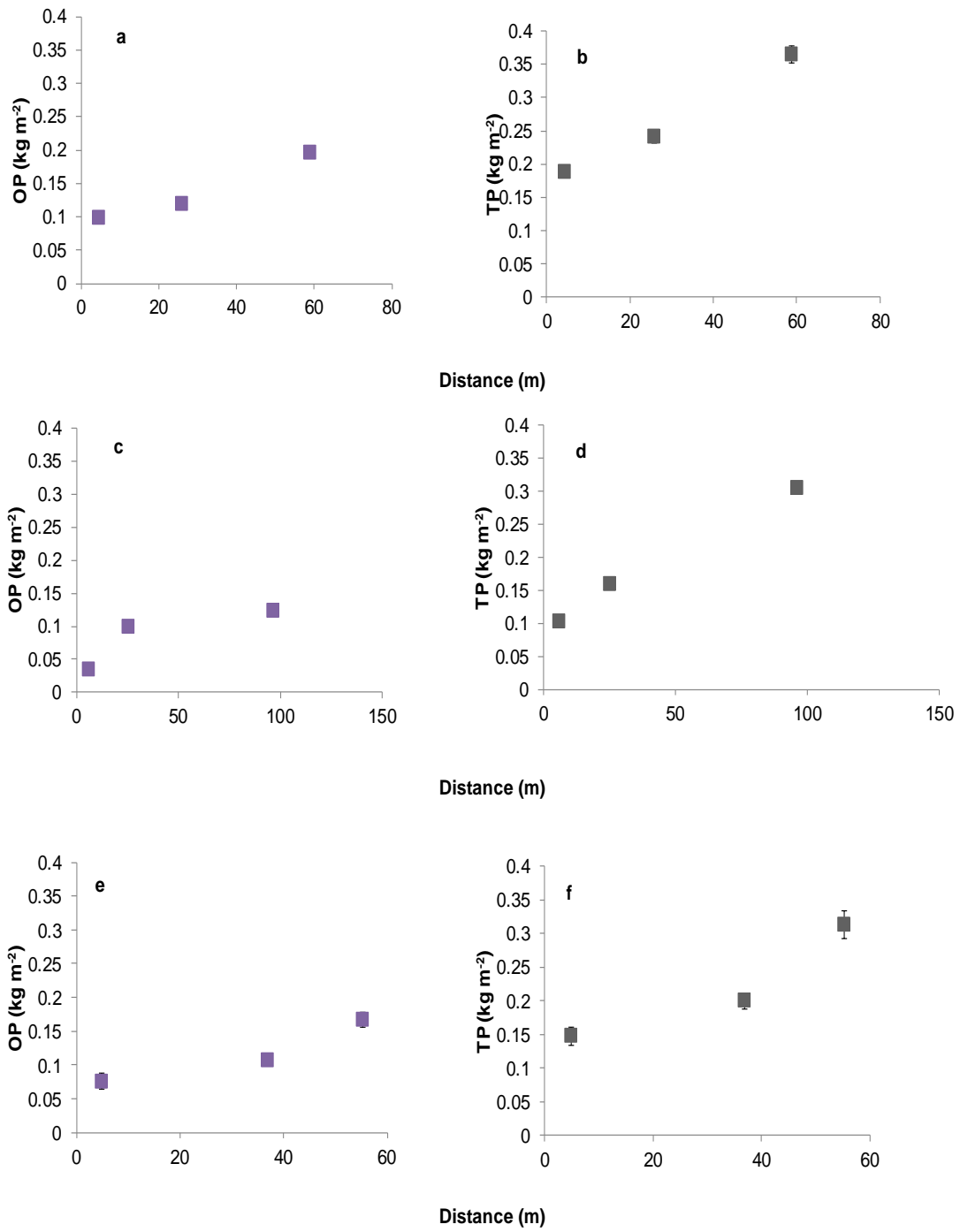


Figure 5.8 Total Inventory of OP and TP to 50 cm soil depth at profiles along a slope transect within field of Site 2 (PSF1: a-b, PSF2:c-d, and PSF3: e-f). P analysed as a composite sample of each depth layer.

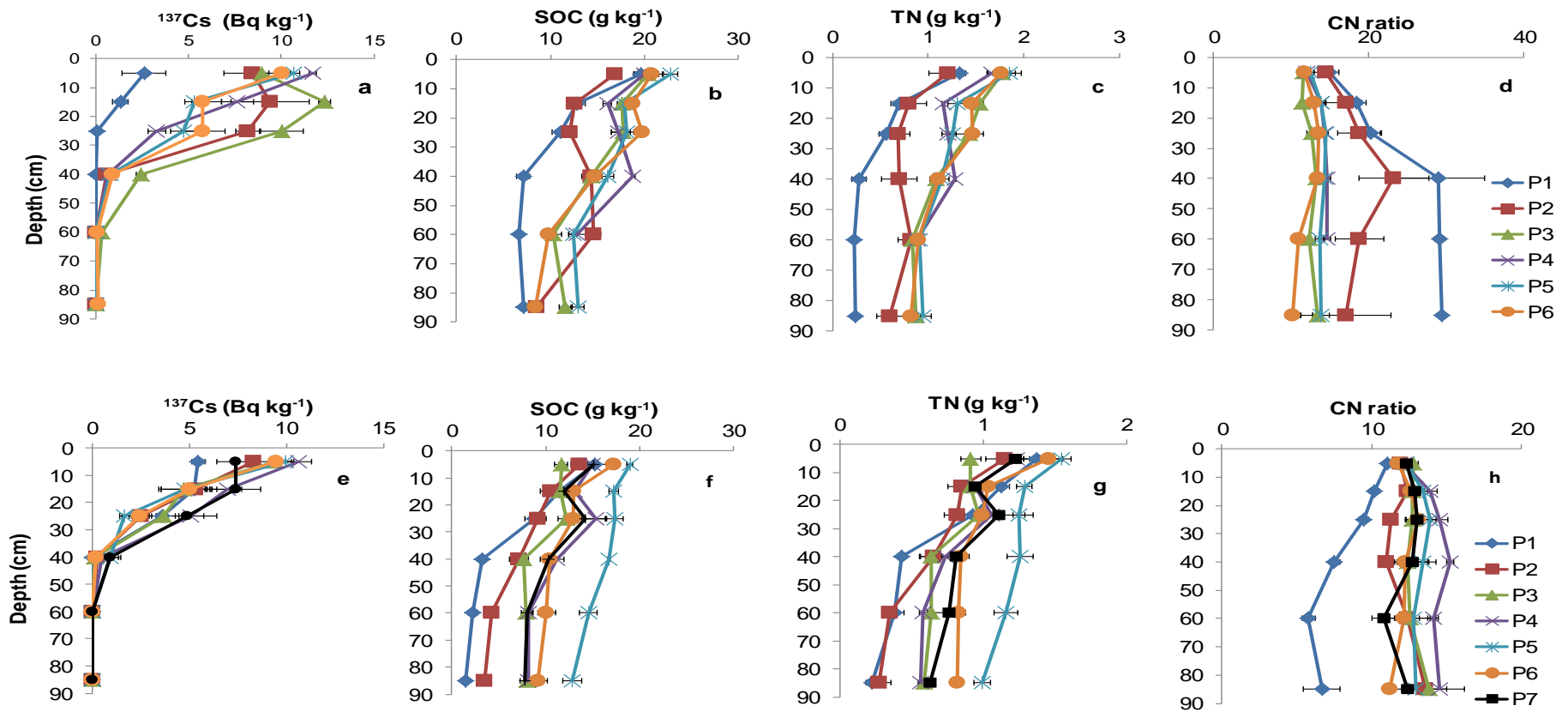


Figure 5.9 Vertical distributions of ^{137}Cs , SOC, total N and C:N in soil profiles along the slope transects within field Site 1 (PSF1: a-d, and PSF2: e-h). Error bars are \pm SE ($n=3$).

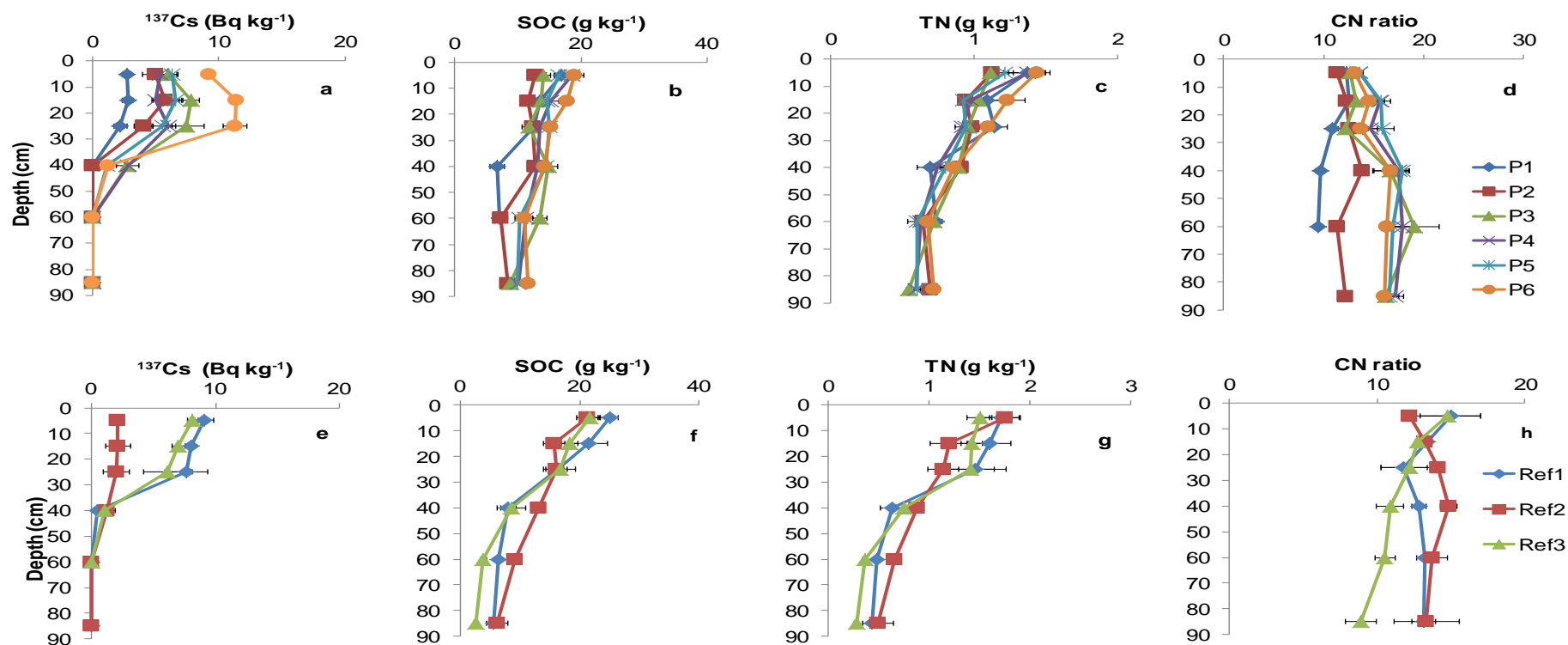


Figure 5.10 Vertical distributions of ^{137}Cs , SOC, total N and C:N in soil profiles along the slope transects within field Site 1 (PSF3: a-d, and PS Ref: e-h). Error bars are \pm SE ($n = 3$).

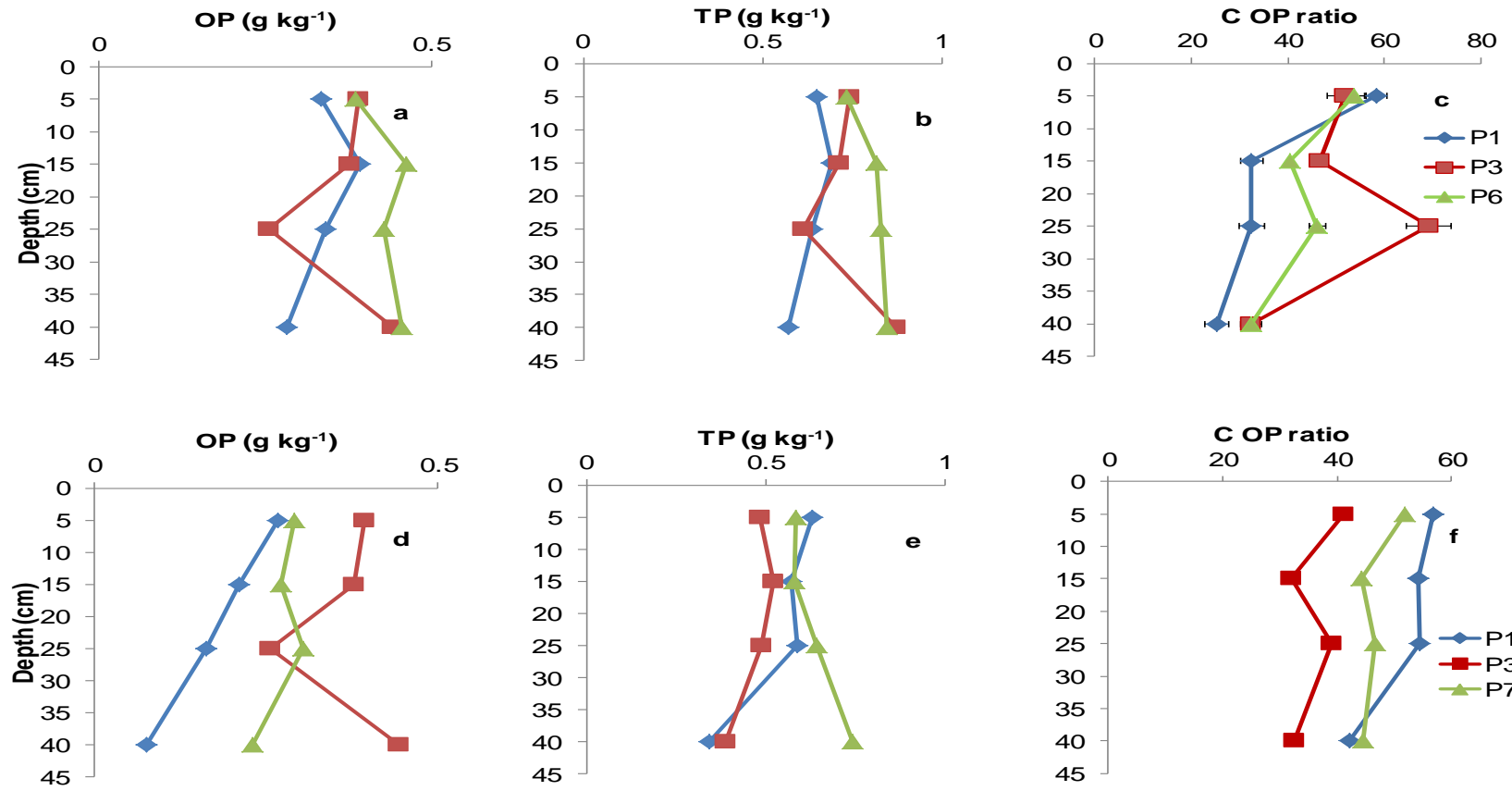


Figure 5.11 Vertical distributions of OP, TP and CP ratio in profiles in Site 2 (PSF1: a-c, and PSF2: d-f). Each depth layer made it into composite and analysed up to 50 cm

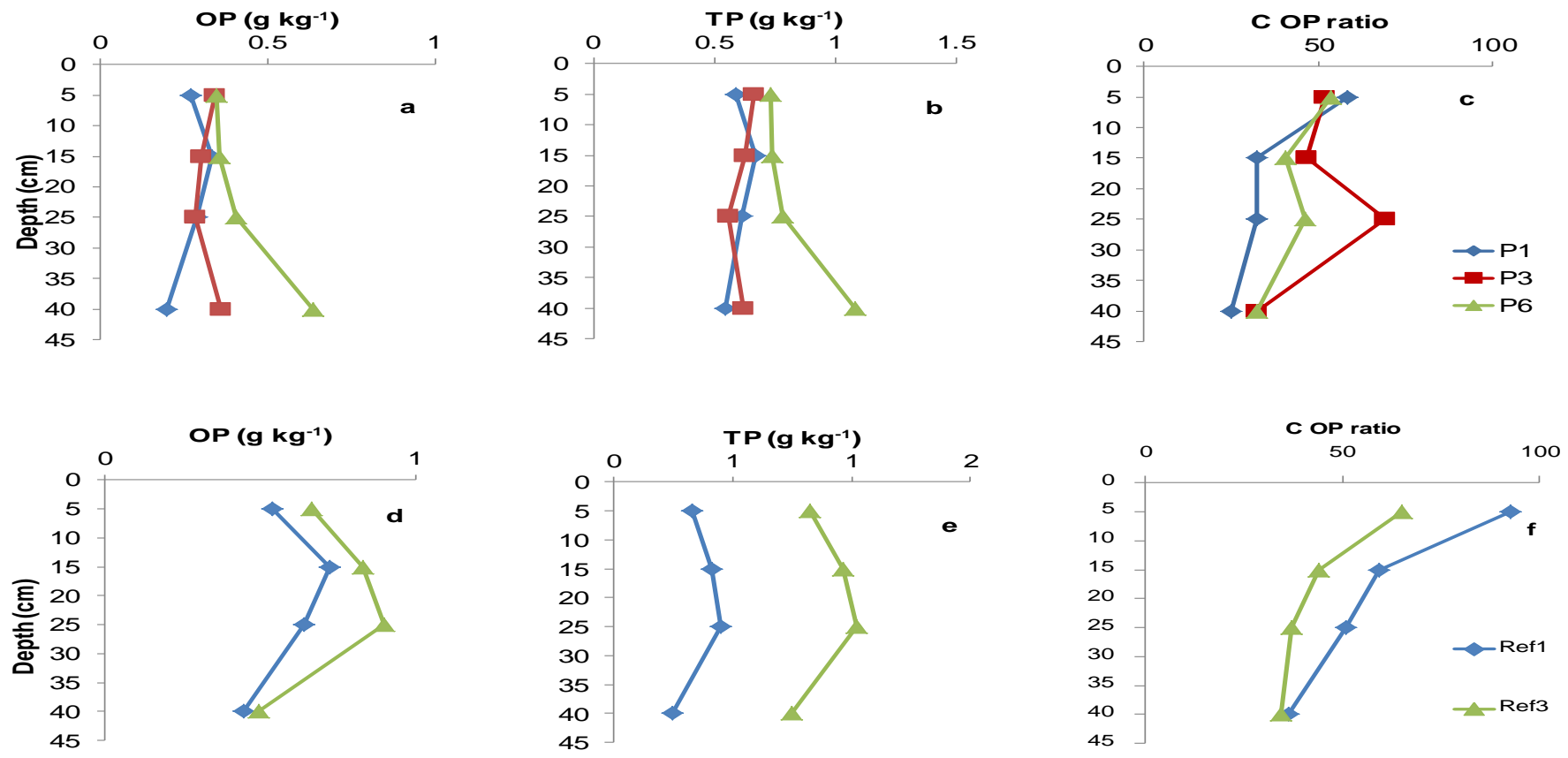


Figure 5.12 Vertical distributions of OP, TP and CP ratio in profiles in Site 2 (PSF3: a-c, and PS Ref: d-f). Each depth layer made it into composite and analysed up to 50 cm

5.3.4 Vertical and lateral distribution of ^{137}Cs , SOC, N and P at Site 3

^{137}Cs

The patterns of ^{137}Cs inventories in all 3 fields at Site 3 are consistent with field topography (Figure 4.2g,h, and i). Each field has a distinct change of slope along the transect and this is reflected in the inventories. Low activity was measured in upslope profiles or those on steep slope sections (probably below a former bund) such as profiles 4 and 5 from BGF2 and profiles 3 and 4 from BGF3. At these maximum activity is observed up to 30 cm. A maximum activity of 30 cm was also observed in BGF2 profile 6, however, this was the maximum soil depth at this location (Figure 5.15a, e). High activities (close to 10 Bq kg^{-1}) were also seen in the pits with high inventories in BGF2 (P6) and BGF3 (P2). The profile distribution of ^{137}Cs at these profiles is consistent with redeposition of eroded material from upslope at these locations on the lower slopes. The BGF1 deposition downslope ^{137}Cs activity was lower than BGF2 which may be due to continuous loss of soil beyond this location because the field is located on steep hills and there was no clear boundary to prevent soil loss, (which is present in BGF2). In BGF1 pit P7 was located at the other corner of the field transect and showed comparatively less activity than the deposition profile (it is also from a location with a slightly higher elevation than P6).

Overall, the ^{137}Cs inventories within Site 3 show statistically significant differences significantly lower ($p < 0.05$) between topographic positions which appear to have been sources of eroded soil and those that have received deposition (Figure 5.13 a, d, g and Table 5.3). The reference field (BG Ref3) of Site 3 have a ^{137}Cs activity (Figure 5.16e and Table 5.3) lower than predicted fallout (1685 Bq m^{-2}) for this study region but close to those seen at Site 2 (BG Ref 1: 1282 ± 63 , BG Ref 2: 1063 ± 33 and BG Ref 3: $799 \pm 40 \text{ Bq m}^{-2}$).

SOC

As at Site 2, the broad trends in ^{137}Cs inventories are seen in all fields in the SOC inventories, with a tendency for SOC to increase down-field. In field BGF1, SOC concentrations were lower at the eroding profile (P1-P5) of upslope and midslope positions and more concentrated in the top soil up to 10 cm depth. Below that there was a sharp decline of concentration, but the deposition down slope profile (P6) had

increased SOC (Figure 5.15b). Although P7 was located at a downslope location, its SOC inventory and concentration reflect the ^{137}Cs pattern and are significantly lower than P6. SOC inventory along the slope transect (Figure 5.13b and Table 5.3) at eroding and mid-slope profiles (P1-P5) are significantly lower ($P < 0.05$) than deposition downslope profile (P6). In field BGF2, SOC concentration was lower at eroding profile (P1-P5) of eroding and mid-slope positions and more concentrated in the top soil up to 10 cm. Below 0-10 cm there was a sharp decline of concentration compared to the deposition (Figure 5.15f) slope profile (P6) which had relatively increased carbon concentrations. SOC inventory along (Figure 5.13d and Table 5.3) slope profiles at eroding and mid-slope positions (P1-P5) were significantly lower ($P < 0.05$) than deposition downslope profile (P6). In field BGF3, SOC concentration (Figure 5.16b) showed a clear pattern along the slope (Figure 5.13h and Table 5.3) transect, but the large difference seen between the upper (P1 and P2) and lower (P3-P5) parts of the field seen in ^{137}Cs activity is not as clear in the SOC data. However, if the data is separated into P1-P2 and P3-P5 then there is a closer fit. For Site 3, there is more variation in the SOC profiles than in the ^{137}Cs profiles, which may indicate that C input or biomass removal rates vary between the reference fields. Total SOC inventory (Table 5.3) up to 50 cm depth was Ref 1 ($8.30 \pm 0.42 \text{ kg m}^{-2}$), Ref 2 ($5.63 \pm 0.17 \text{ kg m}^{-2}$) and Ref 3 ($3.36 \pm 0.13 \text{ kg m}^{-2}$).

Total N

As at Sites 1 and 2, the patterns of lateral variation in total N are broadly similar to those seen in total C and, therefore, the relationships with soil redistribution are similar. In field BGF1, total N concentrations were lower at eroding profile (P1-P5) of upslope positions and more concentrated in the top soil increment up to 10 cm depth, after which there was a sharp decline of concentration, apart from deposition downslope profile (P6) which had increased total N concentrations (Figure 5.15c). Although P7 was located in the deposition profile, it did not have a large total N concentration, possibly reflecting its location at a field boundary susceptible to soil loss by runoff. Total N inventories (Figure 5.13c and Table 5.3) from eroding profiles (P1-P5) were again significantly lower ($p < 0.05$) than the inventory of the deposition downslope profile (P6). In field BGF2, total N concentrations were lower at the eroding profile (P1-P5) of upslope positions and more concentrated in the top soil increment up to 10 cm depth, with a sharp decline of concentration below that. The deposition slope

profile (P6) had comparatively increased total N concentrations (Figure 5.15g). As in BGF1, there was a statistically ($p < 0.05$) significant difference in total N inventory (Figure 5.13f and Table 5.3) between eroding profiles (P1-P5) and the depositional profile (P6). In field BGF3, total N concentration (Figure 5.16c) is easier to interpret when data are separated into two distinct areas, P1-P2 and P3-P5. In both zones, there is an increase in total N inventories towards the depositional section, mirroring the increase in both ^{137}Cs and total C inventories. For Site 3 the reference field total N concentration profiles are similar shapes but have differing maximum concentrations (Figure 5.16g) and this is reflected in the total N inventories (Table 5.3) up to 50 cm depth: Ref 1 ($0.64 \pm 0.014 \text{ kg m}^{-2}$), Ref 2 ($0.44 \pm 0.051 \text{ kg m}^{-2}$) and Ref 3 ($0.26 \pm 0.025 \text{ kg m}^{-2}$).

C:N ratio

In fields BGF1, the C:N ratio for highly eroding profiles (P1-P3) of deeper soil increments layer (below 20 cm) was higher than all other profiles (P4-P7), but up to 20 cm all profiles had similar C:N ratios (Figure 5.15d). However, in field BGF2, except P4, all profiles have similar C:N ratios. P4 was described as an eroding slope and it has a wider C:N ratio than other profiles (Figure 5.15h). In BGF3 there was no clear pattern of C:N ratios observed (Figure 5.16d). Site 3 reference profile looks similar C:N ratio for Ref1 and Ref 2 but Ref 3 looks abnormal (Figure 5.16h).

Total and Organic P (and C:OP ratio)

In field BGF1, OP concentrations (Figure 5.17a) were lower at eroding upslope profiles (P1) and mid slope (P3) than downslope deposition profiles (P6). Deposition downslope profiles had comparatively higher OP concentrations over the entire soil depth. The OP inventory in erosion profiles (P1) was significantly lower ($p < 0.05$) than the deposition profile (P6) and equal to mid slope P3 (Figure 5.14a and Table 5.3). In field BGF1, TP concentrations (Figure 5.17b) were lower at the eroding profile (P1) than mid slope (P3) and deposition profiles (P6). The TP concentrations in deposition profiles was higher than in the mid slope profile at 10 cm depth; after that the mid slope profile TP concentration was higher than the deposition profile. The TP inventory in erosion profile (P1) was significantly lower ($p < 0.05$) than mid-slope (P3) but equal to deposition profile (P6) (Figure 5.14b and Table 5.3). In field BGF1 C:OP ratio (Figure 5.17c) of top soil 10 cm layer of eroding and deposition profiles were similar but the

mid slope profiles have higher ratios than both other profiles. Below 10 cm increments in the mid and deposition profiles C:OP ratios were equal but the eroding profile looks wider at 20 cm depth after that all profiles have similar C:OP ratios.

In field BGF2 OP concentrations (Figure 5.17d) of top 10 cm increments were lower at eroding upslope profile (P1) than deposition downslope (P6) than mid slope profile (P3). Below that at 20 cm depth all profiles had similar OP concentrations. After that eroding and mid slope profiles were similar with lower OP concentrations than the deposition profile. There was no significant ($P > 0.05$) difference in OP inventory between all profiles (Figure 5.14c and Table 5.3). In field BGF2 TP concentration (Figure 5.17e) were almost equal at top 10 cm depth of all profiles and below that depth the concentration in the eroding profile was lower. The mid slope and deposition profiles had similar TP concentrations at 20 cm depth and below that the deposition profile had higher TP concentrations than the mid slope profiles. There was no significant ($p > 0.05$) difference in TP inventory of all the profiles (Figure 5.17e and Table 5.9). In field BGF2, the C: OP ratio (Figure 5.17f) of the top 10 cm increment of eroding and deposition profiles was similar, but mid slope profiles have lower C: OP ratios than both other profiles. Below 10 cm, the eroding profile has lower C: OP ratio than other profiles in entire depth. The C: OP ratio of the mid slope profile is lower at 20 cm and equal at 30 cm depth to the deposition profile.

In field BGF3, OP concentrations (Figure 5.18a) of the top 10 cm increment were lower at eroding upslope profile (P1) than mid (P2) and downslope deposition profiles (P5). Below 20 cm, the P5 deposition profile has lower than OP concentrations than others but the mid slope profile had higher OP concentrations, and after this depth eroding profile had relatively lower OP concentration. The OP inventory in the eroding profile (P1) is significantly ($p < 0.05$) lower than in the mid and deposition profiles (Figure 5.14e and Table 5.3). In field BGF3, TP concentrations (Figure 5.18b) were similar in the top 10 cm increment of all profiles, and below that the deposition profiles had lower concentrations. Eroding and mid slope profiles had similar TP concentrations at 20 cm depth, but below that the mid slope profile had lower concentrations than the eroding profile. The TP inventory in the eroding profile (P1) is significantly ($p < 0.05$) lower than in the mid and deposition profiles (Figure 5.14f and Table 5.3). In field BGF3, the C:OP ratio (Figure 5.18c) of top 10 cm increment of the eroding profile was higher than deposition and mid slope profile. Below 20 cm, the deposition profile had relatively

higher C:OP ratios than the mid and eroding slope profiles. At 30 cm deposition and mid slope profile had equal C OP ratios which were lower than eroding slope position, after this depth mid slope lower than deposition.

At Site 3 the reference OP and TP inventories are respectively 0.04 and 0.40 kg m⁻² for Ref 1 and 0.06 and 0.31 kg m⁻² for Ref 2. OP and TP concentrations and C: OP ratio variation with depth for the reference profiles are presented in Figure 5.18 d,e and f.

Table 5.3 Total Inventory of ^{137}Cs , SOC, total N, OP and TP to 50 cm soil depth along the slope transects at Site 3 (BGF1, BGF2, BGF3 and BG Ref fields). For each profile $n = 3$, differences in inventories were tested by one way Anova at $p = 0.05$, significant sub-sets are denoted. CV is the coefficient of variation in total inventory of three replicates (soil pit faces). Mean values \pm SE are presented.

Pits of BGF1	^{137}Cs Inventory (Bq m ⁻²)	CV %	SOC Inventory (kg m ⁻²)	CV %	TN Inventory (kg m ⁻²)	CV %	OP Inventory (kg m ⁻²)	TP Inventory (kg m ⁻²)
P1	524 \pm 46a	15.0	3.75 \pm 0.38a	17.0	0.35 \pm 0.027b	13.0	0.04a	0.37a
P2	728 \pm 22a	5.0	4.07 \pm 0.09ab	4.0	0.30 \pm 0.013b	8.0		
P3	727 \pm 61a	15.0	2.51 \pm 0.14a	10.0	0.20 \pm 0.001a	1.0	0.04a	0.86b
P4	1093 \pm 63b	10.0	4.37 \pm 0.49ab	19.0	0.42 \pm 0.006c	2.0		
P5	1308 \pm 16b	2.0	4.83 \pm 0.12ab	4.0	0.45 \pm 0.019c	7.0		
P6	1420 \pm 43bc	5.0	6.47 \pm 0.22c	6.0	0.58 \pm 0.009d	3.0	0.07b	0.49a
P7	932 \pm 59ab	11.0	5.14 \pm 0.18b	6.0	0.53 \pm 0.034cd	11.0		

Pits of BGF2	^{137}Cs Inventory (Bq m ⁻²)	CV %	SOC Inventory (kg m ⁻²)	CV %	TN Inventory (kg m ⁻²)	CV %	OP Inventory (kg m ⁻²)	TP Inventory (kg m ⁻²)
P1	815 \pm 89a	19.0	3.82 \pm 0.37a	17.0	0.40 \pm 0.054a	24.0	0.06a	0.31a
P2	832 \pm 93a	19.0	3.95 \pm 0.68a	30.0	0.33 \pm 0.055a	29.0		
P3	1404 \pm 46b	6.0	4.81 \pm 0.09a	3.0	0.45 \pm 0.031a	12.0	0.07a	0.37a
P4	823 \pm 77a	16.0	4.47 \pm 0.41a	16.0	0.37 \pm 0.035a	17.0		
P5	1043 \pm 67ab	11.0	4.58 \pm 0.34a	13.0	0.36 \pm 0.017a	8.0		
P6	2431 \pm 231c	16.0	6.23 \pm 0.79ab	22.0	0.65 \pm 0.011ab	30.0	0.05a	0.34a

Pits of BGF3	^{137}Cs Inventory (Bq m ⁻²)	CV %	SOC Inventory (kg m ⁻²)	CV %	TN Inventory (kg m ⁻²)	CV %	OP Inventory (kg m ⁻²)	TP Inventory (kg m ⁻²)
P1	1246 \pm 178ab	25.0	3.94 \pm 0.31a	13.0	0.48 \pm 0.030ab	11.0	0.02a	0.32a
P2	1471 \pm 142ab	17.0	5.25 \pm 0.18b	6.0	0.68 \pm 0.028b	7.0		
P3	770 \pm 72a	16.0	3.80 \pm 0.13a	6.0	0.36 \pm 0.012a	6.0	0.08b	0.46b
P4	642 \pm 22a	6.0	3.54 \pm 0.20a	10.0	0.42 \pm 0.017a	7.0		
P5	1024 \pm 98a	16.0	7.19 \pm 0.33c	8.0	0.65 \pm 0.037b	10.0	0.07b	0.43b

Pits of BG ref	^{137}Cs Inventory (Bq m ⁻²)	CV %	SOC Inventory (kg m ⁻²)	CV %	TN Inventory (kg m ⁻²)	CV %	OP Inventory (kg m ⁻²)	TP Inventory (kg m ⁻²)
Ref 1	1282 \pm 63	8.0	8.30 \pm 0.42	9.0	0.64 \pm 0.014	4.0	0.04	0.40
Ref 2	1063 \pm 33	5.0	5.63 \pm 0.17	5.0	0.44 \pm 0.051	20.0	0.06	0.31
Ref 3	799 \pm 40	9.0	3.36 \pm 0.13	7.0	0.26 \pm 0.025	17.0	0.03	0.41

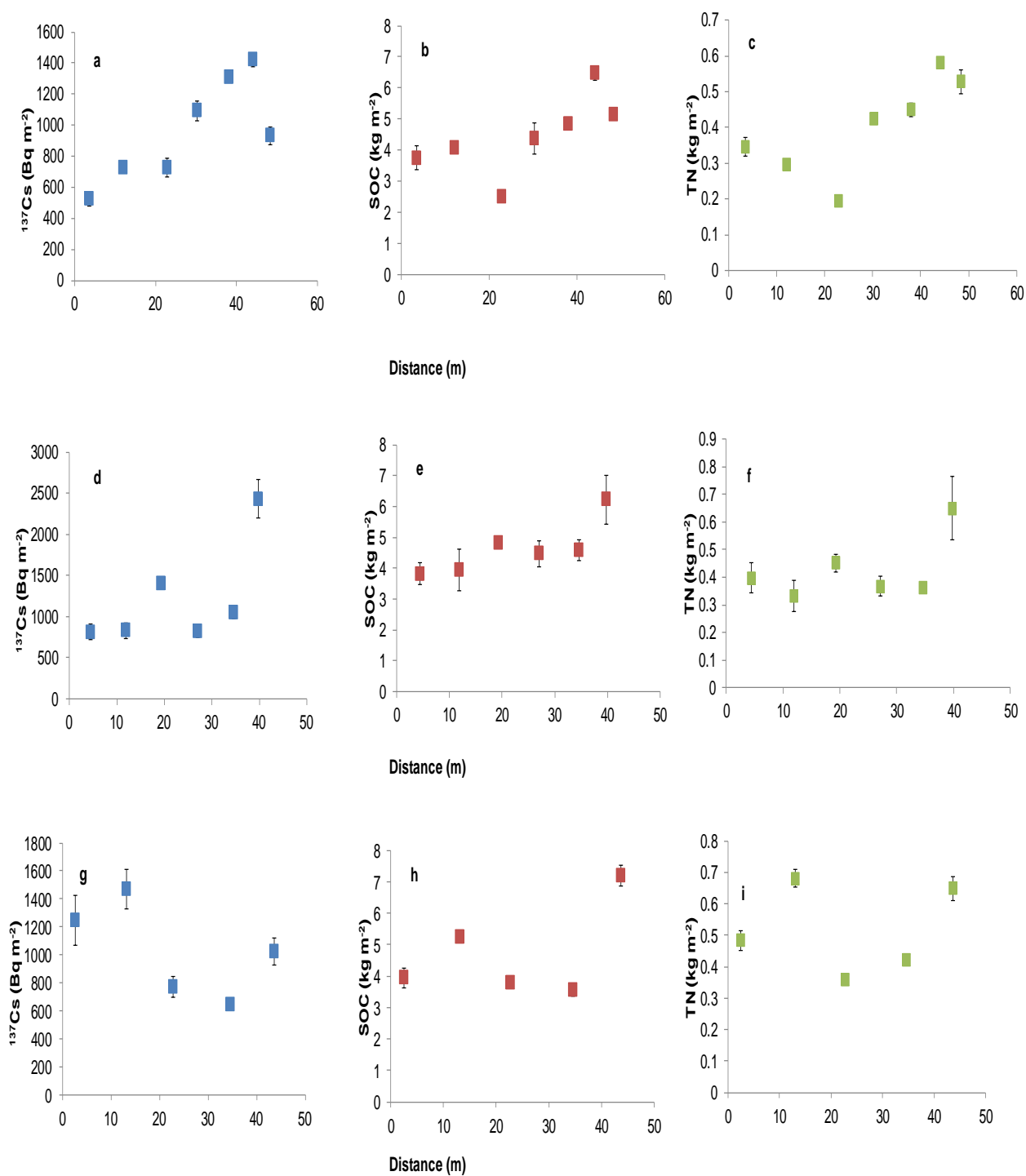


Figure 5.13 Total Inventory of ¹³⁷Cs, SOC, and total N to 50 cm soil depth at profiles along a slope transect within field of Site 3 (BGF1: a-c, BGF2: d-f, and BGF3: g-i). For each profile $n = 3$ and the error bars reflect standard error.

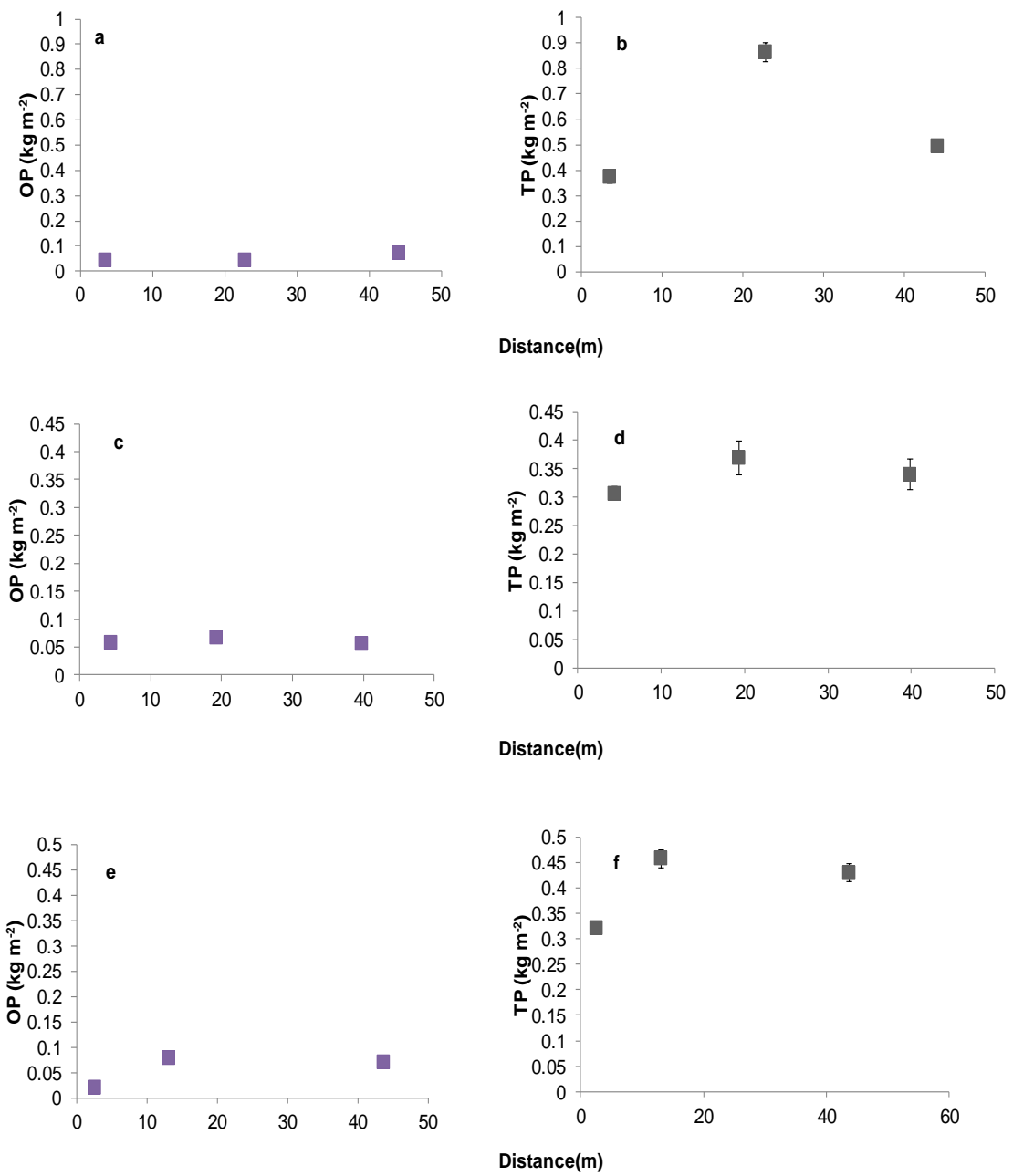


Figure 5.14 Total Inventory of OP and TP to 50 cm soil depth at profiles along a slope transect within field of Site 3 (BGF1: a-b, BGF2: c-d, and BGF3: e-f). P analysed as a composite sample of each depth layer

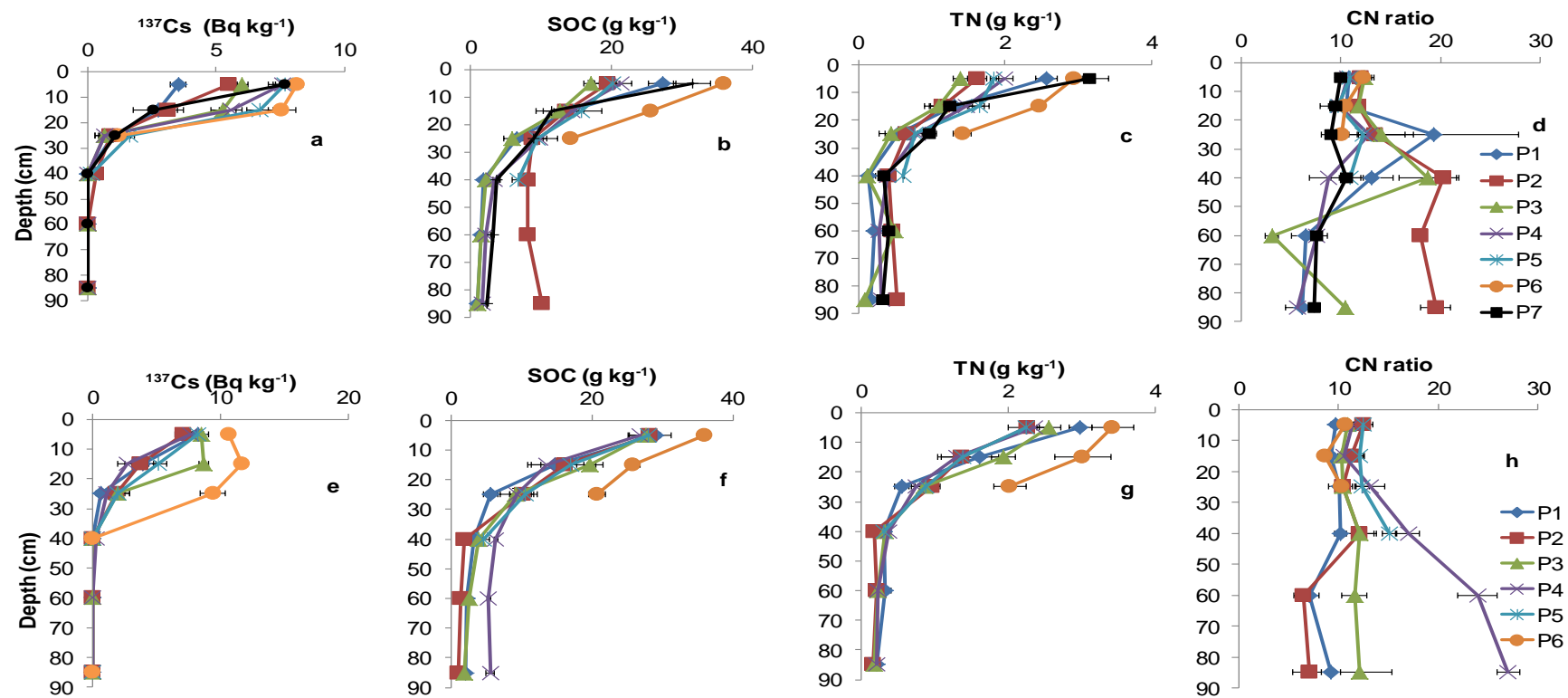


Figure 5.15 Vertical distributions of ^{137}Cs , SOC, total N and C:N in soil profiles along the slope transects within field Site 1 (BGF1: a-d, and BGF2: e-h). Error bars are \pm SE ($n = 3$).

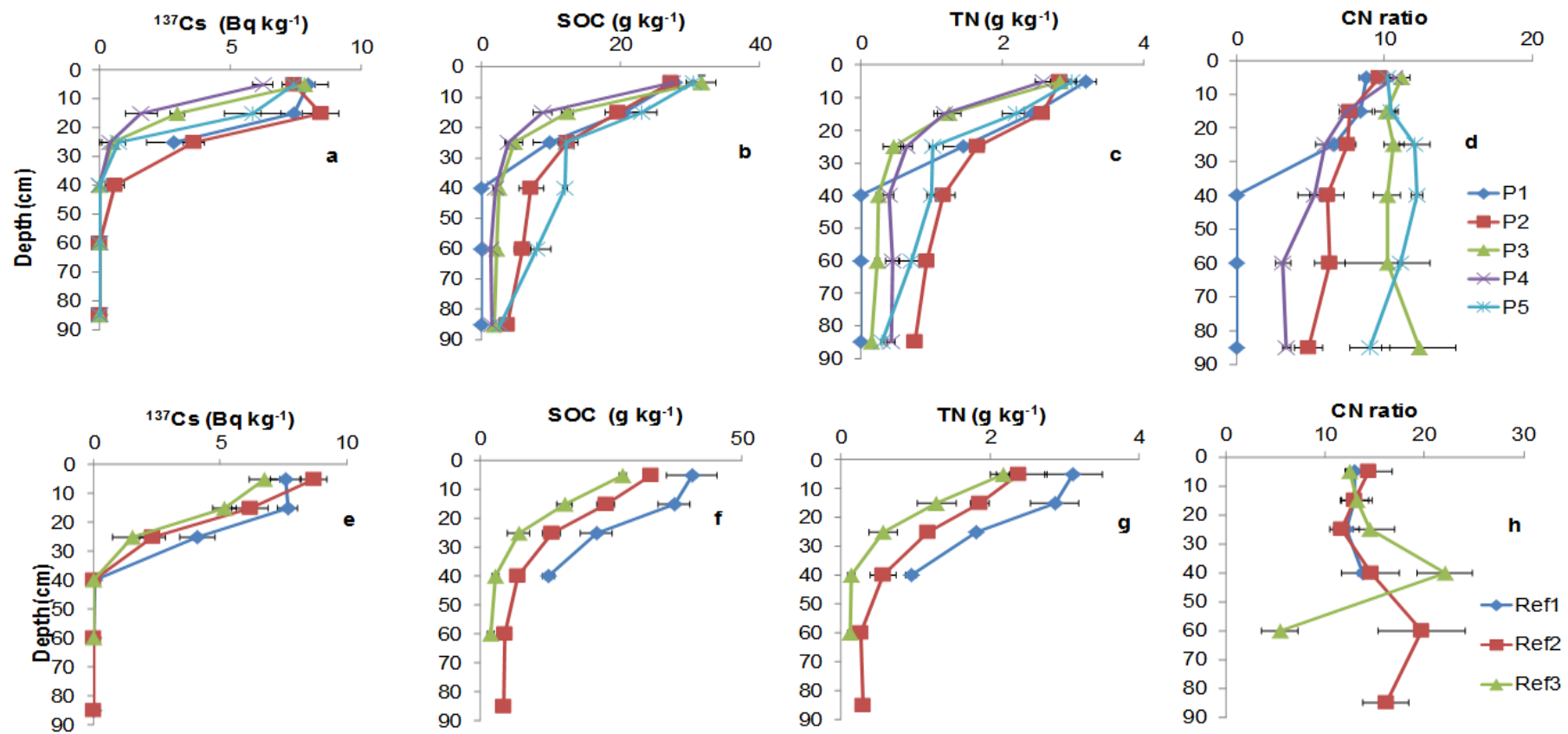


Figure 5.16 Vertical distributions of ^{137}Cs , SOC, total N and C:N in soil profiles along the slope transects within field Site 1 (BGF3: a- d, and BG Ref: e-h). Error bars are \pm SE ($n = 3$).

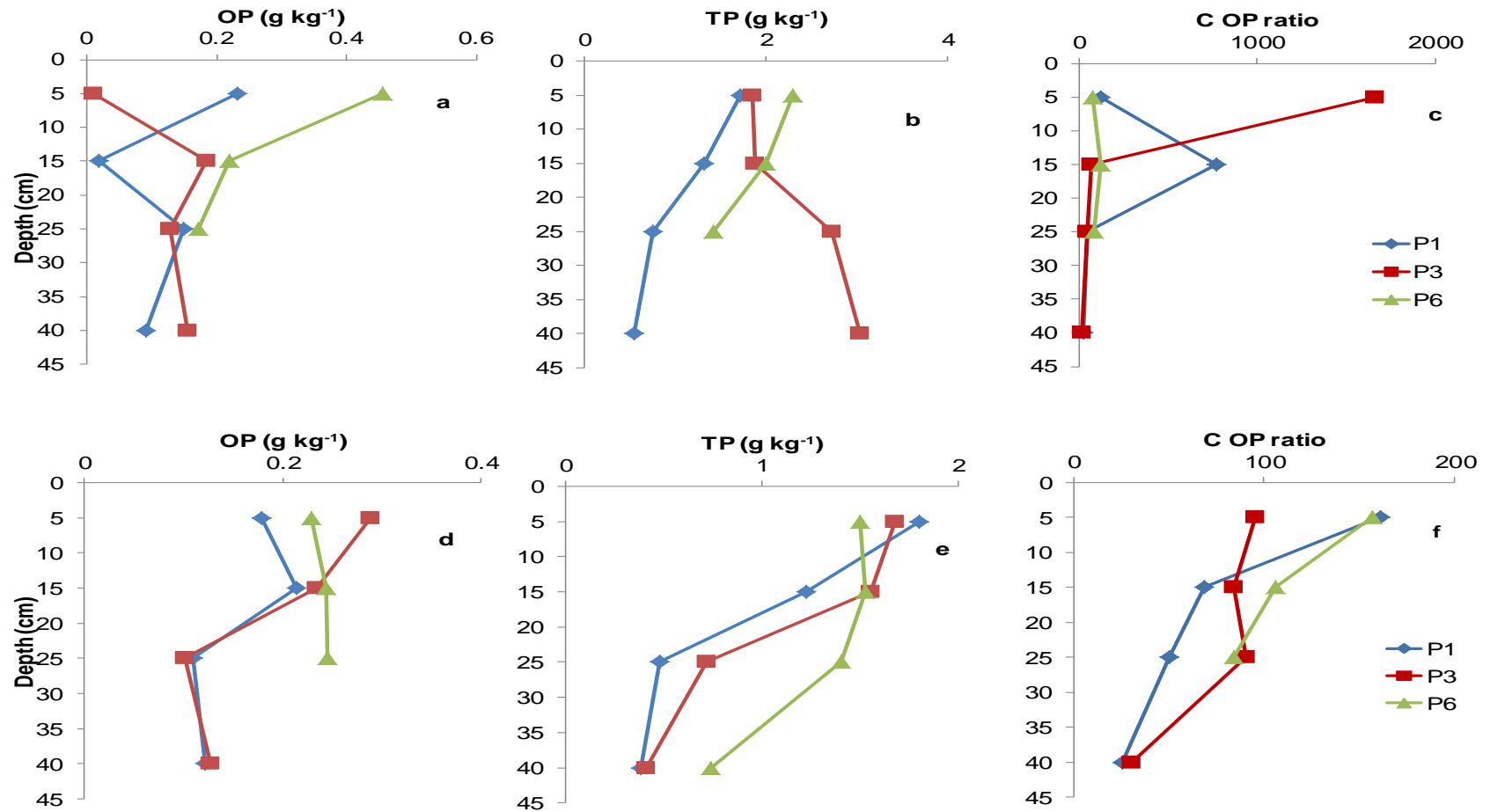


Figure 5.17 Vertical distributions of OP, TP and CP ratio in profiles in field Site 3 (BGF1: a-c, and BGF2: d-f). Each depth layer made it into composite and analysed up to 50 cm

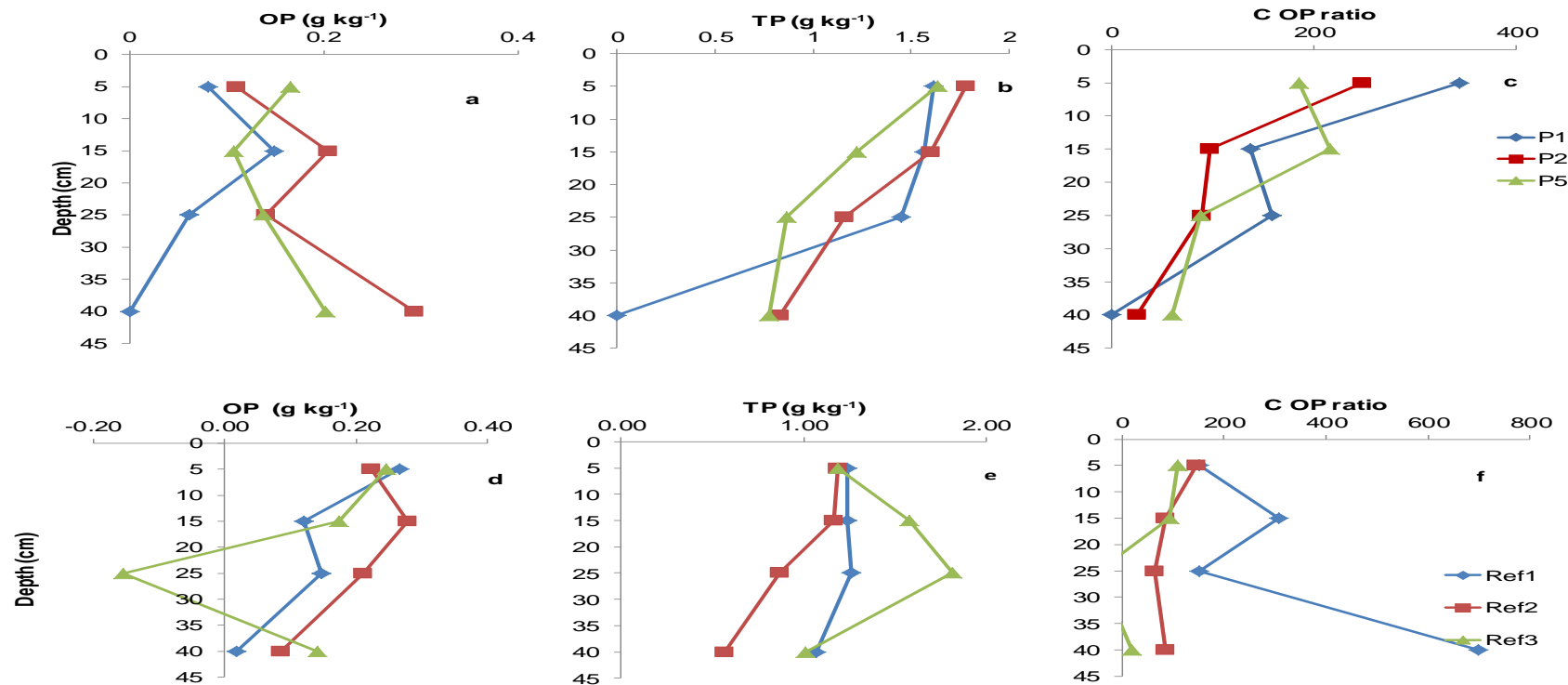


Figure 5.18 Vertical distributions of OP, TP and CP ratio in profiles in field Site 2 (BGF3: a-c, and BG Ref: d-f). Each depth layer made it into composite and analysed up to 50 cm.

Table 5.4 Descriptive statistics for total inventory of ^{137}Cs , SOC, and total N to 50cm depth for all three sites slope field.

Sites	Field id	Parameters	Min	Max	Median	Mean
Site 1	DKF1	^{137}Cs (Bq m^{-2})	472	2196	739	996
	DKF1	SOC (kg m^{-2})	2.89	5.80	3.74	3.98
	DKF1	TN (kg m^{-2})	0.21	0.49	0.33	0.34
Site 1	DKF2	^{137}Cs (Bq m^{-2})	180	2046	680	796
	DKF2	SOC (kg m^{-2})	1.69	4.67	3.66	3.49
	DKF2	TN (kg m^{-2})	0.20	0.49	0.37	0.36
Site 1	DKF3	^{137}Cs (Bq m^{-2})	84	1839	729	701
	DKF3	SOC (kg m^{-2})	2.82	4.77	3.73	3.68
	DKF3	TN (kg m^{-2})	0.32	0.60	0.35	0.37
Site 2	PSF1	^{137}Cs (Bq m^{-2})	202	2680	2094	1836
	PSF1	SOC (kg m^{-2})	3.18	8.68	6.39	6.18
	PSF1	TN (kg m^{-2})	0.17	0.65	0.49	0.44
Site 2	PSF2	^{137}Cs (Bq m^{-2})	566	2446	1546	1475
	PSF2	SOC (kg m^{-2})	1.73	7.31	5.11	4.56
	PSF2	TN (kg m^{-2})	0.17	0.58	0.37	0.36
Site 2	PSF3	^{137}Cs (Bq m^{-2})	332	3161	1504	1481
	PSF3	SOC (kg m^{-2})	2.73	6.29	4.66	4.60
	PSF3	TN (kg m^{-2})	0.25	0.44	0.32	0.33
Site 3	BGF1	^{137}Cs (Bq m^{-2})	477	1500	961	962
	BGF1	SOC (kg m^{-2})	2.23	6.83	4.36	4.29
	BGF1	TN (kg m^{-2})	0.19	0.60	0.42	0.40
Site 3	BGF2	^{137}Cs (Bq m^{-2})	676	2816	1000	1225
	BGF2	SOC (kg m^{-2})	2.82	7.75	4.56	4.64
	BGF2	TN (kg m^{-2})	0.25	0.86	0.40	0.43
Site 3	BGF3	^{137}Cs (Bq m^{-2})	613	1694	892	1031
	BGF3	SOC (kg m^{-2})	3.15	7.56	4.13	4.74
	BGF3	TN (kg m^{-2})	0.34	0.71	0.51	0.52

5.3.5 Relationship between ^{137}Cs , SOC and total N

Relationship between total inventory of ^{137}Cs and SOC and total N were tested for all study site to the sampling depth of 50 cm and found positive and strong statistically significant relationship for Site 1- (Figure 5.19a,b) field 1 (^{137}Cs vs SOC, $r^2 = 0.35$, $p < 0.05$; ^{137}Cs vs total N, $r^2 = 0.38$, $p < 0.05$); for Site 1- field 2 (Figure 5.19c,d) strong relationship found for SOC not for total N (^{137}Cs vs SOC, $r^2 = 0.36$, $p < 0.05$; ^{137}Cs vs total N, $r^2 = 0.06$, $p = 0.39$). For Site 2- (Figure 5.20a,b) field 1 (^{137}Cs vs SOC, $r^2 = 0.43$, $p < 0.05$; ^{137}Cs vs total N, $r^2 = 0.47$, $p < 0.05$); Site 2- (Figure 5.20c,d) field 2 (^{137}Cs vs SOC, $r^2 = 0.55$, $p < 0.05$; ^{137}Cs vs total N, $r^2 = 0.54$, $p < 0.05$) and for Site 2- (Figure 5.20e,f) field 3 (^{137}Cs vs SOC, $r^2 = 0.65$, $p < 0.05$; ^{137}Cs vs total N, $r^2 = 0.70$, $p < 0.05$) has statistical strong relationship between ^{137}Cs and SOC and total N inventory this indicate they moved along similar pathways . In Site 3-(Figure 5.21a,b) field 1 (^{137}Cs vs SOC, $r^2 = 0.55$, $p < 0.05$; ^{137}Cs vs total N, $r^2 = 0.52$, $p < 0.05$) and Site3- (Figure 5.21c,d) field 2 (^{137}Cs vs SOC, $r^2 = 0.72$, $p < 0.05$; ^{137}Cs vs total N, $r^2 = 0.78$, $p < 0.05$) were found statistically strong significant relationship between ^{137}Cs vs SOC and total N but in Site 3- (Figure 5.21e,f) field 3 (^{137}Cs vs SOC, $r^2 = 0.16$, $P = 0.141$; ^{137}Cs vs total N, $r^2 = 0.55$, $p < 0.05$) has statistical strong relationship between ^{137}Cs and total N inventory not with SOC . Descriptive statistics of total inventory of ^{137}Cs and SOC and total N were tested up to 50 cm depth of all sites and results presented in Table 5.4, it display lowest and highest pattern of all inventories in this study region.

5.3.6 Relationship between ^{137}Cs activity and SOC and total N concentration

Relationship between ^{137}Cs activity and SOC and total N concentration were tested for all study sites to the sampling depth of 50 cm with different increment and result presented in Table 5.5 and Figure 5.22a-d, Figure 5.23a-f, and Figure 5.24a-f. Along the slope field relationship between ^{137}Cs activity and SOC and total N concentration at top soil most of the field found less r^2 values than deep soil.

5.3.7 Relationship between ^{137}Cs and P (OP and TP)

Relationship between total ^{137}Cs and OP and TP inventory were tested for all study site to the sampling depth of 50 cm and found positive and strong statistically significant relationship for Site 1- Combined (Figure 5.25a,b) first two field (^{137}Cs vs OP, $r^2 = 0.62$, $p < 0.05$; ^{137}Cs vs TP, $r^2 = 0.54$, $p < 0.05$) and Site 2- combined (Figure 5.25c,d) three field (^{137}Cs vs OP, $r^2 = 0.51$, $p < 0.05$; ^{137}Cs vs TP, $r^2 = 0.58$, $p < 0.05$) but in Site3-combined (Figure.5.25e,f) three field (^{137}Cs vs OP, $r^2 = 0.06$, $p = 0.22$;

^{137}Cs vs TP, $r^2 = 0.07$, $p = 0.19$) no significant relationship between total ^{137}Cs and OP and TP inventory.

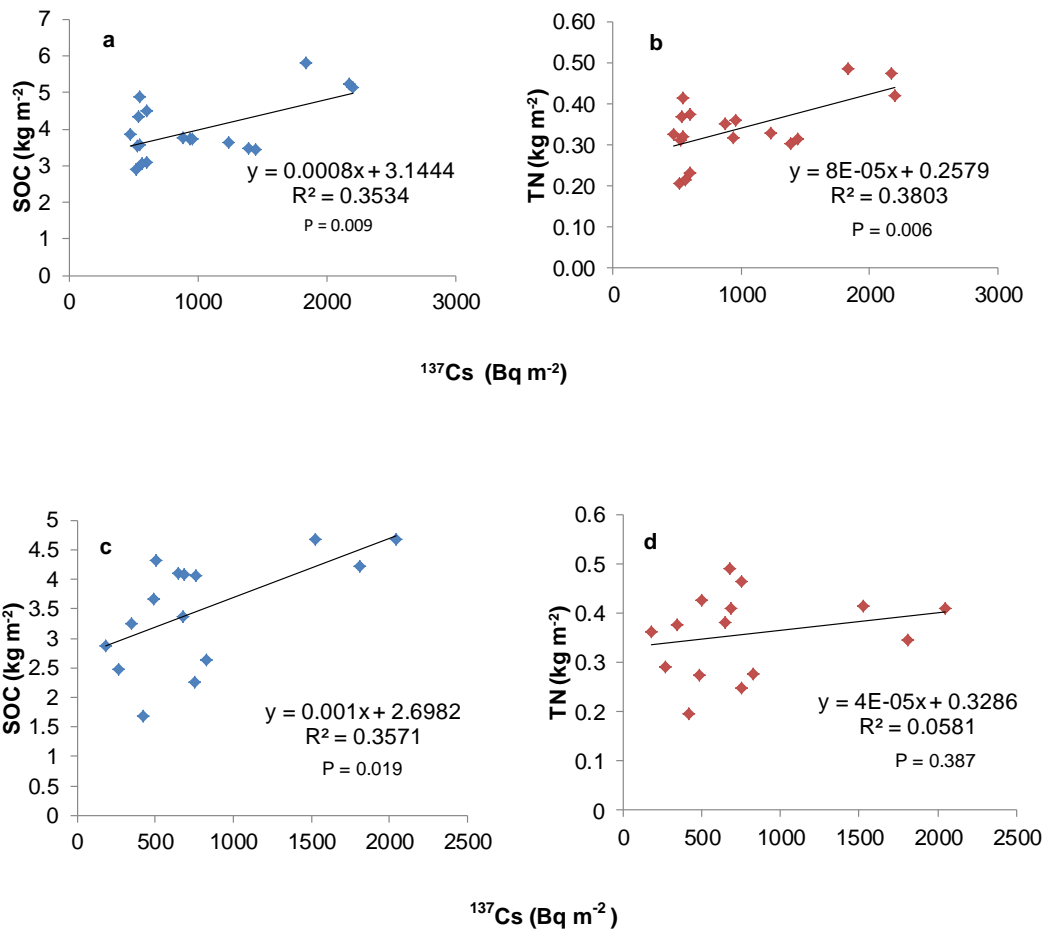


Figure 5.19 Relationship between individual profile face total inventories of ^{137}Cs , SOC and total N within fields of Site 1 (DKF1: a-b, and DKF2: c-d). All inventories to 0.5 m. Linear regression analysis performed and tested significance

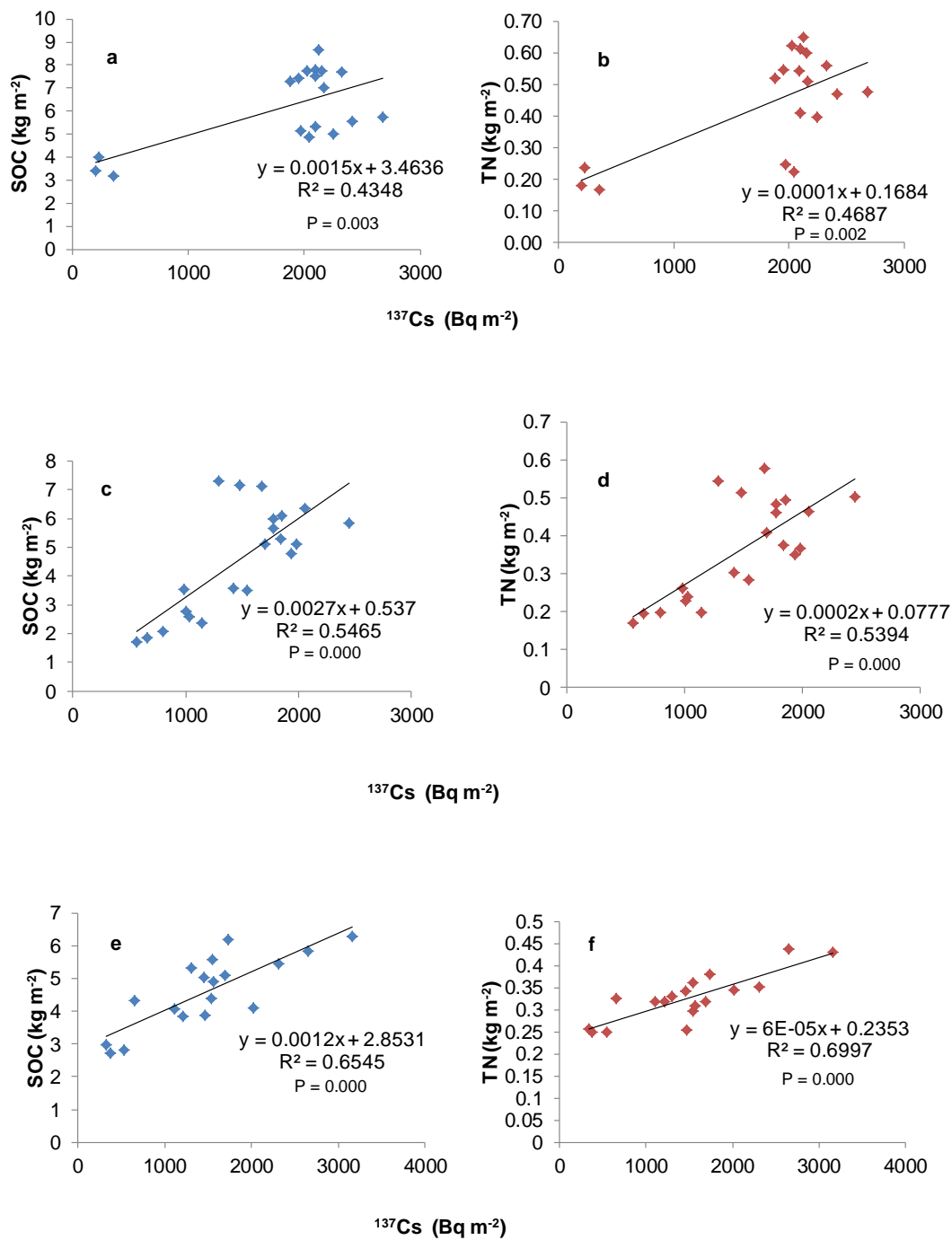


Figure 5.20 Relationship between individual profile face total inventories of ^{137}Cs , SOC and total N within fields of Site 2 (PSF1: a-b, PSF2: c-d, and PSF3: e-f). All inventories to 0.5 m. linear regression analysis performed and tested significance

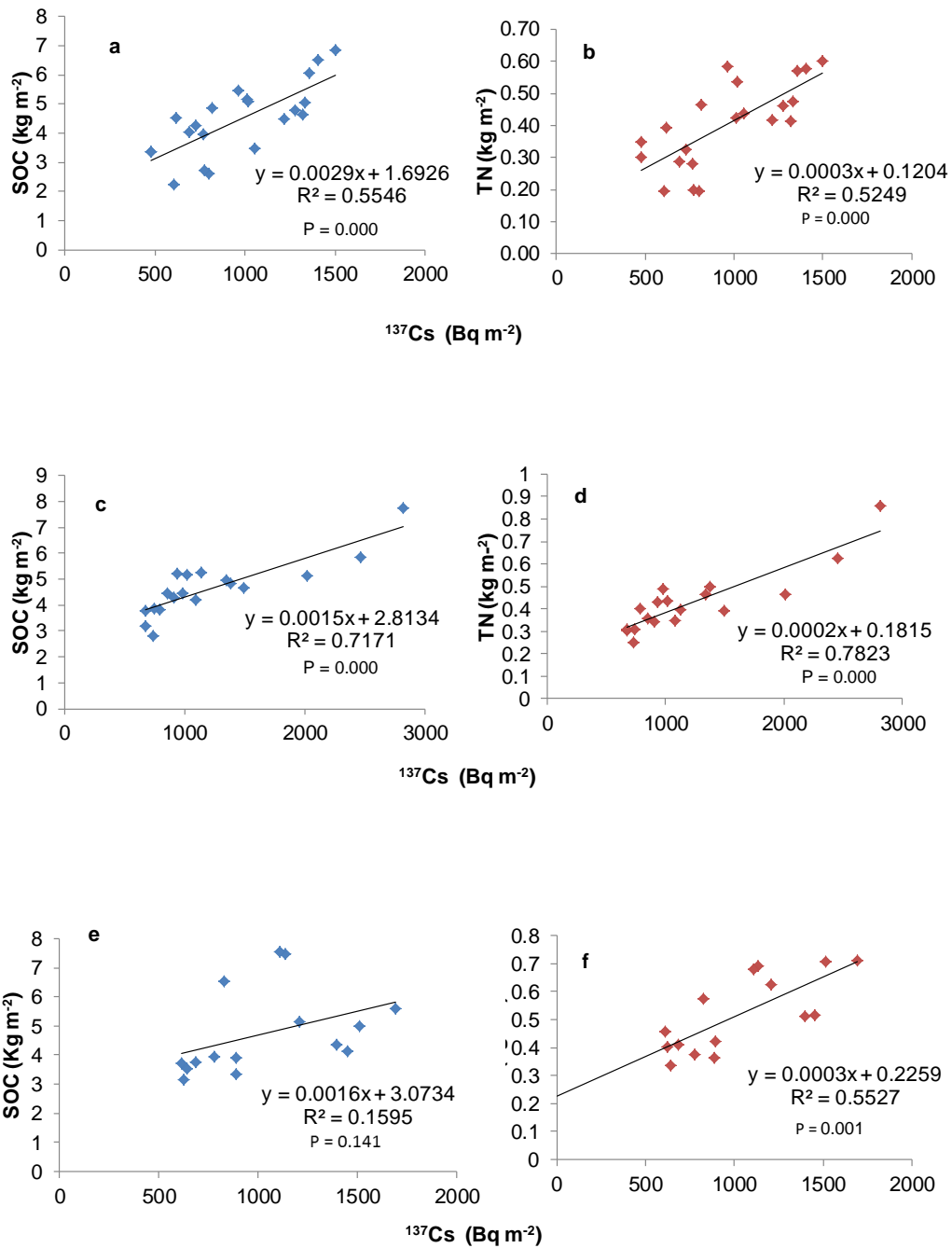


Figure 5.21 Relationship between individual profile face total inventories of ^{137}Cs , SOC and total N within fields of Site 3 (BGF1: a-b, BGF2: c-d, and BGF3: e-f). All inventories to 0.5 m. Linear regression analysis performed and tested significance

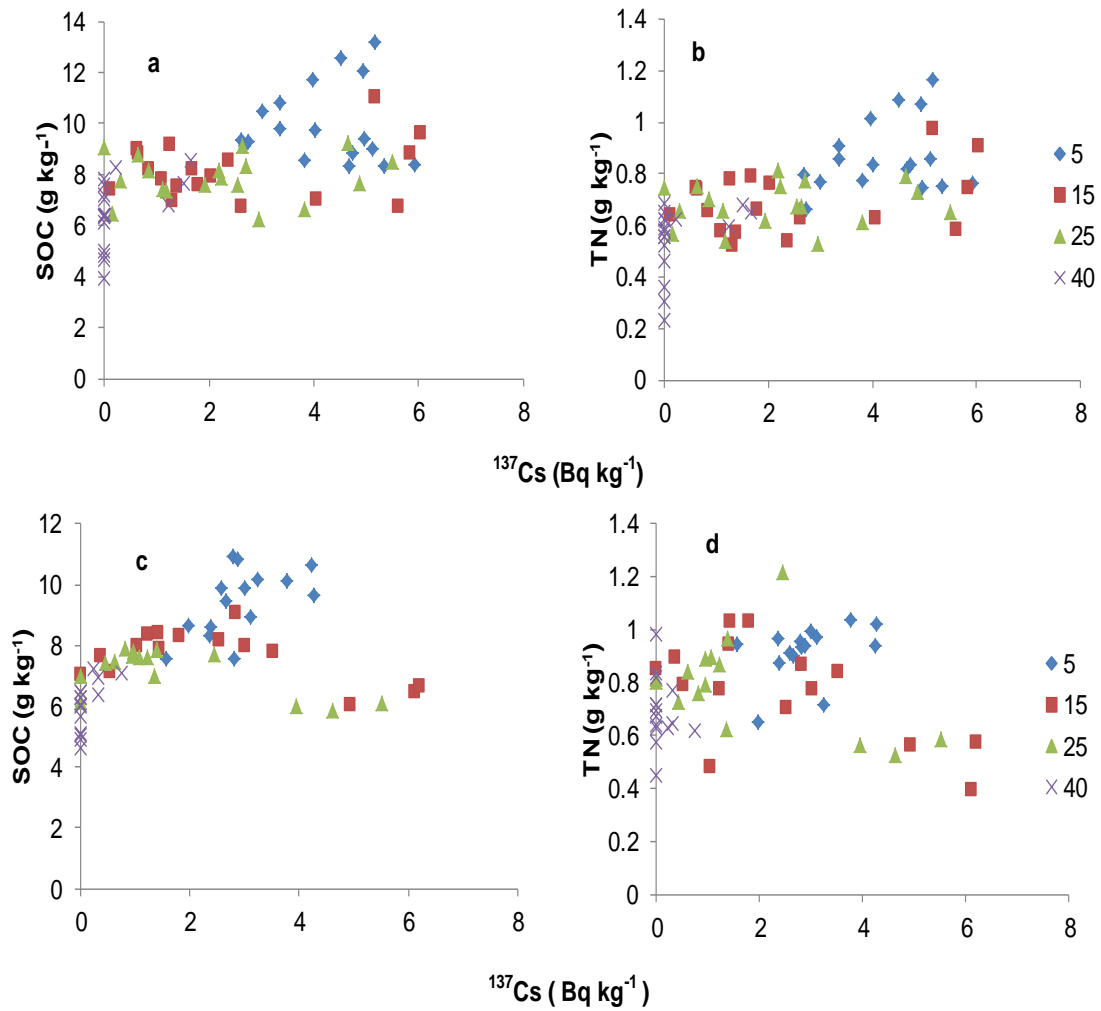


Figure 5.22 Relationship between individual depths profile face activity of ^{137}Cs , concentration of SOC and total N within fields of Site 1 (DKF1: a-b, and DKF2: c-d). All activity and concentration to 0.5 m.

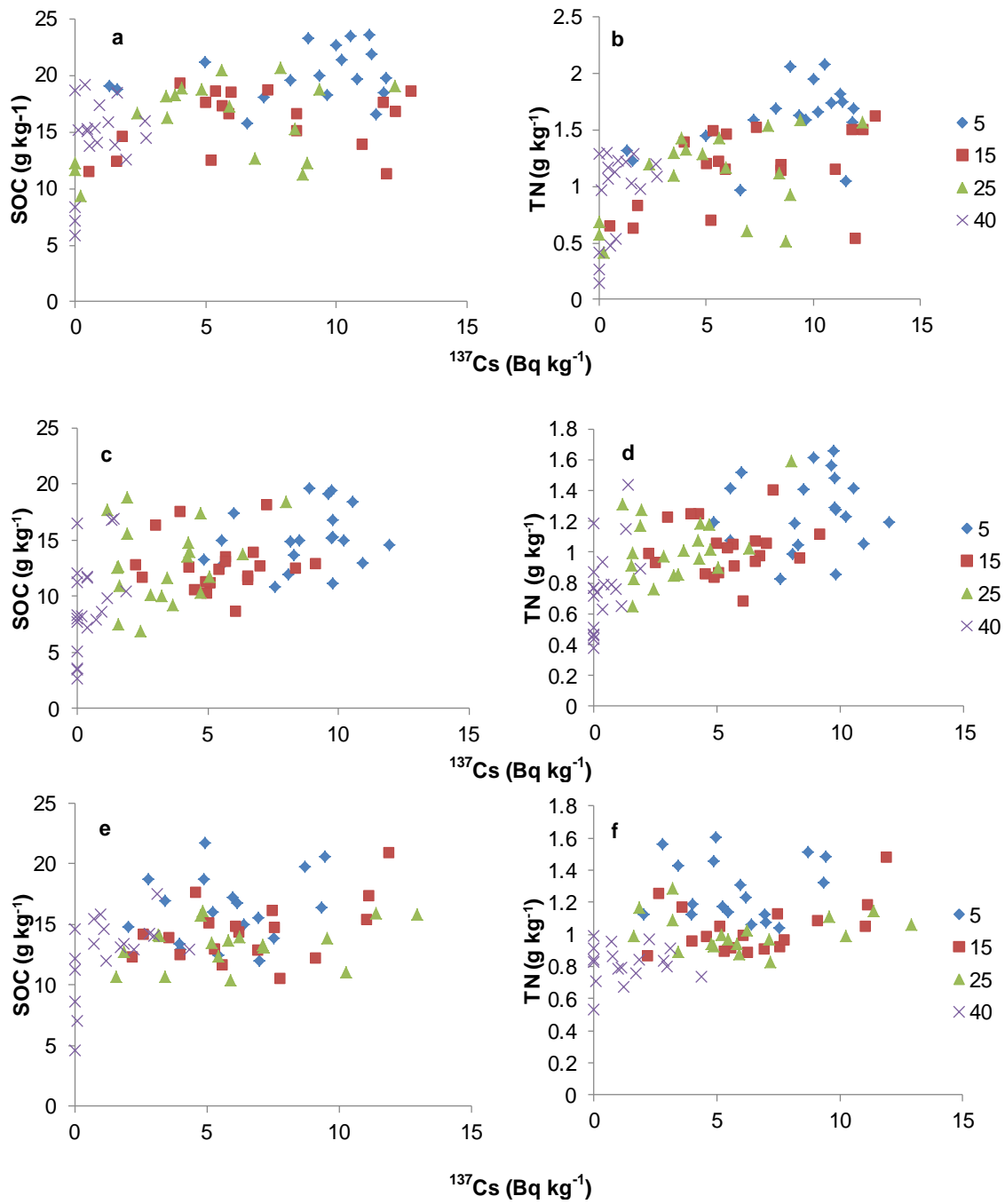


Figure 5.23 Relationship between individual depths profile face activity of ^{137}Cs , concentration of SOC and total N within fields of Site 2 (PSF1: a-b, PSF2: c-d, and PSF3: e-f). All activity and concentration to 0.5 m.

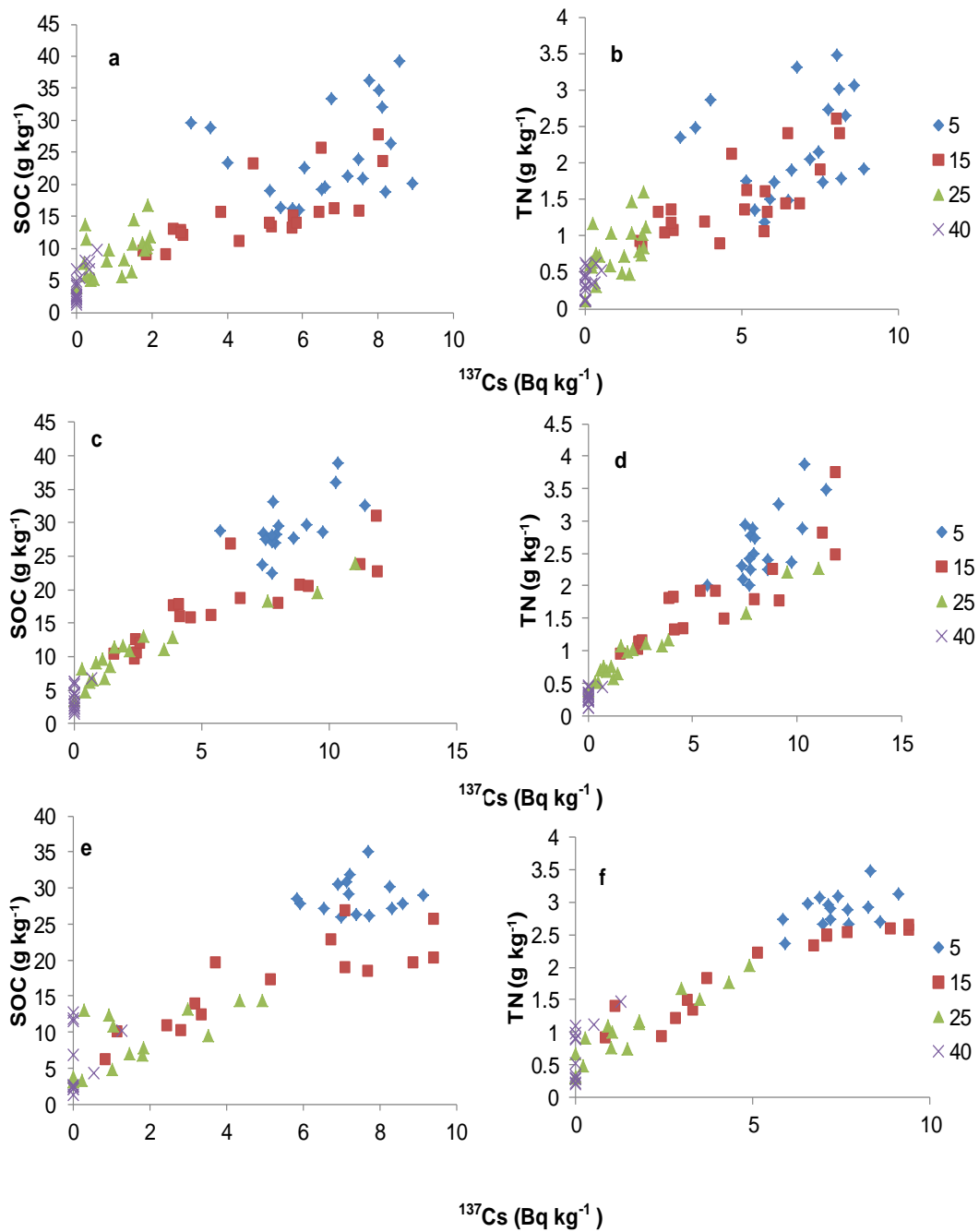


Figure 5.24 Relationship between individual depths profile face activity of ^{137}Cs , concentration of SOC and total N within fields of Site 3 (BGF1: a-b, BGF2: c-d, and BGF3: e-f). All activity and concentration to 0.5 m.

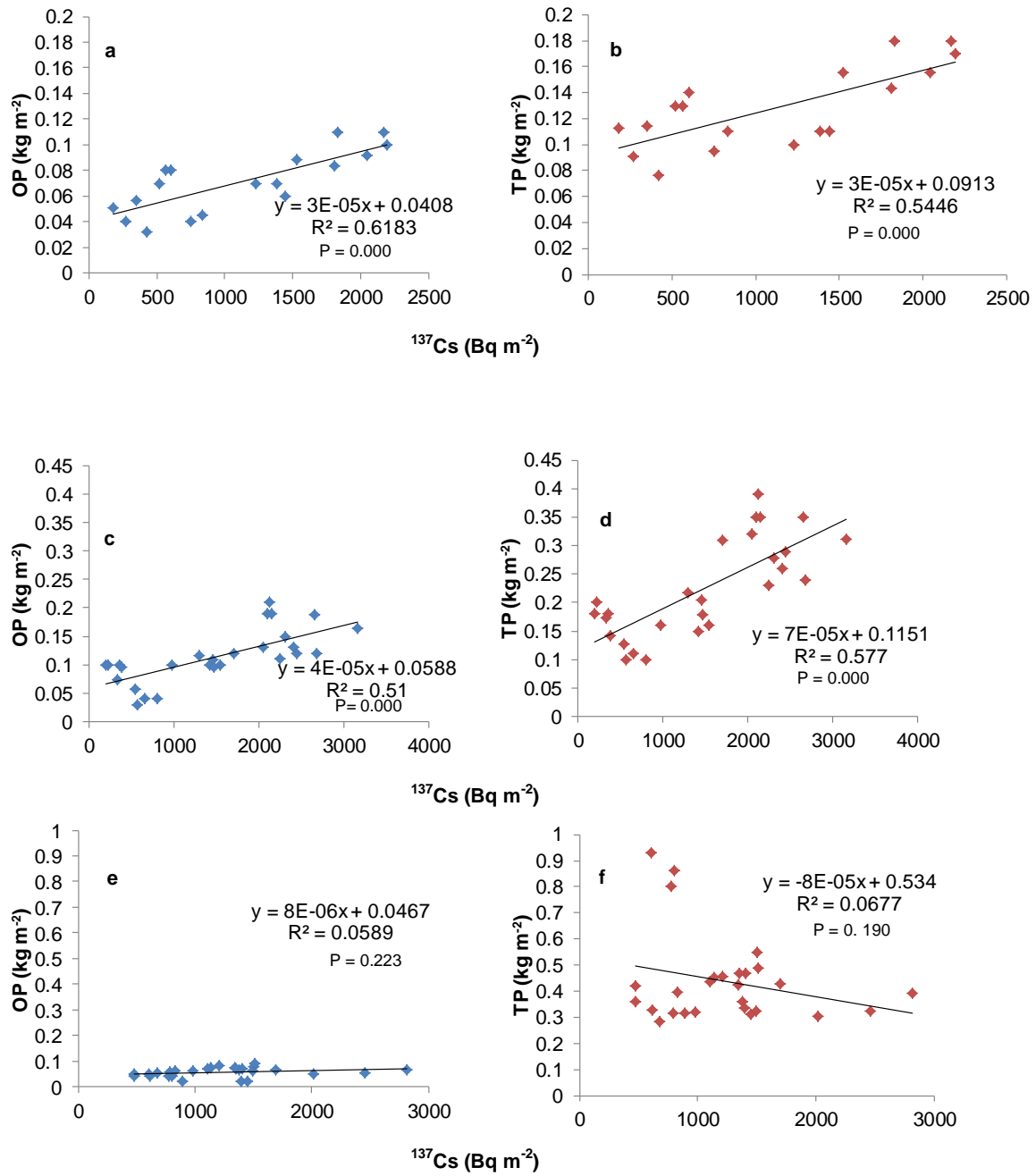


Figure 5.25 Relationship between total inventory of ¹³⁷Cs, OP and TP for Site 1 (a-b), Site 2 (c-d) and Site 3(e-f).

Table 5.5 Linear regression result between ^{137}Cs activity, SOC and total N concentration for three sites field and with depth increment

Site	field	r^2 values for ^{137}Cs (Bq kg^{-1}) vs SOC (g kg^{-1})					r^2 values for ^{137}Cs (Bq kg^{-1}) vs TN (g kg^{-1})				
		Depth (cm)					Depth (cm)				
		5	15	25	40	0-50	5	15	25	40	0-50
Site 1	DKF1	0.00	0.07	0.01	0.23	0.33	0.12	0.14	0.02	0.13	0.38
	DKF2	0.24	0.34	0.38	0.36	0.14	0.15	0.37	0.21	0.03	0.00
Site 2	PSF1	0.07	0.04	0.12	0.08	0.23	0.22	0.20	0.19	0.18	0.34
	PSF2	0.05	0.00	0.06	0.22	0.28	0.00	0.00	0.18	0.27	0.36
	PSF3	0.03	0.22	0.11	0.24	0.16	0.00	0.17	0.00	0.00	0.17
Site 3	BGF1	0.05	0.53	0.28	0.68	0.70	0.04	0.55	0.28	0.20	0.71
	BGF2	0.38	0.72	0.90	0.19	0.85	0.49	0.77	0.94	0.16	0.89
	BGF3	0.01	0.72	0.49	0.06	0.80	0.22	0.89	0.88	0.44	0.9

5.4 Discussion

5.4.1 Vertical and lateral distribution of ^{137}Cs activity and Inventory

Validity of using ^{137}Cs as a tracer

The detailed examination of small-scale variation ($n=3$ within pit) as well as variation with depth, in space (along transects) and between fields ($n=3$ sloping fields at each site) allows evaluation of the validity of using ^{137}Cs as a tracer in this environment. In contrast to suggestions by (Parsons and Foster, 2011 and 2013) relatively low CV were observed in both profile inventories and activities for samples from the same depth within each pit (Presented in Tables 5.1 to 5.3). These results suggest that reliable and replicable measures of ^{137}Cs inventories can be obtained from these soils which is a fundamental requirement for use of the technique in erosion assessment. Furthermore, when depth profiles are compared with total profile inventories (Presented in Tables 5.1 to 5.3 and Figures 5.1, 5.3 to 5.4, 5.7, 5.9 to 5.10 and 5.13, 5.15 to 5.16), there are 2 strong lines of evidence that ^{137}Cs has been redistributed in association with sediment. Firstly, in profiles with low inventories, the ^{137}Cs is strongly concentrated in the upper one or two depth increments; this indicates that there is minimal down-profile migration of ^{137}Cs in solution. Low inventories at these locations are the product of low activities in the surface horizons, consistent with progressive dilution of the cultivation layer with former subsoil as soil, lost by erosion, is replaced by cultivating deeper into formerly sub-plough layers. The second line of evidence comes from those profiles with greatly elevated ^{137}Cs inventories; these also show elevated ^{137}Cs activities to depths in the soil profile that significantly exceed the cultivation depth. This is consistent with movement of ^{137}Cs in association with eroded and redeposited soil, such that former cultivation layer is excluded from the actively mixed layer by 'burial'. That is, as deposition takes place, the absolute depth (with respect to datum) of cultivation is reduced – the base of the cultivation layer rises, year on year. Given these observations, I have confidence that ^{137}Cs can be used as a tracer of soil redistribution within this environment and that those areas with depleted ^{137}Cs inventories can be considered to have suffered erosion and those areas with elevated inventories can be treated as subject to deposition. However, given the uncertainties with respect to definition of the fallout reference inventory (section 4.3), in this chapter, no attempt is made to derive erosion rates from the ^{137}Cs data. Instead,

in this chapter ^{137}Cs is used as a tracer of soil redistribution but this is achieved by comparing spatial patterns of C, N and P directly with spatial patterns of ^{137}Cs .

The spatial patterns of ^{137}Cs inventories are consistent with progressive downslope movement of soil from upslope to downslope as a result of water and tillage erosion (Govers *et al.*, 1996; Quine *et al.*, 1999; Thapa *et al.*, 2001; Van Oost *et al.*, 2005a). In 7 of the 9 fields, minimum ^{137}Cs inventories are found in the uppermost profile, which is often seen in terraced environments and attributed to the influence of tillage erosion (e.g. Quine *et al.*, 1999) because if the direction of flow of runoff is down the field, it is assumed that there would be insufficient flow to generate high erosion rates at these upslope locations. Furthermore, in a number of the fields, an abrupt change in ^{137}Cs activity and inventory is seen close to the mid slope (typically between P3 and P4). This is often represented in a sharp drop from a local high ^{137}Cs inventory to a very low inventory. This pattern would be consistent with former sub-division of the fields at these locations by a field bund that would prevent soil translocation by tillage across the bund line and, therefore, lead to soil and ^{137}Cs depletion below the bund.

In addition to evidence for tillage erosion, there is also ample evidence of the influence of intense water erosion where ^{137}Cs inventories are depressed over much of the field area, for example in DKF1 (lower half), DKF2, BGF2 and BGF3 (lower-half). This is also reflected in the absolute values of the mean inventories for most fields which lie significantly below the estimated fallout to the area (this is discussed further in Chapter 6). Overall, the spatial patterns of ^{137}Cs activity profiles and inventories along the slope transects are consistent with erosion induced soil redistribution leading to transfer of eroded from the upper slopes and some redeposition in lower parts of the fields. Similar observations of erosion-induced spatial variation of ^{137}Cs activity and inventories within field have been found by other study (Quine and Zhang, 2002; Vandenbygaart *et al.*, 2012; Nosrati *et al.*, 2015).

5.4.2 Vertical and lateral distribution of SOC concentration and inventory and relationships with ^{137}Cs

Overall, the pattern of SOC concentrations and inventories in all of the fields is similar and the existence of statistically significant correlations between ^{137}Cs and SOC (concentrations and inventories) suggests that soil redistribution is an important control on SOC distributions. There is a general pattern that SOC concentrations in the eroding (low- ^{137}Cs) upslope profiles are lower than in depositional (high- ^{137}Cs) downslope profiles. Also, in the eroding profiles, the highest SOC concentrations are only seen in the upper 10 cm after which a sharp decline is seen; whereas in deposition profiles higher concentrations are seen up to 30 cm and there is no sharp decline. Similar result also found by other study (Vandenbygaart *et al.*, 2012, Norsati *et al.*, 2015). The topographic association between low SOC inventories over the upper parts of fields and high inventories over the lower areas and the correlation between SOC and ^{137}Cs inventories, both provide strong evidence of the creation of spatial variation through redistribution of eroded material within the fields as has been reported in a number of previous studies (Quine and Zhang, 2002; Van Oost *et al.*, 2005a; Zhang *et al.*, 2006; De gryze *et al.*, 2008; Vandenbygaart *et al.*, 2012; Li *et al.*, 2013; Norsati *et al.*, 2015).

Despite these broad patterns of similarity between ^{137}Cs and SOC distributions, a number of clear differences are also seen. Firstly, the range of variation differs markedly between ^{137}Cs and SOC, with SOC showing smaller proportional differences between the lowest and highest SOC inventories. Secondly, the abrupt changes found in ^{137}Cs inventories that have been interpreted as the result of former field sub-division are either not seen or not as clearly seen in the SOC inventories. Therefore, when SOC inventories are regressed against ^{137}Cs inventories, although statistically significant relationships are found for the great majority of fields, R^2 values range from 0.35 to 0.72. This indicates that while soil redistribution has altered the spatial variability of SOC, there are other important controls on the spatial pattern of SOC. The finding of erosion control on SOC distribution is consistent several previous studies (Ritchie and McCarty, 2003; Afshar *et al.*, 2010; Martinez *et al.*, 2010; Vandenbygaart *et al.*, 2012; Nosrati *et al.*, 2015); however, the strength of the relationships found here are stronger in 7 out of 9 fields (Figure 5.19 to 5.21).

In addition to exploring the relationships between total ^{137}Cs and total SOC inventories, in this study, new insights into the controls on SOC inventories were sought be

comparing ^{137}Cs activity and SOC concentration for separate depth increments (Table 5.5 and Figure 5.22 to 5.24). These figures are quite complicated to interpret because of the range of controls that influence both SOC and ^{137}Cs . Some general patterns can be suggested:

- Higher ^{137}Cs activities per unit mass are indicative of higher proportions of 1960s plough soil (peak fallout occurred in 1963 and 80% fallout occurred before 1964 and it is assumed that the initial fallout was mixed evenly through the plough layer as in Quine and Van Oost, 2007)
- Lower ^{137}Cs activities per unit mass indicate either high proportions of subsoil mixed into cultivation layer or low probability of the layer having been near the surface in the fallout period.
- High ^{137}Cs and high SOC in the upper most depth increment is consistent with a stable or depositional soil in receipt of surface inputs of SOM.
- Low ^{137}Cs and high SOC in the upper most depth increment could be considered to be evidence of effective dynamic replacement in which SOC levels are maintained despite subsoil dilution.
- High ^{137}Cs and high SOC in a lower depth increment could be consistent with preservation of SOC in buried cultivation layer.
- High ^{137}Cs and low SOC in a lower depth increment would suggest that former cultivation layer has been buried but lost much of the initial SOC.

Based on these broad patterns, three examples can be examined that illustrate some of the variation in behaviour (Figure 5.26). At Site 1, field DKF2 (Figure 5.26a) two of these patterns are evident. First, high SOC concentrations are seen in the upper-most depth increment even where ^{137}Cs activity per unit mass is relatively low. Second, there are a group of samples from the 10-20 and 20-30 cm depth increments that have high ^{137}Cs activity, indicating a substantial proportion of former plough soil, but low SOC concentration compared to current plough soil, indicating loss of C from this buried plough soil. At Site 2, field PSF3 (Figure 5.26b), there is again evidence of dynamic replacement in high SOC concentrations in surface samples that are depleted in ^{137}Cs . However, the behaviour of deeper soils contrasts with the previous site and there is evidence of deeper soil increments with high SOC concentration, indicative of effective preservation. At Site 3, field BGF3 (Figure 5.26c), C concentrations in the

surface increments are significantly higher for the same ^{137}Cs activity than deeper soil increments. This emphasises the importance of the redistribution of this surface layer in determining within field SOC variability.

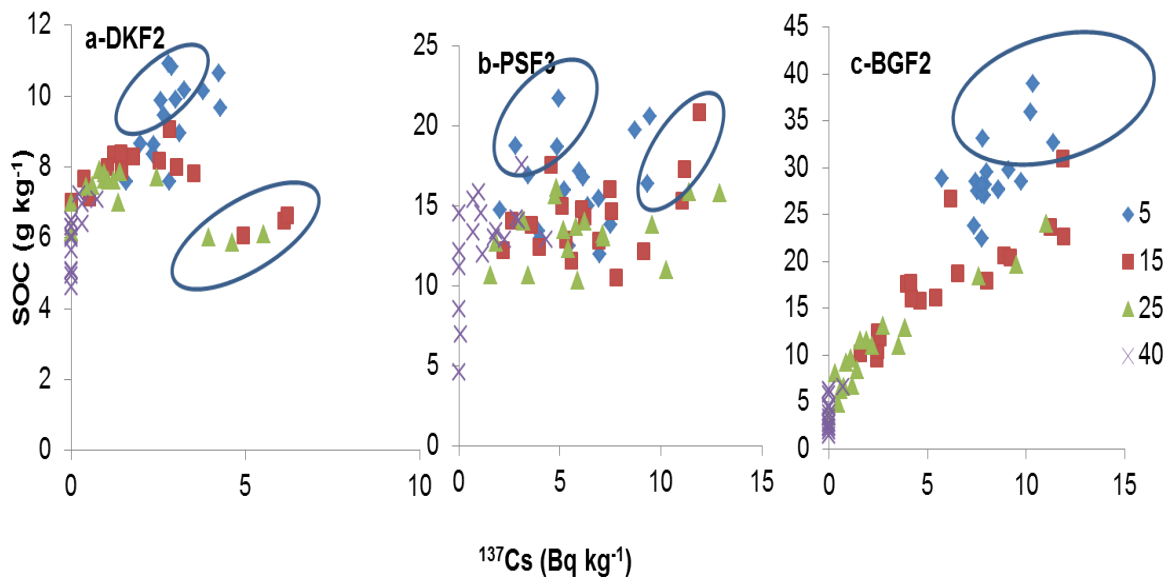


Figure 5.26 Depth wise ^{137}Cs and C reflect possible mechanism on C dynamic based on redistribution process (a-DKF2 from Site 1; b-PSF3 from Site 2 and c-BGF2 from Site 3)

Figures 5.22-5.24 and Figure 5.26 all make clear the variation in SOC concentration among the sites. Mean SOC concentrations at Site 1 are lowest (nearly 1% SOC); followed by Site 2 (nearly 1.5% SOC); and Site 3 has the highest (2.5% of SOC). This variation may be due to usage of organic inputs for crop growth and due to microclimate pattern. At the study Site 1, near to the city (Dehradun), the farmers use less forest litter as manure due to both ease of access and regulation; whereas, at Sites 2 and 3 away from the city and near to forest they use more forest litter as a manure and animal and house hold waste as manure for crop production. Also the higher SOC concentration at Site 3 may be due to climatic effects related to the higher elevation (1600m), including a comparatively low temperature (approximately 3°C lower than other sites) and higher rainfall (approximately 200mm more than other

sites). These may contribute to lower mineralisation of SOC and more crop and biomass production than at other sites.

5.4.3 Vertical and lateral distribution of total N concentration and Inventory and Relationships with ¹³⁷Cs

In general, the patterns of total N concentrations and inventories in all fields are similar and the existence of statistically significant correlations between ¹³⁷Cs and total N (concentrations and inventories) suggest that soil redistribution is an important control on total N distributions. Similar to SOC, total N concentrations in the eroding upslope profiles are lower than in depositional downslope profiles. In eroding and deposition profiles, total N concentrations in the upper 10 cm layer are almost equal; however, it is observed that N concentration declines rapidly below 10 cm in eroding profiles but the decline is much more gradual in depositional profiles. The pattern of low total N inventories in the upper parts of the fields and high inventories over the downslope areas and correlation between total N and ¹³⁷Cs inventories, both provide strong evidence of spatial variation due to redistribution of eroded material within fields (Quine and Zhang, 2002; De Gryze *et al.*, 2008; Berhe *et al.*, 2014).

The relationships between ¹³⁷Cs and total N inventories were tested for all study site to the sampling depth of 50cm. Positive and strong statistically significant relationships were found for the majority of the sites (7 out of 9) and R² values ranged from 0.38 to 0.78 (Figure 5.19 to 5.21). One exception was Site 1, field DKF2, where there was no relationship between ¹³⁷Cs and total N inventory (R² = 0.06). The reason for this is not known but may be due to the pattern of fertilizer application by the farmers. In all the other fields strong significant relationship between ¹³⁷Cs and total N were found, which indicate that erosion induced soil redistribution has altered the spatial variability of total N. This finding is consistent with similar relationships noted in other studies (Quine and Zhang, 2002; Vandenbygaart *et al.*, 2012). The total N concentrations/inventory relationships with ¹³⁷Cs are very similar to those seen with SOC.

5.4.4 Vertical and lateral distribution of P (total and Organic P) concentration and Inventory and Relationships with ¹³⁷Cs

The pattern of P inventories in field from (Site 1 and Site 2) exist statistically significant correlation with ¹³⁷Cs suggest that soil redistribution is an important control on P redistribution but this pattern not exist in Site 3. This indicate the P pattern with ¹³⁷Cs may be influenced by other parameters such as CaCO₃ level, weathering and release of P (Theocharopoulos *et al.*, 2003; Ni and Zhang, 2007) because Site 3 fall under calcareous but other sites are fall in acidic type. Similar like SOC and total N, the P concentrations in the upslope profiles are lower than downslope deposition profiles. Also the pattern of P in top 10 cm soil layer almost similar concentration in all slope positions, this pattern also almost similar with SOC and total N. The pattern of low inventories of P at eroding part and high in aggradation part of field provide strong evidence of spatial variation due to redistribution of eroded material within fields (Quine and Zhang, 2002; Li *et al.*, 2013).

5.4.5 Vertical and lateral distribution of C:N and C:OP ratio

CN ratio along slope transect from eroding upslope to deposition downslope point exist three different pattern in my study area. Some fields eroding profile found narrow C:N ratios (DKF2, PSF2 , PSF3) and some eroding upslope profile found wider CN ratio (DKF1, PSF1). In Site 3 (BGF1 and BGF2) there was no clear pattern observed for C:N ratios. Similar results were also found by other study (Vandenbygaart *et al.*, 2012). This pattern of narrow C:N ratios at eroding profiles may be due to loss of top soil and mixing of subsoil with narrow C:N ratio creating this dilution.

The C:OP ratios show wide variation and no consistent pattern. In some fields top soil along the entire slope looks similar but in deep layers eroding upslope profiles have narrow ratios than deposition profiles. In other fields, eroding profile have narrower C:OP ratios than deposition profiles over the entire depth. Quinton *et al.*, 2010 reported more P variation within agricultural fields than other nutrients. This may be due to fertilization, weathering and other soil properties influence on P dynamics.

5.5. Conclusion

The data analysis undertaken in this chapter had the primary objective of addressing research objective 1: *To quantify the impacts of erosion-induced soil redistribution on SOC and nutrients (lateral and vertical) within agricultural fields.* Additionally, this research objective also provides a foundation for the following research objectives and chapters. The analysis carried out in this chapter assumed the overall null hypothesis: **H₀**: Erosion-induced redistribution of soils (top- / sub-soil) changes within field spatial variation of soil nutrient stocks and stoichiometry (C:N:P ratio), so that eroded sites will have lower SOC and nutrient stocks than sites of deposition.

This null hypothesis cannot be rejected for the following reasons:

- Statistically significant differences were found in nutrient and SOC concentrations and inventories between profiles in different topographic settings, with upslope profiles containing ($p < 0.05$) lower nutrient and SOC inventories than downslope profiles.
- In the majority of fields, strong statistically significant relationships were found between ^{137}Cs inventories and nutrients (total N, and P) and SOC.

5.6. Key findings

^{137}Cs

- Upslope and midslope ^{137}Cs activity profiles show lower activity in the upper 30 cm and lower depth penetration of ^{137}Cs . These are properties consistent with erosion. Several downslope profiles are enriched in ^{137}Cs in the upper 30 cm and demonstrate depth penetration to 50 cm depth. These are properties consistent with deposition.
- The lateral pattern of ^{137}Cs inventories along the slope transects, typically showed statistically significantly lower inventories in upslope and midslope profiles than downslope profiles.
- These patterns are consistent with ^{137}Cs redistribution in association with soil redistribution and the suitability of ^{137}Cs as an erosion tracer in this environment.

- Abrupt changes in ^{137}Cs inventory after midslope positions in a number of fields are considered most likely to be the result of the former presence of a field bund (temporary boundary) that farmers have removed.

SOC

- In up and midslope profiles, SOC exhibits high concentrations in only the top layers and then declines sharply. In deposition profiles, SOC concentrations are high to greater depths and only a gradual decline in concentration is observed.
- The absence of significant variation in SOC in the uppermost layer (0-10 cm) is consistent with rapid dynamic replacement of SOC at eroded locations.
- The lateral pattern of SOC inventories along the slope transects, typically showed statistically significantly lower inventories in upslope and midslope profiles than downslope profiles. This mirrors the pattern seen in ^{137}Cs inventories.
- The abrupt changes in ^{137}Cs along the slope transect, attributed to the former presence of field bunds, are not seen in SOC. This suggests that the timescale of recovery of SOC is relatively short (shorter than the half century associated with ^{137}Cs).

Total N

- In up and midslope profiles, total N exhibits high concentrations in only the top layers and then declines sharply. In deposition profiles, total N concentrations are high to greater depths and only a gradual decline in concentration is observed. This is consistent with the pattern observed in SOC.
- Total N is less consistent in pattern than SOC and while some fields display similar concentrations in the surface layers over the whole field, others do not.
- The lateral pattern of total N inventories along the slope transects, typically showed statistically significantly lower inventories in upslope and midslope profiles than downslope profiles. This mirrors the pattern seen in ^{137}Cs and SOC inventories.
- As in the case of SOC, the abrupt changes in ^{137}Cs along the slope transect, attributed to the former presence of field bunds, are not seen in total N. This suggests that the timescale of recovery of total N is also relatively short (shorter than the half century associated with ^{137}Cs).

- Overall, the along slope within field redistribution pattern is similar for SOC and total N inventories.

CN ratio

- Some eroding profiles have narrow C:N ratio and some have wider C:N ratio and some field don't have clear pattern of C:N ratio.

OP, TP and C OP ratio

- A clear pattern of OP and TP inventory depletion in upslope and enrichment in downslope profiles was observed for acidic soils.
- No relationships between topography and OP and TP were seen in the calcareous fields.

Linear regression for ^{137}Cs vs SOC and total N and P

- In the great majority of the fields, strong statistical relationships were found between ^{137}Cs and SOC and total N inventories.
- Strong significant relationships were found between ^{137}Cs and OP and TP inventories in acidic soils but not in calcareous soils.

6. Effect of soil redistribution on the net flux of C between soil and the atmosphere within the agricultural fields

6.1. Introduction

The review of the literature in chapter 2 and statement of objectives in chapter 3 highlighted the continuing debate concerning the significance and effect of soil redistribution on net C flux between the soil and the atmosphere (Stallard, 1998; Lal *et al.*, 2004; Berhe *et al.*, 2007; Van Oost *et al.*, 2007; Lal and Pimentel, 2008; Doetterl *et al.*, 2016). Where these studies investigated agricultural fields, these were typically in receipt of high nutrient inputs and subject to mechanised farming processes (Quine and Van Oost, 2007; Van Oost *et al.*, 2007). Highly eroding field loss onsite nutrients affect crop growth, reduce net return of biomass and finally reduce C sink. Eroded field managed well with proper nutrient supply, crop production will maintained and C sink continued (Li *et al.*, 2015). There is a need for similar but comparative studies in low input/ low productivity farm lands, where net return of biomass will be low. Based on this existing research gap, I conducted this study in a highly eroding (Singh and Gupta, 1982; Narayana and Ram Babu, 1983; Khola and Sastry., 2005; Singh *et al.*, 2016), low input farm land area low productivity within the foothills of the Indian Himalaya. As a result of low input of fertilizers, cultivation on slopes and high erosion the study area is considered to be an area of low crop productivity when compared with the national average for India and with developed countries (mechanised farm lands) (Tiwari *et al.*, 2005; Tiwari, 2007; Madhu and Sharda, 2011; Ghosh *et al.*, 2012; Singh *et al.*, 2016; FAO-Stat, 2016). This low productivity equates to a low return of biomass, which consequently means a lower return of C to soil. This study area also uses farm residues to feed agricultural farm stock (e.g., farm animals, fuels), which further alters the C return to the soil (Bhattacharyya *et al.*, 2009). As described in Chapter 4, I used ¹³⁷Cs fallout and SOC inventories following the approach adopted by Quine and Van Oost (2007) in order to assess the following null hypothesis:

H₀: Erosion-induced soil redistribution results in a net carbon sink when continuous crop production is maintained, despite low fertiliser inputs, low crop productivity and high biomass removal.

The methods used are described in detail in Chapter 4 (section 4.3) and the SOC and ^{137}Cs data have been discussed in Chapter 5. Here the focus is on the calculated soil redistribution rates and the derived net C fluxes between soil and atmosphere at each soil profile and within each field. Additional data used in calculations are included in Appendix Table 6.1 to 6.3.

6. 2. Result

As discussed in section 4.3, there is significant uncertainty in determining the ^{137}Cs fallout reference inventory and, therefore, the value derived using global data (1685 Bq m^{-2}) is used as the default in sections 6.2.1 – 6.2.3 and sensitivity to this assumption is explored by varying reference inventory in section 6.2.4.

6.2.1. Point/profile scale and field scale soil redistribution rates and budgets

Site1

Soil redistribution rates (derived from ^{137}Cs data using the methodology outlined in section 4.3) for Site 1 (DKF1 to DKF3) are presented in Table 6.1. Negative values indicate net soil loss and those that are positive value indicate net soil deposition. The data in Table 6.1 indicate that (under the assumptions noted above with respect to reference inventory) the site as a whole is dominated by erosion, with only the lower-most pits in fields DKF1 and DKF2 being subject to net deposition. The within-field patterns are as discussed in Chapter 5. Within field 1, there is reduction in erosion rate over the first three pits followed by a sharp increase in erosion, possibly reflecting the former position of a bund (line of zero downslope flux) upslope of pit 4. Field 2 shows a simpler pattern of elevated erosion over most of the field area, consistent with significant water erosion, while field 3 shows lower erosion rates over the upper, lower gradient part of the field and a significant increase in erosion rate over the steeper section (Figure 4.2c). Individual point rates vary as follows in DKF1 soil loss range from 0.72 ± 0.15 to $3.81 \pm 0.13 \text{ kg m}^{-2} \text{ y}^{-1}$ and soil deposition is $1.14 \pm 0.35 \text{ kg m}^{-2} \text{ y}^{-1}$. In field DKF2 four pits fall under soil loss and rates range from 3.10 ± 0.67 to $6.00 \pm 0.60 \text{ kg m}^{-2} \text{ y}^{-1}$ and one pit under deposition is $0.44 \pm 0.45 \text{ kg m}^{-2} \text{ y}^{-1}$. For field DKF3 all pits under eroding condition and rates range from 0.96 ± 0.77 to $7.49 \pm 0.98 \text{ kg m}^{-2} \text{ y}^{-1}$. Field-scale summary data are reported in Table 6.4 and show some consistency between fields with mean erosion rates varying from 2.4 to $3.2 \text{ kg m}^{-2} \text{ y}^{-1}$ and export rates varying from 2.3 to $3.2 \text{ kg m}^{-2} \text{ y}^{-1}$, reflecting the minimal within-field sediment deposition in fields 1 and 2 of $0.1 \text{ kg m}^{-2} \text{ y}^{-1}$.

Site 2

Soil redistribution rate for Site 2 (PSF1 to PSF3) are presented in Table 6.2. Data in this table reflect all three fields upslope pits (P1 and P2) eroded higher than others mid slope (except field 1) and all fields lower most pits deposition occurs. Compare with other two sites (Site 1 and 3) this site has lower net erosion but higher deposition than others. This higher deposition indicates these fields comparatively large area under concave slope than other sites (Figure 4.2d to f). Site 2 in Figure 5.8 all 3 fields ^{137}Cs show pattern consistent with former presence of a bund after mid slope (P3/P4) – this is reflected in within-field patterns of soil erosion (Table 6.2) and nutrient changes. Field 1 is unusual in having high inventories over much of the field area – may be receiving soil from other fields upslope. In PSF1 one pit fall under eroding /soil loss location and remaining pits fall under deposition/ soil gain area, soil deposition range from 0.83 ± 0.17 to $2.01 \pm 0.33 \text{ kg m}^{-2} \text{ y}^{-1}$ and soil loss is $3.76 \pm 0.34 \text{ kg m}^{-2} \text{ y}^{-1}$. In field PSF2 four pits were fall under soil loss and it range from 0.37 ± 0.21 to $2.57 \pm 0.28 \text{ kg m}^{-2} \text{ y}^{-1}$ and three pits under deposition and it range from 0.27 ± 0.06 to $0.86 \pm 0.49 \text{ kg m}^{-2} \text{ y}^{-1}$. In field PSF3 five pits were fall under soil loss and it range from 0.53 ± 0.22 to $4.52 \pm 0.39 \text{ kg m}^{-2} \text{ y}^{-1}$ and one pit under deposition is $1.28 \pm 0.52 \text{ kg m}^{-2} \text{ y}^{-1}$. The summary of soil redistribution rate for each field of Site 3 presented in Table 6.4, the fields with mean erosion rates varying from 0.53 to $1.41 \text{ kg m}^{-2} \text{ y}^{-1}$, export rates from -0.40 to $1.12 \text{ kg m}^{-2} \text{ y}^{-1}$, and within-field sediment deposition is 0.28 to $1.01 \text{ kg m}^{-2} \text{ y}^{-1}$.

Site 3

For Site 3 (BGF1 to BGF3) Soil redistribution rate presented in Table 6.3. Except one pit (P6) in field 2 (BGF2) received soil deposition remaining all pits in Site 3 fields were under exposed soil erosion. This Site 3 erosion rates were higher than Site 2 but not as high as Site 1. In field 2 (BGF2) after P3 increase erosion rate reflecting possible former position of field bund like Site 1 field 1. Similar pattern exists in field 3 (BGF3) after P2 but here still field bund exists this pattern confirmed by ^{137}Cs inventory and topography changes (Figure 4.2g to l and 5.9g). In field 1 and 2 upper slope part of field eroded more than other part. But in field 3 upper part of field less eroded than lower part of field this reflect effect of presence of field bund after P2. The range of soil loss for the field BGF1 is from 0.53 ± 0.09 to $3.57 \pm 0.25 \text{ kg m}^{-2} \text{ y}^{-1}$ and for field BGF3 is from 0.44 ± 0.31 to $2.94 \pm 0.10 \text{ kg m}^{-2} \text{ y}^{-1}$. For the field BGF2 five pits were fall under

eroding/soil loss location and one pit fall under deposition/soil gain area. In this field BGF2 soil loss range from 0.56 ± 0.10 to 2.25 ± 0.33 $\text{kg m}^{-2} \text{y}^{-1}$ and soil deposition is 1.85 ± 0.57 $\text{kg m}^{-2} \text{y}^{-1}$. Over all summary of soil redistribution rate presented in Table 6.4, the fields with mean erosion rates varying from 1.53 to 2.02 $\text{kg m}^{-2} \text{y}^{-1}$, export rates range from 1.31 to 2.02 $\text{kg m}^{-2} \text{y}^{-1}$, and within-field sediment deposition is 0.22 $\text{kg m}^{-2} \text{y}^{-1}$.

Table 6.1 Site 1 Dhulkhot (DK); profile scale soil redistribution rate (SR), CCI, CII and Net C flux derived using the following parameters: ^{137}Cs inventory 1685 Bq m^{-2} , reference C inventory 4.6 kg m^{-2} up to 50 cm and plough depth (PD) 0.14 m. Mean values \pm SE ($n = 3$) are presented.

Sites	Fields	Profile	Mid Leng	SR rate ($\text{kg m}^{-2} \text{ y}^{-1}$)	CCI ($\text{g m}^{-2} \text{ y}^{-1}$)	CII ($\text{g m}^{-2} \text{ y}^{-1}$)	Net C flux ($\text{g m}^{-2} \text{ y}^{-1}$)
Site 1	DKF1	P1	10.1	-3.53 ± 0.13	55.8 ± 1.24	65.7 ± 2.1	-10.6 ± 0.6
		P2	12.2	-1.94 ± 0.08	42.3 ± 1.17	44.5 ± 0.9	-4.0 ± 0.6
		P3	12.9	-0.72 ± 0.15	27.1 ± 1.77	33.1 ± 1.2	-15.7 ± 2.0
		P4	14.3	-3.81 ± 0.13	74.3 ± 5.24	70.5 ± 2.4	3.6 ± 2.6
		P5	10.5	-3.53 ± 0.10	84.9 ± 4.28	65.7 ± 1.7	20.7 ± 3.3
		P6	5.9	1.14 ± 0.35	27.4 ± 2.76	24.2 ± 1.0	12.1 ± 5.9
Site 1	DKF2	P1	8.2	-6.00 ± 0.60	119.8 ± 22.2	125.9 ± 20.0	-3.2 ± 4.1
		P2	10.8	-3.27 ± 0.30	72.3 ± 8.15	62.0 ± 4.8	11.3 ± 3.0
		P3	10.7	-3.10 ± 0.67	35.3 ± 3.03	52.5 ± 9.1	-19.2 ± 2.8
		P4	11.1	-3.16 ± 0.42	61.9 ± 7.79	60.6 ± 6.5	1.3 ± 3.8
		P5	9.2	0.44 ± 0.45	26.6 ± 2.48	26.9 ± 1.7	-1.7 ± 3.8
Site 1	DKF3	P1	8.0	-0.96 ± 0.77	33.7 ± 6.92	36.8 ± 5.5	-9.3 ± 6.1
		P2	18.1	-1.82 ± 0.27	44.8 ± 4.62	43.3 ± 2.8	2.1 ± 3.7
		P3	15.2	-2.01 ± 0.19	47.3 ± 2.51	45.3 ± 2.2	3.8 ± 5.9
		P4	8.9	-7.49 ± 0.98	268.3 ± 103	196.8 ± 56.4	15.8 ± 5.5
		P5	8.8	-5.63 ± 0.86	139.8 ± 32.1	117.0 ± 22.4	10.2 ± 3.5
		P6	14.9	-3.48 ± 0.42	54.5 ± 7.43	65.6 ± 7.2	-12.4 ± 2.2

Table 6.2 Site 2 Pasauli (PS); profile scale soil redistribution rate (SR), CCI, CII and Net C flux derived using the following parameters for PSF1 and PSF2: ^{137}Cs inventory 1685 Bq m^{-2} , reference C inventory 5.3 kg m^{-2} up to 50 cm; plough depth 0.19 m for PSF1 and 0.26 m for PSF2. For PSF3, the following were used ^{137}Cs inventory 2100 Bq m^{-2} and reference C inventory 6.09 kg m^{-2} up to 50cm.

Sites	Fields	Profile	Mid Leng	SR rate ($\text{kg m}^{-2} \text{y}^{-1}$)	CCI ($\text{g m}^{-2} \text{y}^{-1}$)	CII ($\text{g m}^{-2} \text{y}^{-1}$)	Net C flux ($\text{g m}^{-2} \text{y}^{-1}$)
Site 2	PSF1	P1	9.9	-3.76 ± 0.34	244 ± 48.2	104 ± 9.98	39.6 ± 6.78
		P2	10.7	0.93 ± 0.09	42.0 ± 1.13	40.7 ± 0.21	3.27 ± 2.54
		P3	9.5	2.01 ± 0.33	37.2 ± 0.80	38.3 ± 0.75	-3.09 ± 1.78
		P4	10.5	1.22 ± 0.29	57.7 ± 3.01	40.0 ± 0.63	45.0 ± 4.47
		P5	12.3	0.83 ± 0.17	63.6 ± 0.77	40.9 ± 0.38	54.3 ± 1.27
		P6	10.1	1.17 ± 0.04	62.7 ± 2.71	40.1 ± 0.09	57.5 ± 6.96
Site 2	PSF2	P1	10.5	-2.57 ± 0.28	33.8 ± 1.60	51.9 ± 1.84	-20.2 ± 1.76
		P2	9.7	-1.30 ± 0.11	29.3 ± 2.52	44.4 ± 0.57	-26.9 ± 4.62
		P3	10.5	-0.74 ± 0.39	33.6 ± 4.85	41.8 ± 1.87	-19.5 ± 8.16
		P4	15.2	0.54 ± 0.09	31.7 ± 1.42	36.9 ± 0.23	-16.7 ± 4.16
		P5	19.8	-0.37 ± 0.21	59.0 ± 5.01	40.0 ± 0.97	45.4 ± 6.29
		P6	20.3	0.27 ± 0.06	39.4 ± 0.58	37.6 ± 0.16	5.51 ± 1.87
		P7	17.9	0.86 ± 0.49	34.0 ± 2.67	36.2 ± 1.14	-8.57 ± 7.60
Site 2	PSF3	P1	10.3	-4.52 ± 0.39	107 ± 16.3	69.7 ± 4.51	18.8 ± 3.90
		P2	9.7	-2.19 ± 0.54	67.4 ± 16.3	49.7 ± 3.51	17.5 ± 10.3
		P3	10.6	-0.53 ± 0.22	39.5 ± 4.52	40.7 ± 1.01	-4.03 ± 9.44
		P4	10.5	-1.12 ± 0.11	50.7 ± 6.19	43.5 ± 0.54	13.0 ± 10.3
		P5	9.2	-0.74 ± 0.10	51.5 ± 2.20	41.7 ± 0.48	21.4 ± 5.65
		P6	14.8	1.28 ± 0.52	32.7 ± 1.59	35.5 ± 1.11	-10.7 ± 2.73

Table 6.3 Site 3 Bhatta Gaon (BG); profile scale soil redistribution rate (SR), CCI, CII and Net C flux derived using the following parameters: ^{137}Cs inventory 1685 Bg m^{-2} , reference C inventory 5.5 kg m^{-2} up to 50 cm and plough depth 0.24 m. Mean values \pm SE ($n = 3$) are presented.

Sites	Fields	Profile	Mid Length(m)	SR rate ($\text{kg m}^{-2} \text{ y}^{-1}$)	CCI ($\text{g m}^{-2} \text{ y}^{-1}$)	CII ($\text{g m}^{-2} \text{ y}^{-1}$)	Net C flux ($\text{g m}^{-2} \text{ y}^{-1}$)
Site 3	BGF1	P1	7.8	-3.57 ± 0.25	78.5 ± 0.96	67.6 ± 3.50	11.1 ± 5.54
		P2	9.7	-2.56 ± 0.09	61.6 ± 2.45	55.0 ± 0.95	8.65 ± 2.18
		P3	9.1	-2.58 ± 0.27	38.2 ± 1.42	55.4 ± 2.90	-22.5 ± 0.97
		P4	7.6	-1.33 ± 0.17	44.3 ± 6.01	44.3 ± 1.23	-0.43 ± 10.3
		P5	6.9	-0.77 ± 0.04	40.6 ± 0.96	40.5 ± 0.24	0.29 ± 2.28
		P6	5.1	-0.53 ± 0.09	50.0 ± 0.47	35.5 ± 0.48	37.7 ± 3.02
		P7	3.8	-1.82 ± 0.20	60.9 ± 3.11	48.2 ± 1.70	21.4 ± 2.89
Site 3	BGF2	P1	7.1	-2.25 ± 0.33	51.7 ± 0.86	52.2 ± 3.07	0.00 ± 3.61
		P2	7.8	-2.18 ± 0.32	51.6 ± 4.74	51.6 ± 2.88	1.77 ± 10.2
		P3	7.7	-0.56 ± 0.10	37.7 ± 1.88	39.1 ± 0.60	-3.73 ± 3.45
		P4	7.7	-2.21 ± 0.29	59.7 ± 1.46	51.8 ± 2.85	12.6 ± 5.13
		P5	6.7	-1.48 ± 0.20	48.4 ± 2.94	45.4 ± 1.58	5.69 ± 5.64
		P6	5.0	1.85 ± 0.57	28.0 ± 1.21	28.8 ± 0.85	-2.44 ± 5.21
Site 3	BGF3	P1	7.8	-0.99 ± 0.48	35.5 ± 2.91	38.3 ± 2.88	-6.28 ± 1.91
		P2	10.1	-0.44 ± 0.31	39.8 ± 3.50	38.5 ± 1.87	2.82 ± 4.13
		P3	10.7	-2.41 ± 0.29	54.9 ± 3.60	53.7 ± 2.93	1.48 ± 1.53
		P4	10.5	-2.94 ± 0.10	60.7 ± 3.33	59.2 ± 1.19	1.80 ± 3.70
		P5	5.9	-1.55 ± 0.31	78.0 ± 4.39	46.1 ± 2.49	58.7 ± 2.66

Table 6.4 Soil redistribution budgets for all sites based on profile data.

	Site 1 Dhoolkhot			Site 2 Pasauli			Site 3 Bhatta Gaon			Mean	SE
	DKF1	DKF2	DKF3	PSF1	PSF2	PSF3	BGF1	BGF2	BGF3		
	(Soil redistribution rate in $\text{kg m}^{-2} \text{y}^{-1}$)										
<i>Eroded area % of field</i>	91.1	81.7	100.0	16.1	48.6	77.2	100.0	88.0	100.0	78.1	9.5
Mean Erosion /subsoil excavation rate	2.67	3.74	3.24	3.76	1.08	1.83	2.02	1.74	1.73	2.42	0.32
Cultivation layer export	1.71	2.15	1.84	1.71	0.81	1.16	1.40	1.28	1.22	1.47	0.14
Subsoil in export	0.95	1.59	1.42	2.06	0.28	0.67	0.62	0.46	0.51	0.95	0.20
Fraction of cultivation layer in export	0.64	0.58	0.57	0.45	0.74	0.63	0.69	0.74	0.71	0.64	0.03
<i>Deposition area % of field</i>	8.92	18.32	0.00	83.90	51.41	22.79	0.00	12.00	0.00	21.93	9.45
Mean Deposition	1.14	0.44	0.00	1.20	0.54	1.28	0.00	1.85	0.00	0.72	0.23
Burial of Initial cultivation layer	0.84	0.39	0.00	0.75	0.45	0.88	0.00	1.15	0.00	0.50	0.15
Initial cultivation layer in import	0.73	0.25	0.00	0.55	0.40	0.81	0.00	1.36	0.00	0.46	0.15
Sub soil in import	0.41	0.19	0.00	0.66	0.14	0.47	0.00	0.49	0.00	0.26	0.08
Burial of imported Initial cultivation layer	0.19	0.03	0.00	0.20	0.07	0.25	0.00	0.51	0.00	0.14	0.06
Burial of imported subsoil	0.11	0.02	0.00	0.25	0.02	0.15	0.00	0.18	0.00	0.08	0.03
Replacement of cultivation soil by subsoil in cultivation layer	0.30	0.17	0.00	0.41	0.12	0.32	0.00	0.31	0.00	0.18	0.05
<i>Whole field</i>											
Whole field area (ha)	0.13	0.15	0.16	0.13	0.32	0.10	0.06	0.05	0.05	0.13	0.03
Whole field slope %	2.91	2.24	2.84	5.89	6.59	6.15	1.84	4.05	4.21	4.08	0.59
Mean erosion rate	2.43	3.06	3.24	0.61	0.53	1.41	2.02	1.53	1.73	1.84	0.32
Mean aggradation rate	0.10	0.08	0.00	1.01	0.28	0.29	0.00	0.22	0.00	0.22	0.11
Net export rate	2.33	2.98	3.24	-0.40	0.25	1.12	2.02	1.31	1.73	1.62	0.40

6.2.2. Point/profile scale CCI (Carbon Concentration Index) and CII (Carbon Inheritance Index) comparison with SR rate

As discussed in section 4.3, the Carbon Inheritance Index (CII) is a measure of the expected C content of a profile (per unit mass of 1963 plough soil) if equilibrium conditions were maintained across the field and inventories were, therefore, determined by soil redistribution. The Carbon Concentration Index (CCI) is expressed in the same units and provides a measure of the SOC currently in the profiles. Therefore, where CCI exceeds CII, this provides evidence of net sequestration of atmospheric C, whereas where CII exceeds CCI this suggests net loss of C from the soil to the atmosphere. In this section, CCI and CII are plotted against soil redistribution rates (as reported in 6.2.1) to allow the control of erosion on CCI, CII and net exchange with the atmosphere to be explored.

Site 1

The CCI and CII for Site 1 are compared and presented in Table 6.1 and Figure 6.1. At Site 1, profiles are equally split between those in which CCI exceeds CII and in which CII exceeds CCI; however, in all cases the values are similar, suggesting that the C stocks in these fields are close to equilibrium. The largest deviations between CCI and CII are seen in the most eroded locations, whereas in profiles where deposition has occurred there is very little difference. Large differences between CCI and CII values in the most eroded profiles indicate that erosion has induced significant disequilibrium between inputs, respiration and inventory and has facilitated sequestration of C in the most eroded places (Figure 6.1 d-f). In Site 1 the net C flux from atmosphere to soil at the eroded profiles ranges from -19.2 ± 2.8 to $20.7 \pm 3.3 \text{ g m}^{-2} \text{ y}^{-1}$ and in deposition area ranges from -1.7 ± 3.8 to $12.1 \pm 5.9 \text{ g m}^{-2} \text{ y}^{-1}$ (negative values indicate a flux from soil to atmosphere).

Site 2

At Site 2, the pattern is more complex (Figure 6.2). In the eroded area of field PSF1 and of field PSF3 broadly the same pattern is seen, with the most eroded sites associated with high CCI values and the largest differences between CCI and CII. In contrast, at field PSF2, differences between CCI and CII are relatively small and the eroded areas of the field are associated with CCI values that are lower than CII values. These results appear to indicate that high erosion rates are driving a net sink in the most highly eroding areas of fields 1 and 3 but a net source from the most highly eroding areas in field 2. In Field PSF1 (Figure 6.2d) there is only one profile in the

eroded area and this exhibits a field net C flux from atmosphere to soil of $39.6 \pm 6.78 \text{ g m}^{-2} \text{ y}^{-1}$, whereas the deposition locations range from -3.09 ± 1.78 to $57.5 \pm 6.96 \text{ g m}^{-2} \text{ y}^{-1}$. Overall field PSF1 acted as a net C sink. In PSF2 (Figure 6.2e) eroded pits (P1–P3) acted as a net C source range from -19.5 ± 8.16 to $-26.9 \pm 4.62 \text{ g m}^{-2} \text{ y}^{-1}$ and also two deposition pits (P4 and P6) acted as a net C source range from -8.57 ± 7.60 to $-16.7 \pm 4.16 \text{ g m}^{-2} \text{ y}^{-1}$. P5 eroded pit and P6 depositional pit acted as a net C sinks of $45.4 \pm 6.29 \text{ g m}^{-2} \text{ y}^{-1}$ and $5.51 \pm 1.87 \text{ g m}^{-2} \text{ y}^{-1}$, respectively. In field PSF3 (Figure 6.2f) eroded pits (P1,P3,P4 and P5) exhibit net C fluxes from atmosphere to soil that range from 13.0 ± 10.3 to $21.4 \pm 5.65 \text{ g m}^{-2} \text{ y}^{-1}$. Deposition pit (P6) and one eroded pit (P2) acted as a C source with net C fluxes of -10.7 ± 2.73 and $-4.03 \pm 9.44 \text{ g m}^{-2} \text{ y}^{-1}$, respectively.

Note: For Site 2 field PSF3 C flux estimation was undertaken using a higher level of reference ^{137}Cs inventory (2100 Bq m^{-2}) to account for lateral redistribution of sediment to the field.

Site 3

The CCI and CII values for Site 3 are presented in Figure 6.3 and exhibit patterns that are similar to Sites 1 and 2. Most eroded locations acted as C sink and very few erosional pits and one depositional pit acted as a C source. The large differences between CCI and CII values in the most eroded profiles indicate that erosion has induced significant disequilibrium and has facilitated high rates of sequestration in the most eroded places (Figure 6.3 d-e). In Site 3 the net C flux from atmosphere to soil at eroded pits range from 0.00 ± 3.61 to $58.7 \pm 2.66 \text{ g m}^{-2} \text{ y}^{-1}$. Few eroded pits acted as C source with a range from -0.43 ± 10.3 to $-22.5 \pm 0.97 \text{ g m}^{-2} \text{ y}^{-1}$ and one depositional pit also acted C source at $-2.44 \pm 5.21 \text{ g m}^{-2} \text{ y}^{-1}$.

All sites

For each site, the C flux and soil redistribution data from all 3 fields are presented on a single plot in Figure 6.5a to c; while figure 6.5d allows all data to be compared on a single plot. These figures reveal that with few exceptions the relationships between C flux between soil and atmosphere and soil redistribution rates are broadly similar. With the exception of PSF1 and a small number of pits in other fields, fluxes vary between $+30$ and $-30 \text{ g m}^{-2} \text{ y}^{-1}$.

6.2.3. Field-scale and Site C budgets

Following the approach of Quine and Van Oost (2007), carbon budgets were developed for each field in which carbon stores and transfers are inferred using both the equilibrium and measured SOC profile data. The resultant budgets are presented in Table 6.5. At Site 1, the lateral C fluxes reflect high rates of carbon erosion and minimal deposition referred to above and average C erosion, redeposition and net export for all fields is 28.0 ± 2.07 , 0.58 ± 0.29 and 27.5 ± 2.28 g C m⁻² y⁻¹, respectively. The vertical C flux between atmosphere and soil for eroding area, depositional area and whole area are -0.78 ± 0.87 , 0.26 ± 0.42 and -0.52 ± 0.91 g C m⁻² y⁻¹, respectively. For Site 1, the net exchange with the atmosphere is only ca 2% of the lateral erosion flux and, as noted above, the similarity between CCI and CII at this site suggests that C stocks are close to equilibrium. Therefore, if more than 2% of the exported C is sequestered, the in-field source would be cancelled and a landscape-scale net sink would be created.

Site 2 contrasts strongly with Sites 1 and 3 because a large proportion of the eroded SOC is redeposited within the fields with only a very minor part exported from the field. This is seen most clearly in the field level statistics, average C erosion, C redeposition and net C export, which are 12.09 ± 0.72 , 10.7 ± 3.89 and 1.35 ± 4.4 g C m⁻² y⁻¹, respectively. Furthermore, at Site 2, the pattern of vertical C fluxes between soil and atmosphere also differs from that seen at other sites, with comparatively low fluxes at eroding profiles and high fluxes at deposition profiles. Again, this is seen clearly in the summary for vertical C flux statistics for eroding, deposition and the whole field: 3.84 ± 1.29 , 7.34 ± 9.98 and 11.2 ± 11.3 g C m⁻² y⁻¹, respectively. Overall, the eroded and deposited area acted as a net C sink, although because of the high standard error on the estimates this must be treated with caution. Nevertheless, the result suggests that, as at the other sites, there is no evidence of a net source of C to the atmosphere as a result of soil redistribution here.

As was, the case at Site 1, erosion dominates at Site 3 and the average C erosion, C redeposition, net C export for all fields are 37.6 ± 2.66 , 1.49 ± 1.49 and 36.2 ± 3.96 g C m⁻² y⁻¹, respectively. In this site vertical C flux between soil to atmosphere for eroding, deposition and whole field is 5.20 ± 1.49 , -0.10 ± 0.10 and 5.10 ± 1.57 g C m⁻² y⁻¹, respectively. The eroded area acted as a net C sink but deposition area acted

as a small source or was in an equilibrium condition. For Site 3 for all fields, the average net C flux shows the fields acted as net C sinks even if the C export is discounted (assumed lost back to the atmosphere), this C sink may be due to continuous C input. If part of the exported C is preserved in depositional areas away from the fields, then the C sink strength will be further increased.

Taking the mean values for all the study sites near Dehradun, India, the lateral C fluxes demonstrate the dominance of erosion with average C erosion, redeposition, net export of 25.49 ± 3.486 , 4.27 ± 2.02 and 21.7 ± 5.54 g C m⁻² y⁻¹, respectively (Table 6.6). Across these sites, vertical C fluxes between from atmosphere to soil for eroding, deposition and whole field are 2.8 ± 1.10 , 2.50 ± 3.13 and 5.3 ± 4.1 g C m⁻² y⁻¹, respectively. Combining all sites in the study area, the net C flux from atmosphere to soil is 5.3 ± 4.1 g C m⁻² y⁻¹ even if it is assumed that all exported C is lost to atmosphere (21.7 ± 5.54 g C m⁻² y⁻¹). The C stocks at the sites appear to be in dynamic equilibrium.

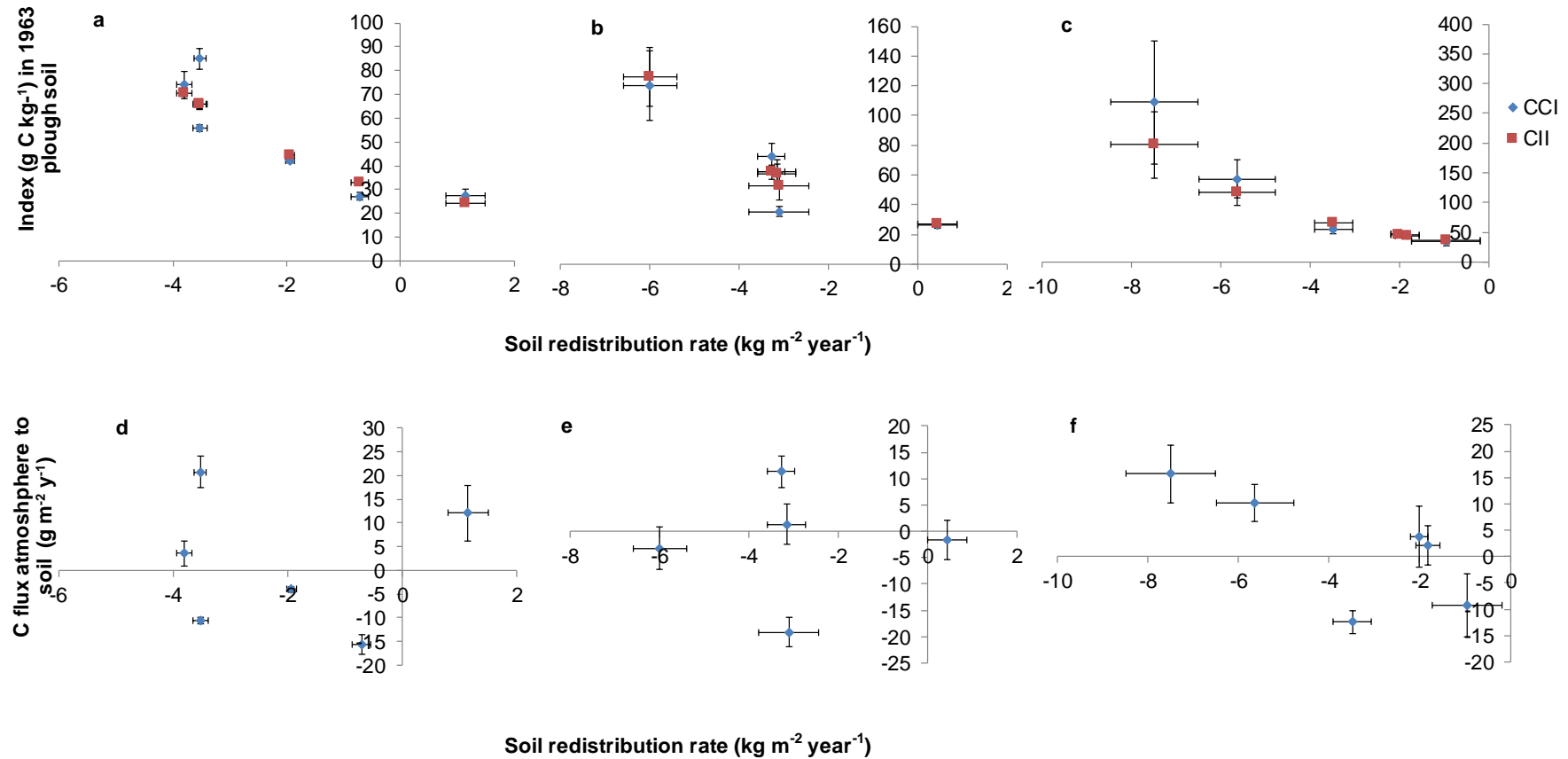


Figure 6.1 Profile /point scale relationship between SR rate, CCI and CII (top: a-DKF1, b-DKF2 and c-DKF3) and net C flux (bottom: d-DKF1, e-DKF2 and f-DKF3) for different field of Site 1 Dhulkhot (DK). Mean values ± SE (*n* = 3) are presented.

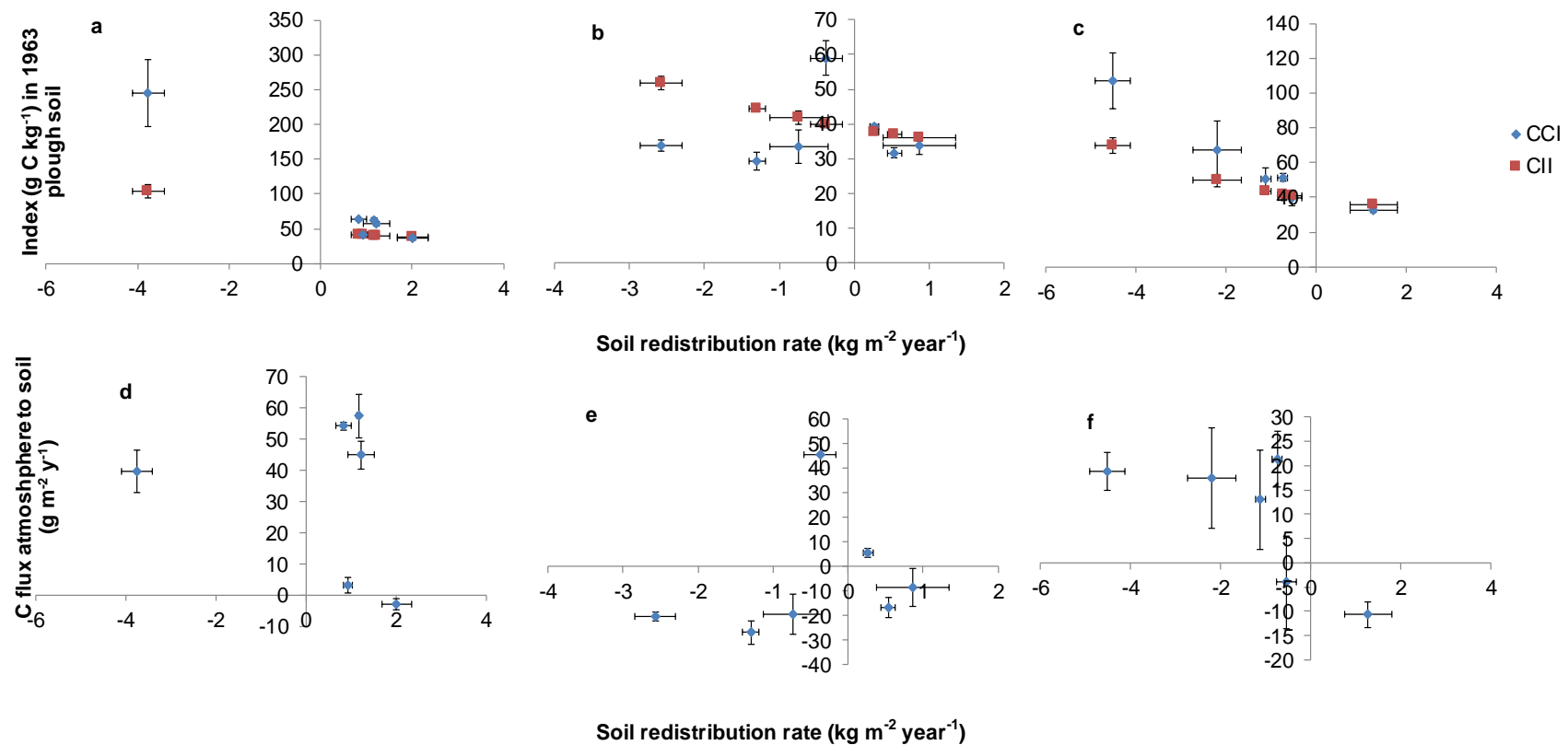


Figure 6.2 Profile / point scale relationship between SR rate, CCI and CII (Top: a-PSF1, b-PSF2 and c-PSF3) and net C flux (Bottom: d-PSF1, e-PSF2 and f-PSF3) for different field of Site 2 Pasauli (PS). Mean values \pm SE (n=3) are presented.

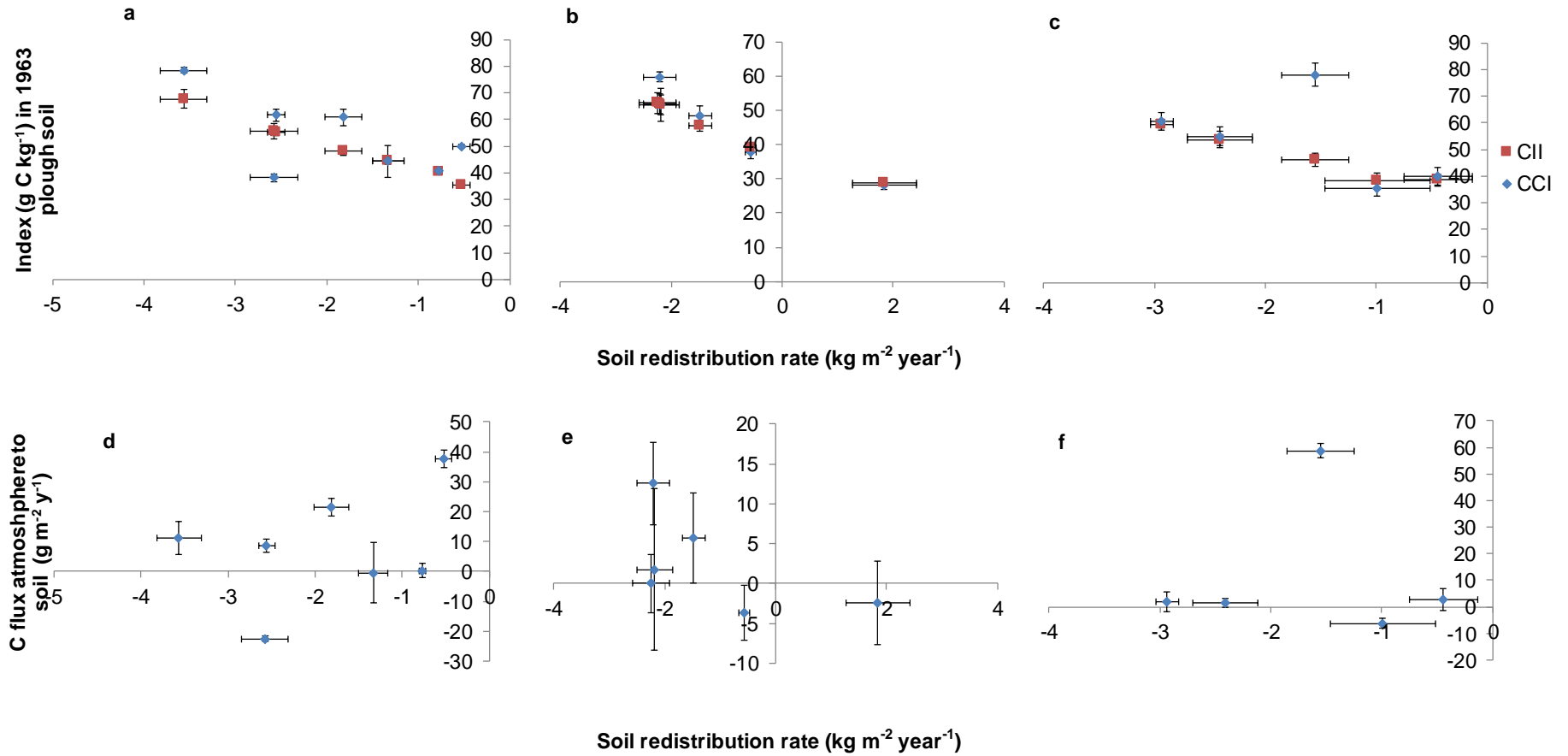


Figure 6.3 Profile/point scale relationship between SR rate, CCI and CII (Top: a-BGF1, b-BGF2 and c-BGF3) and net C flux (Bottom: d-BGF1, e-BGF2 and f-BGF3) for different field of Site 3 Bhatta Gaon (BG). Mean values \pm SE ($n = 3$) are presented.

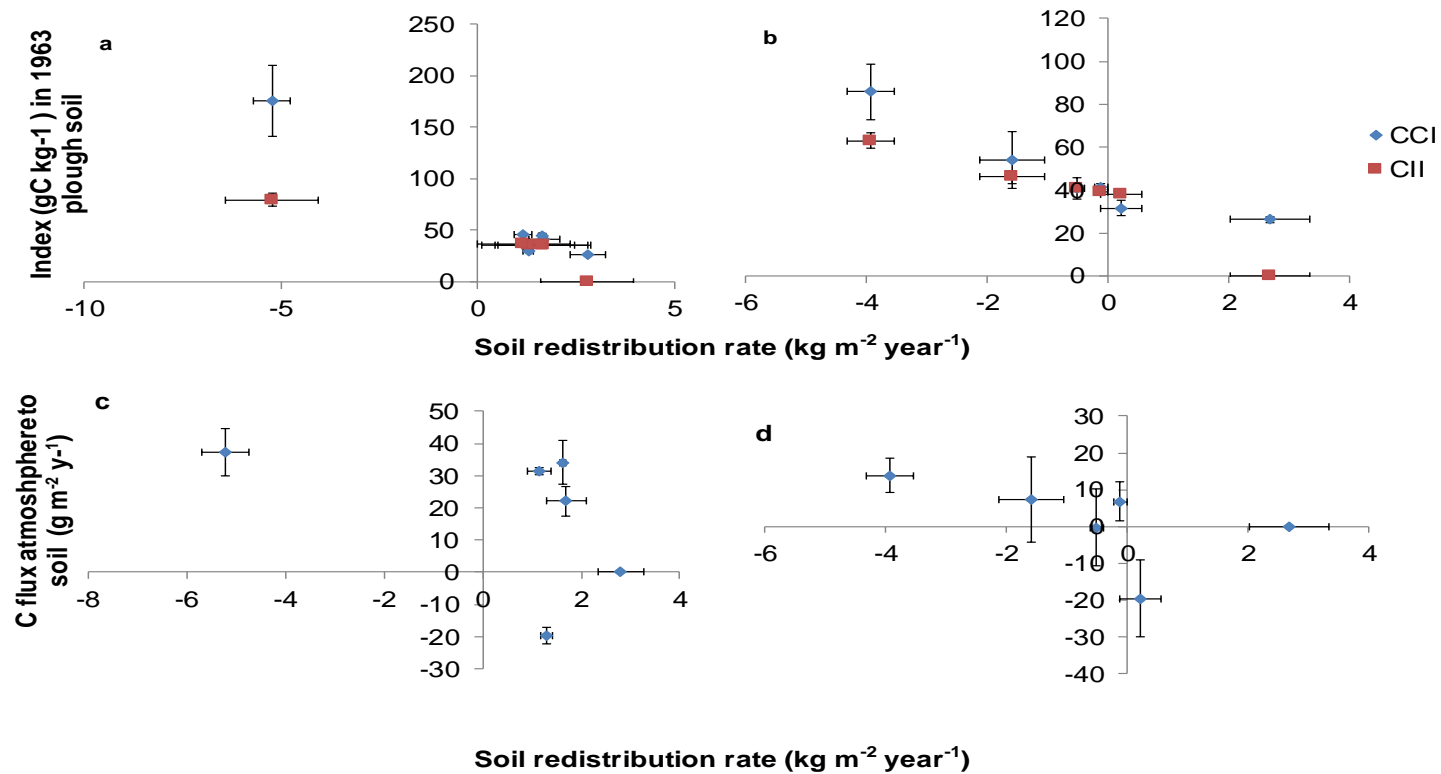


Figure 6.4 Profile / point scale SR rate, CCI, CII and Net C flux for different fields of Site 2 by using default parameter of ¹³⁷Cs inventory 1685 Bq m⁻², reference C inventory 5.3 kg m⁻² up to 50 cm and plough depth 0.26 m for where model not predicting at deposition profile (PSF1 and PSF3). Mean values ± SE (*n* = 3) are presented.

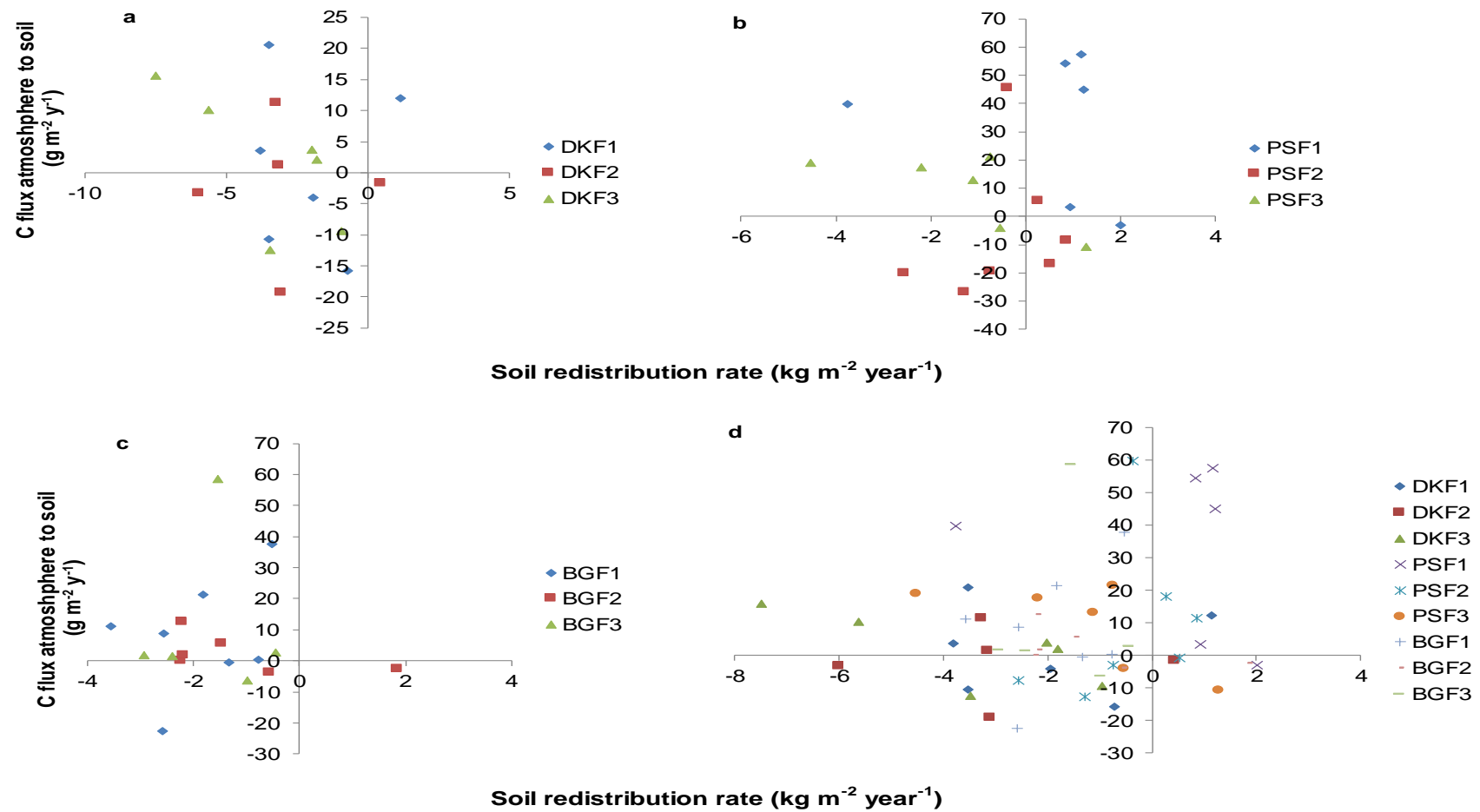


Figure 6.5 Profile /point scale relationship between net C flux and soil redistribution rate combined for all fields of Site 1(a), Site 2(b), Site 3(c) and all site fields(d).

Table 6.5 Soil carbon budget for fields from Dehradun, India Site 1, 2 and 3. Ep- eroding profile, Dp- deposition profile, Ea –eroding area, Da- deposition area, F – whole field.

Soil Carbon Budget for India site 1 (Dhulkhot - DK)															
	DKF1					DKF2					DKF3				
	Ep	Dp	Ea	Da	F	Ep	Dp	Ea	Da	F	Ep	Dp	Ea	Da	F
Carbon stores (kg C m⁻²)															
Measured	3.69	5.39	3.4	0.48	3.84	3.26	4.51	2.66	0.83	3.49	3.71	0.00	3.71	0.00	3.71
Simulated	3.77	4.78	3.4	0.43	3.86	3.38	4.60	2.76	0.84	3.60	3.66	0.00	3.66	0.00	3.66
Excess measured	-0.08	0.61	-0.1	0.05	-0.01	-0.12	-0.08	-0.09	-0.02	-0.11	0.05	0.00	0.05	0.00	0.05
Carbon transfers (g m⁻² y⁻¹)															
Subsoil C transferred to plough layer	21.7		19.8			29.3		23.9			25.2		25.2		
Subsoil C retained Plough layer	13.69		12.5			16.37		13.37			13.99		13.99		
Subsoil C eroded/exported	8.05		7.3			12.91		10.55			11.18		11.18		
Plough soil C eroded/exported	18.3		16.7			23.0		18.8			19.6		19.6		
Burial of Initial cultivation layer C		8.99		0.80			4.15		0.76			0.00		0.00	
Burial of aggraded Carbon		2.62		0.23			0.45		0.08			0.00		0.00	
Addition of aggraded C to plough layer		7.44		0.66			4.11		0.75			0.00		0.00	
Excess C Sequestration from atmospheric	-1.5	12.1	-1.4	1.08	-0.3	-2.3	-1.7	-1.9	-0.31	-2.2	0.9	0.00	0.9	0.00	0.9
Export from the field					23.1					28.5					30.8
Soil Carbon Budget for India site 2 (Pasauli - PS)															
	PSF1					PSF2					PSF3				
	Ep	Dp	Ea	Da	F	Ep	Dp	Ea	Da	F	Ep	Dp	Ea	Da	F
Carbon stores (kg C m⁻²)															
Measured	3.54	6.75	0.57	5.66	6.23	4.44	5.62	2.16	2.89	5.05	2.43	5.85	1.88	1.33	3.21
Simulated	1.56	5.13	0.25	4.30	4.55	4.22	5.90	2.05	3.03	5.08	2.23	6.38	1.73	1.45	3.18
Excess measured	1.98	1.63	0.32	1.36	1.68	0.22	-0.28	0.11	-0.14	-0.04	0.19	-0.53	0.15	-0.12	0.03
Carbon transfers (g m⁻² y⁻¹)															
Subsoil C transferred to plough layer	25.6		4.13			9.74		4.73			7.19		5.55		
Subsoil C retained Plough layer	9.83		1.58			7.15		3.48			4.84		3.73		
Subsoil C eroded/exported	15.82		2.55			2.59		1.26			5.75		4.44		
Plough soil C eroded/exported	53.2		8.57			25.2		12.2			9.37		7.23		
Burial of Initial cultivation layer C		23.5		19.7			14.2		7.29			27.4		6.24	
Burial of aggraded Carbon		8.25		6.92			2.26		1.16			9.05		2.06	
Addition of aggraded C to plough layer		13.8		11.61			11.5		5.93			19.9		4.55	
Excess C Sequestration from atmospheric	39.6	32.5	6.38	27.3	33.7	4.4	-5.54	2.14	-2.85	-0.7	3.88	-10.7	3.00	-2.43	0.57
Export from the field					-7.41					6.41					5.06
Soil Carbon Budget for India site 3 (Bhatta Gaon - BG)															
	BGF1					BGF2					BGF3				
	Ep	Dp	Ea	Da	F	Ep	Dp	Ea	Da	F	Ep	Dp	Ea	Da	F
Carbon stores (kg C m⁻²)															
Measured	4.22	0.00	4.22	0.00	4.22	4.33	6.23	3.81	0.75	4.55	4.53	0.00	4.53	0.00	4.53
Simulated	3.98	0.00	3.98	0.00	3.98	4.16	6.35	3.66	0.76	4.43	4.13	0.00	4.13	0.00	4.13
Excess measured	0.24	0.00	0.24	0.00	0.24	0.16	-0.12	0.14	-0.01	0.13	0.40	0.00	0.40	0.00	0.40
Carbon transfers (g m⁻² y⁻¹)															
Subsoil C transferred to plough layer	20.96		20.96			18.87		16.61			18.26		18.26		
Subsoil C retained Plough layer	14.05		14.05			13.50		11.88			12.50		12.50		
Subsoil C eroded/exported	6.91		6.91			5.37		4.73			5.76		5.76		
Plough soil C eroded/exported	35.6		35.6			32.6		28.7			31.2		31.2		
Burial of Initial cultivation layer C		0.00		0.00			29.41		3.53			0.00		0.00	
Burial of aggraded Carbon		0.00		0.00			14.01		1.68			0.00		0.00	
Addition of aggraded C to plough layer		0.00		0.00			23.33		2.80			0.00		0.00	
Excess C Sequestration from atmospheric	4.8	0.00	4.8	0.00	4.8	3.3	-2.4	2.9	-0.29	2.6	8.0	0.00	8.0	0.00	8.0
Export from the field					42.5					28.9					37.0

Table 6.6 Complete Soil redistribution and C flux budget for study area. E-erosion, D-deposition and EX-export

Site	Fields	Area %		lateral sediment flux (kg m ⁻² y ⁻¹)			lateral C flux (g C m ⁻² y ⁻¹)			Vertical C flux (g C m ⁻² y ⁻¹)		
		E	D	E	D	EX	E	D	EX	E	D	Field
Site 1	DKF1	91.1	8.9	2.43	0.10	2.33	24.0	0.90	23.1	-1.4	1.08	-0.3
Site 1	DKF2	81.7	18.3	3.06	0.08	2.98	29.3	0.83	28.5	-1.9	-0.31	-2.2
Site 1	DKF3	100	0.00	3.24	0.00	3.24	30.8	0.00	30.8	0.9	0.00	0.9
Site 2	PSF1	16.1	83.9	0.61	1.01	-0.40	11.1	18.5	-7.41	6.38	27.3	33.7
Site 2	PSF2	48.6	51.4	0.53	0.28	0.25	13.5	7.09	6.41	2.14	-2.85	-0.7
Site 2	PSF3	77.2	22.8	1.41	0.29	1.12	11.7	6.61	5.06	3.00	-2.43	0.57
Site 3	BGF1	100	0.00	2.02	0.00	2.02	42.5	0.00	42.5	4.8	0.00	4.8
Site 3	BGF2	88.0	12.0	1.53	0.22	1.31	33.4	4.48	28.9	2.9	-0.29	2.6
Site 3	BGF3	100	0.00	1.73	0.00	1.73	37.0	0.00	37.0	8.0	0.00	8.0
	Mean	78.1	21.9	1.84	0.22	1.62	25.9	4.27	21.7	2.8	2.50	5.3
	SE	9.45	9.45	0.32	0.11	0.40	3.86	2.02	5.54	1.10	3.13	4.12

6.2.4. Sensitivity analysis

In Section 4.3, the uncertainty regarding the ^{137}Cs fallout reference inventory was discussed. Comparison of the estimate of fallout derived from global data with that based on in-field measurement, leads to the interpretation that even the level, apparently stable fields may have suffered net ^{137}Cs and soil loss. Nevertheless, the uncertainty bounds on the estimate of fallout based on global data are wide (the latitudinal bands are 10°) and, therefore, in this section the sensitivity of the results to the selected ^{137}Cs inventory is explored. Other key variables in the assessment of sink strength are the estimated SOC equilibrium inventory, because this has a strong control over expected inventories, and the cultivation (mixing) depth, because this controls the ^{137}Cs and C concentration in redistributed soil and the disequilibrium period (td), because this determines the period over which the observed changes have occurred. Therefore, sensitivity analysis also explores the effect of varying these parameters. The sensitivity analysis explored the effect on estimated soil redistribution rate, CCI, CII and net sink strength of variation in reference ^{137}Cs fallout inventory, equilibrium SOC inventory, plough depth, and disequilibrium period.

Variability in ^{137}Cs inventory

The effect of using a significantly higher and significantly lower ^{137}Cs reference inventory (1300, 1685 and 2100 Bq m⁻²) was explored. Inevitably, these result in changes in estimated soil redistribution rates; however, relatively little change is seen in the patterns of CCI and CII (Plots a to c in Figures 6.6, 6.7 and 6.8 for Sites 1 2 and 3, respectively). Using ^{137}Cs reference inventory values from 1300 to 2100 Bq m⁻², C flux varied for eroded, deposition areas and whole field vary respectively, as follows for Site 1: -5.1 to 4.3, -3.7 to 1.6 and -6.7 to 4.3 g C m⁻² yr⁻¹, Site 2: -7.0 to 7.8, -2.43 to 22.0 and 0.57 to 28.6 g C m⁻² yr⁻¹, and for Site 3 -8.2 to 22.8, -0.58 to 2.43 and -5.8 to 22.8 g C m⁻² yr⁻¹. These results highlight the importance of reliable reference inventories and suggest that further investigation to support refinement of reference inventories would be beneficial.

Variability in reference C inventory

The default reference C inventory of each site (Site 1: 4.59, Site 2: 5.30 and Site 3:5.50 kg m⁻²) compared with lower (decided based on measured C inventory at stable profiles) and higher level (used same quantity increase as decreased for lower level)

of C and looked the pattern of CCI vs CII (plots d to f in Figure 6.6; Figure 6.7; Figure 6.8) results consistent with earlier observation above, high level of CCI observed than CII in all fields of eroded locations except certain aggraded point CII is higher than CCI. It's clearly indicating C flux from atmosphere to soil at most eroded location. Using the range of reference C inventory in the sensitivity analysis, the C flux varied for eroded, deposition areas and whole field vary respectively, as follows for Site 1: -8.4 to 10.8, -2.3 to 2.3 and -9.7 to 10.8 g C m⁻² yr⁻¹, Site 2: -4.7 to 15.8, -13.6 to 18.8 and -18.3 to 34.6 g C m⁻² yr⁻¹, and for Site 3 -5.9 to 24.9, -2.9 to 2.3 and -8.8 to 24.9 g C m⁻² yr⁻¹.

Variability in Plough Depth (PD)

Like reference ¹³⁷Cs and C inventory sensitivity analysis performed for changing different level of PD of each site measured value (measured PD for Site 1: 0.14, Site 2: 0.19 and 0.26, Site 3: 0.24 m). Various level of PD compared with SR, CCI and CII, in all condition the pattern of CCI with CII not changed (Figure 6.6g-i) to resulted pattern of default PD and it shows CCI is higher than CII at most eroded location in Site 1. Similar pattern also observed for Site 2 (Figure 6.7g-i) and Site 3 (Figure 6.8g-i). Using the range of plough depths in the sensitivity analysis, the C flux varied for eroded, deposition areas and whole field vary respectively, as follows for Site 1: -6.3 to 0.92, -2.9 to 1.08 and -6.8 to 0.92 g C m⁻² yr⁻¹, Site 2: 0.63 to 14.2, -2.85 to 41.9 and -0.70 to 48.4 g C m⁻² yr⁻¹, and for Site 3; 2.86 to 21.8, -0.29 to 3.3 and 2.57 to 21.8 g C m⁻² yr⁻¹.

Variability in Disequilibrium Period (td)

As for the other variables, sensitivity analysis was performed for different disequilibrium periods (td was set to 40, 50, 70, 100 years). Using these values of td, the predicted (CII) values decrease with increase of td at the most eroded parts of field and increase at deposition sites in the fields (Figure 6.9a-c for Site 1; Figure 6.9d-f for Site 2 and Figure 6.9g-l for Site 3). As has been noted above, with a td period of 50 years most of the eroded sites exhibit a CCI that exceeds CII; therefore, if td is increased there will be an increased tendency for this pattern (as CII is depressed). Using the range of disequilibrium periods (different td is 40, 50, 70, 100 years) in the sensitivity analysis, C flux was found to vary for eroded, deposition areas and whole field respectively, as follows for Site 1: -4.7 to 11.8, -2.1 to 1.3 and -4.8 to 11.8 g C m⁻² yr⁻¹.

yr^{-1} , Site 2: -0.12 to 9.24, -7.7 to -0.86 and -2.36 to -0.57 $\text{g C m}^{-2} \text{yr}^{-1}$, and for Site 3; 0.22 to 22.0, -12.3 to 0.83 and 0.22 to 22.0 $\text{g C m}^{-2} \text{yr}^{-1}$.

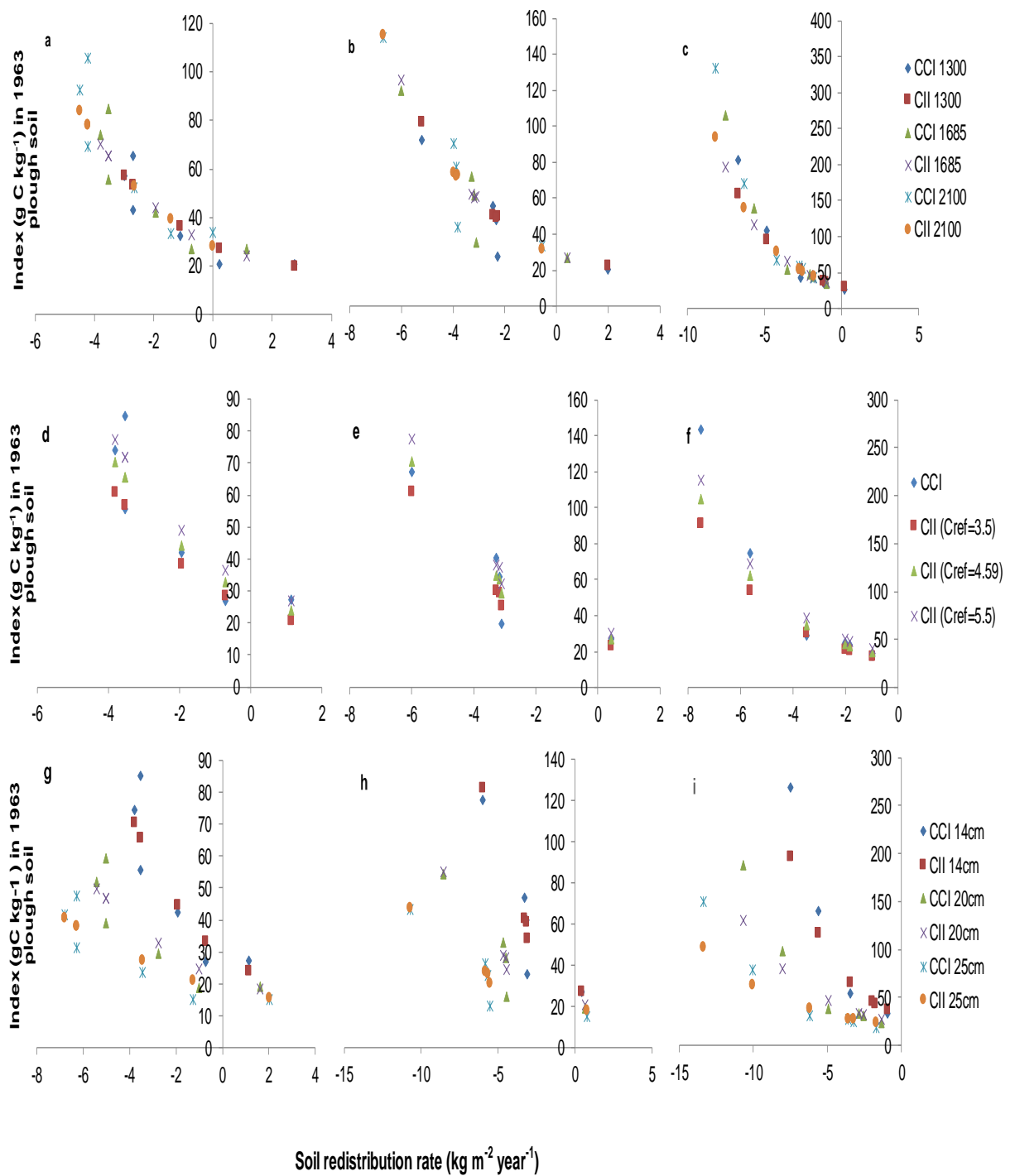


Figure 6.6 Profile/point scale relationship between SR rate, CCI and CII for different reference ^{137}Cs (1300, 1685 and 2100 Bq m^{-2}) inventory (Top : a-DKF1, b-DKF2 and c-DKF3), different reference C (3.5, 4.59 and 5.5 kg m^{-2}) inventory (mid: d-DKF1, e-DKF2 and f-DKF3) and for different (14, 20 and 25 cm) plough depth (Bottom: g-DKF1, h-DKF2 and i-DKF3) of fields to Site 1 Dhulkhot.

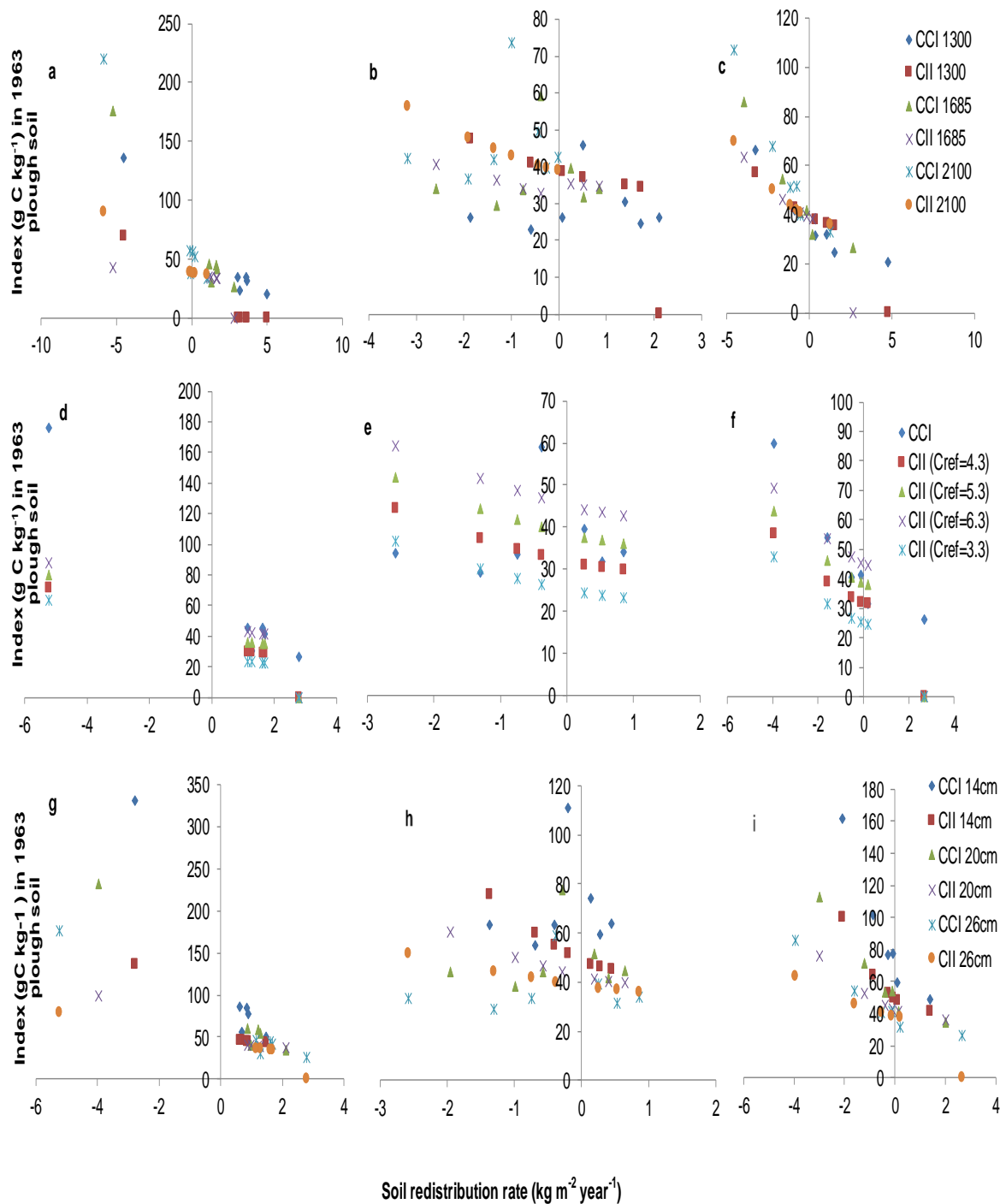


Figure 6.7 Profile/point scale relationship between SR rate , CCI and CII for different reference ^{137}Cs (1300, 1685 and 2100 Bq m^{-2}) inventory (top : a-PSF1, b-PSF2 and c-PSF3), different reference C (3.3, 4.3, 5.3 and 6.3 kg m^{-2}) inventory (mid: d-PSF1, e-PSF2 and f-PSF3) and for different (14, 20 and 26 cm) plough depth (bottom: g-PSF1, h-PSF2 and i-PSF3) of fields to Site 2 Pasauli (PS).

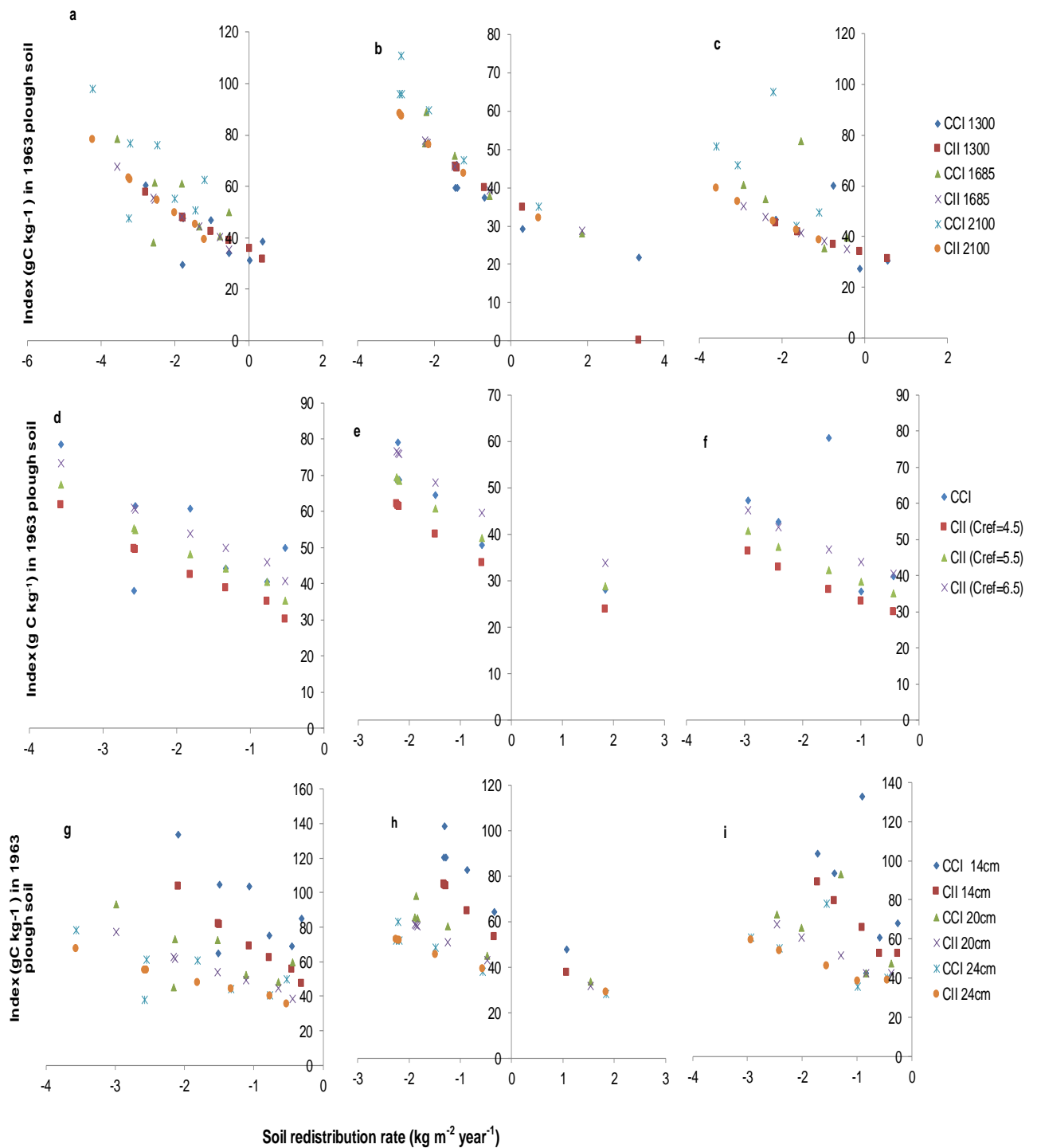


Figure 6.8 Profile/point scale relationship between SR rate , CCI and CII for different reference ^{137}Cs (1300, 1685 and 2100 Bq m^{-2}) inventory (Top : a-BGF1, b-BGF2 and c-BGF3), different reference C (4.5,5.5 and 6.5 kg m^{-2}) inventory (mid: d-BGF1, e-BGF2 and f-BGF3) and for different (14, 20 and 24 cm) plough depth (Bottom: g-BGF1, h-BGF2 and i-BGF3) of fields to Site 3 Bhatta Gaon (BG).

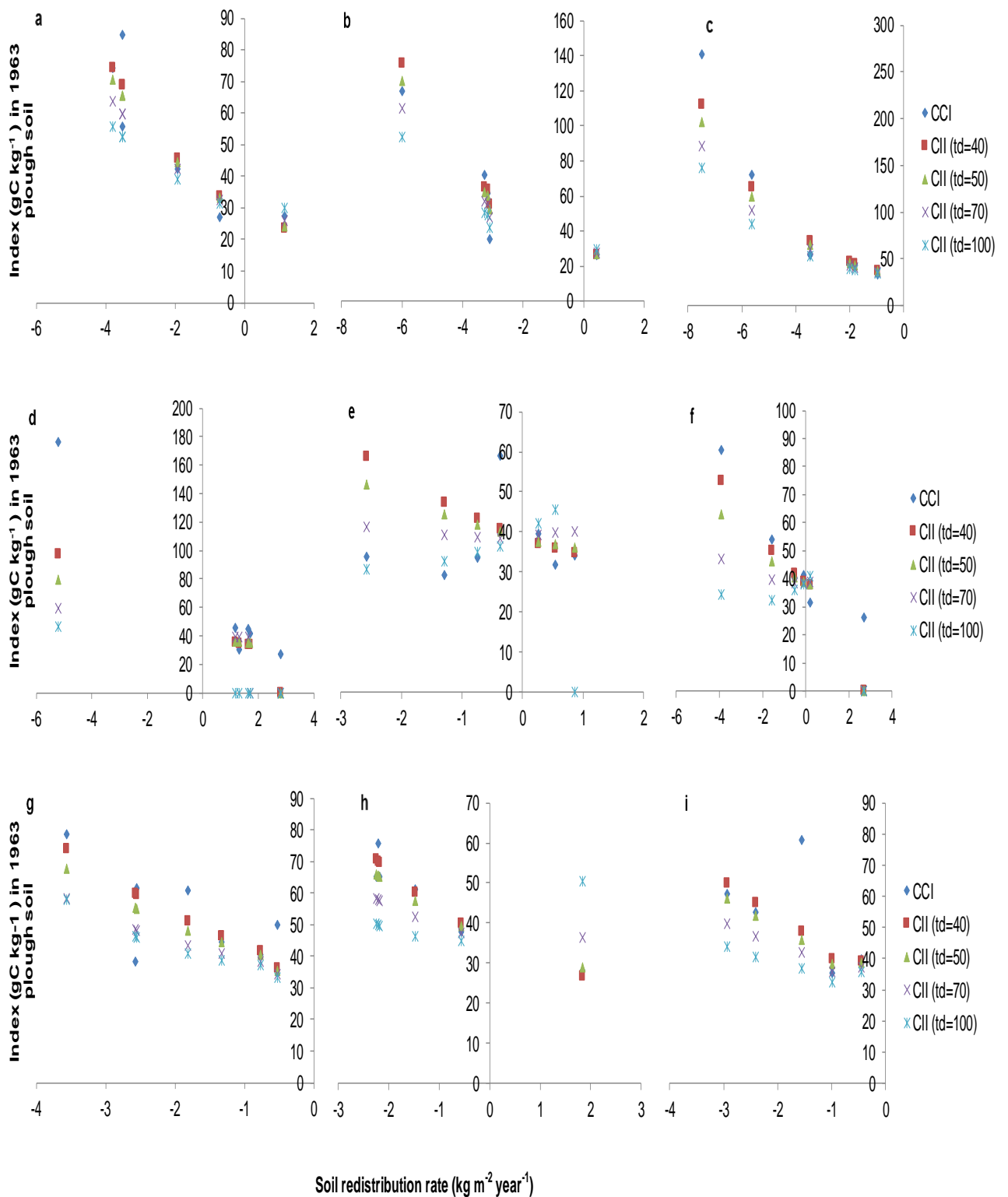


Figure 6.9 Profile/point scale relationship between SR rate , CCI and CII for different disequilibrium period (td: 40,50,70,100 years) (Top : a-DKF1, b-DKF2 and c-DKF3), (mid: d-PSF1, e-PSF2 and f-PSF3), (Bottom: g-BGF1, h-BGF2 and i-BGF3) for all fields at different sites

6.3. Discussion

6.3.1. Profile and field scale soil redistribution rates and budget

In general, all three sites studied are dominated by erosion and areas of net deposition of soil represent only a small percentage of the total. The only exception to this is Site 2, in which one of the three fields is dominated by net deposition and it is likely that this receives sediment transported from other fields (including 2 and 3) located further up the valley slope. Caesium-137 data provide more detail regarding within-field soil redistribution than other approaches and there is, therefore, a lack of data with which to evaluate the spatial patterns. However, the average erosion rate and net export rate across all sites of 1.84 ± 0.32 and $1.62 \pm 0.40 \text{ kg m}^{-2} \text{ y}^{-1}$, respectively, (Table 6.6) can be compared with published studies. The latter have suggested that average erosion rates in the region are comparable ($> 20 \text{ t ha y}^{-1}$) with other erosion estimates (Singh and Gupta, 1982; Narayana and Ram Babu, 1983; Khola and Sastry, 2005 Singh *et al.*, 2016). My results found the soil erosion for this area fall between slight ($<5 \text{ t ha}^{-1} \text{ y}^{-1}$) to severe ($80 \text{ t ha}^{-1} \text{ y}^{-1}$) erosion class for each pits. But in overall average total net soil erosion/loss based on area of field fall under moderate erosion ($10\text{-}20 \text{ t ha}^{-1} \text{ y}^{-1}$) class which is loss of 16.2 t ha y^{-1} . This similar value of soil erosion also measured by Singh *et al.*, 2016 in unmanaged and managed agriculture slope field based on run off plot studies. This measured soil loss value is higher than the soil loss tolerance level of 2.5 to $12.5 \text{ t ha}^{-1} \text{ y}^{-1}$ for this region proposed by Mandal *et al.*, 2010. The high rates of net soil export from the fields clearly indicate that water erosion due to high intensity rainfall on the steeply sloping fields is the major soil redistribution process. However, some of the patterns of within field variation, including maximum erosion rates close to upslope boundaries (DKF2, DKF1, BGF1, PSF2, PSF1, PSF3 and BGF2) and maximum deposition rates close to downslope boundaries (DKF1, DKF2, PSF1, PSF2, PSF3 and BGF2) are consistent with patterns of soil redistribution by tillage observed in other low intensity systems where animal draft dominates (Li and Lindstrom, 2001; Quine *et al.*, 1999; Thapa *et al.*, 2001).

The magnitude of the erosion rates and the consequently high subsoil to plough soil fluxes in the eroding areas (summarised in Figure 2.3) create conditions favourable for carbon sequestration by dynamic replacement (Harden *et al.*, 1999; Van Oost *et al.*, 2007). Nevertheless, the high rates of water erosion, high mean annual

temperatures and high precipitation are also conducive to high rates of SOC mineralisation.

6.3.2. Discussion of net C fluxes

The study area C fluxes for each site average indicate that export of eroded C is very high: 98%, 8% and 96 % for Site 1, Site 2 and Site 3 respectively. Taking the mean for all sites, 84% of the eroded C is exported from the field and only 16% of C redeposited within field (Table 6.5 and 6.6). This export of C is high compared to mechanised and high input farming lands where only small portion of eroded C is typically exported from the field (e.g. 22% in Van Oost *et al.*, 2007). However, the result found here is similar to that found for a field in a highly eroding non-mechanised agricultural field in the Loess Plateau in China (Li *et al.*, 2015). Therefore, the fate of exported C is very important to know if the budget of erosion induced C flux is to be closed and the full source or sink analysis completed (Hoffmann *et al.*, 2013; Li *et al.*, 2015; Wang *et al.*, 2015). There remains disagreement between those who suggest that exported SOC is stored and preserved in low aerated environments that can act as C sinks (Ran *et al.*, 2014; Vandenbygaart *et al.*, 2015; Wang *et al.*, 2015 a, b) and those who suggest that some or most exported SOC is reemitted to atmosphere as C source (Lal and Pimentel, 2008).

In my study restricted up to within field SOC redistribution and its dynamics and not addressed on fate of exported C (remain priority for future research). Interestingly in my fields part of eroded SOC deposited bottom slope of field and get buried below the cultivation layer and get stored this I can confirm by measuring spatial variation of SOC with help of ¹³⁷Cs tracer (results Chapter 5) within field particularly enriched SOC concentration at deposition area. Also I conducted soil respiration measurement for deposition position top, sub and mixed of both soils to know the fate of deposited/buried SOC within field in Chapter 7 results. The results supported buried soil SOC (assumed top soil SOC) less mineralised even provided optimum condition. This less mineralisation due to reaggregation and physical separation facilitate (Six *et al.*, 2002; Doetterl *et al.*, 2012; Vandenbygaart *et al.*, 2015) buried SOC store long time and cause C sink but this buried SOC more vulnerable to loss if it get exposed by changing land use or mixed fresh SOC with old by priming action which I found in Chapter 7 (Fontaine *et al.*, 2007; Van Oost *et al.*, 2012; Wang *et al.*, 2015)

The measured and predicted C Inventories (based on equilibrium conditions) in the eroded area of all three sites (with the exception of PSF1) are similar. At DK, the measured inventories are on average 99% of the predicted inventories; while at PS and BG (with the exception of PSF1) the measured inventories are on average 107% of the predicted inventories. There is, therefore, no evidence for disequilibrium driving a significant source; while at PS and BG there is consistent evidence of net sequestration. This dynamic replacement of eroded C at eroded locations is thought to be due to mixing of less C saturated with high minerals surface subsoil with plough soil cause disequilibrium which facilitate dynamic replacement of C (Stallard, 1998; Harden *et al.*, 1999; Quine and Van Oost, 2007; Van Oost *et al.*, 2007; Berhe *et al.*, 2007, 2008; Dungait *et al.*, 2013; Li *et al.*, 2015; Doetterl *et al.*, 2015, 2016; Nie *et al.*, 2016). Nevertheless, the rate of dynamic replacement of C at eroded sites is far lower than the rate of lateral carbon export by erosion and, therefore, the net C inventories at the eroded area of each site when compared with reference C inventories (up to 0.5m) demonstrates a deficit of 23 % , 35% and 21% of C for Site DK, Site PS and Site BG, respectively. Therefore, the eroded areas of the field are subject to net reduction in C stocks.

At depositional locations, the situation is mixed. In 3 of the 5 fields with areas of net deposition, the measured inventories are very close to the predicted inventories (92-98%). In the remaining 2 fields (DKF1 and PSF1) the measured inventories significantly exceed the predicted inventories (113% and 132%, respectively). This suggests that burial of deposited C has led to protection and facilitated some C sink formation (Van Oost *et al.*, 2007). This is particularly evident in Site PSF1 in which the deposition area occupies a large proportion of the field and has the highest net sequestration. The high C sink in the depositional area in Site 2 field PSF1 may be due to high redeposition of sequestered SOC from the eroded area within the field and imported from other fields. While surprising, similar patterns have been reported in some previous studies (Quine and Van Oost, 2007).

In summary, despite high rates of erosion, all fields in this study acted as small local C sink; and there is no evidence for a net C source to the atmosphere. This finding is comparable with other recent studies (Quine and Van Oost, 2007; Van Oost *et al.*, 2007; Li *et al.*, 2015). In this study, the area of net deposition of C within fields is low compared to studies from mechanised farm lands. In this study, most of eroded C was found to have been exported outside the field and this has significant implications for the net carbon balance. If the majority of the exported C is rapidly returned to the atmosphere then this would tip the landscape-scale system towards a net source of C

to the atmosphere. Therefore, investigation of the fate of the exported C remains a priority for future study. Finally, it is interesting to note that the eroded areas of the studied fields all acted as C sink with similar magnitude to those typically seen in mechanised farm lands (Van Oost *et al.*, 2007) despite relatively low nutrient inputs.

6. 4. Conclusion

This chapter addressed research objective 2: *To quantify erosion-induced soil carbon redistribution on the net effect of carbon exchange between soil and atmosphere in low input/productivity and highly eroding agricultural fields from the foothills of the Indian Himalaya by using ¹³⁷Cs fallout and SOC inventories.* This objective seeks to determine whether C sink exist in low input/productivity farm lands where net return of biomass is less. The analysis for this research objective assumed the overall null hypothesis:

H₀: Erosion-induced soil redistribution results in a net carbon sink when continuous crop production is maintained, despite low fertiliser inputs, low crop productivity and high biomass removal

Soil redistribution rate and C flux derived for study site of low input/productivity non mechanised and highly eroding agricultural fields from foot hills of Indian Himalaya, Dehradun, India. For all the study fields from Dehradun, India the average sediment erosion, deposition and net export is 1.84 ± 0.32 , 0.22 ± 0.11 and 1.62 ± 0.40 kg m⁻² y⁻¹, respectively. This result depicts around 88% of sediment exported from field and only 12% of sediment redeposited within field. This result of soil loss measured based on ¹³⁷Cs tracer technique comparable with other study measured soil loss for this area based on runoff plot study. This study confirmed again ¹³⁷Cs tracer technique more suitable for erosion studies. Over all to the study area all fields lateral C flux such as average C loss, redeposition, net export for all field is 25.5 ± 3.5 , 4.3 ± 2.0 and 21.7 ± 5.5 g C m⁻² y⁻¹, respectively. In this site vertical C flux between soil to atmosphere for eroding, deposition and whole field is 2.8 ± 1.10 , 2.50 ± 3.13 and 5.3 ± 4.1 g C m⁻² y⁻¹, respectively. Complete study fields eroded area acted as net C sink higher than deposition area. For all fields average net C flux is 5.3 ± 4.1 g C m⁻² y⁻¹ from atmosphere to soil sequestered even after assuming all exported C lost to atmosphere (21.7 ± 5.54 g C m⁻² y⁻¹). If I consider part of exported C preserved in burial /depositional area then C sink strength further increased. This study further confirmed dynamic replacement of eroded C at eroded location of highly eroding low input /low productivity agricultural

fields. Even at deposition area of within field also net C sink found due to continuous deposition C from eroded area and its burial at deposition area of field. In final my study conclude ^{137}Cs tracer technique much suitable for erosion and C dynamic studies, the fields from low input /highly eroding field acted C sink and need to further study about fate of exported C from field. Because 84% of C exported from field is partly preserved the sink strength of these fields further increase and almost comparable with C sink estimated in mechanised fields because this field C exported from the field is very less. Based on these results the null hypothesis for this research objective cannot be rejected and it is accepted that erosion induced soil redistribution act as a net C sink or creates SOC stock equilibrium under low input/productivity farm lands.

6.5. Key Findings

- Study area fall under high erosion category and maximum eroded sediment exported from the field very less redeposited within field
- Fields under eroded area completely acted as a C sink and but some field of deposition area acted C sink and source over all field level acted C sink but this C sink is less than mechanised farm lands.
- Interesting finding from this field maximum eroded C exported from the field which is opposite to mechanised farm lands where maximum eroded C redeposited within field only small fraction exported.
- Remaining priority on fate of exported C from the field decide ultimate C sink. Need further study on this.

7. Erosion as a carbon sink: effects of lateral and vertical carbon redistribution on decomposition rates?

7. 1. Introduction

Previous studies of the effect of soil redistribution on soil respiration rates at eroding and deposition topographic sites have been conducted along a soil depth gradient (Doetterl *et al.*, 2012; Wang *et al.*, 2013; Vandenbygaart *et al.*, 2015; Wang *et al.*, 2015) and found that spatial variation of soil respiration rates and overall result supported erosion induced redistribution of soil/SOC facilitate C sink to atmospheric CO₂ by dynamic C replacement at eroded positions and burial of eroded C at deposition positions. However, to the authors knowledge there has been no study regarding the effect of erosion/redistribution induced vertical mixing on respiration rates or on the potential priming effect it may have. Microcosm incubation experiments were conducted to determine whether there were differences in soil respiration from different soil layers of eroding and deposition topographic landscape positions in (a) separate layers and (b) mixed layers for a period of a year. Complete methods and experimental setups are described in Section 4.4. In this chapter result and discussion section used Site 1 and Site 2, which means Site 1 represent field DKF1 and Site 2 represent field PSF3.

Chapter 7 addresses the research objective 3: *To study the effect of erosion- and deposition-induced vertical soil/SOC mixing on soil respiration rates at various landscapes positions.*

Specifically this chapter addresses the following null hypotheses:

- 1) **H₀:** In eroded position, mixing topsoil with organic matter-poor subsoil will reduce decomposition rates as organic matter from topsoils may become bound onto unsaturated soil particles in the subsoil.
- 2) **H₀:** In depositional areas, mixing fresh organic matter from top soils into organic matter-rich subsoils will promote C release through a positive priming effect.

7. 2. Results

7.2.1. Caesium -137 (¹³⁷Cs) inventory distribution

The comparison of the ¹³⁷Cs activity along the topographic gradient (up to 50 cm depth) indicates that in both sites (Site 1 and 2) confirmed that the eroding sample pits had a lower ¹³⁷Cs activity than the deposition soil pits. Table 7.1 shows the soil redistribution rate (SR) estimated for each pit along the topographic gradient and the convention used is that negative values indicate soil loss, whilst positive value indicate deposition (soil gain). Both sites eroding and mid-slope positions appear to be losing soil, whilst the deposition position indicates soil gain. The depth distribution of ¹³⁷Cs is clearly different between topography pit locations. The eroding sites had activity up to 30 cm, whilst deposition locations had ¹³⁷Cs activity down to 50 cm depth. Mid-slope soil pits showed intermediate activity for both sites. Overall, Site 2 showed evidence of higher activity than Site 1.

7.2.2. Soil and C mixing (lateral and vertical redistribution) at each landscape (eroding and deposition)

Based on the model proposed by Quine and Van Oost (2007) (described in section 4.3) lateral and vertical soil C mixing is calculated for eroding (all eroding profiles combined) and deposition positions for each sites. For Site 1 and Site 2, soil erosion, deposition and net export was calculated as 1.92 ± 0.51 , 0.20 ± 0.09 and 1.72 ± 0.60 $\text{kg m}^{-2} \text{y}^{-1}$, respectively (Table 7.2). Of the net export of soil around 64% and 36% of the plough and sub plough soil is lost every year, respectively. Currently at eroding landscape positions (position based) 47% is sub-plough and 53% is ploughed soil (Figure 7.2), this indicates at eroding position equal proportion of plough and sub-plough soil present at current plough layer. At the deposition position due to continuous soil accumulation the initial plough soil layer has been buried, and imported plough and sub-plough layer has been buried by 0.86 ± 0.02 , 0.22 ± 0.03 and 0.13 ± 0.03 $\text{kg m}^{-2} \text{y}^{-1}$, respectively. At present in the deposition position, the plough layer is a mixture of imported plough, sub-plough and initial plough layer in proportions of 44%, 27% and 29%, respectively. This indicates though that there is plough layer soil now buried below the cultivation depth, and at present the maximum plough depth is within the plough layer (initial and imported) of deposition positions. Individual site based soil

erosion, deposition and mixing profiles are presented in Table 7.2. It is also clearly evident that Site 1 has experience a higher rate of erosion than Site 2.

If both sites are combined (Site 1 and Site 2) and the area of occupation of each landscape position (erosion, mid slope and depositional) considered, then C erosion, deposition and net export is 17.8 ± 6.2 , 3.75 ± 2.86 and 14.1 ± 9.02 g C m⁻² y⁻¹, respectively (Table 7.3). Of the net exported C, it is estimated that 62% and 38% are derived from the plough and sub-plough layers, respectively. At deposition positions, as a result of the continuous soil aggradation there is 18.2 ± 9.19 , 4.96 ± 2.93 and 0.65 ± 0.06 g C m⁻² y⁻¹ of buried initial plough layer, imported plough and sub-plough layer C, respectively. The plough layer of the deposition site consists of a mixture of imported sub plough, plough, initial plough and plant derived new C. This indicates that although some of the initial plough layer C buried is below the cultivation depth, presently plough layer at deposition positions is enriched with plough soil C. Again, Site 1 shows evidence of having a higher rate of erosion than Site 2.

7.2.3. Soil organic carbon (SOC), Total Nitrogen (TN) and CN ratio

SOC, TN concentration, and C:N ratio was greater at Site 2. At both sites, top soil had a significantly greater ($p < 0.05$) SOC and TN content than the sub-soil. Overall in both sites the eroding position (Table 7.4, 7.5 and Figure 7.1c, d) has less SOC and TN than other topographic position (mid-slope and deposition). C:N for both sites and soils along topographic gradient showed no significant ($p > 0.05$) difference. SOC concentration (Table 7.4) of the top 15 cm was significantly ($p < 0.05$) higher at deposition profile than eroding or the mid-slope profiles of Site 1. In Site 2 the deposition profile had a significantly ($p < 0.05$) higher SOC concentration than mid-slope and eroding profiles, with mid-slope also having a significantly higher concentration than the eroded profiles ($p < 0.05$). In both sites eroding pits (eroding and mid-slope) SOC concentration is significantly ($p < 0.05$) lower than in the deposition sampling pits in both depths. For sub-soil (45-60 cm) SOC concentration was significantly ($p < 0.05$) higher in the deposition profiles than the other profiles at both sites (Table 7.4). TN concentration (Table 7.4) of top (0 - 15 cm) soils did not significantly ($p > 0.05$) differ along the topographic gradient for Site 1. However, in Site 2 the deposition and mid-slope profiles had a significantly ($p < 0.05$) higher TN content than eroding profiles. Furthermore, there was no significant ($p > 0.05$) difference

between deposition and mid-slope profiles for Site 2. For sub-soil (45 - 60cm) TN concentration was significantly ($p < 0.05$) lower at eroding sampling pits than other position profiles of Site 1 (Table 7.4). In Site 2 TN concentration in the sub-soil layer was significantly ($p < 0.05$) higher in the mid-slope than the eroding profile. However, there were no significant ($p > 0.05$) differences between the eroding and deposition profiles. In addition, there was no significant difference observed between the mid-slope and deposition profile ($p > 0.05$). C:N of the top soil and sub-soils showed no significant difference ($p > 0.05$) for both sites. For both sites the mid-slope and deposition profiles C:N was significantly ($p < 0.05$) higher in the sub-soil than top soil.

Table 7.1 Total ^{137}Cs inventory, soil pH and other properties along the slope transect. Within a site, values labelled with different letters differ significantly ($p < 0.05$). Mean values $\pm 1\text{SE}$ ($n = 3$) are presented. Here Site 1 = field DKF1 and Site 2 = field PSF3.

Sites	Positions	^{137}Cs (Bq m^{-2})	SR rate ($\text{kg m}^{-2} \text{y}^{-1}$)	Depth (cm)	Soil pH	Latitude	Longitude	Elevation (m)
Site 1 (LIA)	Eroding	562 \pm 23 ^a	-3.53 \pm 0.13	<70	5.09 \pm 0.05	30°21.052' N	77°53.483' E	538
	Mid-slope	1352 \pm 63 ^b	-0.72 \pm 0.15	<90	5.19 \pm 0.04	30°21.062' N	77°53.472' E	537
	Deposition	2065 \pm 117 ^c	1.14 \pm 0.35	>100	5.10 \pm 0.04	30°21.076' N	77°53.457' E	536
Site 2 (LIA)	Eroding	417 \pm 63 ^a	-4.52 \pm 0.39	<70	5.17 \pm 0.05	30°27.205' N	77°52.759' E	674
	Mid-slope	1409 \pm 54 ^b	-1.12 \pm 0.11	>100	4.93 \pm 0.12	30°27.191' N	77°52.767' E	673
	Deposition	2707 \pm 248 ^c	1.28 \pm 0.52	>100	4.99 \pm 0.07	30°27.181' N	77°52.773' E	672

LIA: Low input agriculture - acidic

Table 7.2 Soil lateral and vertical redistribution ($\text{kg m}^{-2} \text{y}^{-1}$) budget for India sites based on profile means from Segment (E/D) and field area. Mean values \pm SE (n=2 sites value) are presented

Parameters	Site 1	Site 2	Mean	SE
	DKF1	PSF3		
Eroded area % of field and mixing	91.1	77.2	84	6.94
Mean Erosion /subsoil excavation rate	2.67	1.83	2.25	0.42
Cultivation layer in export	1.71	1.16	1.44	0.28
Subsoil in export	0.95	0.67	0.81	0.14
Cultivation soil lost in 50 yrs (kg m^{-2})	85.7	57.8	71.8	13.9
Subsoil lost in 50 yrs (kg m^{-2})	47.7	33.6	40.6	7.0
Remaining cultivation soil at eroding positions(kg m^{-2})	76.3	82.4	79.4	3.1
Subsoil mixed at eroding plough layer (kg m^{-2})	86	58	72	13.9
Fraction of cultivation layer in export	0.64	0.64	0.64	0.00
Fraction of subsoil at eroding cultivation soil	0.53	0.41	0.47	0.06
Aggraded area % of field and mixing	8.92	22.8	15.9	6.94
Mean Deposition	1.14	1.28	1.21	0.07
Initial cultivation import /deposit	0.73	0.77	0.75	0.02
Subsoil deposit/import	0.41	0.51	0.46	0.05
Burial of Initial cultivation layer	0.84	0.87	0.86	0.02
Burial of imported Initial cultivation layer	0.19	0.24	0.22	0.03
Burial of imported subsoil	0.11	0.16	0.13	0.03
Replacement of imported cultivation soil to initial cultivation layer	0.54	0.53	0.53	0.01
Replacement of imported sub soil in cultivation layer	0.30	0.35	0.33	0.02
Presence of remaining initial cultivation	0.30	0.40	0.35	0.05
Whole field				
Whole field area ha	0.13	0.10	0.11	0.02
Eroded Area ha	0.12	0.08	0.10	0.02
Aggraded Area ha	0.01	0.02	0.02	0.01
Whole field slope %	2.91	6.15	4.53	1.62
Mean erosion rate	2.43	1.41	1.92	0.51
Mean aggradation rate	0.10	0.29	0.20	0.09
Net export rate	2.33	1.12	1.72	0.60
Net export of plough soil	1.50	0.72	1.11	0.39
Net export of subplough	0.83	0.40	0.62	0.21

Table 7.3 C lateral and vertical redistribution ($\text{g C m}^{-2} \text{y}^{-1}$) budgets for the study sites sites based on profile means from erosional and depositional segments and the whole field area. Mean values \pm SE ($n = 2$ sites value) are presented.

Parameters	Site 1	Site 2	Mean	SE
	DKF1	PSF3		
Eroded area % of field and mixing	91.1	77.2	84.1	6.94
Mean C Erosion /subsoil excavation rate	26.3	15.1	20.7	5.61
Cultivation layer C in export	18.3	9.4	13.8	4.46
Subsoil C in export	8.05	5.75	6.90	1.15
Cultivation soil C lost in 50 yrs (g C m^{-2})	914	468	691	223
Subsoil C lost in 50 yrs (g C m^{-2})	403	287	345	57.65
Remaining cultivation soil C at eroding positions(g C m^{-2})	815	3902	2359	1544
Subsoil C mixed at eroding plough layer (g C m^{-2})	914	468	691	223
Fraction of cultivation layer C in export	0.69	0.62	0.66	0.04
Aggraded area % of field and mixing	8.92	22.79	15.85	6.94
Mean C Deposition	10.1	29.0	19.5	9.47
Initial cultivation C import /deposit	7.80	25.3	16.5	8.74
Subsoil C deposit/import	2.26	3.73	3.00	0.73
Burial of Initial cultivation layer C	8.99	27.4	18.2	9.19
Burial of imported Initial cultivation layer C	2.03	7.89	4.96	2.93
Burial of imported subsoil C	0.59	0.72	0.65	0.06
Replacement of imported cultivation soil C to initial cultivation layer C	5.77	17.4	11.6	5.81
Replacement of imported sub soil C in cultivation layer C	1.67	1.58	1.63	0.05
Whole field				
Whole field area ha	0.13	0.10	0.11	0.02
Eroded Area ha	0.12	0.08	0.10	0.02
Aggraded Area ha	0.01	0.02	0.02	0.01
Whole field slope %	2.91	6.15	4.53	1.62
Mean C erosion rate	24.0	11.7	17.8	6.16
Mean C aggradation rate	0.90	6.61	3.75	2.86
Net C export rate	23.1	5.06	14.1	9.02
Net export of plough soil C	16.0	1.47	8.72	7.24
Net export of subplough C	7.13	3.59	5.36	1.77

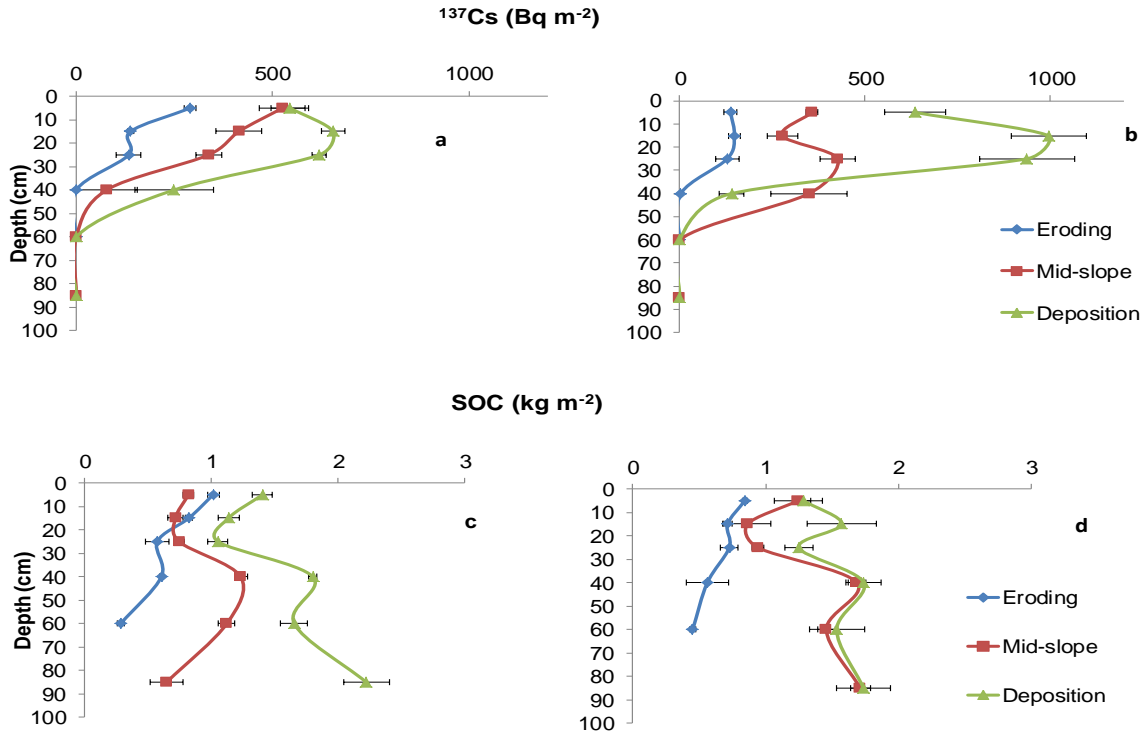


Figure 7.1 Depth distribution of ^{137}Cs and SOC inventory in profiles from different slope positions at Site 1 -Low Input Acidic (Figure 7.1a and c) and Site 2-Low Input Acidic (Figure 7.1b and d). Mean values \pm 1SE ($n = 3$) are presented

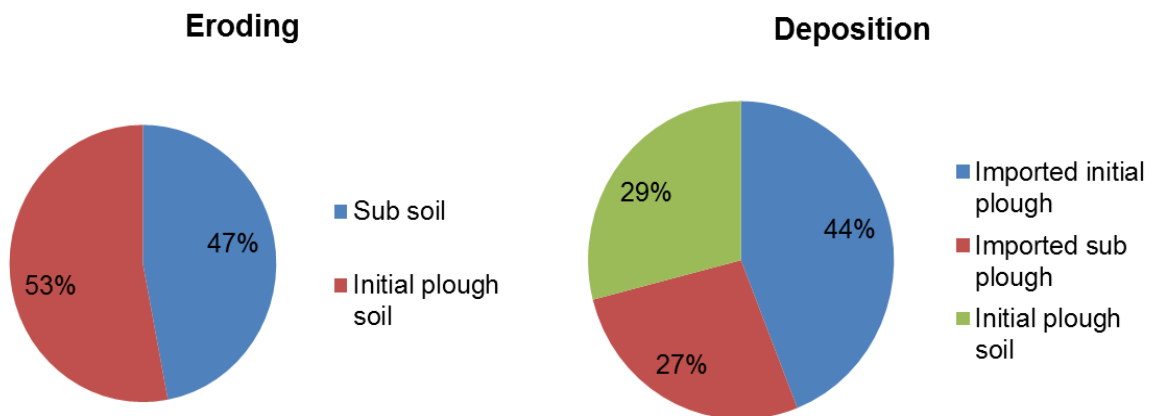


Figure 7.2 Percentages mixing of soils at eroding and deposition positions plough layer for both sites

Table 7.4 SOC, TN and C:N of Site1 and Site 2 by position and depth. Within a site and depth interval, values labelled with different letters differ significantly ($p < 0.05$). Mean values ± 1 SE ($n = 5$) are presented.

Sites	Depth (cm)	SOC (g kg^{-1})		TN (g kg^{-1})		CN ratio	
		0-15	45-60	0-15	45-60	0-15	45-60
Site 1	Eroding	9.60 \pm 0.12 ^a	4.38 \pm 0.18 ^a	0.64 \pm 0.03 ^a	0.21 \pm 0.03 ^a	15.1 \pm 0.78 ^a	18.6 \pm 0.81 ^a
	Mid-slope	9.02 \pm 0.12 ^a	6.75 \pm 0.18 ^b	0.85 \pm 0.14 ^a	0.39 \pm 0.01 ^b	11.7 \pm 1.56 ^a	17.5 \pm 0.76 ^a
	Deposition	12.6 \pm 0.32 ^b	8.05 \pm 0.15 ^c	0.88 \pm 0.05 ^a	0.41 \pm 0.04 ^b	14.4 \pm 0.44 ^a	20.2 \pm 1.58 ^a
Site 2	Eroding	13.6 \pm 0.75 ^a	6.94 \pm 0.66 ^a	1.22 \pm 0.07 ^a	0.81 \pm 0.04 ^a	11.3 \pm 0.84 ^a	10.5 \pm 0.53 ^a
	Mid-slope	16.4 \pm 0.63 ^b	11.8 \pm 0.90 ^b	1.53 \pm 0.05 ^b	0.99 \pm 0.06 ^b	10.7 \pm 0.12 ^a	11.9 \pm 0.24 ^a
	Deposition	19.5 \pm 0.57 ^c	12.1 \pm 0.45 ^c	1.72 \pm 0.07 ^c	0.92 \pm 0.03 ^a	11.3 \pm 0.11 ^a	13.2 \pm 0.08 ^a

Table 7.5 SOC and TN inventory up to 70 cm in depth by position. Mean values ± 1 SE ($n = 3$) are presented.

Sites	Positions	SOC (kg m^{-2})		TN (kg m^{-2})	
		Up to 70 cm depth			
Site 1	Eroding	3.29 \pm 0.07	0.23 \pm 0.03		
	Mid-slope	4.63 \pm 0.12	0.42 \pm 0.02		
	Deposition	5.39 \pm 0.32	0.46 \pm 0.03		
Site 2	Eroding	3.29 \pm 0.09	0.30 \pm 0.00		
	Mid-slope	6.19 \pm 0.41	0.39 \pm 0.02		
	Deposition	7.39 \pm 0.14	0.50 \pm 0.02		

7.2.4. Soil respiration cumulative pattern over the experimental period

Top Soils

Total cumulative C release from top soils was greater in the Site 1 soils. The top soils of Site 1 at the eroding and mid-slope sampling pits showed significantly ($p < 0.05$) higher respiration rates than in Site 2. However, in deposition profiles, top soil respiration rates did not differ between Site 1 and Site 2. After one year of incubation, the cumulative C release per unit SOC (gram) for top soils (Figure 7.3.a, b and Figure 7.5a,b) of different landscape positions along the slope transect were not significantly ($p > 0.05$) different (Site 1: eroding: 103.4 ± 6.2 , mid-slope: 102.6 ± 6.0 , deposition: 84.6 ± 6.0 mg CO₂-C g⁻¹ SOC; and Site 2: eroding: 70.6 ± 7.0 , mid-slope: 61.8 ± 3.0 , deposition: 71.9 ± 4.0 mg CO₂-C g⁻¹ SOC).

Although, there was no significant difference in cumulative C release at different landscape positions for top soils at both sites, over the period there was a trend for greater C release rates from eroding profiles (Figure 7.3 a, b). Initially respiration rates were higher in this eroded soils compared to the other sampling sites, but later in the incubation a decrease in respiration was observed relative to the other positions.

For Site 1, respiration rates between landscape positions were equivalent up to day 56 (Figure 7.4a). Samples collected from the eroding locations showed higher respiration rates than the mid-slope and deposition profiles between days 56 and 140. Thereafter, all profiles converged in terms of respiration and stabilized between 140-364 days. Site 2 (Figure 7.4b) initially had a higher respiration rate in the eroding profiles in comparison to the other sampling sites (up to 49 days). Thereafter the rate decreased between 49-98 days and converged with the respiration rates evident from the other sampling locations, stabilising after 250 days.

Sub-Soils

When comparing both sites the total cumulative C release for sub soils, in Site 1 was higher than Site 2. However, sub-soil cumulative C release from eroding and mid-slope profiles in both sites show no significant ($p > 0.05$) difference. The deposition profiles of Site 1 show significantly ($p < 0.05$) higher respiration than Site 2. For sub-

soils after the one year incubation period the cumulative C release per unit SOC (gram) (Figure 7.3c, d and Figure 7.5a,b) was significantly greater from eroding profiles ($p < 0.05$) than the other sampling locations in both the sites (Site 1. eroding: 20.4 ± 1.1 , mid-slope: 16.2 ± 1.1 , deposition: 14.0 ± 1.3 mg CO₂- C g⁻¹ SOC and Site 2. eroding: 14.0 ± 1.6 , mid- slope: 9.7 ± 1.2 , deposition: 9.5 ± 0.6 mg CO₂- C g⁻¹ SOC). Cumulative C release did not differ between mid-slope and deposition locations ($p > 0.05$) for both sites.

The flux rate trend over the experimental period for Site 1 and Site 2 show that the eroding profiles had a higher respiration rate than other positions (7.3c, d). Stabilization for sub-soils of both sites occurred rapidly by day 100 (7.4c, d).

7.2.5. Mixed-soils observed Vs expected cumulative respiration

After the year long incubation the mixed soil cumulative C release were compared with observed and expected cumulative C release at each slope position for both the sites as illustrated in Figure 7.5a,b.

The observed cumulative C release in deposition profiles were significantly ($p < 0.05$) highly than expected based on the respiration rates of top and sub-soils when incubated separately. 11.2% more C was released than expected representing an excess of 2.5 to 10 mg CO₂-C g⁻¹ SOC at Sites 2 and 1, respectively. When the analysis was carried within a sites, differences between observed and expected release at the depositional sites were no longer significantly ($p > 0.06$). At the other sampling positions showed no difference between observed and expected C release.

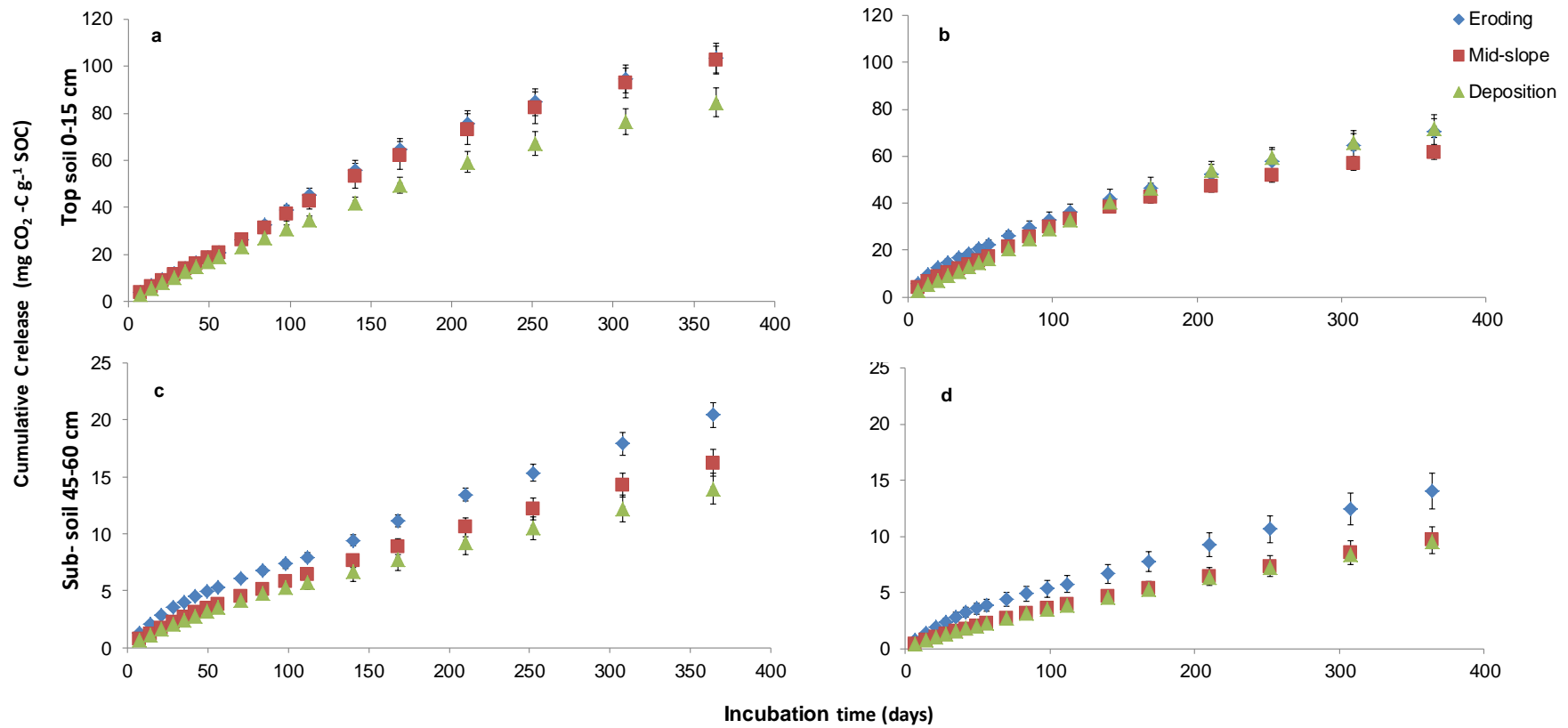


Figure 7.3 Cumulative CO₂-C release from the 0-15 cm (a,b) and 45-60 cm (c,d) depths from Site 1 (a,c) and Site 2 (b,d). Mean values ±1SE (*n* = 5) are presented.

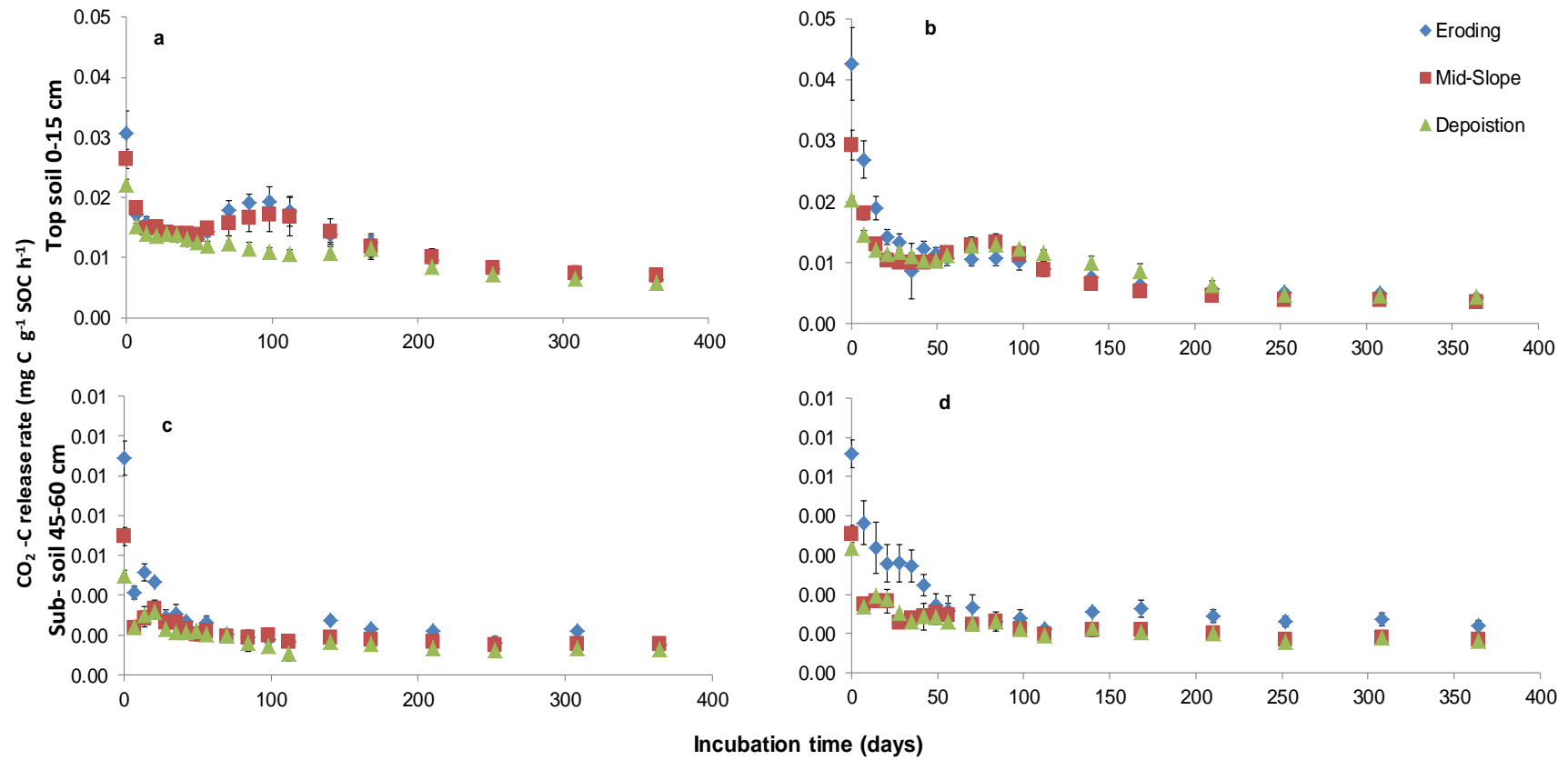


Figure 7.4 Soil respiration rate from the 0-15 cm (a,b) and 45-60 cm (c,d) depths from Site 1 (a,c) and Site 2 (b,d) . Mean values \pm 1SE ($n = 5$) are presented.

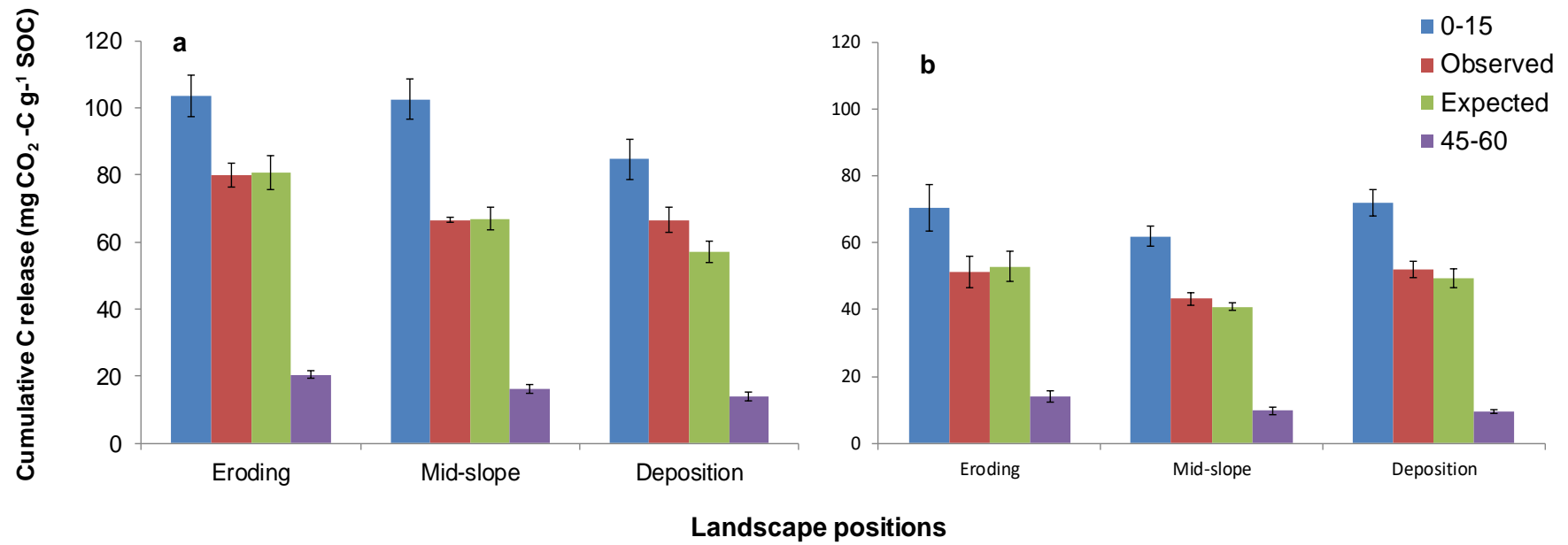


Figure 7.5 Cumulative CO₂-C release per gram SOC from the 0-15 cm, 45-60 cm depths, observed and expected (mixed soil) incubated different landscape positions from Site 1 (a) and Site 2 (b). Mean values ±1SE (n = 5) are presented.

7.2.6. Absolute difference between observed vs expected cumulative respiration release in mixed soils

The absolute difference of C release between observed and expected for the mixed soils from various landscape positions were estimated for the different sites, landscape position and for different time periods within the incubation (Figure 7.6a and b). It is important to note that for the depositional soils from Site 1, rates of C release were greater than expected in the mixed soils in all time periods. The same pattern was not observed for the depositional soils at Site 2. There was a suggestion of greater than expected C release from the mixed mid-slope soils in Site 2 but the overall difference was not statistically significant (Figure 7.5a,b)

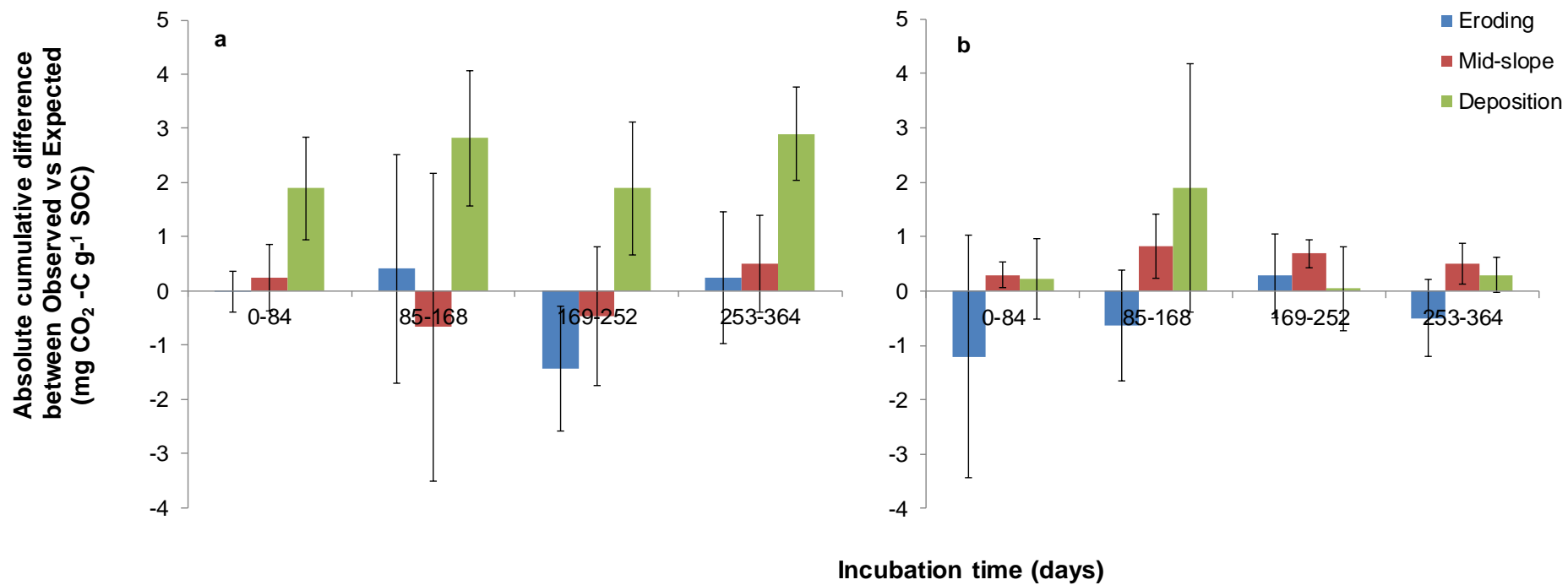


Figure 7.6 Absolute cumulative difference of C release between observed vs expected at different time interval of within 364 days for various landscape positions from Site 1 (a) and Site 2 (b). Mean values $\pm 1SE$ ($n = 5$) are presented

7.3. Discussion

7.3.1. ¹³⁷Cs inventory, SOC and TN concentration and CN ratio

The ¹³⁷Cs inventory pattern along the slope clearly confirmed erosion and deposition has occurred in Site 1 and Site 2 (Table 7.1 and Figure 7.1a.b). The sites concur with other studies such as Walling and Quine (1991) and Quine and Zhang (2002). The low total ¹³⁷Cs activity and lower depth distributed at eroding profiles (eroding and mid-slope) was evident in comparison to deposition sampling sites that had higher total ¹³⁷Cs activity and to a greater depth. The eroding locations have lost a considerable amount of soil in comparison to the mid-slope sampling locations in both sites. Depositional locations at both sites had considerable gains in soil, with Site 2 reflecting a higher rate of deposition than Site 1. The low input/non-mechanized study sites show a net soil export from the higher than mechanized/high input farm lands (Van Oost *et al.*, 2007). This may be due to water erosion, which is the major form of erosion in this region, whilst in mechanized agriculture tillage is predominant erosion causing agent (Singh *et al.*, 1992; Quine and Zhang, 2002; Singh *et al.*, 2016).

Soil erosion processes lead to high loss of top soil, which contains C and nutrients. Thereafter, some of this eroded material will be redeposited and buried at deposition sites, with the remaining material being exported from the farming area. In the eroded profiles there were almost equal amounts of top and sub-soil due to the losses observed and the tendency of C to move towards the surface (Harden *et al.*, 1999; Quine and Zhang, 2002; Van Oost *et al.*, 2005; Quine and Van Oost *et al.*, 2007). The sub-soil, with low SOC content, rises to surface and becomes mixed with the top soil, which creates a disequilibrium, which facilitates either the soil to sequester more atmospheric C or cause C loss through priming. At the deposition sampling sites burial of topsoils occurs with the deposited soil containing approximately 27% sub-plough soil originating from the eroded areas.

Redistribution of soils and sediments has implications for carbon budgets. Top and sub-soils at the eroded sampling sites had significantly lower SOC concentration (Table 7.4) than deposition profiles for both sites (1 and 2). This is likely to be a result of continuous deposition and burial (Van Oost *et al.*, 2005, 2012; Wang *et al.*, 2013; Doetterl *et al.*, 2012, Vandenbygaart *et al.*, 2012, 2015). In this study the continuous top soil loss at the eroding sampling sites leads to an almost equal proportion of top

and sub-soil being present in the eroding profile plough layer. So if there is no dynamic replacement of new photosynthate at the eroding sampling sites then the top soil SOC should be equal or slightly higher than the sub-soil SOC concentration (Quine and Zhang, 2002; Van Oost *et al.*, 2005). However, in the eroding sampling sites, the top soil has almost double the amount of SOC as compared to the sub-soil, which suggests that there is a dynamic replacement of SOC.

Similarly at deposition sampling sites the proportion of top- to sub-soil is greater, with SOC almost equal to current SOC concentration of top soil at this position; this is likely a result of burial (Van Oost *et al.*, 2012; Wang *et al.*, 2014, 2015). However, in my study sites C contents do still decline with depth suggesting that there is a has been some loss of SOC during burial. In deposition profiles the sub-soil SOC is higher than in the eroding profiles, this confirms continuous burial of top soil SOC (Vandenbygaart *et al.*, 2012).

Soil redistribution processes influence TN concentration across a topographic gradient (Quine and Zhang, 2002; Zhang *et al.*, 2006; Vandenbygaart *et al.*, 2012). The top soil TN concentration along the slope at Site 1 showed no significant difference between sampling pits. However, in Site 2 the eroding sampling points had a significantly lower TN concentration than either the mid-slope or deposition profiles. The result observed in Site 1 maybe a due to the farmers applying fertilizers as this plot was under intense cultivation. In the sub-soil, TN concentration was significantly lower at eroding sampling points than mid-slope or deposition sampling locations in Site 1. However, in Site 2 the mid-slope profiles showed a higher concentration than either the eroding or deposition sampling points. The spatial pattern of TN is likely to be caused by soil redistribution processes, which ultimately also affect C flux (e.g., through crop production and microbial activity (Hartley *et al.*, 2010)).

There is no significant difference observed along the topographic gradient with respect to the CN ratio of top and sub-soil (Table 4). However, when top- and sub-soil C:N is directly compared at each slope stage, some differences were observed. Within the eroding profiles top and sub-soil show no significant difference, however, within mid-slope and deposition profiles the sub-soil CN ratio is significantly higher than within the top soils. This suggests that buried SOC may contain a labile portion which is relatively fresh in terms of SOC (with a wider range of C:N). In the eroding sampling

sites the top- and sub-soil SOC is older and more passive and the C:N has a narrower range (Wang *et al.*, 2013; Vandenbygaart *et al.*, 2012) .

7.3.2. Cumulative C release

In this study there was no significant difference between eroding, mid-slope and deposition positions with respect to top- and sub-soil C release. After one year of incubation, top soils from eroding, mid-slope and deposition sampling profiles showed no significant difference between Site 1 and Site 2 for cumulative C release (Figure 7.5a, b). Although there is a significant difference in SOC concentration along slope positions with respect to the top soils, there was no different in C mineralization per unit SOC. This may be due to a continuous plant derived SOC uniformly being added to the top soils of all positions, or more labile SOC being replaced at eroding positions (equal to the amounts in the mid-slope and deposition sampling locations). Similar results have also been reported by other authors for similar landscape level studies (Doetterl *et al.*, 2012; Wang *et al.*, 2013). At deeper depth, rates of decomposition per unit SOC were lower in the depositional sites than in the eroded locations despite the buried layers likely to contain a greater amount of relatively young organic matter (^{137}Cs activity much greater in depositional sites at depth). Either there is a small amount of labile C in the eroded deep layers responsible for the higher rate of respiration per unit SOC, or the burial is effective in reducing rates of decomposition in the depositional areas potentially through reaggregation and physical protection (Six *et al.*, 2002; VonLutzow *et al.*, 2006; Doetterl *et al.*, 2012; Vandenbygaart *et al.*, 2015).

Vertical mixing

Based on ^{137}Cs tracer technique this study confirms for the two sites that vertical mixing/redistribution of SOC within the top and sub-soils occurs at both eroding and deposition sampling positions. To determine whether this should result in carbon uptake or release, I aimed to test two hypotheses. Firstly, in eroded sites, mixing topsoil with organic matter-poor subsoil will reduce decomposition rates as organic matter from topsoils may become bound onto unsaturated soil particles in the subsoil. This can be measured by comparing observed and expected C release for eroded sites locations. I observed no significant (Figure 7.5 a, b) difference between observed and expected cumulative C release in this soil samples and thus reject this hypothesis. Equally I did not observe any evidence for positive priming effects associated with

could have been caused by fresh organic matter in the topsoil promoting decomposition of older subsoil C. This may be related to the relatively low organic matter content of subsoils in eroded areas and/or a predominance of physically or chemically protected SOC (Quine and Van Oost., 2007; Six *et al.*, 2002). This result confirms that the mixing of the top and sub-soil SOC at the eroding position does not cause sizeable losses of C due to priming or promote C sequestration onto unsaturated soil particles (Kuzyakov *et al.*, 2000; Fontaine *et al.*, 2007; Salome *et al.*, 2010). Despite this, as highlighted above there remains the potential for dynamic replacement of eroded C in these areas as evidenced by the high C contents in the eroded surface samples which should have been a mixture of top and subsoils.

My second hypothesis was that in depositional areas, mixing fresh organic matter from top soils into organic matter-rich subsoils will promote C release through a positive priming effect. This hypothesis was supported by the results with greater than expected losses from the combined soils, compared with the results from the individual incubations (Figure 7.5 a, b). When depositional subsoils were incubated on their own the rate of respiration per unit SOC was lower than in eroded locations despite the expectation that there should be more young C present in these samples. If the assumption is made that the additional C released from the mixed samples was derived from the sub-soil part of the mixture (justifiable given that it was the subsoils that differed more between eroded and depositional locations, especially at Site 1), then the additional 2.5 to 10 mg CO₂-C g⁻¹SOC would represent an increase in decomposition of 25 to 100%. This suggests strongly that in these buried depositional soils, microbial activity is strongly limited by the availability of readily decomposable organic matter (Fontaine *et al.*, 2007). From this result it can be proposed that the deposition profiles facilitate a C-sink when there is rapid and continuous burial by burying organic matter below the depths that receive large amounts of contemporary C inputs. It is important to emphasize that unlike many previous experiments (e.g. Hartley *et al.*, 2010) priming effects were studied over a 1-year incubation in this study and positive effects of mixing were observed throughout in the soils from Site 1 suggesting that these effects are meaningful for long-term controls on agricultural SOC dynamics (Figure 7.6a). Therefore, it should also be mentioned that if deep ploughing or any other practices mixes horizons together buried SOC could be lost and C sink

strength will be reduced (Fontaine *et al.*, 2007; Van Oost *et al.*, 2012; Vandenbygaart *et al.*, 2012, 2015; Wang *et al.*, 2013; Wang *et al.*, 2014; Wang *et al.*, 2015).

7.4. Conclusion

The results of this study suggest that erosion-induced redistribution can promote a C sink through dynamic replacement of SOC at eroding positions, and burial of SOC at deposition positions. The former is illustrated by the high topsoil C contents in eroded locations, while positive priming effects following the mixing of depositional top and subsoils suggests that microbial activity is strongly limited by the availability of readily-decomposable organic matter in organic matter rich buried horizons.

7.5. Key findings

- ^{137}Cs activity inventory clearly showed areas of erosion and deposition within the study area.
- SOC, TN and CN ratio pattern also changed according to soil redistribution within the study fields. There is an eroding profile deficit apparent for SOC and TN, and an accumulation apparent in the deposition areas. The similarity of organic matter contents in eroded topsoils compared with the other locations indicates a dynamic replacement has occurred.
- Sub-soil eroding profiles showed a higher rate of respiration than deposition samples, suggesting that either there is a small amount of labile C in the eroded deep layers responsible for the higher rate of respiration per unit SOC, or that burial is effective in reducing rates of decomposition in the depositional areas.
- Mixed soils respiration eroding profiles showed no detectable positive or negative priming effect, however, the deposition samples showed a positive priming effect, with up to a doubling of the rate of decomposition of sub soil organic matter.
- The incubation study (one year in duration) confirmed erosion induced redistribution/mixing process favours a C sink, with no evidence that burial in depositional areas reduces microbial activity by isolating organic matter from contemporary C inputs.

8. Conclusion

8.1 Introduction

Recent studies have shown the importance of the effect of soil redistribution on the spatial variation of: nutrients, C fluxes between soil and atmosphere; and soil respiration; and these emphasise the importance of these for better understanding of SOC dynamics (Quine and Van Oost., 2007; Van Oost *et al.*, 2007; Doetterl *et al.*, 2012; Li *et al.*, 2015; Doetterl *et al.*, 2016). These studies also demonstrate the need to extend understanding of these processes to low productivity agricultural systems. Therefore, this study has focussed on developing an understanding of the soil redistribution/erosion induced spatial variation of nutrients (C, N and P), net C flux between soil and atmosphere and soil respiration rates across a topographic gradient within low input and productivity agricultural fields in the foot hills of the Indian Himalaya.

Based upon a review of current understanding, presented in Chapter 2, there remained a need to gain further understanding supported by experimental data in several critical areas. Chapter 3 identified the key aims of this project. Based upon identified areas for further research, Chapter 4 outlined the methodological approach to address identified objectives, whilst Chapters 5-7 presented results and analysis. Key findings of each objective are summarised individually, within the context of the main aim of this study.

8.2. Summary of key results for each objective

Objective 1: *To quantify the impacts of erosion-induced soil redistribution on SOC and nutrients distributions (lateral and vertical) within agricultural fields.*

Chapter 5 addressed objective 1 by characterising lateral (along slope transect) and vertical (depth increment) distributions of ^{137}Cs , SOC, TN, and P concentration (activity or mass per unit mass) and inventory (activity or mass per unit land surface area) and C:N and C:OP ratio for each field from all study sites. The ^{137}Cs tracer technique was adopted to characterise soil redistribution, the basic principle is that where soil loss occurs ^{137}Cs inventories are low (lower than fallout input) and where soil accumulation occurs inventories are high (higher than fallout input). The complete results presented in Chapter 5 (Section 5.3.1) reveal a consistent pattern in which profiles from the upslope positions in most of fields are characterised by ^{137}Cs inventories significantly ($p < 0.05$) lower than profiles located in the mid and downslope positions of the fields. This provides strongly evidence of within field soil redistribution. This pattern of inventories is also reflected in differences in the activity depth distributions with lower maximum depth of elevated ^{137}Cs activity in the eroding upslope pits and elevated ^{137}Cs activity at greater depths in the downslope pits. The pattern of ^{137}Cs variation within field and pit is consistent with the influence of both water and tillage erosion within the fields. The ^{137}Cs tracer results also provide strong support for the suitability of the approach for tracing and studying soil redistribution in this environment.

The SOC and TN distributions with depth and along the slopes (Section 5.3.2-5.3.8) followed a similar pattern to ^{137}Cs . Upslope positions, which on the basis of ^{137}Cs inventories are considered eroded, exhibited significantly lower ($p < 0.05$) inventories than were observed in ^{137}Cs -enriched downslope areas, considered to be depositional. Like SOC and TN, P (OP and TP) also followed similar pattern except at Site 3 (calcareous soil fields). The fields, therefore, display a pattern of nutrient loss over the eroding upslope sections and nutrient and SOC burial in aggradation areas. In the eroded sections, loss of top soil and the consequent mixture of remaining plough soil, nutrients and SOC-poor sub-soil creates the potential for SOC sequestration and other nutrient stabilization (Harden *et al.*, 1999). There is evidence that this is occurring in the fields studied here in the relatively small depletion of SOC, N and P at eroding locations compared to the high levels of depletion of ^{137}Cs . Although burial of nutrient

and SOC rich topsoil at depositional areas may suggest that these play an important role in C and nutrient sequestration, the soil erosion budgets presented in Chapter 6 indicate that within field storage of redistributed soil accounts for a smaller proportion of eroded soil than in mechanised farm lands (Quine and Van Oost, 2007; Van Oost *et al.*, 2007). At the study sites, most of eroded sediment, SOC and sediment-associated N and P is exported beyond the field boundaries and this creates a deficit of nutrient in these low input farm lands. The implications of subsoil C excavation and mixing at eroding positions and top soil burial and mixing at deposition positions are addressed in chapter 6 and 7. Over all spatial variation within field pattern of ^{137}Cs , SOC and nutrients strongly evidenced influence of soil redistribution process on within-field soil variability.

Objective 2: *To quantify the effect of erosion-induced soil carbon redistribution on the net carbon exchange between soil and atmosphere in low input/productivity and highly eroding agricultural fields from the foothills of the Indian Himalaya by using ^{137}Cs fallout and SOC inventories*

Soil redistribution rates and net C flux between soil and atmosphere derived using the ^{137}Cs and SOC inventory and depth distribution data (from Chapter 5) for study area are presented in Chapter 6. The C flux quantification model (Section 4.3), based on the method developed by Quine and Van Oost (2007), was used to estimate lateral and vertical soil and SOC redistribution under an assumption of equilibrium conditions and the net exchange of C between soil and atmosphere was derived from the difference between measured and 'equilibrium' SOC inventories. Net C fluxes were derived for each landscape position within the agricultural fields studies and calculated at field and site scale (Section 6.2). The result indicate that erosion rates (1.31 to $3.2 \text{ kg m}^{-2} \text{ y}^{-1}$) are in the mid-range for the region and that the great majority of eroded soil (88%) is exported from the fields and only 12% of sediment redeposited within fields. Eroded SOC is exported and redeposited in the same proportions. The effect of high rate of soil and SOC redistribution was to create disequilibrium in SOC dynamics at eroding and deposition positions and this supported the formation of a field scale C sink. The sink strength is highest in the most eroded parts of the fields due to dynamic replacement of eroded C (Harden *et al.*, 1999). This is assumed to be due to the high rate of incorporation of SOC-poor subsoil, with a large C-unsaturated surface area,

into the cultivation layer. The C sink is smaller to those reported from high nutrient-input mechanised farm lands (Quine and Van Oost, 2007; Van Oost *et al.*, 2007). Irrespective of the fate of exported SOC, the SOC stocks in the fields appear to be in dynamic equilibrium condition and, therefore, there is no evidence of a direct C source to atmosphere due to erosion. This is very similar to the recent finding of equilibrium soil C stocks in highly eroding fields in the Loess Plateau (Li *et al.*, 2015). Also the rate of SOC export from the fields is very high, especially when compared with mechanised field, and if it is assumed that some portion of exported C is stored in some part of low lying area then the C sink strength would be comparable to mechanised farm lands.

Nevertheless, despite the field SOC stocks appearing to be in dynamic equilibrium, the SOC stocks and the surface concentrations over the most eroded parts of the fields are significantly depleted compared to the stable and depositional areas within the fields (section 5.3). This has potentially important implications because of the important role that SOC plays in regulating soil quality and soil productivity. First, it is likely that the depletion of SOC over the eroded field area affects soil function and limits crop production. Second, because my results suggest that the soils of the most eroded part of field have low SOC saturation, there is potential to store more C in these soils if they can be improved. Therefore, notwithstanding the observed net C sink in the eroded landscape elements, it is suggested that adoption of best management practice (nutrient management, crop residue, erosion-control, etc) should be adopted to increase the SOC saturation level and target co-benefits for crop productivity and other ecosystem services. This is particularly important as there is some circumstantial evidence that the current 'equilibrium' state in SOC stocks within the field is in part maintained by import of biomass from neighbouring forest ecosystems. This is an aspect of the C-dynamics of these field systems that warrants further investigation.

Objective 3: *To study the effect of erosion- and deposition-induced vertical soil/SOC mixing on soil respiration rates at various landscapes positions.*

As discussed in Chapter 5 and 6, the soil redistribution and C flux study confirmed the existence of spatial variation in C flux at various landscapes position and was consistent with an important role for vertical mixing of soil and SOC in determining net C exchange with the atmosphere. This informed the design of the final element of the research that examined soil respiration differences in soil from shallow and deep

layers in eroding and aggrading landscapes position (Objective 3 addressed in Chapter 7). Respiration was measured over a one year period in samples derived from separate depth layers and in mixtures of soil from different depths from each landscape position. No significant difference was found in C release rate (per unit mass of C) from topsoil of eroding and deposition position but the subsoil of eroding pits exhibited significantly ($p < 0.05$) higher C release than the subsoil from deposition positions. This is similar to the observations made by Doetterl et al. (2012) working in mechanised agricultural landscapes in Western Europe. The results found in this study are considered to demonstrate that topsoil in both locations has almost equal and similar C origin. The relatively high rate of respiration in sub soils from eroding pits may be due to the presence of a larger proportion of SOC formed from recently incorporated plant material (crop roots) at these locations. In buried and deposition locations the reduced mineralisation is consistent with the proposition that burial of top soil can contribute to formation of a C sink. In the samples containing mixed topsoil and subsoil, evidence for priming was seen where the respiration rate in the mixed sample was significantly higher than the expected rate based on the respiration rate seen in the separate depth samples. No priming was evident in mixed soils from eroding locations, suggesting that mixing of subsoil and surface soil does not accelerate loss of old SOC from the subsoil. In contrast, significant ($p < 0.05$) priming action was evident in mixed soils from aggrading locations suggesting that buried SOC at depositional locations may be subject to accelerated respiration as long as it is exposed to fresh plant input (as found in surface soils).

8.3. Areas for further research

- There is good evidence in this study for the viability of using ^{137}Cs to trace erosion in the study region. However, if this is to be undertaken on a routine basis it will be essential to obtain reliable data for ^{137}Cs fallout reference inventories. An initial investment in systematic activity to define patterns of fallout input to the region would be a strong basis for future work across multiple field sites.
- There is clear potential to use or adapt existing coupled erosion-C dynamics models (Van Oost *et al.*, 2005a) to gain further insights into the relationship between erosion, C-dynamics and soil quality and to explore the relative importance of tillage and water erosion. Such work could incorporate the data obtained in this study.

- Due to presence of inorganic carbon in one site it was difficult to interpret soil respiration results. Future studies could use the isotopic signature of respired C to discriminate between inorganic and organic sources. The equipment needed to do this is now much more readily available than when this study began.
- Phosphorus redistribution studied in carbonate soil did not show any systematic relationship with soil redistribution. This implies that interaction between the P-cycle and carbonate weathering may be important at these sites and this requires further investigation.
- The observed results of priming action at deposition sites in this study are potentially important for the survival of SOC in depositional locations and, by implication, the C-dynamics of erosion-deposition systems. Further investigation is needed to more clearly isolate the controls on this important process and temporal evolution of the priming effect over long time-scales.
- While this study demonstrated dynamic replacement of C occurred in eroding agricultural fields, further investigation of the mechanisms is required. Greater understanding could be achieved if the origin of replaced C was known and there is potential to use the contrasting isotopic C signatures of C₃ and C₄ plant material to advance this field.
- Most of the eroded sediment and SOC was exported from the fields of this region and there is a need for further study of the fate of exported SOC beyond field boundaries.
- The possibility that these field systems are in receipt of additional C inputs from other ecosystems warrants further investigation because this has significant implications for assessment of landscape-scale C fluxes.

8.4. Broader Context and Conclusions

In conclusion, despite the low input and low productivity of the farmlands in the Indian Himalaya region studied here, there is consistent evidence that high rates of soil erosion and soil redistribution have induced spatial variation of nutrients and SOC, net C flux and soil respiration rates that combine to create a pattern of soil SOC stocks that are close to equilibrium and, if some of the exported C is sequestered, to create a net C sink. This result again confirms that erosion induced redistribution of C does not directly cause a net release of C to the atmosphere. Similar results have also been found in the highly eroding environment of the Loess Plateau in China (Li *et al.*, 2015).

However, this remains a controversial topic and many soil scientists express concern at the suggestion that erosion creates a sink, as can be seen in the Lal and Pimentel (2008) response to the paper by Van Oost et al. (2007) that provided evidence for a global C sink associated with erosion on agricultural land. The conclusions of this study should not be read as justifying land degradation; however, it does mean that care is needed in establishing the C sequestration benefits of land use change, especially if such estimates are used to justify or offset C-releasing activity such as fossil fuel combustion.

The results and conclusions raise three broader questions that I will attempt to address here.

1. *What are the impacts of the high rates of erosion observed at these sites and what would be the potential benefits of reducing erosion?*

The evidence in Chapters 5 and 6 makes clear the effect of soil redistribution and the significantly reduced nutrients and SOC over the most eroded parts of the fields and the high rates of nutrient export from the fields. These results are consistent with earlier studies that reported high net loss of soil for this region, based on run off plot and survey techniques (Singh and Gupta, 1982; Singh *et al.*, 1992; Singh *et al.*, 2016). To sustain crop production in this highly eroding region it is recommended that N P K doses of 120:60:40 kg ha⁻¹ are applied for Maize–wheat cropping systems (Ghosh *et al.*, 2015b). Nevertheless, in this low income region inorganic fertilisers are rarely used and farmers rely on farmyard manure as the principal amendment. While the organic amendments contribute to maintenance of SOC stocks in an equilibrium state, they are less effective in making up for the loss of nutrients. Furthermore, as mentioned above, there is some observational and oral reporting evidence that local forest ecosystems are currently used to supplement organic amendments to the fields and there is a risk that, if this were to increase, it could lead to degradation of these ecosystems. Therefore, despite the appearance of an equilibrium state, the fields are neither in a sustainable nor optimal state for crop production.

In summary, my study results identify the need for erosion control measures and sustainable nutrient management program for this region to support continued crop production. Otherwise due to continued loss of nutrients, it is expected that crop productivity will be reduced and this will affect total food production in this region.

Furthermore, the nutrient loss has implications for water quality and for regional economics if the government subsidises fertilizers input to address the problems.

2. What are the implications for current land use in the region?

My study found that despite erosion, SOC stocks appear to be in dynamic equilibrium (Chapter 6). Nevertheless, as discussed above this equilibrium state is associated with depleted SOC and nutrient stocks across the eroded part of the landscape (78% area) and with significant loss of SOC and nutrients from the fields. If these fields are to be retained in continuous sustainable crop production there is a need for improved management including integrated nutrient management techniques (Ghosh *et al.*, 2014 and 2015a). These crop management practices would be based on supply of combined nutrient from inorganic and organic and use a wide variety of the latter including: farm yard manure, vermicompost, poultry manure and other indigenously available manures.

This study also reported key result on spatial variation of nutrients and SOC within fields which has not been previously reported for this high eroding region. These results demonstrate the potential for farmers to 'precision' manage land by specific interventions at the sub-field scale to improve the nutrient-poor locations without unnecessary amendments to the nutrient- rich land to reduce cost and support environmental friendly farming. The high rates of soil and nutrient export can be addressed by adopting erosion management measures such as crop selection (erosion resistant), crop space management (intercrops) management, crop residue management, proper tillage practice, sub-field level crop management (upslope field - grown less water demanding crop and downslope field- more water demanding crops) and adopting conservation engineering measures (field bund across slope to reduce erosion). These erosion control measures help to reduce soil loss but complete eradication of soil erosion in this region is impossible because of nature of the fields' topography (slope/hill farming), soil type (more susceptible to soil loss), and the high intensity rain fall (nearly 1400mm rain fall within July to September). My study result suggests that strong site specific management of field for sustainable crop management are required.

An alternative strategy would be to convert from continuous cultivation on the slopes to adoption of Horticulture (fruit trees), Agri-horticulture, Agro-forestry, Animal farming

(managed grass lands). This would follow the “Grain to Green” model adopted in China where cultivation was stopped in the most eroded part of the land and the area was given over to growing other permanent trees etc to stop degradation of land and enhance ecosystem service delivery. Nevertheless, this would be very challenging in this region because of the large population reliant on farming for subsistence purposes.

3. How should these results influence ICAR advice and Indian government policy regarding erosion prevention, carbon sequestration, etc.?

At present, although there are many programmes run by state and central government to control erosion, promote better crop production on site, and reduce off site erosion effects, there has been little less focus on C sequestration on eroded landscapes. However, ICAR and the Indian Soil and Water Conservation Institute have a developing programme with a main focus on C sequestration on eroded landscapes through the adoption of better land management/conservation measures (Bhattacharya *et al.*, 2009; Ghosh *et al.*, 2014 and 2015a). This study will complement and inform this developing research programme by providing the first study from this region to address the influence of erosion on C sequestration. The consistency of my results with previous studies suggests that there is both scope and need for soil erosion induced carbon fluxes to be incorporated into carbon budgets, research frameworks, land management and climate change mitigation strategies at policy-relevant scales. It is clearly essential that the C sequestration potential of soil redistribution is recognised and accounted for when quantifying the very real benefits to be gained from interventions that increase local SOC inventories and benefit the delivery of ecosystem services through management practices that control erosion. As strategies are developed to address the 95 m ha undergoing erosion in India, it is imperative that win-win (erosion-reduction and productivity increase) potential is recognised but not overstated as win-win-win with assumed C sequestration benefits embedded without accounting for the offset created by loss of erosion-induced C sequestration. If this is not undertaken then, errors made in estimation of C-sequestration benefit of land use change over an area of this magnitude could have far-reaching consequences.

Appendix from chapter 4 to 7

Appendix for Chapter 4 include from Appendix Table 4.1 to 4.5, Appendix Figure 4.1 to 4.5 and Appendix text 4.1

DKF1



DKF2



DKF3



DK Ref 1



DK ref 2



Appendix Figure 4.1 Field shape images for Site 1 (All slope fields and non slope fields)

PSF1



PSF2



PSF3



PS Ref1



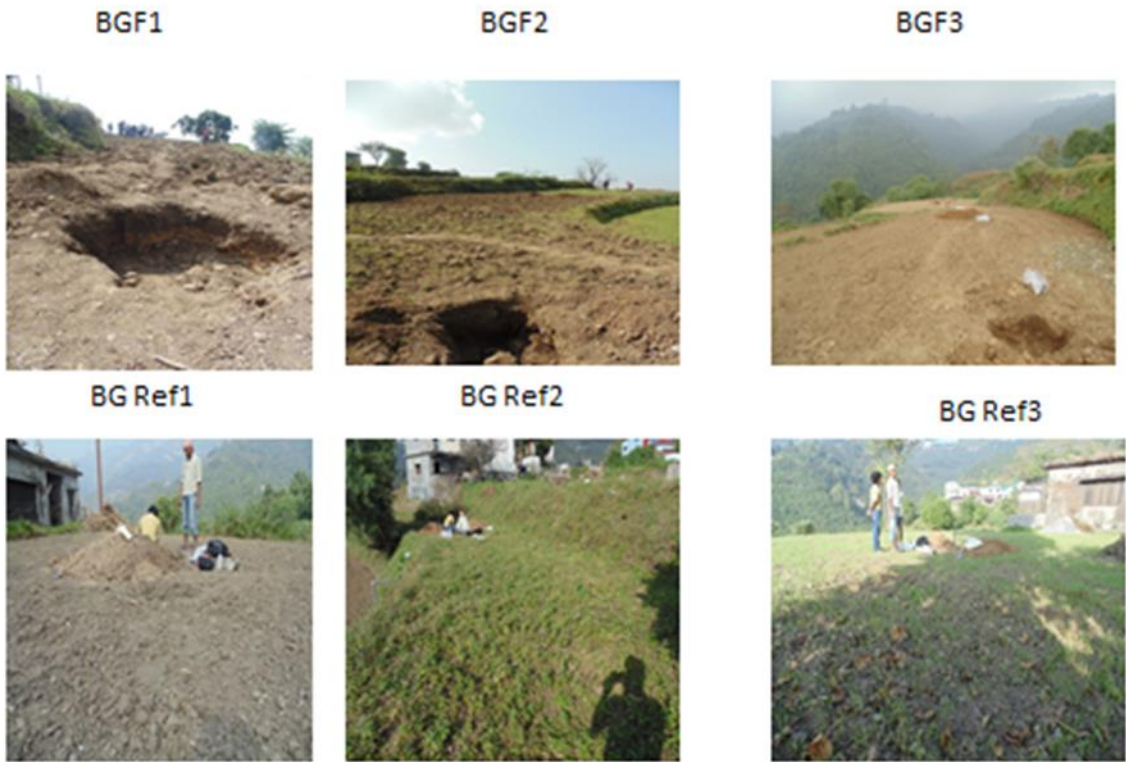
PS Ref2



PS Ref3



Appendix Figure 4.2 Field shape images for Site 2 (All slope fields and non slope fields)



Appendix Figure 4.3 Field shape images for Site 3 (All slope fields and non slope fields)

Soil pH and EC

Appendix Table 4.1 Soil pH and EC (dsm^{-1}) for composite soils of various depths (vertical) and along slope (lateral) for fields from Site 1(Dhulkhot).

Site 1 Fields	Depth	P1		P2		P3		P4		P5		P6	
		pH	EC	pH	EC	pH	EC	pH	EC	pH	EC	pH	EC
DKF1	0-10	5.25	0.27	4.9	0.15	5.13	0.12	5.21	0.12	5.04	0.21	5.2	0.24
	10-20	5.05	0.1	5	0.06	5.23	0.06	5.13	0.06	5.08	0.07	5.2	0.14
	20-30	5.05	0.16	4.91	0.08	5.23	0.07	5.02	0.06	4.97	0.08	5.04	0.12
	30-50	4.98	0.07	5.09	0.03	5.21	0.04	5.05	0.03	4.92	0.06	5.05	0.05
	50-70	5.13	0.06	5.05	0.03	5.14	0.04	5.07	0.03	4.95	0.04	5.02	0.04
	70-100					4.99	0.04	5.15	0.02	4.72	0.08	5	0.03
DKF2	0-10	5.49	0.17	5.28	0.39	5.35	0.22	5.22	0.12	5.21	0.24		
	10-20	5.95	0.07	5.59	0.13	5.5	0.08	5.46	0.06	5.59	0.07		
	20-30	5.77	0.09	5.45	0.14	5.38	0.15	5.28	0.09	5.39	0.08		
	30-50	5.72	0.07	5.44	0.07	5.47	0.08	5.38	0.03	5.16	0.07		
	50-70	5.56	0.06	5.35	0.05			5.33	0.02	5.15	0.05		
	70-100			4.9	0.2			5.28	0.07	4.86	0.18		
DKF3	0-10	5.07	0.11	5.08	0.13	5.13	0.16	5.38	0.08	5.28	0.12	5.31	0.09
	10-20	5.36	0.05	5.32	0.04	5.45	0.05	5.63	0.03	5.57	0.04	5.62	0.04
	20-30	5.27	0.05	5.28	0.05	5.38	0.06	5.47	0.04	5.45	0.04	5.57	0.04
	30-50	5.24	0.04	5.26	0.04	5.42	0.03	5.31	0.02	5.35	0.02	5.51	0.02
	50-70	5.04	0.06	4.8	0.16	5.39	0.02	5.3	0.01	5.33	0.01	5.61	0.01
	70-100			4.97	0.09	4.4	2.46	5.02	0.04	4.87	0.08	4.92	0.66
DKRef	0-10	5	0.14	5.12	0.15	5.16	0.13						
	10-20	5.32	0.04	5.43	0.06	5.47	0.05						
	20-30	5.31	0.05	5.4	0.06	5.43	0.06						
	30-50	5.37	0.03	5.38	0.04	5.32	0.04						
	50-70	5.3	0.03	5.3	0.04	5.28	0.04						
	70-100	5.31	0.02	5.11	0.16								

Appendix Table 4.2 Soil pH and EC (dsm⁻¹) for composite soils of various depth (vertical) and along slope (lateral) for fields from Site 2 (Pasauli)

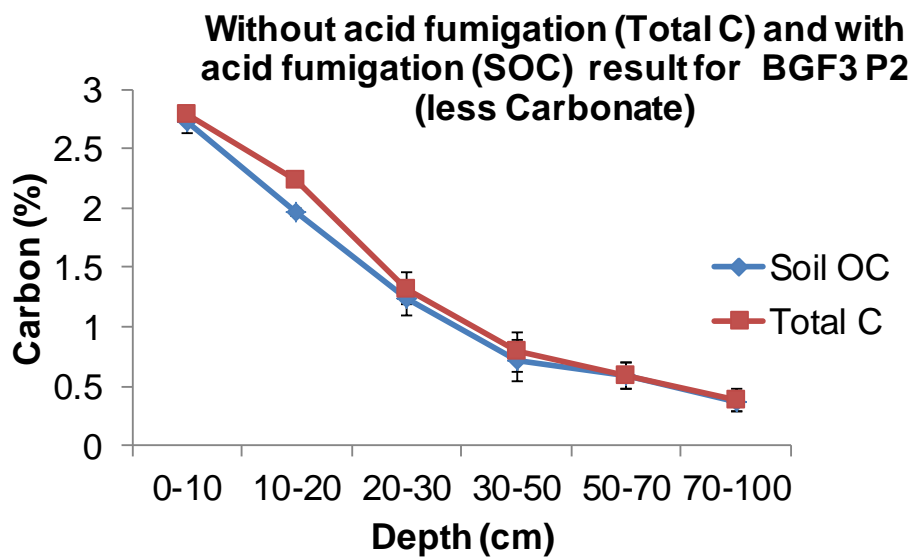
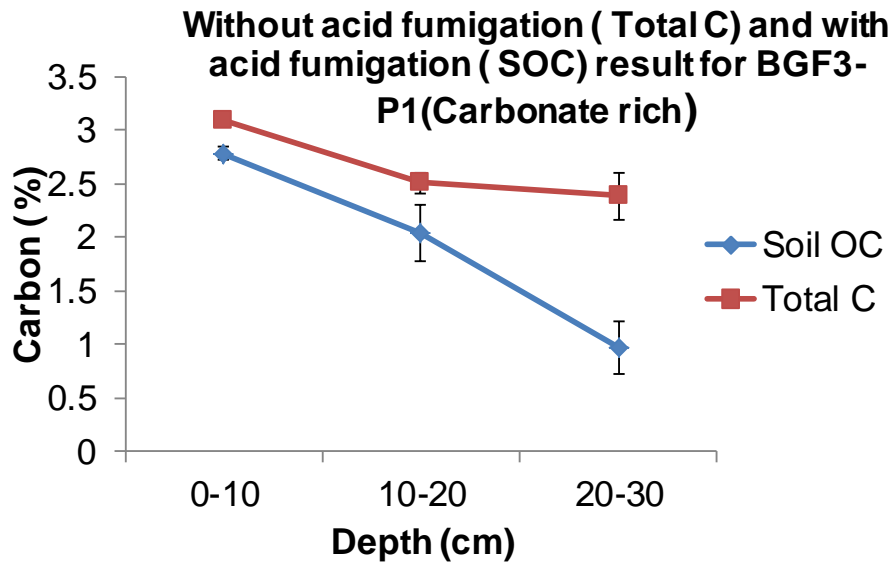
Site 2	Depth	P1		P2		P3		P4		P5		P6		P7	
Fields		pH	EC	pH	EC	pH	EC	pH	EC	pH	EC	pH	EC	pH	EC
PSF1	0-10	5.78	0.09	5.46	0.13	5.75	0.1	5.59	0.07	5.61	0.07	5.39	0.09		
	10-20	5.72	0.05	5.5	0.07	5.72	0.09	5.43	0.05	5.46	0.06	5.41	0.06		
	20-30	5.65	0.04	5.51	0.06	5.71	0.08	5.36	0.05	5.41	0.05	5.35	0.05		
	30-50	5.55	0.02	5.32	0.06	5.38	0.06	5.15	0.05	5.18	0.05	5.24	0.05		
	50-70	5.6	0.02	5.27	0.05	5.33	0.04	5.1	0.03	5.22	0.03	5.3	0.04		
	70-100	5.51	0.03	5.19	0.07	5.3	0.04			5.23	0.03	5.3	0.03		
PSF2	0-10	5.97	0.21	5.15	0.14	5.12	0.05	5.14	0.12	5.34	0.1	5.12	0.13	5.16	0.1
	10-20	6.14	0.1	5.12	0.08	5.21	0.04	5.26	0.07	5.43	0.05	5.41	0.04	5.28	0.07
	20-30	6.12	0.09	5.13	0.08	5.15	0.05	5.14	0.11	5.41	0.05	5.39	0.04	4.93	0.31
	30-50	6.08	0.05	5.21	0.06	5.23	0.04	5.21	0.04	4.8	0.36	5.36	0.04	5.37	0.05
	50-70	5.95	0.04	5.37	0.03	5.36	0.03	5.34	0.04	4.68	1.43	5.38	0.03	5.34	0.05
	70-100	6.02	0.02	5.49	0.03	5.38	0.02	5.35	0.04	4.78	0.36	5.35	0.04	5.33	0.04
PSF3	0-10	5.01	0.19	4.89	0.12	4.76	0.09	4.66	0.17	4.87	0.14	4.78	0.17		
	10-20	5.15	0.13	5.09	0.06	4.84	0.06	4.75	0.09	5.07	0.09	4.97	0.08		
	20-30	5.15	0.12	5.18	0.05	4.84	0.06	4.78	0.09	5.13	0.1	4.86	0.12		
	30-50	5.34	0.05	5.36	0.04	5.17	0.04	5.14	0.06	5.44	0.05	5.1	0.05		
	50-70	5.22	0.09	5.5	0.03	5.38	0.02	5.34	0.03	5.4	0.03	5.22	0.03		
	70-100			5.31	0.03	5.43	0.03	5.28	0.02	5.36	0.03	5.08	0.05		
PSRef	0-10	5.58	0.33	7.45	0.17	6.16	0.22								
	10-20	5.54	0.25	7.46	0.16	6.18	0.18								
	20-30	5.62	0.31	7.41	0.17	6.2	0.19								
	30-50	5.78	0.06	7.14	0.07	6.35	0.08								
	50-70	5.83	0.04	6.72	0.05	6.43	0.04								
70-100	5.82	0.04	6.47	0.06	6.45	0.03									

Appendix Table 4.3 Soil pH and EC (dsm⁻¹) for composite soils of various depth (vertical) and along slope (lateral) for fields from Site 3 (Bhatta Gaon)

Site 3	Depth	P1		P2		P3		P4		P5		P6		P7	
Fields		pH	EC	pH	EC	pH	EC	pH	EC	pH	EC	pH	EC	pH	EC
BGF1	0-10	6.91	0.48	6.90	0.22	6.90	0.20	6.84	0.32	7.03	0.30	7.10	0.39	6.98	0.58
	10-20	6.87	0.29	6.88	0.15	6.89	0.19	6.93	0.27	7.25	0.27	7.27	0.30	7.21	0.25
	20-30	7.04	0.14	6.85	0.12	6.96	0.15	6.93	0.20	7.43	0.27	7.44	0.25	7.23	0.21
	30-50	7.17	0.07	6.90	0.10	7.18	0.07	7.11	0.11	7.68	0.26			7.39	0.18
	50-70	7.21	0.09	6.80	0.13	7.27	0.10	7.45	0.19					7.66	0.17
	70-100	7.54	0.10	6.84	0.11	7.29	0.12	7.69	0.22					7.69	0.17
BGF2	0-10	7.01	0.36	7.10	0.42	7.35	0.30	7.31	0.27	7.42	0.26	7.40	0.35		
	10-20	7.19	0.22	7.28	0.18	7.38	0.26	7.26	0.22	7.63	0.20	7.48	0.34		
	20-30	7.24	0.13	7.29	0.15	7.23	0.18	7.19	0.15	7.73	0.20	7.59	0.23		
	30-50	7.20	0.12	7.40	0.11	7.17	0.11	7.09	0.12	7.79	0.11				
	50-70	7.25	0.09	7.46	0.08	7.25	0.10	7.15	0.11						
	70-100	7.31	0.07	7.43	0.11	7.28	0.08	7.11	0.12						
BGF3	0-10	7.07	0.36	7.22	0.28	7.14	0.37	7.16	0.33	7.24	0.34				
	10-20	7.35	0.3	7.27	0.24	7.43	0.31	7.34	0.21	7.34	0.18				
	20-30	7.66	0.28	7.24	0.21	7.55	0.26	7.43	0.14	7.27	0.16				
	30-50			7.27	0.1	7.36	0.12	7.61	0.14	7.34	0.15				
	50-70			7.28	0.08	7.49	0.11	7.78	0.11	7.41	0.12				
	70-100			6.97	0.28	7.79	0.17	7.37	0.42	6.88	0.31				
BGRRef	0-10	7.24	0.37	7.37	0.29	7.25	0.34								
	10-20	7.3	0.35	7.4	0.24	7.31	0.26								
	20-30	7.38	0.31	7.31	0.2	7.15	0.24								
	30-50	7.52	0.22	7.26	0.14	7.11	0.2								
	50-70			7.3	0.12	7.08	0.17								
	70-100			7.23	0.13	7.29	0.1								

Appendix Table 4.4 Inorganic carbon (IOC) content in soils from calcareous soils of Site 3. Mean values \pm SE ($n = 3$) are presented

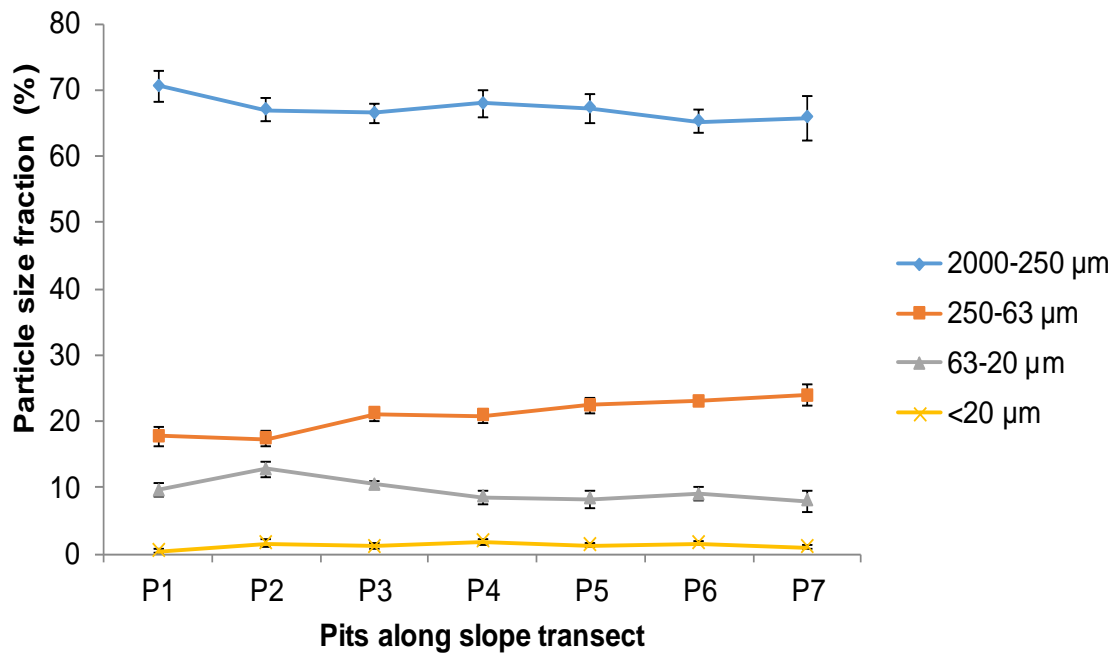
Fields ID	Depth (cm)	P1		P2		P3		P4		P5		P6		P7	
		IOC %	SE	IOC %	SE	IOC %	SE	IOC %	SE	IOC %	SE	IOC %	SE	IOC %	SE
BGF1	0-10	0.07	0.29	0.06	0.04	-0.04	0.10	-0.02	0.02	0.08	0.12	-0.17	0.16	0.40	0.04
	10-20	0.06	0.06	0.00	0.11	0.03	0.03	0.08	0.08	0.25	0.17	0.33	0.10	-0.03	0.09
	20-30	0.05	0.02	0.07	0.04	0.08	0.01	-0.26	0.30	0.18	0.07	0.22	0.06	0.12	0.02
	30-50	0.03	0.03	-0.02	0.04	-0.01	0.01	-0.04	0.10	-0.05	0.37			0.00	0.01
	50-70	0.00	0.01	0.00	0.00	-0.02	0.01	0.32	0.21					0.08	0.07
	70-100	0.54	0.53	0.07	0.03	-0.01	0.01	0.71	0.62					0.31	0.19
			P1		P2		P3		P4		P5		P6		
		IOC %	SE	IOC %	SE	IOC %	SE	IOC %	SE	IOC %	SE	IOC %	SE		
BGF2	0-10	0.37	0.12	-0.30	0.21	0.39	0.15	0.16	0.16	0.03	0.13	0.76	0.32		
	10-20	0.21	0.07	-0.21	0.20	0.39	0.20	0.19	0.10	0.53	0.32	1.07	0.10		
	20-30	-0.04	0.02	-0.09	0.07	0.08	0.09	0.06	0.07	1.12	1.04	0.45	0.08		
	30-50	-0.02	0.02	-0.01	0.00	0.01	0.02	0.01	0.02	0.30	0.24				
	50-70	-0.02	0.01	0.05	0.05	0.02	0.02	-0.02	0.02						
	70-100	-0.04	0.02	0.00	0.00	0.02	0.01	0.01	0.01						
			P1		P2		P3		P4		P5				
		IOC %	SE	IOC %	SE	IOC %	SE	IOC %	SE	IOC %	SE				
BGF3	0-10	0.32	0.12	0.07	0.13	-0.11	0.26	-0.11	0.05	0.35	0.10				
	10-20	0.47	0.34	0.27	0.05	0.45	0.35	0.08	0.02	0.09	0.08				
	20-30	1.42	0.07	0.08	0.01	0.21	0.20	0.00	0.03	-0.06	0.09				
	30-50			0.07	0.03	0.02	0.01	0.01	0.00	0.01	0.04				
	50-70			0.00	0.01	0.04	0.04	-0.02	0.00	-0.01	0.03				
	70-100			0.01	0.01	0.10	0.08	-0.01	0.00	0.00	0.01				
			Ref1		Ref2		Ref3								
		IOC %	SE	IOC %	SE	IOC %	SE								
BGRref	0-10	1.12	0.29	1.02	0.52	0.68	0.08								
	10-20	1.24	0.06	0.82	0.39	0.59	0.23								
	20-30	1.26	0.35	0.50	0.11	0.28	0.13								
	30-50	1.18	0.44	0.09	0.05	0.00	0.01								
	50-70			0.02	0.01	0.01	0.01								
	70-100			0.04	0.01	0.00	0.00								



Appendix Figure 4.4 Trial for IOC removal conducted with more carbonate soil (above) and less carbonate soil (bottom). Mean values \pm SE ($n = 3$) are presented

Appendix Table 4.5 Soil particle size fractionation along slope transect up to 50 cm depth for BGF1. Mean values \pm SE ($n = 3$) are presented

Pits	Depth (cm)	Particle size fraction (%)							
		2000-250 μm	SE	250-63 μm	SE	63-20 μm	SE	<20 μm	SE
P1	0-10	68.49	1.37	18.50	0.90	10.51	1.01	0.78	0.27
	10-20	71.00	2.84	17.81	1.72	9.24	1.41	0.34	0.24
	20-30	72.50	2.58	16.58	1.47	9.43	1.02	0.41	0.12
	30-50	70.57	2.54	18.45	1.75	9.47	1.19	0.33	0.14
P2	0-10	68.47	3.09	18.27	1.94	11.00	0.99	0.80	0.42
	10-20	67.60	0.58	17.40	0.69	12.73	1.12	1.07	0.67
	20-30	66.00	2.01	16.07	1.49	15.07	0.59	1.73	0.74
	30-50	65.60	1.33	17.67	0.27	12.33	2.02	2.93	0.79
P3	0-10	67.33	1.57	19.73	0.79	10.67	0.93	1.33	0.48
	10-20	68.73	0.94	18.73	0.68	10.67	0.64	1.07	0.35
	20-30	64.67	1.27	22.40	1.30	11.40	0.31	0.80	0.23
	30-50	65.33	2.07	23.73	1.22	9.07	0.55	1.07	0.67
P4	0-10	65.46	1.71	21.98	0.63	9.77	1.39	2.01	0.92
	10-20	67.72	1.47	19.80	1.10	9.23	0.75	2.51	0.40
	20-30	68.49	3.17	20.82	1.27	8.37	1.57	1.41	0.40
	30-50	70.35	1.71	20.80	0.99	6.69	0.86	1.37	0.23
P5	0-10	65.71	2.69	22.41	1.64	9.13	1.18	1.78	0.32
	10-20	68.66	1.89	22.61	0.99	6.99	0.76	0.97	0.17
	20-30	68.74	2.71	21.49	0.79	7.99	1.83	1.03	0.21
	30-50	65.90	1.24	23.09	0.94	8.85	1.08	1.29	0.30
P6	0-10	62.73	1.67	23.93	0.57	10.14	0.92	2.08	0.32
	10-20	65.23	0.17	23.48	0.16	8.79	0.03	1.38	0.29
	20-30	65.97	2.70	22.38	1.11	9.03	1.78	1.51	0.13
P7	0-10	65.87	2.21	23.29	0.97	8.29	0.90	1.51	0.25
	10-20	68.09	4.09	22.65	2.23	6.89	1.52	1.21	0.51
	20-30	62.96	3.39	24.88	1.68	9.68	1.85	1.04	0.44
	30-50	66.20	3.76	25.07	1.46	7.00	2.36	0.40	0.12



Appendix Figure 4.5 Soil particle size fractionation along slope transect total of up to 50 cm depth for BGF1. Mean values \pm SE ($n = 3$) are presented

Appendix Table 4.6 Soil particle size distributions at various slope positions and depths and Enrichment Ratios (ER), representing the downslope % divided by the upslope %. At sites 1 and 2 there appears to be modest silt enrichment in the surface soil layer at the downslope sites. In contrast, at Site 3 there is no clear evidence of enrichment of any fraction at the downslope pit with the possible exception of some clay depletion in the sub-surface downslope.

Sites	Slope	Pits	Depth in cm	Clay %	D/U	Silt %	D/U	F.Sand	C.Sand	Sand %	D/U	Soil texture type
				< 0.002 mm	ER	0.002-0.02 mm	ER	0.02-0.2 mm	0.2-2 mm	ER	Based on ISSS	
Site 1	Upslope (U)	DKF1 P1	0-10	16.8		25.6		57.1	0.5	57.6		Loam
			30-50	18.4		29.6		39.38	12.62	52		Loam
	Downslope (D)	DKF1 P6	0-10	15.2	0.90	33.6	1.31	45.56	5.64	51.2	0.89	Loam
			30-50	18.4	1.00	34.4	1.16	45.96	1.24	47.2	0.91	Loam
Site 2	Upslope (U)	PSF3 P1	0-10	15.2		20.8		33	31	64		Sandy loam
			30-50	11.2		25.6		33.6	29.6	63.2		Sandy loam
	Downslope (D)	PSF3 P6	0-10	13.6	0.89	36	1.73	40.32	10.08	50.4	0.79	Loam
			30-50	15.2	1.36	32.8	1.28	40.6	11.4	52	0.82	Loam
Site 3	Upslope (U)	BGF2 P1	0-10	19.2		34.4		30	16.4	46.4		Loam
			30-50	24		30.4		22.4	23.2	45.6		Loam
	Downslope (D)	BGF2 P6	0-10	16.8	0.88	32.8	0.95	36.3	14.1	50.4	1.09	Loam
			20-30	16.8	0.70	31.2	1.03	31.4	20.6	52	1.14	Loam

Appendix Text 4.1 Soil particle size distribution by dry Sieving:

- Soil air dried and crushed with pestle and mortar and sieved with <2 mm sieve.
- 50 g air dried soils < 2mm size put on nest of sieve 2000 μm (coarse sand), 250 μm (fine sand), 63 μm (silt and clay) and 20 μm and shaken for 5-10 minutes by using shaker. Particles retained and passed through the sieves will be weighed and put into original bags separately (this soil can be reused but it may be very slightly contaminated due to particle struck in sieves). After each sample sieving, sieves will be cleaned properly.
- This particle size decided based on International society of soil science.

Appendix text 4.2

Inorganic carbon (IOC) removal procedures

There are four common methods adopted by many researchers to remove Inorganic carbon from soil:

Acid rinse/ washing method: here the soils are entirely mixed with diluted acid and washed with de-ionised water and followed drying and measuring the organic carbon and $\delta^{13}\text{C}$ content (Midwood and Boutton, 1998; Collin *et al.*, 1999; Fernandes and Krull, 2008).

Limitation: a. loss of OC and change in $\delta^{13}\text{C}$ signature and loss fine soil materials
b. time and labour consuming

Capsule method/ aqueous acid addition: Addition of stepwise diluted acid and water directly into soil which is in Silver capsule and transferred to metal tray and kept on hot plate. The sample monitored for effervescence and indicating IOC reaction. After end of reaction capsule folded and packed in Tin capsule and measured OC and $\delta^{13}\text{C}$ content (Verardo *et al.*, 1990).

Limitation: soil contamination by violent effervescence and soil loss affect OC

Acid fumigation by HCL: soil samples weighed in Silver capsule and placed in microtiter tray. Add water to moisten in soils and keep tray in Desiccator. 100 ml of Conc HCL acid in beaker placed inside desiccator. Keep both in desiccator leave it for 6-8 hrs and remove tray and dry in oven and cool then pack fold the capsule and measure OC and $\delta^{13}\text{C}$ (Harris *et al.*, 2001).

Limitation: it will alter N content and $\delta^{15}\text{N}$. Brittle capsule and loss of soil

Benefit: many samples can processed, no effect on OC and $\delta^{13}\text{C}$

Loss on Ignition (LOI): LOI calculates %OM by comparing the weight of a sample before and after the soil has been ignited. Before ignition the sample contains OM, but after ignition all that remains is the mineral portion of the soil. The difference in weight before and after ignition represents the amount of the OM that was present in the sample (Ball, 1964; Schulte and Hopkins, 1996)

Problems with LOI:

- a. Abella and Zimmer, 2007 suggest LOI is not accurate than Elemental analysis SOC estimation for arid forest soil of USA.
- b. combust IC, clay structure water, not all SOM ignites (Ball, 1964; Schulte and Hopkins, 1996)
- c. Optimal temperature and duration for heating determine is difficult.
- d. LOI varies with soil type and depth of same soil (Konen *et al.*, 2002)
- e. If soil has low SOC (1.5%) LOI is unreliable (Soon and Abboud, 1991)
- f. Conversion of LOI- OM to OC is difficult because of conversion factors may differs vegetation to vegetation (Batti and Bauer, 2002)

Recent suggestion is that to remove IOC without affect OC and $\delta^{13}\text{C}$ is acid fumigation (Harris *et al.*, 2001) is best method. But this method reviewed and tested by several authors (Bisutti *et al.*, 2004; Komada *et al.*, 2008; Walthert *et al.*, 2010 ; Brodie *et al.*, 2011) and given modification and further upgraded the methods.

Stepwise acidification as modification for acid fumigation Walthert *et al.*, 2010 modified Harris *et a.*, 2001 acid fumigation procedure (Used in my soil samples);

1. Weigh 25 mg of the ground sample into small silver capsules (9 mm by 5mm) and place the capsules in the wells of a titter plate (Capsule thickness if I increased I can avoid corroding)
2. Add 50 μL of 1% HCL to each capsule,
3. In a desiccator, expose the titter plate with the open capsules for 8 h to the vapour produced by 100 mL of 37% HCL in a beaker,
4. If sample give excess foam during step 3: then repeat 1 and 2; then expose the samples in the desiccator for 24 h to the vapour produced by 32% HCL, add 50 μL of deionised water, and finally expose the samples for 8 h to the vapour produced by 37% HCL.

5. Place the titter plate with the open capsules for 24 h in a continuously vacuumed desiccator containing drying granules,
6. Place the titter plate with the open capsules inside the desiccator with drying granules under the fume hood for 3 d (low temperature drying minimize the volatilize OC) (the steps 5 and 6 drying process help to reduce acid effect on CN instrument life and also drying at vacuum/fume hood is necessary to avoid forming crust on surface of samples during drying otherwise it affect desiccation of sample)
7. Immediately after removal from the desiccator, quickly pack the capsules containing the dried samples into larger new tin capsules (10 mm by 10 mm) forming compact balls, (small capsule with acid treated soil will packed in large size capsule to avoid brittle and loss of soil from corroded capsule)
8. Store the balls until measurement in a desiccator containing drying granules,
9. Measure the samples with a CN analyser involving high temperature combustion.

Modification to method from Harris et al., 2001 by Walthert et al., 2010 :

The modification is to moisten the soil samples with 1% HCL to accelerate wetting instead of Deionized water; strongly foaming samples will be treated separately by adopting gentle fumigation step to avoid sample loss due to excess foaming; include drying in vacuum oven to ensure complete drying; after drying pack the small silver capsules used in fumigation into larger silver capsules to avoid sample loss from corroded and perforated capsules.

Other comments:

- Acid fumigation affects OC loss due to acid volatilization, oxidation and spills suggested by Bisutti *et al.*, 2004
- Komada *et al.*, (2008) recommend acid fumigation better when comparing with Capsule acid method for measuring OC and $\delta^{13}\text{C}$ is successful but maximum time is 6-24 hrs only

Stepwise acidification limitation:

Placing treated samples and capsules into a second capsule prior to folding is more difficult, time consuming and increase cost. Double encapsulating the sample is also problematic for the mass spectrometer because more oxygen is required for combustion and results in frequent replacement of copper wires used to trap excess oxygen (Ramarine *et al.*, 2011). But I can outer wrap by tin capsules may reduce the cost (Brodie *et al.*, 2011) and increase burning.

Soil pH (decide IOC removal required/not):

Schumacher, 2002 reported soil pH >7.4 need to remove inorganic carbon, and Walthert *et al.*, 2010 observed IC at further low pH so >6.00 soil samples need to remove IOC.

Acid Selection:

HCL is better than other acids (H₃PO₄ – C contamination, Viscous and Hydroscopic and H₂SO₄ - is too weak to remove Dolomite type IOC). But in HCL –Cl may affect instrument it will reduced by proper drying in vacuum oven. Also Cl will change the mass of soil if I not measure pre acid treatment so need correction factors.

Appendix Text 4.3

P estimation methods and review

Introduction

The Total P test estimates the amount of inorganic and organic P in a soil. It is therefore a useful diagnostic test in that it gives a better appreciation of the reason plants may not be performing optimally in a certain soil i.e. it helps to determine whether this is because P levels in the soil are simply too low (and thus more fertiliser should be added) or whether the problem is simply one of P availability (there is an adequate total amount present in the soil). In the latter case, availability may be improved by methods other than applying fertiliser i.e. stimulating soil microbes to breakdown organic matter and speed up nutrient cycling or altering pH to levels that are more optimal for P availability.

Phosphorus in agricultural soils occurs in many forms, both organic and inorganic. Inorganic forms of phosphorus include fertiliser residues, various calcium, iron and aluminium phosphates, and phosphorus adsorbed on mineral surfaces, especially hydrous oxides of iron and aluminium. Organic forms of phosphorus often account for a large fraction of the phosphorus in soil, especially in soils under permanent pasture where the percentage of organic phosphorus may exceed 70% of the total. Much of this organic phosphorus occurs as poorly characterised, high molecular weight material which originates from microbial activity in the soil and from the decomposition of plant and animal residues. Organic forms of phosphorus are generally not directly available for plant uptake, but can provide a source of plant-available phosphorus upon mineralisation. This is usually a slow process and organic phosphorus is usually considered to be mostly unavailable to annual crops. The ratio of organic carbon: organic phosphorus may provide an index to its availability (Black and Goring, 1953). Net immobilisation of inorganic phosphorus into organic forms usually occurs if this ratio exceeds 300.

Estimation: Organic P estimation by many methods (Appendix Table 4.6), has complex and time consuming

- Most common to measure O.P is dry combustion methods of Saunders and Williams (1955) as modified by Walker and Adams (1958). But this method

recovery of P is erratic and varies from Ca –domination to Fe/Al dominated soils weathering intensity.

- Ignition method highly inaccurate for weathered soils rich in Fe/Al oxides particularly tropical soils because ignition changes Fe/Al oxides/Hydroxide and water molecules. (Olsen and Sommers ,1982) for comments about ignition
- Ignition may underestimate Organic P due to Incomplete extraction of P during ignition and volatilization of P (Williams *et al.*, 1970; Anderson, 1975) but these losses are minimum at 800°C (Saunders and Williams, 1955; Anderson, 1975). After ignition solubility of P compounds may be increased result increase P values

Soils of study area fall under Alluvial soil / Entisol and Inceptisol. This soil not fall under the category of high Fe /Al oxides. Ignition methods is not suitable for tropical soils. In India tropical soils fall under Tamil Nadu, Andhra Pradesh, Kerala and Karnataka (Red and lateritic highly weathered soils which has more Iron and Aluminium). But my study area fall under subtropical and sub humid region. Soils mostly brown and alluvial soils in that region study. In Acidic soil P availability restricted due to Fe and Al fixation of P. In alkaline soil P fixed by Calcium. P availability more at neutral soils.

Appendix Table 0.7 Agronomical P / Available P estimation methods to recommend fertilizer for crop Production

Method name	Extracting solution	Suitable for	Remarks
Bray and Kurtz P-1	0.025M HCL in 0.03 M NH ₄ F	Acid to Neutral soil	Not suitable for Alkaline soil. 25-30 mg P /kg soil Optimum for crop production
Mehlich – 1	0.0125M H ₂ SO ₄ + 0.05 M HCL	Acidic soil	25-30 mg P /kg soil Optimum for crop production
Mehlich – 3	EDTA, NH ₄ F, CH ₃ COOH, NH ₄ NO ₃ and HNO ₃	All soils	45-50 mg P /kg soil Optimum for crop production
Olsen P	0.5M NaHCO ₃	Alkaline Soil	

Determination of inorganic and organic phosphate in soil (Saunders and Williams, 1955)

Principle

From dried soils samples: two samples (ca. 0.5g each) from each soil batch are needed, one for the determination of inorganic phosphate, the other one for the determination of organic phosphate.

Inorganic Phosphate

A known sample of soil is transferred into a centrifuge tube and soaked overnight in (a known quantity) of 0.5M H₂SO₄. Due to this the inorganic (ortho) phosphate in the soil will go into the solution.

Total phosphate (organic phosphate = total – inorganic)

This soil sample is weighted into a crucible and then burnt. Heating the sample at 55^oC transfers the organic phosphate into inorganic phosphate, so the total amount of P in the soil is analysed. The organic phosphate can be calculated as the difference between a heated (total P) and an unheated (inorg P) sample.

The burnt sample is transferred into a centrifuge tube and soaked overnight in (a known quantity) of 0.5M H₂SO₄ so that the (inorganic) phosphate in the sample will go into the solution

2nd day: The phosphate concentration in a known quantity of the solution is determined; from this the inorganic and organic phosphate content in the soil can be calculated.

In order to determine the phosphate concentration reagents are added to the acid solution with the dissolved orthophosphate so that a highly coloured molybdenum blue complex is formed. The same reagents are added to different phosphate standards (solutions with a known concentration of P). The intensity of the colour is proportional to the P content but unfortunately not very stable. The different standards are measured photometrical at 880nm so that a calibration curve is obtained. The reading from the spectrophotometer of the soil sample solutions can now be converted into the phosphate concentration of each sample.

Steps involved in P analysis

Analysis of total phosphate (T)



0.5g of sample in crucible

Burn at 550C for an hour

Remove, cool in desiccators

Transfer sample in centrifuge tube

Fill up tubes with 0.5M H₂SO₄ to 45ml mark (the acid is dissolving the inorganic phosphate)

Vortex each tube

Shake overnight

Analysis of inorganic phosphate (I)



0.5g of sample in centrifuge tube

- Label 25ml volumetric flasks for samples, for standards and for blank
- Centrifuge samples for 10min at 3000rpm
- Prepare colour reagent
- Pipette a known volume of supernatant into a labelled volumetric flask (can be between 0.1 ml and 10 ml), for every sample
- add 0.5M sulphuric acid to *blank flask*, use same amount (ml) as you use for soil samples
- Add 5 drops of 0.25% p-nitrophenol indicator to each flask (Total and inorg. P and repeats and Blank)
- Neutralise by adding drops of 5M NaOH until colour change from clear to bright yellow
- Add 4ml of colour reagent
- Fill up to the mark with distilled water
- Let colour develop for 1h
- Measure absorbance in photometer at 880 nm

Appendix for Chapter 5

Appendix Table 5.1 Soil profile ^{137}Cs , SOC, and total N to 100 cm or maximum soil depth along the gradient transect within field Site 1 (DKF1 and DKF2 fields). Mean values \pm SE ($n = 3$) are presented

DKF1	^{137}Cs Inventory (Bq m^{-2})						SOC inventory (kg m^{-2})						TN inventory (kg m^{-2})						
	Depth	P1	P2	P3	P4	P5	P6	P1	P2	P3	P4	P5	P6	P1	P2	P3	P4	P5	P6
	0-10	290 \pm 15	479 \pm 3.2	525 \pm 56	349 \pm 27	420 \pm 7.0	545 \pm 48	1.01 \pm 0.05	0.89 \pm 0.02	0.82 \pm 0.04	1.01 \pm 0.06	1.16 \pm 0.05	1.40 \pm 0.08	0.07 \pm 0.004	0.08 \pm 0.004	0.08 \pm 0.003	0.09 \pm 0.004	0.10 \pm 0.005	0.12 \pm 0.008
	10-20	138 \pm 8.0	204 \pm 35	414 \pm 57	103 \pm 59	88 \pm 25	654 \pm 30	0.82 \pm 0.03	0.82 \pm 0.07	0.72 \pm 0.06	0.87 \pm 0.03	0.93 \pm 0.06	1.13 \pm 0.08	0.06 \pm 0.001	0.07 \pm 0.005	0.07 \pm 0.006	0.07 \pm 0.003	0.08 \pm 0.005	0.10 \pm 0.009
	20-30	134 \pm 31	237 \pm 20	337 \pm 33	62 \pm 29	54 \pm 31	618 \pm 18	0.57 \pm 0.09	0.81 \pm 0.04	0.74 \pm 0.05	0.71 \pm 0.03	0.97 \pm 0.12	1.05 \pm 0.08	0.04 \pm 0.008	0.08 \pm 0.003	0.07 \pm 0.003	0.06 \pm 0.003	0.08 \pm 0.009	0.09 \pm 0.010
	30-50	0	3.2 \pm 3.2	77 \pm 77	0	0	248 \pm 100	0.60 \pm 0.02	1.23 \pm 0.05	1.23 \pm 0.05	1.07 \pm 0.08	1.50 \pm 0.06	1.80 \pm 0.03	0.04 \pm 0.002	0.12 \pm 0.004	0.11 \pm 0.002	0.10 \pm 0.005	0.12 \pm 0.004	0.14 \pm 0.009
	50-70	0	0	0	0	0	0	0.28 \pm 0.03	0.79 \pm 0.22	1.12 \pm 0.07	0.86 \pm 0.09	1.36 \pm 0.05	1.65 \pm 0.11	0.02 \pm 0.003	0.08 \pm 0.018	0.10 \pm 0.007	0.08 \pm 0.005	0.11 \pm 0.005	0.13 \pm 0.009
	70-100			0	0	0	0			0.65 \pm 0.13	1.00 \pm 0.08	1.86 \pm 0.05	2.22 \pm 0.19			0.06 \pm 0.02	0.11 \pm 0.007	0.16 \pm 0.003	0.19 \pm 0.007

DKF2	^{137}Cs Inventory (Bq m^{-2})					SOC inventory (kg m^{-2})					TN inventory (kg m^{-2})						
	Depth	P1	P2	P3	P4	P5	P1	P2	P3	P4	P5	P1	P2	P3	P4	P5	
	0-10	221 \pm 24	232 \pm 13	332 \pm 87	318 \pm 63	476 \pm 46	0.87 \pm 0.05	1.06 \pm 0.07	1.05 \pm 0.20	0.91 \pm 0.03	1.47 \pm 0.10	0.10 \pm 0.005	0.10 \pm 0.004	0.11 \pm 0.019	0.09 \pm 0.012	0.12 \pm 0.015	
	10-20	14 \pm 15	146 \pm 49	226 \pm 94	141 \pm 8.0	631 \pm 58	0.80 \pm 0.04	0.96 \pm 0.02	0.61 \pm 0.11	0.90 \pm 0.09	0.70 \pm 0.06	0.09 \pm 0.006	0.09 \pm 0.004	0.07 \pm 0.010	0.09 \pm 0.013	0.06 \pm 0.010	
	20-30	31 \pm 15	152 \pm 19	55 \pm 8.8	161 \pm 34	587 \pm 88	0.61 \pm 0.03	0.90 \pm 0.03	0.34 \pm 0.04	0.78 \pm 0.06	0.74 \pm 0.05	0.07 \pm 0.007	0.09 \pm 0.004	0.04 \pm 0.005	0.09 \pm 0.014	0.07 \pm 0.005	
	30-50	0	0	0	21 \pm 21	99 \pm 42	0.58 \pm 0.15	1.25 \pm 0.02	0.19 \pm 0.04	1.11 \pm 0.09	1.60 \pm 0.08	0.08 \pm 0.020	0.13 \pm 0.007	0.025 \pm 0.004	0.13 \pm 0.030	0.14 \pm 0.005	
	50-70	0	0		0	0	0.18 \pm 0.05	0.99 \pm 0.06		0.95 \pm 0.08	1.19 \pm 0.06	0.02 \pm 0.006	0.10 \pm 0.012		0.14 \pm 0.034	0.12 \pm 0.002	
	70-100		0		0	0			1.27 \pm 0.02		1.03 \pm 0.02	0.90 \pm 0.04		0.17 \pm 0.024		0.20 \pm 0.039	0.10 \pm 0.005

Appendix Table 5.2 Soil profile ^{137}Cs , SOC, and total N to 100 cm or maximum soil depth along the gradient transect within field Site 1 (DKF3 and DK Ref fields). Mean values \pm SE (n = 3) are presented.

DKF3	^{137}Cs Inventory (Bq m^{-2})						SOC inventory (kg m^{-2})						TN inventory (kg m^{-2})					
	Depth	P1	P2	P3	P4	P5	P6	P1	P2	P3	P4	P5	P6	P1	P2	P3	P4	P5
0-10	506 \pm 58	509 \pm 47	455 \pm 23	111 \pm 44	175 \pm 25	293 \pm 54	0.89 \pm 0.01	1.00 \pm 0.02	0.97 \pm 0.07	0.91 \pm 0.02	0.93 \pm 0.04	0.94 \pm 0.09	0.08 \pm 0.002	0.08 \pm 0.001	0.10 \pm 0.014	0.01 \pm 0.002	0.10 \pm 0.004	0.10 \pm 0.005
10-20	385 \pm 96	333 \pm 31	284 \pm 27	62 \pm 3.5	99 \pm 70	202 \pm 37	0.78 \pm 0.04	0.83 \pm 0.05	0.77 \pm 0.03	0.72 \pm 0.05	0.80 \pm 0.05	0.76 \pm 0.02	0.07 \pm 0.004	0.07 \pm 0.003	0.09 \pm 0.003	0.08 \pm 0.005	0.09 \pm 0.006	0.09 \pm 0.004
20-30	252 \pm 96	123 \pm 97	166 \pm 84	0	24 \pm 17	81 \pm 49	0.75 \pm 0.05	0.87 \pm 0.05	1.07 \pm 0.19	0.67 \pm 0.03	0.69 \pm 0.01	0.55 \pm 0.03	0.07 \pm 0.004	0.07 \pm 0.003	0.12 \pm 0.032	0.07 \pm 0.001	0.07 \pm 0.001	0.07 \pm 0.002
30-50	131 \pm 131	0	0	0	13 \pm 13	3 \pm 3	1.32 \pm 0.05	1.39 \pm 0.07	1.31 \pm 0.10	1.26 \pm 0.09	1.20 \pm 0.04	0.68 \pm 0.05	0.12 \pm 0.003	0.11 \pm 0.005	0.13 \pm 0.040	0.13 \pm 0.002	0.11 \pm 0.017	0.10 \pm 0.004
50-70	0	0	0	0	0	0	1.13 \pm 0.04	1.20 \pm 0.05	0.92 \pm 0.07	0.84 \pm 0.02	1.01 \pm 0.05	0.43 \pm 0.05	0.11 \pm 0.003	0.11 \pm 0.006	0.10 \pm 0.007	0.10 \pm 0.004	0.08 \pm 0.012	0.09 \pm 0.012
70-100		0	0	0	0	0		1.42 \pm 0.04	0.96 \pm 0.06	1.20 \pm 0.13	1.21 \pm 0.13	0.50 \pm 0.05		0.14 \pm 0.010	0.20 \pm 0.020	0.17 \pm 0.008	0.12 \pm 0.026	0.17 \pm 0.040

DKRef	^{137}Cs Inventory (Bq m^{-2})			SOC inventory (kg m^{-2})			TN inventory (kg m^{-2})			
	Depth	Ref 1	Ref 2	Ref 3	Ref 1	Ref 2	Ref 3	Ref 1	Ref 2	Ref 3
0-10	235 \pm 71	382 \pm 34	476 \pm 62		0.84 \pm 0.04	1.00 \pm 0.11	0.97 \pm 0.07	0.08 \pm 0.004	0.10 \pm 0.012	0.09 \pm 0.012
10-20	128 \pm 74	333 \pm 31	210 \pm 28		0.70 \pm 0.06	0.87 \pm 0.05	0.84 \pm 0.04	0.07 \pm 0.006	0.09 \pm 0.010	0.09 \pm 0.012
20-30	65 \pm 31	123 \pm 97	8 \pm 8		0.68 \pm 0.01	0.79 \pm 0.05	0.84 \pm 0.03	0.07 \pm 0.003	0.08 \pm 0.012	0.09 \pm 0.008
30-50	0	0	0		1.16 \pm 0.03	1.05 \pm 0.06	1.05 \pm 0.14	0.11 \pm 0.002	0.11 \pm 0.011	0.12 \pm 0.029
50-70	0	0	0		1.18 \pm 0.03	0.71 \pm 0.03	1.04 \pm 0.12	0.11 \pm 0.002	0.09 \pm 0.009	0.12 \pm 0.019
70-100	0	0			1.35 \pm 0.10	0.90 \pm 0.06		0.15 \pm 0.004	0.17 \pm 0.031	

Appendix Table 5.3 Soil profile ^{137}Cs , SOC, and total N to 100 cm or maximum soil depth along the gradient transect within field Site 1 (PSF1 and PSF2 fields). Mean values \pm SE (n = 3) are presented.

PSF1	^{137}Cs Inventory (Bq m^{-2})						SOC inventory (kg m^{-2})						TN inventory (kg m^{-2})						
	Depth	P1	P2	P3	P4	P5	P6	P1	P2	P3	P4	P5	P6	P1	P2	P3	P4	P5	P6
	0-10	165 \pm 74	526 \pm 111	559 \pm 20	1004 \pm 72	1034 \pm 57	874 \pm 57	1.25 \pm 0.04	1.03 \pm 0.02	1.28 \pm 0.10	1.71 \pm 0.08	2.21 \pm 0.15	1.80 \pm 0.09	0.08 \pm 0.004	0.07 \pm 0.008	0.11 \pm 0.009	0.14 \pm 0.008	0.18 \pm 0.019	0.15 \pm 0.010
	10-20	91 \pm 31	699 \pm 170	833 \pm 46	760 \pm 59	469 \pm 20	675 \pm 72	0.86 \pm 0.13	0.92 \pm 0.03	1.19 \pm 0.06	1.61 \pm 0.10	1.57 \pm 0.09	1.91 \pm 0.18	0.05 \pm 0.008	0.06 \pm 0.012	0.10 \pm 0.005	0.12 \pm 0.004	0.11 \pm 0.012	0.15 \pm 0.009
	20-30	3.4 \pm 3.4	724 \pm 67	783 \pm 90	286 \pm 57	393 \pm 72	526 \pm 117	0.64 \pm 0.09	1.07 \pm 0.07	1.38 \pm 0.10	1.48 \pm 0.15	1.49 \pm 0.06	1.79 \pm 0.09	0.03 \pm 0.006	0.06 \pm 0.013	0.11 \pm 0.012	0.10 \pm 0.011	0.10 \pm 0.003	0.13 \pm 0.006
	30-50	0	88 \pm 22	272 \pm 17	97 \pm 74	104 \pm 47	153 \pm 52	0.80 \pm 0.07	2.10 \pm 0.12	1.60 \pm 0.02	2.59 \pm 0.09	2.36 \pm 0.11	2.49 \pm 0.17	0.03 \pm 0.009	0.10 \pm 0.026	0.12 \pm 0.000	0.18 \pm 0.007	0.16 \pm 0.003	0.19 \pm 0.011
	50-70	0	0	6.3 \pm 6.3	5.2 \pm 5.2	0	18 \pm 18	0.70 \pm 0.08	1.74 \pm 0.04	1.12 \pm 0.09	1.54 \pm 0.08	1.81 \pm 0.14	1.27 \pm 0.06	0.02 \pm 0.003	0.10 \pm 0.013	0.09 \pm 0.007	0.11 \pm 0.006	0.13 \pm 0.017	0.12 \pm 0.008
	70-100	0	0	0	0	9.1 \pm 9.1		1.16 \pm 0.04	1.48 \pm 0.10	1.91 \pm 0.08		2.68 \pm 0.22	0.72 \pm 0.19	0.04 \pm 0.001	0.10 \pm 0.023	0.14 \pm 0.001		0.20 \pm 0.024	0.07 \pm 0.013

PSF2	^{137}Cs Inventory (Bq m^{-2})							SOC inventory (kg m^{-2})							TN inventory (kg m^{-2})							
	Depth	P1	P2	P3	P4	P5	P6	P7	P1	P2	P3	P4	P5	P6	P7	P1	P2	P3	P4	P5	P6	P7
	0-10	338 \pm 30	617 \pm 44	666 \pm 69	851 \pm 39	761 \pm 40	1075 \pm 184	671 \pm 126	0.95 \pm 0.10	1.00 \pm 0.04	0.97 \pm 0.03	1.20 \pm 0.07	1.45 \pm 0.04	1.89 \pm 0.14	1.36 \pm 0.20	0.08 \pm 0.007	0.08 \pm 0.008	0.08 \pm 0.001	0.10 \pm 0.006	0.12 \pm 0.004	0.16 \pm 0.014	0.11 \pm 0.015
	10-20	209 \pm 30	309 \pm 32	344 \pm 89	575 \pm 44	440 \pm 124	452 \pm 111	744 \pm 144	0.42 \pm 0.03	0.60 \pm 0.04	0.84 \pm 0.02	1.10 \pm 0.06	1.59 \pm 0.07	1.22 \pm 0.09	1.19 \pm 0.07	0.04 \pm 0.004	0.05 \pm 0.004	0.07 \pm 0.002	0.08 \pm 0.002	0.12 \pm 0.006	0.10 \pm 0.005	0.09 \pm 0.009
	20-30	127 \pm 30	120 \pm 35	290 \pm 86	430 \pm 60	145 \pm 28	250 \pm 107	493 \pm 178	0.33 \pm 0.04	0.43 \pm 0.08	0.80 \pm 0.02	1.28 \pm 0.04	1.50 \pm 0.04	1.28 \pm 0.11	1.42 \pm 0.29	0.03 \pm 0.004	0.04 \pm 0.005	0.06 \pm 0.001	0.09 \pm 0.001	0.11 \pm 0.004	0.10 \pm 0.011	0.11 \pm 0.029
	30-50	0	15 \pm 15	16 \pm 16	65 \pm 44	137 \pm 69	26 \pm 18	158 \pm 87	0.19 \pm 0.02	0.53 \pm 0.07	0.92 \pm 0.02	1.48 \pm 0.12	2.64 \pm 0.10	1.52 \pm 0.25	1.79 \pm 0.12	0.02 \pm 0.003	0.05 \pm 0.006	0.08 \pm 0.009	0.10 \pm 0.007	0.20 \pm 0.015	0.12 \pm 0.017	0.14 \pm 0.003
	50-70	0	0	0	0	0	0	0	0.12 \pm 0.02	0.24 \pm 0.06	0.82 \pm 0.04	1.23 \pm 0.11	1.97 \pm 0.26	1.52 \pm 0.30	1.00 \pm 0.09	0.02 \pm 0.003	0.02 \pm 0.003	0.07 \pm 0.005	0.09 \pm 0.008	0.15 \pm 0.013	0.12 \pm 0.020	0.09 \pm 0.013
	70-100	0	0	0	0	0	0	0	0.16 \pm 0.01	0.29 \pm 0.06	1.08 \pm 0.05	1.48 \pm 0.07	2.96 \pm 0.22	1.69 \pm 0.08	1.33 \pm 0.12	0.03 \pm 0.006	0.02 \pm 0.006	0.08 \pm 0.004	0.10 \pm 0.005	0.23 \pm 0.008	0.15 \pm 0.005	0.11 \pm 0.007

Appendix Table 5.4 Soil profile ¹³⁷Cs, SOC, and total N to 100 cm or maximum soil depth along the gradient transect within field Site 1 (PSF3 and PS Ref fields). Mean values ± SE (n = 3) are presented.

PSF3	¹³⁷ Cs Inventory (Bq m ⁻²)						SOC inventory (kg m ⁻²)						TN inventory (kg m ⁻²)						
	Depth	P1	P2	P3	P4	P5	P6	P1	P2	P3	P4	P5	P6	P1	P2	P3	P4	P5	P6
	0-10	137±18	289±57	378±39	357±16	436±50	635±82	0.84±0.02	0.74±0.06	0.88±0.04	1.24±0.18	1.13±0.09	1.29±0.06	0.07±0.003	0.06±0.003	0.07±0.005	0.09±0.014	0.08±0.007	0.10±0.007
	10-20	148±16	406±83	470±51	277±42	553±87	995±102	0.71±0.04	0.80±0.05	0.81±0.04	0.86±0.18	1.20±0.10	1.57±0.26	0.06±0.006	0.07±0.003	0.06±0.003	0.05±0.011	0.08±0.006	0.11±0.020
	20-30	128±31	294±70	520±129	426±48	471±97	936±128	0.73±0.07	0.88±0.05	0.80±0.06	0.94±0.05	1.24±0.08	1.25±0.10	0.07±0.006	0.07±0.004	0.07±0.005	0.06±0.004	0.08±0.007	0.09±0.005
	30-50	3 ±3	0	383±50	349±102	155±24	140±33	0.56±0.16	1.66±0.21	2.04±0.25	1.69±0.07	1.98±0.27	1.74±0.13	0.06±0.016	0.12±0.011	0.12±0.005	0.10±0.003	0.11±0.014	0.11±0.017
	50-70	0	0	0	0	0	0	0.45±0.02	0.80±0.05	2.19±0.26	1.46±0.07	1.19±0.01	1.56±0.21	0.05±0.002	0.07±0.005	0.12±0.002	0.08±0.003	0.07±0.005	0.09±0.010
	70-100		0	0	0	0	0		1.53±0.07	1.76±0.05	1.71±0.07	1.51±0.15	1.74±0.20		0.13±0.008	0.11±0.000	0.10±0.001	0.09±0.012	0.11±0.010

PS Ref	¹³⁷ Cs Inventory (Bq m ⁻²)			SOC inventory (kg m ⁻²)			TN inventory (kg m ⁻²)			
	Depth	Ref 1	Ref 2	Ref 3	Ref 1	Ref 2	Ref 3	Ref 1	Ref 2	Ref 3
	0-10	526±72	151± 8	411±61	1.45±0.16	1.53±0.19	1.07±0.10	0.10±0.016	0.13±0.016	0.08±0.013
	10-20	389±57	154±70	404±28	1.04±0.23	1.17±0.17	1.05±0.10	0.08±0.016	0.09±0.016	0.08±0.006
	20-30	386±64	142±73	316±76	0.83±0.05	1.18±0.07	0.89±0.14	0.07±0.012	0.08±0.007	0.07±0.007
	30-50	35 ±15	178±92	63 ±4	0.57±0.08	1.59±0.38	0.47±0.11	0.04±0.008	0.11±0.026	0.04±0.006
	50-70	0	0	0	0.42±0.06	0.65±0.03	0.31±0.03	0.03±0.004	0.05±0.003	0.03±0.002
	70-100	0	0	0	0.47±0.04	0.41±0.18	0.29±0.03	0.03±0.001	0.03±0.014	0.03±0.004

Appendix Table 5.5 Soil profile ¹³⁷Cs, SOC, and total N to 100 cm or maximum soil depth along the gradient transect within field Site 1 (BGF1 and BGF2 fields). Mean values ± SE (n = 3) are presented.

Depth	¹³⁷ Cs Inventory (Bq m ⁻²)							SOC inventory (kg m ⁻²)							TN inventory (kg m ⁻²)						
	P1	P2	P3	P4	P5	P6	P7	P1	P2	P3	P4	P5	P6	P7	P1	P2	P3	P4	P5	P6	P7
0-10	247±56	386±23	342±30	565±64	581±64	681±57	568±92	1.91±0.13	1.35±0.09	0.97±0.11	1.59±0.15	1.52±0.06	3.01±0.36	2.27±0.26	0.18±0.031	0.11±0.004	0.08±0.004	0.15±0.013	0.14±0.012	0.24±0.018	0.23±0.027
10-20	181±41	235±17	339±18	459±32	552±49	630±30	254±8	0.95±0.23	1.01±0.04	0.82±0.03	1.18±0.05	1.29±0.10	2.14±0.09	1.13±0.08	0.09±0.019	0.09±0.002	0.07±0.007	0.12±0.010	0.13±0.003	0.21±0.004	0.12±0.013
20-30	95 ±60	59 ±27	46 ±24	69 ±40	154±28	108±42	110±43	0.63±0.26	0.59±0.04	0.42±0.02	1.01±0.23	0.89±0.013	1.31±0.10	0.92±0.19	0.05±0.032	0.04±0.002	0.03±0.004	0.08±0.011	0.07±0.009	0.13±0.010	0.10±0.012
30-50	0	48 ±12	0	0	21 ±16		0	0.26±0.03	1.12±0.18	0.30±0.01	0.60±0.17	1.13±0.13		0.82±0.12	0.02±0.002	0.06±0.009	0.02±0.002	0.07±0.016	0.10±0.008		0.08±0.010
50-70	0	0	0	0			0	0.21±0.03	0.90±0.08	0.20±0.07	0.36±0.03			0.68±0.07	0.03±0.005	0.05±0.005	0.06±0.008	0.05±0.006			0.09±0.013
70-100	0	0	0	0			0	0.20±0.08	1.36±0.24	0.19±0.04	0.27±0.04			0.64±0.13	0.03±0.012	0.07±0.019	0.02±0.004	0.05±0.005			0.09±0.013

Depth	¹³⁷ Cs Inventory (Bq m ⁻²)						SOC inventory (kg m ⁻²)						TN inventory (kg m ⁻²)					
	P1	P2	P3	P4	P5	P6	P1	P2	P3	P4	P5	P6	P1	P2	P3	P4	P5	P6
0-10	472±48	487±28	600±46	512±41	464±19	720±61	1.66±0.14	1.95±0.23	1.97±0.15	1.79±0.19	1.59±0.12	2.43±0.26	0.17±0.022	0.15±0.014	0.18±0.013	0.16±0.013	0.13±0.008	0.23±0.036
10-20	294±51	244±106	639±36	187±42	429±74	959±83	1.12±0.11	1.05±0.46	1.44±0.10	0.94±0.10	1.41±0.12	2.15±0.39	0.12±0.013	0.09±0.030	0.14±0.020	0.09±0.014	0.12±0.008	0.25±0.052
20-30	49 ±26	102±22	165±53	96 ±35	151±55	752±96	0.48±0.09	0.58±0.03	0.85±0.06	0.82±0.12	0.89±0.03	1.65±0.14	0.05±0.011	0.06±0.002	0.08±0.002	0.06±0.016	0.07±0.003	0.16±0.027
30-50	0	0	0	28 ±28	0		0.57±0.19	0.37±0.07	0.54±0.05	0.92±0.09	0.68±0.09		0.05±0.018	0.03±0.011	0.04±0.002	0.05±0.005	0.05±0.009	
50-70	0	0	0	0			0.35±0.11	0.28±0.04	0.52±0.08	0.75±0.02			0.05±0.019	0.04±0.003	0.04±0.005	0.03±0.003		
70-100	0	0	0	0			0.25±0.06	0.34±0.02	0.53±0.07	1.55±0.19			0.03±0.006	0.05±0.016	0.05±0.017	0.06±0.009		

Appendix Table 5.6 Soil profile ^{137}Cs , SOC, and total N to 100 cm or maximum soil depth along the gradient transect within field Site 1 (BGF3 and BG Ref fields). Mean values \pm SE (n = 3) are presented.

BGF3 ^{137}Cs Inventory (Bq m^{-2})						SOC inventory (kg m^{-2})					TN inventory (kg m^{-2})				
Depth	P1	P2	P3	P4	P5	P1	P2	P3	P4	P5	P1	P2	P3	P4	P5
0-10	505 \pm 75	509 \pm 17	506 \pm 85	475 \pm 20	491 \pm 7.3	1.74 \pm 0.13	1.87 \pm 0.12	1.99 \pm 0.14	2.11 \pm 0.20	2.03 \pm 0.11	0.20 \pm 0.022	0.19 \pm 0.017	0.18 \pm 0.016	0.20 \pm 0.020	0.20 \pm 0.013
10-20	536 \pm 82	606 \pm 58	229 \pm 12	137 \pm 54	459 \pm 79	1.49 \pm 0.20	1.41 \pm 0.07	0.95 \pm 0.01	0.74 \pm 0.08	1.81 \pm 0.11	0.18 \pm 0.005	0.18 \pm 0.010	0.09 \pm 0.006	0.10 \pm 0.005	0.17 \pm 0.013
20-30	206 \pm 71	279 \pm 29	35 \pm 35	30 \pm 19	73 \pm 24	0.71 \pm 0.16	0.95 \pm 0.08	0.41 \pm 0.05	0.33 \pm 0.02	1.16 \pm 0.06	0.10 \pm 0.019	0.13 \pm 0.002	0.04 \pm 0.007	0.06 \pm 0.004	0.10 \pm 0.009
30-50		77 \pm 39	0	0	0		1.02 \pm 0.10	0.44 \pm 0.01	0.36 \pm 0.06	2.18 \pm 0.15		0.17 \pm 0.022	0.04 \pm 0.003	0.07 \pm 0.004	0.18 \pm 0.012
50-70		0	0	0	0		1.01 \pm 0.11	0.45 \pm 0.02	0.25 \pm 0.02	1.44 \pm 0.33		0.16 \pm 0.013	0.05 \pm 0.011	0.08 \pm 0.017	0.13 \pm 0.031
70-100		0	0	0	0		0.98 \pm 0.26	0.57 \pm 0.02	0.46 \pm 0.05	0.93 \pm 0.03		0.20 \pm 0.026	0.05 \pm 0.008	0.13 \pm 0.016	0.11 \pm 0.015

BGRef ^{137}Cs Inventory (Bq m^{-2})				SOC inventory (kg m^{-2})			TN inventory (kg m^{-2})		
Depth	Ref 1	Ref 2	Ref 3	Ref 1	Ref 2	Ref 3	Ref 1	Ref 2	Ref 3
0-10	399 \pm 18	483 \pm 76	402 \pm 51	2.12 \pm 0.20	1.79 \pm 0.18	1.62 \pm 0.12	0.16 \pm 0.015	0.13 \pm 0.023	0.13 \pm 0.013
10-20	555 \pm 21	408 \pm 56	319 \pm 53	2.68 \pm 0.20	1.57 \pm 0.05	0.99 \pm 0.15	0.21 \pm 0.021	0.12 \pm 0.014	0.08 \pm 0.023
20-30	325 \pm 62	172 \pm 31	78 \pm 39	1.76 \pm 0.30	1.03 \pm 0.10	0.40 \pm 0.07	0.14 \pm 0.009	0.09 \pm 0.001	0.03 \pm 0.010
30-50	2.5 \pm 1.3	0	0	1.73 \pm 0.21	1.24 \pm 0.06	0.35 \pm 0.07	0.13 \pm 0.014	0.09 \pm 0.019	0.02 \pm 0.005
50-70		0	0		0.84 \pm 0.06	0.23 \pm 0.05		0.05 \pm 0.012	0.06 \pm 0.03
70-100		0	0		1.36 \pm 0.08	0.19 \pm 0.04		0.09 \pm 0.012	0.03 \pm 0.003

Chapter. 6 Appendix Soil and C redistribution lateral and vertical (Include Appendix Table 6.1 to 6.3).

Appendix Table 6.1 Basic data used in C flux estimation model

Parameters	Site 1	Dhoolkhot			Site 2	Pasauli			Site 3	Bhatta Gaon	
	DKF1	DKF2	DKF3	PSF1	PSF2	PSF3	BGF1	BGF2	BGF3		
Field slope %	2.91	2.20	2.84	5.89	6.59	6.15	1.84	4.05	4.21		
Field size (ha)	0.13	0.15	0.16	0.13	0.32	0.10	0.03	0.05	0.04		
Eroded area %	91.1	74.5	100.0	16.1	48.6	77.2	100.0	77.8	100.0		
Deposition area %	8.92	25.5	0.00	83.9	51.4	22.8	0.00	22.2	0.00		
Number of ¹³⁷ Cs/SOC Pits with 3 replicate	6.00	5.00	6.00	6.00	7.00	6.00	7.00	6.00	5.00		
Number of pits from											
Eroded area	5	4	6	1	4	4	7	5	5		
Deposition area	1	1	0	5	3	1	0	1	0		
Tillage depth (m)	0.14	0.14	0.14	0.19	0.26	0.26	0.24	0.24	0.24		
year of sampling	2013	2013	2013	2013	2013	2013	2013	2013	2013		
Reference ¹³⁷ Cs inventory (Bq m ⁻²)	1685	1685	1685	1685	1685	2100	1685	1685	1685		
Reference C inventory (kg m ⁻²) upto 0.5 m	4.59	4.59	4.59	5.30	5.30	5.30	5.50	5.50	5.50		
Mean annual temperature(°C)/precipitation (mm)	20/1600	20/1600	20/1600	20/1600	20/1600	20/1600	20/1600	20/1600	20/1600		
k (m ⁻¹) depth coefficient	3.53	3.53	3.53	6.29	6.29	6.29	10.3	10.3	10.3		
Cmin (0.9 of 1m depth C concentration) (kg m ⁻³)	3.36	3.36	3.36	1.63	1.63	1.63	3.97	3.97	3.97		

Appendix Table 6.2 Soil lateral and vertical redistribution budget ($\text{kg m}^{-2} \text{y}^{-1}$) for India sites based on profiles mean from Segment (E/D) . Mean values \pm SE ($n = 9$) are presented

Parameters	Site 1	Dhoolkhot			Site 2	Pasauli			Site 3	Bhatta Gaon		
	DKF1	DKF2	DKF3	PSF1	PSF2	PSF3	BGF1	BGF2	BGF3	Mean	SE	
Eroded area (%) of field and mixing	91.1	81.7	100.0	16.1	48.6	77.2	100.0	88.0	100.0	78.1	9.45	
Mean Erosion /subsoil excavation rate	2.67	3.74	3.24	3.76	1.08	1.83	2.02	1.74	1.73	2.42	0.32	
Cultivation layer in export	1.71	2.15	1.84	1.71	0.81	1.16	1.40	1.28	1.22	1.47	0.14	
Subsoil in export	0.95	1.59	1.42	2.06	0.28	0.67	0.62	0.46	0.51	0.95	0.20	
Cultivation soil lost in 50 yrs (kg m^{-2})	85.7	107.7	91.9	85.4	40.3	57.8	69.8	63.8	61.2	73.7	6.88	
Subsoil lost in 50 yrs (kg m^{-2})	47.7	79.4	71.0	102.8	13.8	33.6	31.2	23.0	25.6	47.6	10.07	
Remaining cultivation soil at eroding positions(kg m^{-2})	76.3	54.4	70.2	15.6	99.9	82.4	83.6	89.6	92.2	73.8	8.52	
Subsoil mixed at eroding plough layer (kg m^{-2})	85.7	107.7	91.9	85.4	40.3	57.8	69.8	63.8	61.2	73.7	6.88	
Fraction of cultivation layer in export	0.64	0.58	0.57	0.45	0.74	0.64	0.69	0.74	0.71	0.64	0.03	
Fraction of subsoil at eroding cultivation soil	0.53	0.66	0.57	0.85	0.29	0.41	0.45	0.42	0.40	0.51	0.06	
Aggraded area (%)of field and mixing	8.92	18.3	0.00	83.9	51.4	22.8	0.00	12.0	0.00	21.9	9.45	
Mean Deposition	1.14	0.44	0.00	1.20	0.54	1.28	0.00	1.85	0.00	0.72	0.23	
Initial cultivation import /deposit	0.73	0.25	0.00	0.55	0.40	0.77	0.00	1.36	0.00	0.45	0.15	
Subsoil deposit/import	0.41	0.19	0.00	0.66	0.14	0.51	0.00	0.49	0.00	0.27	0.08	
Burial of Initial cultivation layer	0.84	0.39	0.00	0.75	0.45	0.87	0.00	1.15	0.00	0.50	0.14	
Burial of imported Initial cultivation layer	0.19	0.03	0.00	0.20	0.07	0.24	0.00	0.51	0.00	0.14	0.06	
Burial of imported subsoil	0.11	0.02	0.00	0.25	0.02	0.16	0.00	0.18	0.00	0.08	0.03	
Replacement of imported cultivation soil to initial cultivation layer	0.54	0.22	0.00	0.34	0.34	0.53	0.00	0.85	0.00	0.31	0.10	
Replacement of imported sub soil in cultivation layer	0.30	0.17	0.00	0.41	0.12	0.35	0.00	0.31	0.00	0.18	0.05	
Presence of remaining initial cultivation	0.30	0.05	0.00	0.45	0.09	0.40	0.00	0.69	0.00	0.22	0.08	
Whole field												
Whole field area ha	0.13	0.15	0.16	0.13	0.32	0.10	0.06	0.05	0.05	0.13	0.03	
Eroded area (ha)	0.12	0.12	0.16	0.02	0.16	0.08	0.06	0.04	0.05	0.09	0.02	
Aggraded area (ha)	0.01	0.03	0.00	0.11	0.17	0.02	0.00	0.01	0.00	0.04	0.02	
Whole field slope (%)	2.91	2.24	2.84	5.89	6.59	6.15	1.84	4.05	4.21	4.08	0.59	
Mean erosion rate	2.43	3.06	3.24	0.61	0.53	1.41	2.02	1.53	1.73	1.84	0.32	
Mean aggradation rate	0.10	0.08	0.00	1.01	0.28	0.29	0.00	0.22	0.00	0.22	0.11	
Net export rate	2.33	2.98	3.24	-0.40	0.25	1.12	2.02	1.31	1.73	1.62	0.40	
Net export of plough soil	1.50	1.71	1.84	-0.18	0.18	0.72	1.40	0.96	1.22	1.04	0.23	
Net export of subplough	0.83	1.26	1.42	-0.22	0.06	0.40	0.62	0.35	0.51	0.58	0.18	

Appendix Table 6.3 SOC lateral and vertical redistribution budget ($\text{g C m}^{-2} \text{y}^{-1}$) for India sites based on profiles mean from segment (E/D). Mean values \pm SE ($n = 9$) are presented

Parameters	Site 1	Dhoolkhot			Site 2	Pasauli			Site 3	Bhatta Gaon			Mean	SE
	DKF1	DKF2	DKF3	PSF1	PSF2	PSF3	BGF1	BGF2	BGF3					
Eroded area (%) of field and mixing	91.1	81.7	100.0	16.1	48.6	77.2	100.0	88.0	100.0	78.1	9.45			
Mean C Erosion /subsoil excavation rate	26.3	35.9	30.8	69.1	27.8	15.1	42.5	37.9	37.0	35.8	4.95			
Cultivation layer C in export	18.3	23.0	19.6	53.2	25.2	9.4	35.6	32.6	31.3	27.6	4.20			
Subsoil C in export	8.05	12.91	11.18	15.82	2.59	5.75	6.91	5.37	5.76	8.26	1.41			
Cultivation soil C lost in 50 yrs (g C m^{-2})	914	1149	981	2662	1260	468	1781	1629	1562	1378	210			
Subsoil C lost in 50 yrs (g C m^{-2})	403	646	559	791	129	287	346	268	288	413	70			
Remaining cultivation soil C at eroding positions(g C m^{-2})	815	580	748	486	3111	3902	2134	2286	2352	1824	410			
Subsoil C mixed at eroding plough layer (g C m^{-2})	914	1149	981	2662	1260	468	1781	1629	1562	1378	210			
Fraction of cultivation layer C in export	0.69	0.64	0.64	0.77	0.91	0.62	0.84	0.86	0.84	0.76	0.04			
Aggraded area (%) of field and mixing	8.92	18.32	0.00	83.90	51.41	22.79	0.00	12.00	0.00	21.93	9.45			
Mean C Deposition	10.1	4.55	0.00	22.1	13.8	29.0	0.00	37.3	0.00	13.0	4.59			
Initial cultivation C import/deposit	7.80	3.32	0.00	17.0	12.5	25.3	0.00	34.7	0.00	11.2	4.14			
Subsoil C deposit/import	2.26	1.23	0.00	5.06	1.34	3.73	0.00	2.68	0.00	1.81	0.60			
Burial of Initial cultivation layer C	8.99	4.15	0.00	23.5	14.2	27.4	0.00	29.4	0.00	12.0	4.05			
Burial of imported Initial cultivation layer C	2.03	0.33	0.00	6.36	2.04	7.89	0.00	13.01	0.00	3.52	1.53			
Burial of imported subsoil C	0.59	0.12	0.00	1.14	0.22	0.72	0.00	1.01	0.00	0.42	0.15			
Replacement of imported cultivation soil C to initial cultivation layer C	5.77	2.99	0.00	10.7	10.4	17.4	0.00	21.7	0.00	7.65	2.66			
Replacement of imported sub soil C in cultivation layer C	1.67	1.11	0.00	1.91	1.12	1.58	0.00	1.68	0.00	1.01	0.27			
Whole field														
Whole field area (ha)	0.13	0.15	0.16	0.13	0.32	0.10	0.06	0.05	0.05	0.13	0.03			
Eroded area (ha)	0.12	0.12	0.16	0.02	0.16	0.08	0.06	0.04	0.05	0.09	0.02			
Aggraded area (ha)	0.01	0.03	0.00	0.11	0.17	0.02	0.00	0.01	0.00	0.04	0.02			
Whole field slope (%)	2.91	2.24	2.84	5.89	6.59	6.15	1.84	4.05	4.21	4.08	0.59			
Mean C erosion rate	24.0	29.3	30.8	11.1	13.5	11.7	42.5	33.4	37.0	25.9	3.86			
Mean C aggradation rate	0.90	0.83	0.00	18.53	7.09	6.61	0.00	4.48	0.00	4.27	2.02			
Net C export rate	23.1	28.5	30.8	-7.41	6.41	5.06	42.5	28.9	37.0	21.7	5.54			
Net export of plough soil C	16.0	18.2	19.6	-5.71	5.84	1.47	35.6	24.5	31.3	16.3	4.55			
Net export of subplough C	7.13	10.32	11.18	-1.70	0.57	3.59	6.91	4.40	5.76	5.35	1.40			

Chapter 7 Appendix: Site 3 Low input Agriculture-Calcareous soil - soil respiration rate - Include Appendix Table 7.1 to 7.7, Appendix Figure 7.1 to 7.5 and Appendix Text 7.1.

Appendix Table 7.1 Total ^{137}Cs inventory, soil pH and other properties along slope transect. Mean values \pm 1SE ($n = 3$) are presented.

Sites	Positions	^{137}Cs (Bq m^{-2})	SR rate ($\text{kg m}^{-2} \text{y}^{-1}$)	Depth (cm)	Soil pH	Latitude	Langitude	Elevation (m)
Site 3(LIC)	Eroding	1246 \pm 178 ^a	-0.99 \pm 0.48	<50	7.36 \pm 0.17	30°26.327' N	78°04.698' E	1548
	Mid-slope	1471 \pm 142a	-0.44 \pm 0.31	>100	7.21 \pm 0.05	30°26.331' N	78°04.702' E	1548
	Deposition	1023 \pm 98a	-1.55 \pm 0.31	>100	7.25 \pm 0.08	30°26.342' N	78°04.713' E	1548

LIC- Low input agriculture-Calcareous

Appendix Table 7.2 Soil lateral and vertical redistribution ($\text{kg m}^{-2} \text{y}^{-1}$) budget for India Site 3 based on profiles mean from segment (E/D) and field area

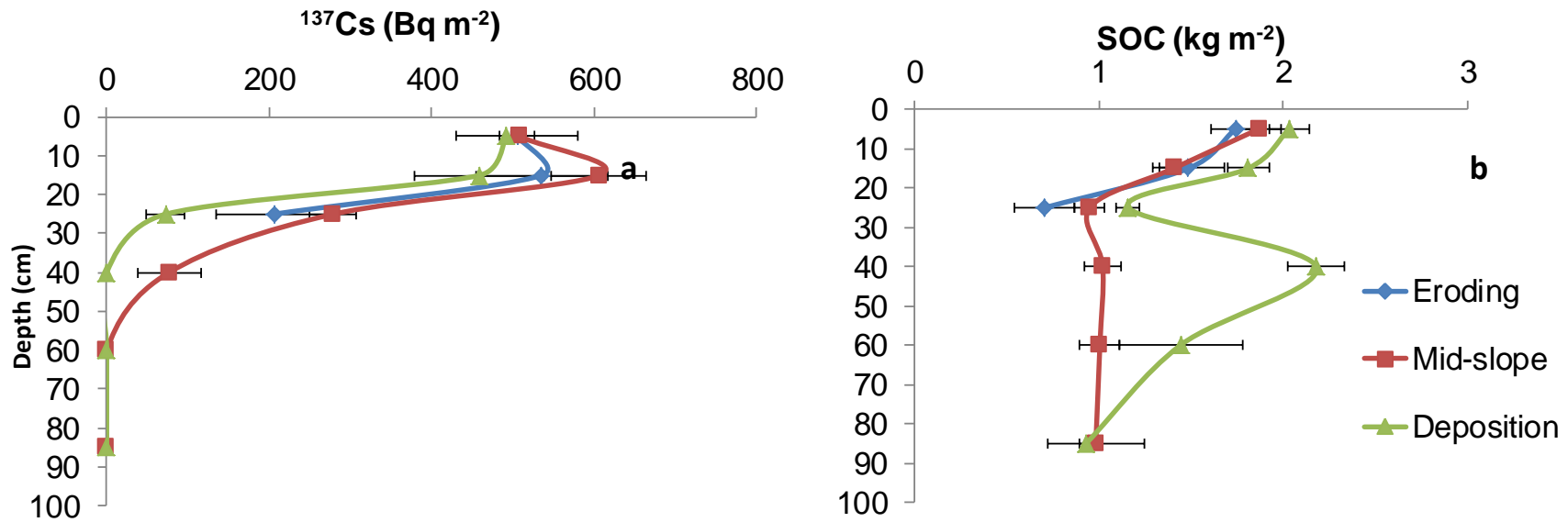
Parameters	Site 3 BGF3
Eroded area % of field and mixing	100
Mean Erosion /subsoil excavation rate	1.73
Cultivation layer in export	1.22
Subsoil in export	0.51
Cultivation soil lost in 50 yrs (kg m^{-2})	61
Subsoil lost in 50 yrs (kg m^{-2})	26
Remaining cultivation soil at eroding positions(kg m^{-2})	92
Subsoil mixed at eroding plough layer (kg m^{-2})	61
Fraction of cultivation layer in export	0.71
Fraction of subsoil at eroding cultivation soil	0.40
Aggraded area % of field and mixing	0.00
Mean Deposition	0.00
Initial cultivation import /deposit	0.00
Subsoil deposit/import	0.00
Burial of Initial cultivation layer	0.00
Burial of imported Initial cultivation layer	0.00
Burial of imported subsoil	0.00
Replacement of imported cultivation soil to initial cultivation layer	0.00
Replacement of imported sub soil in cultivation layer	0.00
Presence of remaining initial cultivation	0.00
Whole field	
Whole field area ha	0.05
Eroded Area ha	0.05
Aggraded Area ha	0.00
Whole field slope %	4.21
Mean erosion rate	1.73
Mean aggradation rate	0.00
Net export rate	1.73
Net export of plough soil	1.22
Net export of subplough	0.51

Appendix Table 7.3 C lateral and vertical redistribution ($\text{g C m}^{-2} \text{y}^{-1}$) budget for India Site 3 based on profiles mean from segment (E/D) and field area

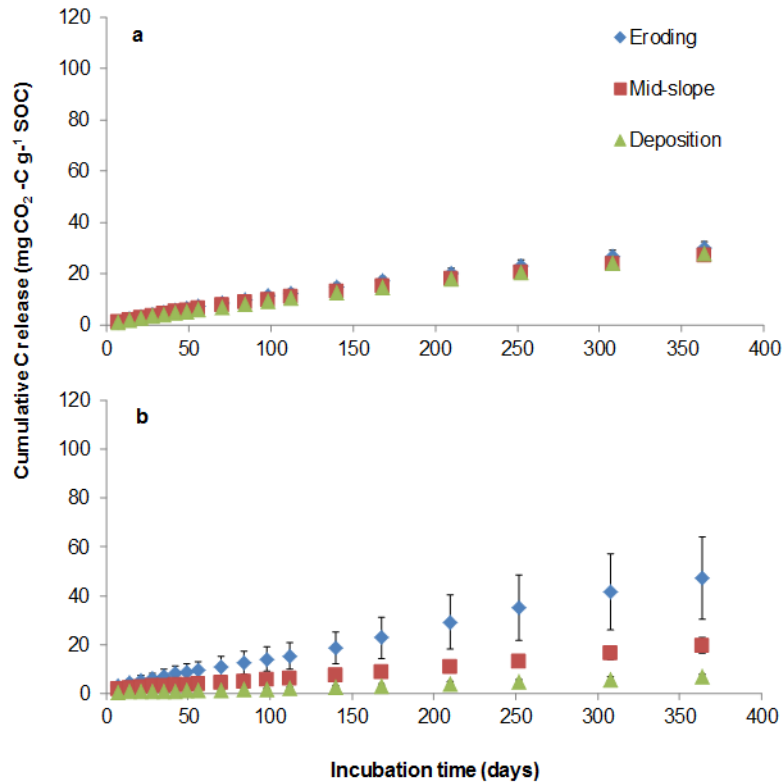
Parameters	Site 3 BGF3
Eroded area % of field and mixing	100.0
Mean C Erosion /subsoil excavation rate	37.01
Cultivation layer C in export	31.25
Subsoil C in export	5.76
Cultivation soil C lost in 50 yrs (g C m^{-2})	1562
Subsoil C lost in 50 yrs (g C m^{-2})	288
Remaining cultivation soil C at eroding positions(g C m^{-2})	2352
Subsoil C mixed at eroding plough layer (g C m^{-2})	1562
Fraction of cultivation layer C in export	0.84
Aggraded area % of field and mixing	
Mean C Deposition	0.00
Initial cultivation C import /deposit	0.00
Subsoil C deposit/import	0.00
Burial of Initial cultivation layer C	0.00
Burial of imported Initial cultivation layer C	0.00
Burial of imported subsoil C	0.00
Replacement of imported cultivation soil C to initial cultivation layer C	0.00
Replacement of imported sub soil C in cultivation layer C	0.00
Whole field	
Whole field area ha	0.05
Eroded Area ha	0.05
Aggraded Area ha	0.00
Whole field slope %	4.21
Mean C erosion rate	37.01
Mean C aggradation rate	0.00
Net C export rate	37.01
Net export of plough soil C	31.25
Net export of subplough C	5.76

Appendix Table 7.4 Important properties of experimental Site 3 by topo-position and different depths. Differences in letter symbol indicate significance at $p < 0.05$ along slope position of each depth layer. Mean values ± 1 SE ($n = 5$) are presented.

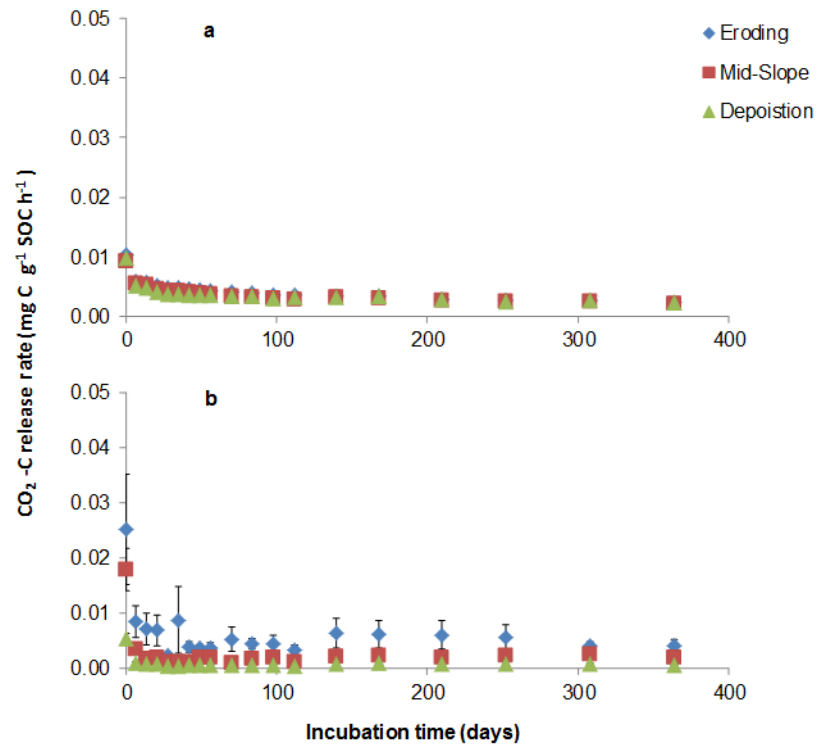
Sites	Depth (cm)	SOC (g kg^{-1})		TN (g kg^{-1})		CN ratio	
		0-15	45-60	0-15	45-60	0-15	45-60
Site 3	Eroding *	24.6 ± 0.77^a	5.34 ± 1.04^a	2.46 ± 0.06^b	0.48 ± 0.06^a	10.0 ± 0.51^a	12.8 ± 1.88^a
	Mid-slope	23.2 ± 0.28^a	5.44 ± 1.42^a	2.22 ± 0.02^a	0.40 ± 0.17^a	10.5 ± 0.19^a	16.1 ± 1.52^a
	Deposition	28.8 ± 0.92^b	13.0 ± 1.60^b	2.59 ± 0.07^b	1.07 ± 0.18^b	11.2 ± 0.66^a	13.2 ± 1.71^a



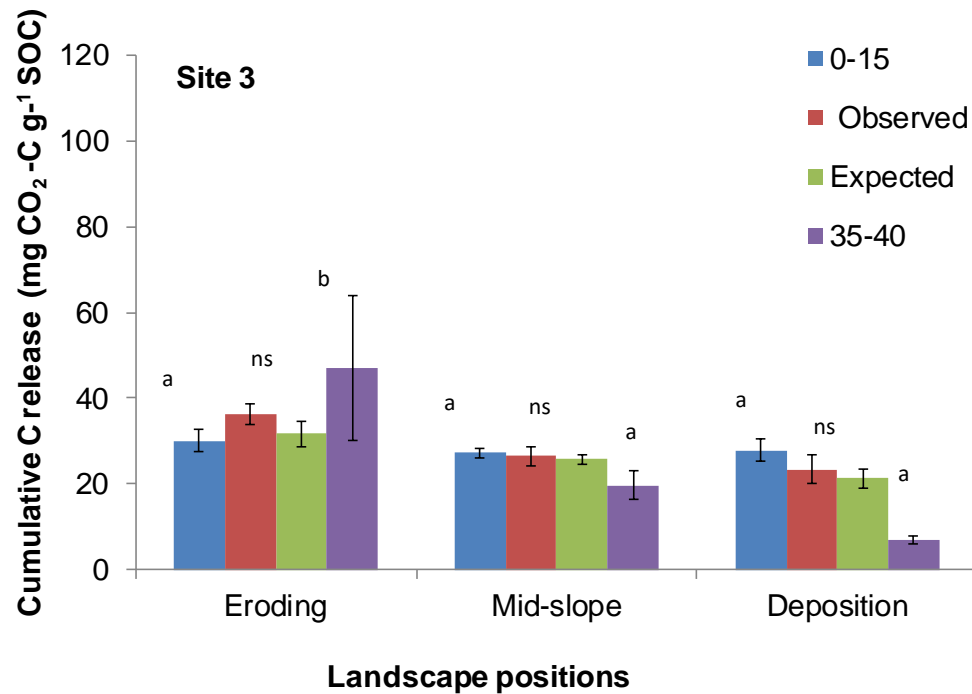
Appendix Figure 7.1 Depth distribution of ^{137}Cs and SOC inventory in profiles from different slope positions at Site 3- Low Input calcareous Agriculture fields . Mean values \pm 1SE ($n=3$) are presented.



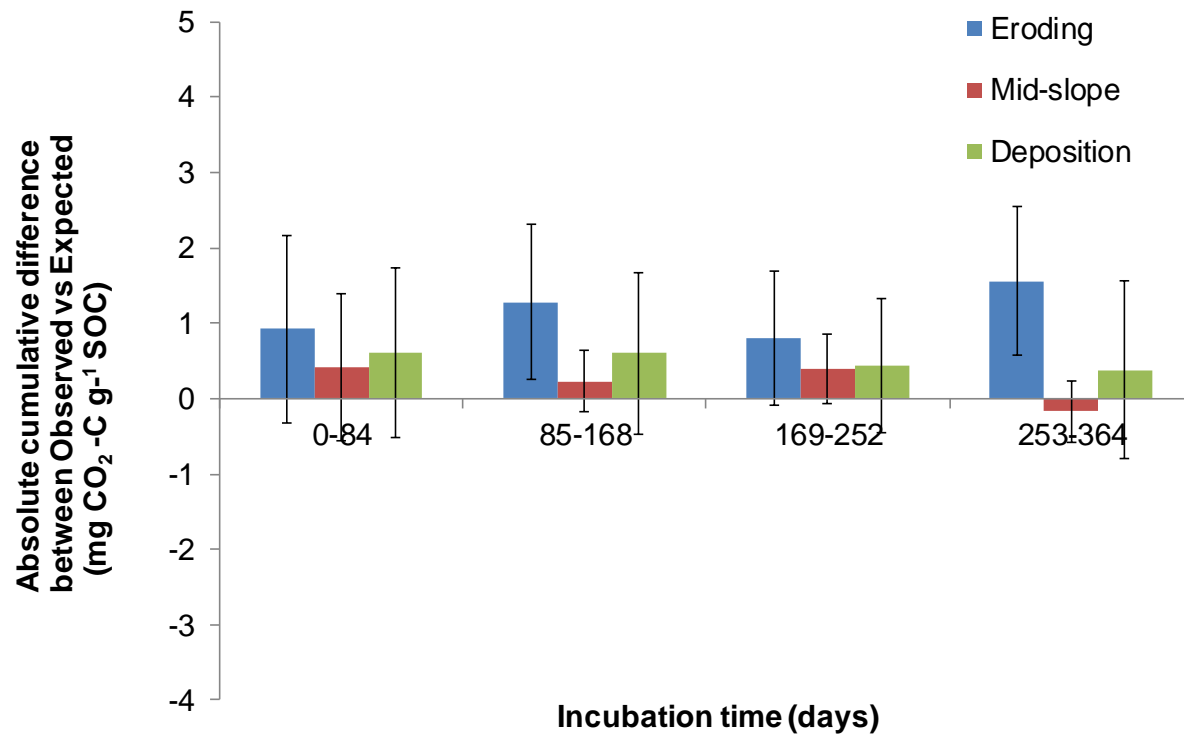
Appendix Figure 7.2 Cumulative CO₂-C release from the 0-15 cm (a) and 35-40 cm (b) depths from Site 3. Mean values $\pm 1SE$ ($n = 5$) are presented. *Figure eroding profile depth ended after 35-40 cm and exposed calcareous stones / rocks.



Appendix Figure 7.3 Soil respiration rate from the 0-15 cm (a) and 45-60 cm (b) depths from Site 3 . Mean values ± 1 SE ($n = 5$) are presented



Appendix Figure 7.4 Cumulative CO₂-C release per gram SOC from the 0-15 cm, 35-40 cm depths, Observed and Expected (mixed soil) incubated different Landscape positions from Site 3. Mean values ± 1 SE ($n = 5$) are presented. Letters changes in graph indicate significance at $p < 0.05$ and need to compare along slope position (p values reflect One way anova for top and subsoil. For mixed Observed and expected comparison tested by Pairwise t.test. “ns” means no significant).



Appendix Figure 7.5 Absolute cumulative difference of C release between observed vs expected at different time interval of within 364 days for various landscape positions from Site 3. Mean values $\pm 1SE$ ($n = 5$) are presented.

Appendix Table 7.5 Cumulative C release from different soil depths and mixed of non-eroded fields from different sites. Mean values ± 1 SE ($n = 5$) are presented.

Sites	layers	Days	Cumulative C release (mg C release g ⁻¹ soil OC)																	
			7	14	21	28	35	42	49	56	70	84	98	112	140	168	210	252	308	364
Site 1	0-15	Mean	2.99	5.16	6.88	8.35	9.70	10.97	12.17	13.42	16.03	18.53	20.75	22.70	26.34	29.86	34.84	39.84	46.44	52.32
		SE	0.32	0.54	0.70	0.83	0.95	1.07	1.17	1.26	1.49	1.75	2.00	2.23	2.63	3.03	3.59	4.13	4.93	5.67
	45-60	Mean	0.95	1.50	2.07	2.55	2.96	3.34	3.70	4.02	4.61	5.26	5.78	6.24	7.37	8.42	9.72	11.02	12.92	14.71
		SE	0.10	0.19	0.29	0.38	0.45	0.49	0.51	0.54	0.60	0.67	0.75	0.83	0.98	1.13	1.34	1.47	1.59	1.66
	Observed	Mean	2.26	3.87	5.22	6.37	7.46	8.48	9.39	10.30	12.14		15.88	17.53	20.39	23.10	27.06	30.48	34.76	38.79
		SE	0.18	0.30	0.41	0.48	0.56	0.65	0.72	0.79	0.92	1.03	1.14	1.26	1.52	1.81	2.08	2.33	2.67	3.05
Expected	Mean	2.21	3.77	5.05	6.14	7.13	8.06	8.94	9.84	11.69	13.49	15.05	16.43	19.12	21.68	25.24	28.82	33.62	37.94	
	SE	0.19	0.33	0.44	0.52	0.59	0.66	0.71	0.76	0.87	1.01	1.15	1.29	1.53	1.76	2.07	2.37	2.83	3.24	
Site 2	0-15	Mean	3.01	5.18	7.09	8.88	10.65	12.35	14.01	15.66	18.97	22.25	25.48	28.69	35.25	41.93	50.99	58.36	66.52	72.94
		SE	0.36	0.56	0.72	0.87	1.04	1.18	1.31	1.42	1.70	2.01	2.34	2.73	3.71	4.93	6.33	6.99	7.41	7.71
	45-60	Mean	1.25	2.09	2.87	3.53	4.20	4.82	5.38	6.04	7.23	8.27	9.26	10.13	12.04	14.00	16.52	19.03	22.63	25.80
		SE	0.31	0.50	0.64	0.73	0.86	0.99	1.12	1.28	1.52	1.73	1.96	2.20	2.75	3.22	3.72	4.21	4.99	5.59
	Observed	Mean	2.69	4.67	6.43	8.09	9.74	11.28	12.81	14.41	17.68	21.07	24.50	28.05	35.53	42.87	51.28	57.61	65.52	71.73
		SE	0.33	0.58	0.80	1.01	1.22	1.40	1.58	1.76	2.14	2.57	3.01	3.52	4.73	6.05	7.51	8.40	9.73	10.86
Expected	Mean	2.61	4.50	6.17	7.72	9.27	10.75	12.18	13.62	16.49	19.32	22.10	24.86	30.50	36.28	44.09	50.49	57.69	63.45	
	SE	0.26	0.42	0.55	0.69	0.84	0.99	1.11	1.24	1.52	1.83	2.15	2.53	3.45	4.52	5.78	6.45	6.97	7.36	
Site 3	0-15	Mean	1.99	3.48	4.77	5.90	7.05	8.18	9.23	10.24	12.24	14.25	16.22	18.11	21.81	25.27	30.01	34.37	39.78	44.54
		SE	0.06	0.12	0.17	0.21	0.24	0.25	0.25	0.26	0.28	0.30	0.33	0.35	0.42	0.53	0.66	0.75	0.94	1.10
	45-60	Mean	4.86	6.65	8.11	9.00	9.87	10.61	11.23	12.11	14.00	16.08	17.95	19.48	23.02	26.80	32.39	39.32	49.23	56.52
		SE	0.91	1.14	1.33	1.38	1.48	1.61	1.69	1.89	2.46	3.00	3.43	3.91	5.11	6.14	7.26	8.55	10.90	12.78
	Observed	Mean	2.19	3.55	4.63	5.63	6.70	7.74	8.77	9.77	11.71	13.65	15.61	17.51	21.26	24.77	29.55	34.09	39.86	44.61
		SE	0.18	0.30	0.34	0.42	0.58	0.71	0.82	0.95	1.16	1.39	1.61	1.83	2.27	2.73	3.33	3.81	4.46	4.97
Expected	Mean	2.20	3.72	5.03	6.15	7.28	8.38	9.40	10.40	12.40	14.43	16.39	18.27	21.96	25.46	30.27	34.83	40.62	45.58	
	SE	0.09	0.16	0.22	0.26	0.29	0.31	0.32	0.34	0.41	0.47	0.54	0.61	0.80	0.99	1.20	1.39	1.75	2.05	

Appendix Table 7.6 SOC content in different fractionated soil particles from different slope positions. Mean values ± 1 SE ($n = 3$) are presented.

Sites	Slope Position	Depth (cm)	SOC %			TN %		
			2000-250 μm	250-63 μm	63-20 μm	2000-250 μm	250-63 μm	63-20 μm
Site 1	Eroding	0-15	0.83 \pm 0.01	0.92 \pm 0.02	1.04 \pm 0.01	0.06 \pm 0.00	0.07 \pm 0.00	0.09 \pm 0.00
		45-60	0.37 \pm 0.01	0.45 \pm 0.02	0.58 \pm 0.04	0.02 \pm 0.00	0.04 \pm 0.01	0.04 \pm 0.01
	Midslope	0-15	0.89 \pm 0.11	0.75 \pm 0.05	1.00 \pm 0.01	0.07 \pm 0.01	0.06 \pm 0.01	0.09 \pm 0.00
		45-60	0.62 \pm 0.02	0.62 \pm 0.02	0.66 \pm 0.03	0.05 \pm 0.01	0.05 \pm 0.00	0.05 \pm 0.01
	Deposition	0-15	1.30 \pm 0.08	1.43 \pm 0.23	0.98 \pm 0.00	0.09 \pm 0.01	0.11 \pm 0.02	0.08 \pm 0.00
		45-60	0.86 \pm 0.06	0.73 \pm 0.06	0.78 \pm 0.05	0.06 \pm 0.00	0.05 \pm 0.00	0.05 \pm 0.00
	DKRef1	0-15	0.72 \pm 0.05	0.60 \pm 0.04	0.79 \pm 0.00	0.05 \pm 0.00	0.04 \pm 0.01	0.06 \pm 0.01
		45-60	0.52 \pm 0.01	0.49 \pm 0.02	0.56 \pm 0.02	0.03 \pm 0.00	0.04 \pm 0.00	0.03 \pm 0.00
Site 2	Eroding	0-15	1.14 \pm 0.05	1.73 \pm 0.16	2.30 \pm 0.04	0.08 \pm 0.01	0.13 \pm 0.01	0.17 \pm 0.00
		45-60	0.39 \pm 0.04	0.83 \pm 0.10	1.44 \pm 0.23	0.04 \pm 0.00	0.06 \pm 0.00	0.10 \pm 0.01
	Midslope	0-15	1.09 \pm 0.13	1.65 \pm 0.13	2.35 \pm 0.06	0.07 \pm 0.00	0.12 \pm 0.01	0.18 \pm 0.01
		45-60	1.08 \pm 0.07	1.36 \pm 0.05	1.78 \pm 0.15	0.06 \pm 0.00	0.09 \pm 0.01	0.11 \pm 0.01
	Deposition	0-15	1.59 \pm 0.09	2.12 \pm 0.11	2.39 \pm 0.03	0.12 \pm 0.01	0.16 \pm 0.01	0.18 \pm 0.01
		45-60	1.02 \pm 0.04	1.35 \pm 0.06	1.68 \pm 0.06	0.06 \pm 0.00	0.08 \pm 0.00	0.11 \pm 0.00
	PSRef1	0-15	1.42 \pm 0.03	2.30 \pm 0.06	2.99 \pm 0.04	0.10 \pm 0.00	0.18 \pm 0.00	0.23 \pm 0.00
		45-60	0.23 \pm 0.05	0.60 \pm 0.11	1.47 \pm 0.07	0.01 \pm 0.01	0.04 \pm 0.01	0.11 \pm 0.01
Site 3	Eroding	0-15	2.05 \pm 0.21	2.67 \pm 0.14	2.56 \pm 0.11	0.22 \pm 0.01	0.31 \pm 0.02	0.30 \pm 0.04
		45-60	0.49 \pm 0.15	0.62 \pm 0.18	0.66 \pm 0.16	0.18 \pm 0.06	0.24 \pm 0.05	0.22 \pm 0.04
	Midslope	0-15	2.28 \pm 0.08	2.75 \pm 0.09	2.69 \pm 0.04	0.40 \pm 0.02	0.42 \pm 0.02	0.36 \pm 0.05
		45-60	0.63 \pm 0.25	0.71 \pm 0.29	0.79 \pm 0.25	0.07 \pm 0.02	0.07 \pm 0.03	0.07 \pm 0.02
	Deposition	0-15	2.67 \pm 0.06	3.16 \pm 0.13	3.29 \pm 0.03	0.25 \pm 0.01	0.29 \pm 0.01	0.32 \pm 0.01
		45-60	1.21 \pm 0.26	1.34 \pm 0.25	1.57 \pm 0.29	0.08 \pm 0.02	0.11 \pm 0.02	0.14 \pm 0.04
	BGRef3	0-15	2.17 \pm 0.07	3.24 \pm 0.26	3.20 \pm 0.06	0.20 \pm 0.02	0.29 \pm 0.02	0.28 \pm 0.03
		45-60	0.21 \pm 0.04	0.25 \pm 0.05	0.41 \pm 0.11	0.03 \pm 0.01	0.03 \pm 0.01	0.04 \pm 0.01

Appendix Text 7.1 Review of methods for SOM fractionation

Option 1 Dry Sieving: Adapted

Real procedure: Aggregates dry sieving (Mendes *et al.*, 1999; Schutter and Dick, 2002; Sainju *et al.*, 2003 and 2006). (Aim to estimate C and N from aggregates and Microbial C and water soluble C and N).

- Soil should be field capacity moisture (fresh soil dry at 4°C for 7 days to get 8-14% of moist- this condition represents real field condition of soil and this temperature not affect Microbes).
- <4.75 mm size soil 500 g placed on nest of sieve <2 mm, 0.25 mm with shaker. Sieves were shaken at 200 Oscillation / minute for 3 minute and aggregates (4.75-2.00, 2.00-0.25, and <0.25 mm) retained and passed through the sieves were weighed.
- Samples were air dried and stored in plastic bags until measure C and N.
- Mean weight diameter of aggregate measured.

I modified Aggregates Dry Sieving Procedure:

- Step 1 Dry the fresh soil at 60°C at Oven (I was not measuring Microbial Carbon/activity)
- Step 2 dried soil sieve manually sieve through 9.5 mm or 8 mm sieve (remove stones and roots) this step facilitate keep aggregates less disturbed
- Step 3 passes the soil <9.5 mm into nest of Sieve 2000, 250, 53 and 20 µm with a shaker. Sieves were shaken at 200 Oscillation / minute for 3 minute and aggregates retained and passed through the sieves will be weighed
- Step 4 these samples will be used for measuring C and N.

This dry sieved aggregates suggest distribution of Sand (Active), Silt and Clay associated (Intermediate / passive pools) SOM pools at eroding / deposition profiles.

Advantages of dry sieving

- Reduce disruption of physical habitat of microbial communities (Mendes *et al.*, 1999; Schutter and Dick, 2002).
- I can estimate water soluble C and N while wet sieving creates under-estimation of C and N (Seech and Beauchamp, 1988; Beauchamp and Seech, 1990)

- Aggregates separated by dry sieving may represent more closely those in field during the absence of rain / irrigation
- There may be chance of soil loss during wet sieving /decantation of water.

Option 2 : Aggregate Wet sieving: Performed based on Elliot (1986) and Six *et al.*, (1998,2000, 2002 and Doetterl *et al.*, 2012 modified)

- Dry the fresh soil at 60°C at Oven (I am not measuring Microbial Carbon/activity)
- Dried soil sieve manually sieves through 9.5 mm or 8 mm sieve (remove stones and roots) this step facilitate keep aggregates less disturbed
- Take 50g air-dried soil sample (< 9.5/8 mm) submerged for 5 min at room temperature in deionized water – on top of a 2000 µm sieve
- Aggregate separation achieved by manually moving sieve up and down 3 cm, 50 repetitions per 2 minutes
- After 2 min: stable >2000 µm aggregates back washed off sieve onto aluminium pan/ or plastic bowl, floating OM >2000 µm decanted and put into a weighed and labelled glass beaker and oven dried (*Not considered SOM, but might be important to know how much macro OM is present, so keep it*). Sediment sample >2000 µm decanted into a weighed glass glass and oven dried at 60°C
- Water and soil passing through 2000 µm poured into next sieve
- Sieving repeated (250 µm), floating material >250 retained with sediment sample, aggregate sample decanted into a weighed glass jar and oven dried
- Repeated through 53 µm, floating material >53 retained with sediment sample, material passing through the 53 µm sieve is then filtered and oven dried – weigh and label the filter paper before filtering (use a Whatman 100).
- Aggregates oven dried (60°C), after drying samples are weighed and stored in plastic bags then measure C and N for each fraction total 5 fraction per sample (2000-250 (light and heavy fraction), 250 – 53 (light and heavy fraction) and < 53 µm (heavy fraction)).
-

Six et al 1998 procedure modification:

- I am not going to do density fraction by Sodium polytungstate because my soils from intensively cultivated land so there is less presence of Light fraction (free Particulate Organic Matter and Intra aggregate particulate Organic Matter) due

to Loss during continue cultivation (Six *et al*, 1998; Doetterl *et al.*, 2012). But I will collect floating light fraction on water for macroaggregates / microaggregates size if it presence.

Modified Aggregates Dry Sieving Procedure:

- Step 1 soil sieve manually through 9.5 mm Sieve (remove stones and roots) this step facilitate keep aggregates less disturbed
- Step 2 Dry the fresh soil at 35°C at Oven (one day and remaining air dried)
- Step 3 passes the soil < 9.5 mm into nest of Sieve 2000, 250, 63 and 20 µm with a shaker. Sieves were shaken at for 3 minute and aggregates retained and passed through the sieves will be weighed and stored in plastic bags. (This provide Macro Aggregates-Coarse Sand, Fine sand - Micro aggregates, more silt - Silt/clay –more clay associated SOM)
- Step 4 these samples used for measuring C and N.

This dry sieved aggregates suggest distribution of sand (active), silt and clay associated (intermediate/passive pools) SOM pools at eroding /deposition profiles. This method favours low SOM soil because I may loose further water soluble SOC In wet sieving. And also this method favour to link relationship with site characters because most of the time these field under dry condition. Only three months only rainfall.

Appendix Table 7.7 Soil moisture content and Water holding capacity of soils from various landscapes positions (soils used for respiration). Mean values $\pm 1SE$ ($n = 5$) are presented

Sites	Positions	Pits	Depth (cm)	Soil moisture content (%)		Water holding capacity (%)	
				Mean	SE	Mean	SE
Site 1	Upslope	P1	0-15	8.47	0.66	32.59	0.27
			45-60	9.52	0.37	31.07	1.42
	Midslope	P3	0-15	8.07	0.56	32.02	0.72
			45-60	14.38	0.52	36.12	0.94
	Downslope	P6	0-15	12.99	0.24	34.04	0.91
			45-60	14.55	0.34	40.68	0.48
	Stable	Ref	0-15	6.92	0.34	34.87	0.67
			45-60	13.20	0.46	37.87	0.46
Site 2	Upslope	P1	0-15	3.28	0.43	30.70	0.84
			45-60	6.97	0.95	31.64	1.26
	Midslope	P3	0-15	4.22	0.44	31.38	0.57
			45-60	13.89	0.85	37.37	0.56
	Downslope	P6	0-15	9.45	0.75	38.90	0.71
			45-60	15.35	0.62	41.13	0.98
	Stable	Ref	0-15	7.95	0.54	31.56	1.78
			45-60	7.60	1.24	27.94	1.23
Site 3	Upslope	P1	0-15	17.82	0.33	35.97	0.62
			45-60	15.36	1.76	33.13	1.04
	Midslope	P2	0-15	17.56	0.34	35.99	0.93
			45-60	20.58	0.82	40.34	0.70
	Downslope	P5	0-15	17.12	1.29	39.83	0.67
			45-60	18.09	1.24	39.78	0.79
	Stable	Ref	0-15	14.21	0.66	33.77	0.42
			45-60	17.15	1.15	34.36	0.66

References

- Abella, S.R., and B.W. Zimmer (2007), Estimating organic carbon from loss-on-ignition in northern Arizona forest soils. *Soil Sci. Soc. Am. J.*, 71, 545–550, doi:10.2136/sssaj2006.0136.
- Afshar, F. A., S. Ayoubi, and A. Jalalian (2010), Soil redistribution rate and its relationship with soil organic carbon and total nitrogen using ^{137}Cs technique in a cultivated complex hillslope in western Iran, *Journal of Environmental Radioactivity*, 101, 606–614, doi:10.1016/j.jenvrad.2010.03.008.
- Anderson, G. (1975), Other organic phosphorus compounds, pp. 305-331. In: J.E. Gieseking (ed.), *Soil Components. Vol. 1: Organic Components*. Springer-Verlag, New York, NY.
- Aufdenkampe, A. K., E. Mayorga, and P.A. Raymond, (2011), Riverine coupling of biogeochemical cycles between land, oceans, and atmosphere, *Frontiers in Ecology and the Environment*, 9, 53–60, doi:10.1890/100014.
- Bajracharya, R. M., R. Lal, and J.M. Kimble, (2000), Diurnal and seasonal $\text{CO}_2\text{-C}$ flux from soil as related to erosion phases in central Ohio, *Soil Sci. Soc. Am. J.*, 64, 286–293, doi:10.2136/sssaj2000.641286.
- Ball, D.E. (1964), Loss-on-ignition as an estimate of organic matter and organic carbon in non-calcareous soils, *J Soil Science*, 15, 84-92, doi: 10.1111/j.1365-2389.1964.tb00247.x
- Batjes, N. H. (1996), The total C and N in soils of the world, *Eur J Soil Sci*, 47, 151 – 63.
- Batti, J. S., and I. E. Bauer. (2002), Comparing loss-on-ignition with dry combustion as a method for determining carbon content in upland and lowland forest ecosystems, *Commun. Soil Sci. Plant Anal*, 33, 3419–3430.
- Beauchamp, E. G., and A. G. Seech, (1990), Denitrification with different sizes of soil aggregates obtained from dry sieving and from sieving with water, *Biol. Fertil. Soils*, 10, 188–193.

Bellamy, P.H., P.J. Loveland, R.I. Bradley, R.M. Lark, and G.J.D. Kirk. (2005), Carbon losses from all soils across England and Wales 1978–2003, *Nature*, 437, 245–248, doi: 10.1038/nature04038.

Beniston, J. W., M. J. Shipitalo, R. Lal, E. A. Dayton, D. W. Hopkins, F. Jones, A. Joynes, and J. A. J. Dungait, (2015), Carbon and macronutrient losses during accelerated erosion under different tillage and residue management, *European Journal of Soil Science*, 66, 218–225, doi: 10.1111/ejss.12205.

Berhe, A. A., J. W. Harden, M. S. Torn, M. Kleber, S. D. Burton, and J. Harte, (2012), Persistence of soil organic matter in eroding versus depositional landform positions, *J. Geophys. Res.*, 117, G02019, doi: [10.1029/2011JG001790](https://doi.org/10.1029/2011JG001790).

Berhe, A. A. (2012), Decomposition of organic substrates at eroding vs. depositional landform positions, *Plant and Soil*, 350, 261-280. doi:10.1007/s11104-011-0902-z,

Berhe, A. A., J. Harte, J.W. Harden, and M. S. Torn, (2007), The significance of the erosion induced terrestrial carbon sink, *Bioscience*, 57, 337-346, doi: 10.1641/B570408.

Berhe, A. A., J. W. Harden, M. S. Torn, and J. Harte, (2008), Linking soil organic matter dynamics and erosion-induced terrestrial carbon sequestration at different landform positions, *Journal of Geophysical Research-Biogeosciences*, 113, G04039, doi:10.1029/2008JG000751

Berhe, A. A. and M. Kleber, (2013), Erosion, deposition and the persistence of soil organic matter: important considerations and problems with terminology, *Earth Surface Processes and Landforms*, 38(8), 908-912, Doi: 10.1002/esp.3408.

Berhe, A. A., C. Arnold, E. M. Stacy, R. Lever, E. McCorkle, and S. N. Araya, (2014), Soil erosion controls on biogeochemical cycling of carbon and nitrogen, *Nature Education Knowledge* 5(8):2.

Beuselinck, L., A. Steegen, G. Govers, J. Nachtergaele, I. Takken, and J. Poesen, (2000), Characteristics of sediment deposits formed by major rainfall events in small agricultural catchments in the Belgian Loam Belt, *Geomorphology*, 32, 69–82, doi:10.1016/j.catena.2015.10.024.

Beyer, L., C. Köbbemann, J. Finnern, D. Elsner, and W. Schluß,(1993), Colluvisols under cultivation in Schleswig-Holstein, 1: Genesis, definition and geo-ecological significance, *Journal of Plant Nutrition and Soil Science*,156, 197–202, doi: 10.1002/jpln.19931560302.

Bhattacharyya, R., R. B. Ved-Prakash, S. Kundu, A.K. Srivastava, and H.S. Gupta, (2009), Soil aggregation and organic matter in a sandy clay loam soil of the Indian Himalayas under different tillage and crop regimes, *Agriculture, Ecosystems & Environment*, 132, 126–134, doi:10.1016/j.agee.2009.03.007.

Bhattacharyya, R., B. N. Ghosh, P. K. Mishra, B. Mandal, C. H. Srinivasa Rao, D. Sarkar, K. Das, K. S. Anil, M. Lalitha, K.M. Hati, and A.J. Franzluebbers, (2015), Soil degradation in India: challenges and potential solutions, *Sustainability* 7, 3528–3570, doi:[10.3390/su7043528](https://doi.org/10.3390/su7043528).

Bingeman, C. W., J. E. Varner, and W. P. Martin. (1953), The Effect of the addition of organic materials on the decomposition of an organic soil¹. *Soil Sci. Soc. Am. J.* 17,34-38, doi:10.2136/sssaj1953.03615995001700010008x.

Bisutti, I., I. Hilke, and M. Raessler, (2004), Determination of total organic carbon – an overview of current methods. *Trends Anal. Chem.* 23, 716–726. doi:[10.1016/j.trac.2004.09.003](https://doi.org/10.1016/j.trac.2004.09.003)

Black, C. A., and C. A. I. Goring, (1953), Organic phosphorus in soils. In "Soil and fertiliser phosphorus," pp. 123-52, Academic Press, New York.

Brady, N.C. & Weil, R.R. 2000. *Elements of the Nature and Property of Soils*, Prentice Hall.

Bray, R.H., and L.T. Kurtz, (1945), Determination of total, organic, and available forms of phosphorus in soils, *Soil Sci*, 59, 39 -45.

Brodie, C.R., M.J. Leng, J.S.L. Casford, C.P. Kendrick, J.M. Lloyd, Y.Q. Zong, and M.I. Bird, (2011a), Evidence for bias on C and N concentrations and $\delta^{13}\text{C}$ composition of terrestrial and aquatic organic materials due to pre-analysis acid preparation methods, *Chem.Geo*,282, 67- 83, DOI: 10.1016/j.chemgeo.2011.01.007.

Burman, S.G. (1984), Land resource-Physical aspects. In Lal, J. S. et al. (eds.), Development of Himalayan Resources-Regional Perspectives. Indian Council of World Affairs, New Delhi (mimeographed) dynamics and erosion-induced terrestrial carbon sequestration at different landform positions. *Journal of Geophysical Research* 113:G04039.

Burwell, G.E., D.R. Timrnons, and R.F. Holt, (1975), Nutrient transport in surface runoff as influenced by surface cover and seasonal periods, *Soil Sci. Soc. Amer. Proc*, 39, 523-528.

Century figure: <http://www.nrel.colostate.edu/projects/century>

Chirinda, N., L. Elsgaard, I.K.Thomsen, G. Heckrath, and J.E. Olesen, (2014), Carbon dynamics in topsoil and subsoil along a cultivated toposequence, *Catena* 140, 20–28, [doi:10.1016/j.catena.2014.03.014](https://doi.org/10.1016/j.catena.2014.03.014).

Christensen, B.T. (1992), Physical fractionation of soil and organic matter in primary particle size and density separates. In B.A. Stewart (Ed.). *Advances in soil science*, 20, Springer, New York. pp. 1-90.

Collins, H. P., D. R. Christenson, R. L. Blevins, L. G. Bundy, W. A. Dick, D. R. Huggins, and E. A. Paul, (1999), Soil carbon dynamics in corn-based agroecosystems: Results from carbon- 13 natural abundance. *Soil Sci. Soc. Am. J.* 63, 584-591, [doi:10.2136/sssaj1999.03615995006300030022x](https://doi.org/10.2136/sssaj1999.03615995006300030022x).

De Alba, S., M. Lindstrom, T.E. Schumacher, and D.D. Malo, (2004). Soil landscape evolution due to soil redistribution by tillage: a new conceptual model of soil catena evolution in agricultural landscapes, *Catena*, 58, 77–100, [doi:10.1016/j.catena.2003.12.004](https://doi.org/10.1016/j.catena.2003.12.004).

De Gryze, S., J. Six, H. Bossuyt, V.O. Kristof, and R. Merckx, (2008), The relationship between landform and the distribution of soil C, N and P under conventional and minimum tillage, *Geoderma*, 144, 180–188. [doi:10.1016/j.geoderma.2007.11.013](https://doi.org/10.1016/j.geoderma.2007.11.013).

Dick, W.A. and E. G. Gregorich, (2004), Developing and maintaining soil organic matter levels. In: Schjonning, P., Elmholt, S., Christensen, B.T. (Eds.), *Managing Soil*

Quality: Challenges in Modern Agriculture. CAB International, Wallingford, UK, pp.103– 120.

Dlugoß. V. (2011), Impacts of Soil Redistribution Processes on Soil Organic Carbon Stocks and Fluxes in a Small Agricultural Catchment. PhD thesis, Geographisches Institut der Universität zu Köln, Köln, Germany.

Doetterl, S. A.A. Berthe, E .Nadeu, Z. Wang, M. Sommer, and P. Fiener, (2016), Erosion, deposition and soil carbon: A review of process-level controls, experimental tools and models to address C cycling in dynamic landscapes, *Earth Science Reviews*, 154, 102-122.

Doetterl. S., J.Six, B .Van Wesemael, and K. Van Oost. (2012), Carbon cycling in eroding landscapes: geomorphic controls on soil organic C pool composition and C stabilization, *Global Change Biology*, 18(7), 2218–2232, DOI: 10.1111/j.1365-2486.2012.02680.x

Dungait, J. A. J., C. Ghee, J.S. Rowan, B. M. McKenzie, C.Hawes, E. R. Dixon, E. Paterson, and D.W. Hopkins (2013), Microbial responses to the erosional redistribution of soil organic carbon in arable fields, *Soil Biology and Biochemistry*, 60,195-201, [doi:10.1016/j.soilbio.2013.01.027](https://doi.org/10.1016/j.soilbio.2013.01.027).

Dungait, J. A. J., D. W.Hopkins, A. S. Gregory, and A. P. Whitmore. (2012), Soil organic matter turnover is governed by accessibility not recalcitrance. *Global Change Biology*, 18, 1781–1796, DOI: 10.1111/j.1365-2486.2012.02665.x

Schulte, E.E., and B.G. Hopkins, (1996), Estimation of organic matter by weight loss-on-ignition. F.R. Magdoff (Ed.), *et al.*, Soil Organic Matter: Analysis and Interpretation. SSSA Spec. Pub. No. 46, SSSA, Madison (1996), pp. 21–31.

Eisenbud, M (1987), Environmental Radioactivity, Academic Press, Inc., London, UK.

Elliott, E. T. (1986), Aggregate structure and carbon, nitrogen, phosphorus in native and cultivated soils, *Soil Sci. Soc. Am. J.* 50, 627–633, [doi:10.2136/sssaj1986.03615995005000030017x](https://doi.org/10.2136/sssaj1986.03615995005000030017x).

El-Swaify, S. A., E. W. Dangler, and C. L. Armstrong, (1982), Soil Erosion by Water in the Tropics. College of Tropical Agriculture and Human Resources, University of Hawaii. 173 pp.

Eswaran, H., E. Van den Berg, P. Reich, and J. Kimble (1995) Global soil carbon resources. In: Lal R, Kimble JM, Levine E, Stewart BA, editors. Soils and global change. Boca Raton, CRC/Lewis, 27 – 43.

FAOSTAT: <http://faostat.fao.org/site/567/default.aspx#ancor>

Fernandes, M., and E. Krull, (2008), How does acid treatment to remove carbonates affect the isotopic and elemental composition of soils and sediments?, *Environ. Chem*, 5, 33–39, DOI: [10.1071/EN07070](https://doi.org/10.1071/EN07070)

Fiener, P., G. Govers, and K. Van Oost. (2008), Evaluation of a dynamic multi-class sediment transport model in a catchment under soil-conservation agriculture. *Earth Surface Processes and Landforms*, 33, 1639-1660, DOI: [10.1002/esp.1634](https://doi.org/10.1002/esp.1634).

Fiener, P., V. Dlugoš, W. Korres, and K. Schneider (2012), Spatial variability of soil respiration in a small agricultural watershed – are patterns of soil redistribution important? , *Catena*, 94, 3-16, [doi:10.1016/j.catena.2011.05.014](https://doi.org/10.1016/j.catena.2011.05.014).

Fierer, N., A.S. Allen, J.P. Schimel, P.A. Holden, (2003), Controls on microbial CO₂ production: a comparison of surface and subsurface soil horizons, *Glob. Chang. Biol.* 9, 1322–1332, DOI: [10.1046/j.1365-2486.2003.00663.x](https://doi.org/10.1046/j.1365-2486.2003.00663.x).

Fontaine, S., S. Barot, P. Barre, N. Bdioui, B. Mary, and C. Rumpel. (2007), Stability of organic carbon in deep soil layers controlled by fresh carbon supply, *Nature*, 450, 277–280. [doi:10.1038/nature06275](https://doi.org/10.1038/nature06275).

Ghosh, B. N., P. Dogra, R. Bhattacharyya, N. K. Sharma, and K. S. Dadhwal, (2012), Effects of grass vegetation strips on soil conservation and crop yield under rainfed conditions in the Indian sub-Himalayas, *Soil Use and Management*, 28, 635–646. [doi: 10.1111/j.1475-2743.2012.00454.x](https://doi.org/10.1111/j.1475-2743.2012.00454.x).

Ghosh, B. N., P. Dogra, N.K. Sharma, and K.S. Dadhwal, (2012), Soil erosion-productivity relationship assessment in sloping lands of north-west Himalayas. *Indian Journal of Agricultural Science*, 82 (12), pp. 1068–1071.

Ghosh, B.N. , P. Dogra, N.K. Sharma, R.J. Singh, and P.K. Mishra, (2015a), Effects of resource conservation practices on productivity, profitability and energy budgeting in maize–wheat system of Indian sub-Himalayas, *Proc. Natl. Acad. Sci. India Biol. Sci.* <http://dx.doi.org/10.1007/s40011-015-0492-2>.

Ghosh, B.N. , P. Dogra, N.K. Sharma, R.Bhattacharyya, and P.K. Mishra, (2015b), Conservation agriculture impact for soil conservation in maize–wheat cropping system in the Indian sub-Himalayas, *International Soil and Water Conservation Research*,3(2), pp. 112-118,. doi:10.1016/j.iswcr.2015.05.001

Ghosh, B.N., N.K. Sharma, N.M. Alam, R.J. Singh, and G.P. Juyal, (2014), Elevation, slope aspect and integrated nutrient management effects on crop productivity and soil quality in North-West Himalayas. India, *J. Mountain Sci.* 11 (5), 1208–1217, <http://dx.doi.org/10.1007/s11629-013-2674-9>.

Gottschalk, P., J.U. Smith, M. Wattenbach, J. Bellarby, E. Stehfest, N. Arnell, T. J. Osborn, C. Jones, and P. Smith, (2012), How will organic carbon stocks in mineral soils evolve under future climate? Global projections using RothC for a range of climate change scenarios, *Biogeosciences*, 9, 3151-3171, doi:10.5194/bg-9-3151-2012.

Govers, G., D. A. Lobb, and T. A. Quine, (1999), Tillage erosion and translocation: emergence of a new paradigm in soil erosion research, *Soil and Tillage Research*, 51, 167–174, [doi:10.1016/S0167-1987\(99\)00035-5](https://doi.org/10.1016/S0167-1987(99)00035-5).

Govers, G., T.A.Quine, P.J.J. Desmet, and D.E. Walling, (1996), The relative contribution of soil tillage and overland flow erosion to soil redistribution on agricultural land, *Earth Surf. Process. Landforms* 21, 929–946, doi: 10.1002/(SICI)1096-9837(199610)21:10<929.

Govers, G., K. Vandaele, P. Desmet, J. Poesen, and K. Bunte, (1994), The role of tillage in soil distribution on hill slopes, *Eur. J. Soil Sci.* 45, 469–478, DOI: [10.1111/j.1365-2389.1994.tb00532.x](https://doi.org/10.1111/j.1365-2389.1994.tb00532.x)

Gulati, A., and S.C .Rai, (2014), Cost estimation of soil erosion and nutrient loss from a watershed of the Chotanagpur Plateau, India, *Current Science*, 105 (4), 670-674.

Harden, J. W., J. M. Sharpe, W. J. Parton, D. S. Ojima, T. L. Fries, T. G. Huntington, and S. M. Dabney, (1999), Dynamic replacement and loss of soil carbon by eroding cropland, *Global Biogeochemical Cycles*, 13, 885-901, DOI: 10.1029/1999GB900061

Harris, D., W. R. Horwath, and C. Van Kessel, (2001), Acid fumigation of soils to remove carbonates prior to total organic carbon or carbon-13 isotopic analysis, *Soil Sci. Soc. Am. J.* 65, 1853-1856.

Hartley, I. P., D. W. Hopkins, M. Sommerkorn, and P. A. Wookey, (2010), The response of organic matter mineralisation to nutrient and substrate additions in sub-arctic soils, *Soil Biol. Biochem.* 42, 92-100, [doi:10.1016/j.soilbio.2009.10.004](https://doi.org/10.1016/j.soilbio.2009.10.004).

Heckrath, G., J. Djurhuus, , T. A. Quine, K. Van Oost, G. Govers, and Y. Zhang, (2005), Tillage erosion and its effect on soil properties and crop yield in Denmark, *J. Environ. Qual.* 34, 312–324.

Heimann, M. and M. Reichstein. (2008), Terrestrial ecosystem carbon dynamics and climate feedbacks, *Nature*, 451, 289-292. doi:10.1038/nature06591.

Herbst, M., N. Prolingheuer, A. Graf, J. A. Huisman, L. Weihermüller, and J. Vanderborght , (2009), Characterization and understanding of bare soil respiration spatial variability at plot scale, *Soil Sci. Soc. Am. J.* 8 , 762–771, doi:10.2136/vzj2008.0068.

Hoffmann, T., M. Schlummer, B. Notebaert, G. Verstraeten, and O. Korup, (2013), Carbon burial in soil sediments from Holocene agricultural erosion, Central Europe, *Global Biogeochemical Cycles*, 27(3), 828-835. doi: 10.1002/gbc.20071

<http://www.gadm.org/>

IPCC, (2007), Climate change impacts, adaptation and vulnerability. Working Group II. Geneva, Switzerland.

Jacinthe, P, and R. Lal, (2001), A mass balance approach to assess carbon dioxide evolution during erosional events, *Land Degrad Dev* 12, 329 – 39, DOI: 10.1002/ldr.454

Jacinthe, P. A., R. Lal, L. B. Owens, and D. L. Hothem, (2004), Transport of labile carbon in runoff as affected by land use and rainfall characteristics, *Soil & Tillage Research*, 77, 111–123, [doi:10.1016/j.still.2003.11.004](https://doi.org/10.1016/j.still.2003.11.004).

Jenkinson, D.S. and J. H. Rayner, (1977), The turnover of soil organic matter in some of the Rothamsted classical experiments, *Soil Science*, 123, 298–305.

Jobbagy, E. G. and R. B. Jackson (2000), The vertical distribution of soil organic carbon and its relation to climate and vegetation, *Ecological Applications*, 10, 423-436, DOI: 10.1890/1051-0761(2000)010[0423:TVDOSO]2.0.CO;2.

Kang, S., S. Doh, D. Lee, V. L. Jin, and J. S. Kimball (2003), Topographic and climatic controls on soil respiration in six temperate mixed-hardwood forest-slopes, Korea, *Global Change Biol.* 9, 1427–1437, DOI: 10.1046/j.1365-2486.2003.00668.x.

Karhu, K., M.D. Auffret, J.A.J. Dungait, D.W. Hopkins, J.I. Prosser, B.K.Singh, J.A. Subke, P.A. Wookey, G.I. Agren, M.T. Sebastia, F. Gouriveau, G. Bergkvist, P. Meir, A.T. Nottingham, N. Salinas, and I.P. Hartley (2014), Temperature sensitivity of soil respiration rates enhanced by microbial community response, *Nature*, 513, 81-84, [doi:10.1038/nature13604](https://doi.org/10.1038/nature13604).

Khola O.P.S., and G. Sastry (2005), Conservation efficiency of mechanical measures and productivity of maize-wheat cropping sequence under different land slopes in foothills of western Himalaya, *Indian Journal of Soil Conservation* 33(3), 221-224.

Komada, T., M.R. Anderson, and C.L. Dorfmeier (2008), Carbonate removal from coastal sediments for the determination of organic carbon and its isotopic signatures, $\delta^{13}\text{C}$ and $\Delta^{14}\text{C}$: comparison of fumigation and direct acidification by hydrochloric acid, *Limnol. Oceanogr-Meth.* 6, 254–262, DOI: 10.4319/lom.2008.6.254.

Konen, M.E., P.M. Jacobs, C.L. Burras, B.J. Talaga, and J.A. Mason (2002), Equation for predicting soil organic carbon using loss-on-ignition for north central U.S. soils, *Soil Sci. Soc. Am. J.*, 66, 1878–1881.

Kuzyakov, Y. (2000), Priming effects: Interactions between living and dead organic matter, *Soil Biology and Biochemistry*, 42,1363–1371, doi: 10.1016/j.soilbio.2010.04.003.

Kuzyakov, Y. (2002), Review: factors affecting rhizosphere priming effects, *Journal of Plant Nutrition and Soil Science*, 165, 382-396, DOI: 10.1002/1522-2624(200208)165:4<382::AID-JPLN382>3.0.CO;2

Kuzyakov, Y., J.K. Friedel, and K. Stahr (2000), Review of mechanisms and quantification of priming effects, *Soil Biology & Biochemistry* 32, 1485-1498, doi:10.1016/S0038-0717(00)00084-5

Lal, M., and S.K.Mishra (2015), Characterization of Surface Runoff, Soil Erosion, Nutrient Loss and their Relationship for Agricultural Plots in India, *Current world environment*, 10(2), 593-601, DOI : <http://dx.doi.org/10.12944/CWE.10.2.24>.

Lal, R. (2003), Soil erosion and the global carbon budget, *Environment International* 29, 437- 450, doi:10.1016/S0160-4120(02)00192-7.

Lal, R. (2004), Soil carbon sequestration impacts on global climate change and food security, *Science*, 304, 1623-1627, DOI: 10.1126/science.1097396.

Lal, R. (2005), Soil erosion and carbon dynamics, *Soil and Tillage Research*, 81(2),137-142.

Lal, R. (2009), Challenges and opportunities in soil organic matter research, *European Journal of Soil Science*, 60, 158-169, DOI: 10.1111/j.1365-2389.2008.01114.x.

Lal, R., and D. Pimentel (2008), Letter on ‘Soil Erosion: A carbon sink or source?’, *Science*, 319, 1040–1041, doi: 10.1126/science.319.5866.1040.

Lal, R., J.M. Kimble, R. F. Follett, and C.V. Cole (1998), The Potential of U.S. Cropland to Sequester Carbon and Mitigate the Greenhouse Effect, Ann Arbor Press, Chelsea, MI, 128 pp.

Lal, R., M.Griffin, J. Apt, L. Lave, and M.G. Morgan (2004), Ecology. Managing soil carbon, *Science*, 304, 393.

Li, S., D.A. Lobb, and M.J. Lindstrom (2007a), Tillage translocation and tillage erosion in cereal-based production in Manitoba, Canada, *Soil Tillage Research*, 94, 164–182.

Li, S., D.A. Lobb, M.J. Lindstrom, and A. Farenhorst (2007b), Tillage and water erosion on different landscapes in the northern North American Great Plains evaluated using ¹³⁷Cs technique and soil erosion models, *Catena*, 70, 493–505, [doi:10.1016/j.catena.2006.12.003](https://doi.org/10.1016/j.catena.2006.12.003).

Li, F. C., J. H. Zhang, and Z. Su (2012), Changes in SOC and nutrients under intensive tillage in two types of slope landscapes, *J. Mt. Sci.* 9, 67–76.

Li, F., J. Zhang, Z. Su, and H. Fan (2013), Simulation and ¹³⁷Cs tracer show tillage erosion translocating soil organic carbon, phosphorus, and potassium, *J. Plant Nutr. Soil Sci.*, 176, 647–654, [doi: 10.1002/jpln.201200341](https://doi.org/10.1002/jpln.201200341).

Li, S., D.A. Lobb, M.J. Lindstrom, S.K. Papiernik, and A. Farenhorst (2008), Modeling tillageinduced redistribution of soil mass and its constituents within different landscapes, *Soil Sci. Soc. Am. J*, 72, 167–179.

Li, X. G., F. M. Li, S. Bhupinderpal, Z. Rengel, and Z. Y. Zhan (2007), Soil management changes organic carbon pools in alpine pasture land soils, *Soil & Tillage Research*, 93, 186–196, [doi:10.1016/j.still.2006.04.003](https://doi.org/10.1016/j.still.2006.04.003).

Li, Y., and M. J. Lindstrom (2001), Evaluating soil quality-soil redistribution relationship on terraces and steep hillslope, *Soil Sci. Soc. Am. J.* 65, 1500–1508, [doi:10.2136/sssaj2001.6551500x](https://doi.org/10.2136/sssaj2001.6551500x).

Li, Y., T.A. Quine, H. Yu, G. Govers, J. Six, D.Gong, Z. Wang, Y .Zhang, and K. Van Oost (2015), Sustained high magnitude erosional forcing generates an organic carbon sink: Test and implications in the Loess Plateau, China, *Earth and Planetary Science Letters*, 411, 281–289, [doi:10.1016/j.epsl.2014.11.036](https://doi.org/10.1016/j.epsl.2014.11.036).

Li, Y., G. Tian, M. J. Lindstrom, and H. R. Bork (2004), Variation of surface soil quality parameters by intensive donkey-drawn tillage on steep slope, *Soil Sci. Soc. Am. J.* 68, 907–913.

Li, Y., Q. W. Zhang, D. C. Reicosky, L. Y. Bai, M. J. Lindstrom, and L. Li (2006), Using ¹³⁷Cs and ²¹⁰Pb-ex for quantifying soil organic carbon redistribution affected by intensive tillage on steep slopes, *Soil Till. Res.* 86, 176–184, [doi:10.1016/j.still.2005.02.006](https://doi.org/10.1016/j.still.2005.02.006).

Lindstrom, M.J., J.A. Schumacher, and T.E. Schumacher (2000), TEP: A tillage erosion prediction model to calculate soil translocation above the initial surface soil by long-term intensive till- rates from tillage, *J. Soil Water Conserv*, 55,105–108.

Lindstrom, M.J., W.W. Nelson, T.E. Schumacher and G.D. Lemme (1990), Soil movement by soil tillage as affected by slope, *Soil Tillage Res.* 17, 255– 264, [doi:10.1016/0167-1987\(90\)90040-K](https://doi.org/10.1016/0167-1987(90)90040-K).

Lobb, D.A., R.G. Kachanoski, and M.H. Miller (1995), Tillage translocation and tillage erosion on shoulder slope landscape positions measured using ¹³⁷Cs as a tracer, *Canadian Journal of Soil Science*, 75, 211–218, [doi:10.4141/cjss95-029](https://doi.org/10.4141/cjss95-029).

Lowery, B., G. L. Hart, J. M. Bradford, K.J.S. Kung, and C. Huang (1998), Erosion impact on soil quality and properties and Model estimates. In R Lal (ed). “Soil quality and soil erosion”, CRC Press, Boca Raton, FL: 75-93.

Madhu, M., and V.N. Sharda (2011), Agricultural scenario in Indian Himalayan region- Status, potentials and strategies, Published in workshop on Mountain agriculture in Himalayan region; status, constraints and potentials, April 2-3.

Mandal, D., and V.N. Sharda (2011), Assessment of permissible soil loss in India employing a quantitative bio-physical model, *Curr Sci India* 100(3),383–390.

Mandal, D., V. N. Sharda, and K. P. Tripathi (2010), Relative efficacy of two biophysical approaches to assess soil loss tolerance for Doon Valley soils of India, *J. Soil Water Conserv*, 65, 42–49, [doi: 10.2489/jswc.65.1.42](https://doi.org/10.2489/jswc.65.1.42).

Martinez, C., G.R. Hancock, and J.D. Kalma (2010), Relationships between ^{137}Cs and soil organic carbon (SOC) in cultivated and never-cultivated soils: An Australian example, *Geoderma*, 158, 137–147, [doi:10.1016/j.geoderma.2010.04.019](https://doi.org/10.1016/j.geoderma.2010.04.019).

Mehlich, A. (1984), Mehlich 3 soil test extractants: A modification of Mehlich 2 extractant, *Commun. Soil Sci. Plant Anal.* 15, 1409 – 1415, DOI:10.1080/00103628409367568.

Meir, P., P. Cox, and J. Grace (2006), The influence of terrestrial ecosystems on climate, *Trends in Ecology & Evolution* 21(5), 254, [doi:10.1016/j.tree.2006.03.005](https://doi.org/10.1016/j.tree.2006.03.005).

Mendes, I. C., A. K. Bandick, R. P. Dick, and P. J. Bottomley (1999), Microbial biomass and activities in soil aggregates affected by winter cover crops. *Soil Sci. Soc. Am. J.* 63, 873–881, [doi:10.2136/sssaj1999.634873x](https://doi.org/10.2136/sssaj1999.634873x).

Midwood, A. J., and T. W. Boutton (1998), Soil carbonate decomposition by acid matters has little effect on $\delta^{13}\text{C}$ of organic matter, *Soil Biol. Biochem.* 30, 1301–1307.

Mikhailova, E. A., P. B. Bryant, I. I. Vassenev, S. J. Schwager, and C. J. Post (2000), Cultivation effects on soil carbon and nitrogen contents at depth in the Russian chernozem, *Soil Sci. Soc. Am. J.* 64, 738–745, [doi:10.2136/sssaj2000.642738x](https://doi.org/10.2136/sssaj2000.642738x).

Millennium Ecosystem Assessment. (2005), Ecosystems and Human Well-being: Current State and Trends, Volume 1, Hassan R, Scholes, R and Neville, A (Eds), Findings of the Condition and Trends Working Group of the Millennium Ecosystem Assessment, Islanders, London, 47p

Ministry of Agriculture. (2011), <http://dacnet.nic.in>

Nadeu, E., A. A. Berhe, J. de Vente, and C. Boix-Fayos (2012), Erosion, deposition and replacement of soil organic carbon in Mediterranean catchments: a geomorphological, isotopic and land use change approach, *Biogeosciences*, 9, 1099-1111, [doi:10.5194/bg-9-1099-2012](https://doi.org/10.5194/bg-9-1099-2012), 2012.

Narayana V.V.D., and Ram Babu, (1983), Estimation of soil erosion in India, *Journal of Irrigation and Drainage Engineering* 109(4), 419-434, [10.1061/\(ASCE\)0733-9437\(1983\)109:4\(419\)](https://doi.org/10.1061/(ASCE)0733-9437(1983)109:4(419)).

Ni, S. J., and J. H. Zhang (2007), Variation of chemical properties as affected by soil erosion on hillslopes and terraces, *Eur. J. Soil Sci.* 58, 1285–1292, DOI: 10.1111/j.1365-2389.2007.00921.x

Nie X.J., J.H.Zhang, J.X. Cheng, H. Gao, and Z.M.Guan (2016), Effect of soil redistribution on various organic carbons in a water- and tillage-eroded soil, *Soil and Tillage Resear*, 155, 1-8, [doi:10.1016/j.still.2015.07.003](https://doi.org/10.1016/j.still.2015.07.003).

NOAA. (2016), <http://www.esrl.noaa.gov/gmd/ccgg/trends/>

Nosrati K., A. Haddadchi, M.Reza Zare, and L.Shirzadi (2015), An evaluation of the role of hillslope components and land use in soil erosion using ¹³⁷Cs inventory and soil organic carbon stock, *Journal Geoderma*, 243–244, 29–40, [doi:10.1016/j.geoderma.2014.12.008](https://doi.org/10.1016/j.geoderma.2014.12.008).

Olsen, S.R., and L.E. Sommers (1982), Phosphorus. p. 403-430 In A.L. Page et al. (Ed.) *Methods of soil analysis. Part 2.* 2nd ed. Agronomy Monogr. 9. ASA and SSSA, Madison, WI.

Oskarsson, H., O. Arnalds, J .Gudmundsson, and G .Gudbergsson (2004), Organic carbon in Icelandic Andosols: geographical variation and impact of erosion, *Catena* 56, 225-238, [doi:10.1016/j.catena.2003.10.013](https://doi.org/10.1016/j.catena.2003.10.013).

Pálsson, S.E., B.J.Howard, and S.M. Wright, (2006), Prediction of spatial variation in global fallout of ¹³⁷Cs using precipitation, *Sci. Total Environ*, 367, 745-756. [doi:10.1016/j.scitotenv.2006.01.011](https://doi.org/10.1016/j.scitotenv.2006.01.011)

Papiernik, S. K., M. J.Lindstrom, J. A. Schumacher, A. Farenhorst, K. D. Stephans, T. E. Schumacher, and D. A. Lobb (2005), Variation in soil properties and crop yield across an eroded prairie landscape, *J. Soil Water Conserv.* 60, 388–395.

Papiernik, S. K., M. J. Lindstrom, T. E. Schumacher, J. A. Schumacher, D. D. Malo, and D. A. Lobb (2007), Characterization of soil profiles in a landscape affected by long-term tillage, *Soil & Tillage Research*, 93,335-345.

Parfitt, R. L., W. T. Baisden, C. W.Ross, and B. J. Rosser (2013), Influence of erosion and deposition on carbon and nitrogen accumulation in resampled steepland soils

under pasture in New Zealand. *Geoderma*, 192, 154–159, doi:10.1016/j.geoderma.2012.08.006.

Parsons, A. J., and I. D. L. Foster (2011), What can we learn about soil erosion from the use of ^{137}Cs ?, *Earth-Sci. Rev.*, 108, 101–113, doi:10.1016/j.earscirev.2011.06.004.

Parsons, A. J., and I. D. L. Foster (2013), The assumptions of science a reply to Mabit et al. (2013), *Earth-Science Reviews*. <http://dx.doi.org/10.1016/j.earscirev.2013.05.011>.

Paustian K., J. Lehmann, S. Ogle, D. Reay, G.P. Robertson, and P. Smith (2016), Climate-smart soils. *Nature* 532, 49-57, doi:10.1038/nature17174.

Paustian, K., W.J. Parton, and J. Persson (1992), Modelling soil organic matter in organic amended and nitrogen-fertilized long-term plots, *Soil Science Society of America Journal*, 56, 476–488.

Pennock, D. J. (2000), Suitability of ^{137}Cs redistribution as an indicator of soil quality. *Acta Geologica Hispanica*, 35, 213–217.

Polyakov, V. O., and R. Lal (2004), Soil erosion and carbon dynamics under simulated rainfall, *Soil Science* 169, 590–599, <http://dx.doi.org/10.1097%2f01.ss.0000138414.84427.40>.

Poreba, G.J. and P. Prokop (2011), Estimation of soil erosion on cultivated fields on the hilly Meghalaya Plateau, North-East India, *Geochronometria* 38(1), 77-84.

Prokop, P., and G. J. Poreba (2012), Soil erosion associated with an upland farming system under population pressure in northeast India, *Land Degrad. Dev.*, 23, 310–321. doi: 10.1002/ldr.2147

Quine, T.A. (1995), Estimation of erosion rates from caesium-137 data: the calibration question. In: *Sediment and Water Quality in River Catchments* (eds Foster IDL, Gurnell AM, Webb BW), pp. 307–329. John Wiley, Chichester.

Quine, T.A., and K. Van Oost (2007), Quantifying carbon sequestration as a result of soil erosion and deposition: Retrospective assessment using caesium-137 and carbon

inventories, *Glob Change Biol*, 13(12), 2610–2625, DOI: 10.1111/j.1365-2486.2007.01457.x.

Quine, T. A., and Y. Zhang (2002), An investigation of spatial variation in soil erosion, soil properties and crop production within an agricultural field in Devon, UK, *Journal of Soil and Water Conservation*, 57, 55–65.

Quine, T.A., D.E. Walling, O.K. Chakela, O.T. Mandiringana, and X. Zhang (1999), Rates and patterns of tillage and water erosion physical properties under contour hedgerow systems on sloping on terraces and contour strips: Evidence from cesium-137 measurements, *Catena* 36,115–142.

Quinton, J. N., G. Govers, K. Van Oost, and R. D. Bardgett (2010), The impact of agricultural soil erosion on biogeochemical cycling, *Nature Geoscience* 3, 311-314, doi:10.1038/ngeo838.

Ramnarine, R., R. Voroney, C .Wagner-Riddle, and K. Dunfield (2011), Carbonate removal by acid fumigation for measuring the $\delta^{13}\text{C}$ of soil organic carbon, *Can J Soil Sci*, 91, 247–50, DOI:10.4141/cjss10066.

Ran, L., X.X.Lu, and Z. Xin (2014), Erosion-induced massive organic carbon burial and carbon emission in the Yellow River basin, China, *Biogeosciences*, 11, 945–959, <http://dx.doi.org/10.5194/bg-11-945-2014>.

Raymond, P. A., and J. E. Bauer (2001), Riverine export of aged terrestrial organic matter to the North Atlantic Ocean, *Nature* ,409, 497 – 500, doi:10.1038/35054034.

Rhoton, F. E., and D.D. Tyler (1990), Erosion-induced changes in the properties of a Fragipan soil, *Soil Sci Soc Am J*,54, 223 – 228, doi:10.2136/sssaj1990.03615995005400010035x.

Ritchie, J. C., and G. W. McCarty (2003), Using $^{137}\text{Cesium}$ to understand soil carbon redistribution on agricultural watersheds, *Soil Tillage Res*, 69, 45–51.

Ritchie, J. C., and J.R. McHenry (1990), Application of radioactive fallout cesium-137 for measuring soil-erosion and sediment accumulation rates and patterns – a review,

Journal of Environmental Quality, 19, 215–233,
DOI: [10.2134/jeq1990.00472425001900020006x](https://doi.org/10.2134/jeq1990.00472425001900020006x).

Ritchie, J. C., G. W. McCarty, E. R. Venteris, and T. C. Kaspar (2007), Soil and soil organic carbon redistribution on the landscape, *Geomorphology*, 89,163-171, doi:[10.1016/j.geomorph.2006.07.021](https://doi.org/10.1016/j.geomorph.2006.07.021).

Rosenbloom, N.A., J.W.Harden, J.C. Neff, and D.S.Schimel (2006), Geomorphic control of landscape carbon accumulation, *J Geophys Res* 111(1), G01004, DOI: [10.1029/2005JG000077](https://doi.org/10.1029/2005JG000077).

Rumpel, C., and I.Kogel-Knabner (2011), Deep soil organic matter-a key but poorly understood component of terrestrial C cycle, *Plant Soil* 338(1–2),143–158.

Sainju, U.M., A. Lenssen, T. Caesar-Thonthat, and J.Waddell (2006), Carbon sequestration in dryland soils and plant residue as influenced by tillage and crop rotation, *J. Environ. Qual.* 35, 1341–1347.

Sainju, U.M., W.F.Whitehead, and B.R.Singh (2003), Cover crops and nitrogen fertilization effects on soil aggregation and carbon and nitrogen pools, *Canadian Journal of Soil Science* 83 (2), 155 – 165, DOI:[10.4141/S02-056](https://doi.org/10.4141/S02-056).

Salomé, C., N. Nunan, V. Pouteau, T. Z. Lerch, and C. Chenu (2010), Carbon dynamics in topsoil and in subsoil may be controlled by different regulatory mechanisms, *Global Change Biology* 16, 416-426, DOI: [10.1111/j.1365-2486.2009.01884.x](https://doi.org/10.1111/j.1365-2486.2009.01884.x)

Saunders, W. M. H. and E. G. Williams (1955), Observations on the determination of total organic phosphorus in soils, *Journal of Soil Science* 6(2), 254-267, DOI: [10.1111/j.1365-2389.1955.tb00849.x](https://doi.org/10.1111/j.1365-2389.1955.tb00849.x).

Schlesinger, W. H. (1999), Carbon sequestration in soils, *Science* 284, 2095.

Schlunz ,B., and R. R. Schneider (2000), Transport of terrestrial organic carbon to the oceans by rivers: re-estimating flux and burial rates, *Int J Earth Sci*, 88, 599 – 606

Schumacher, T.E., M.J. Lindstrom, J.A. Schumacher, and G.D.Lemme (1999), Modeling spatial variation in productivity due to tillage and water erosion, *Soil Tillage Res.* 51,331–339.

Schutter, M. E. and Dick, R. P (2002), Microbial community profiles and activities among aggregates of winter fallow and cover cropped soil, *Soil Sci. Soc. Am. J.* 66, 142–153, doi:10.2136/sssaj2002.1420.

Scott Van Pelt, R., T.M. Zobeck, J.C. Ritchie, and T.E. Gill (2007), Validating the use of ¹³⁷Cs measurements to estimate rates of soil redistribution by wind, *Catena*, 70, 455-464, doi:10.1016/j.catena.2006.11.014.

Seech, A. G., and E. G.Beauchamp (1988), Denitrification in soil aggregates of different sizes, *Soil Sci. Soc. Am. J.* 52, 1616–1621.

Sharda, V. N., and D.Mandal (2010), Land resources: food and livelihood security, In Looking Back to Change Track, TERI, New Delhi.

Sharda, V.N., and R. Singh (2004), Erosion control measures for improving productivity and farmer's profitability, *Fertilizer News*, 48, 71–78.

Singh, D. R. and P. N. Gupta (1982), Assessment of siltation in Tehri reservoir. Proc. International Symp. on Hydrological Aspect of Mountainous Watershed, Univ. of Roorkee, Roorkee (Nov. 4-6, 1982). Mangalik Prakashan, Saharanpur, pp. VIII-60 to VIII-66.

Singh,G., Ram Babu, P. Narain, L.S.Bhushan, and I. P. Abrol (1992), Soil erosion rates in India, *Journal of Soil and Water Conservation*, 47, 97-99.

Singh, R. J., B. N.Ghosh, N. K. Sharma, S.Patra, K. S. Dadhwal, and P. K.Mishra (2016), Energy budgeting and emergy synthesis of rainfed maize-wheat rotation system with different soil amendment applications, *Ecological Indicators*, 61(2), 753–765. doi:10.1016/j.ecolind.2015.10.026.

Six, J., E.A. Conant, E.A. Paul, and K. Paustian (2002), Stabilization mechanisms of soil organic matter: implications for C-saturated soil, *Plant Soil*, 241, 155–176.

Six, J., E. T. Elliott, K. Paustian, and J. W. Doran (1998), Aggregation and soil organic matter accumulation in cultivated and native grassland soils, *Soil Sci. Soc. Am. J.* 62, 1367–1377.

Six, J., K. Paustian, E. T. Elliott, and C. Combrink (2000), Soil structure and organic matter: I. Distribution of aggregate-size classes and aggregated-associated carbon. *Soil Sci. Soc. Am. J.* 64, 681–689.

Smith, P., J.U. Smith, D.S. Powlson, W.B. McGill, J.R.M. Arah, O.G. Chertov, K.Coleman, U.Franko, S.Frolking, D.S. Jenkinson, L.S. Jensen, R.H. Kelly, H. Klein-Gunnewiek, A.S. Komarov, C. Li, J.A.E. Molina, T. Mueller, W.J. Parton, J.H.M. Thornley, A.P. Whitmore (1997), A comparison of the performance of nine soil organic matter models using datasets from seven long-term experiments, *Geoderma*, 81, 153–225. [doi:10.1016/S0016-7061\(97\)00087-6](https://doi.org/10.1016/S0016-7061(97)00087-6)

Smith, S.V., R.O. Slezzer, W.H. Renwick, and R.W. Buddemeier (2005), Fates of eroded soil organic carbon: Mississippi Basin case study, *Ecological Applications*, 15, 1929–1940. DOI: 10.1890/05-0073.

Smith, J., P. Smith, M. Wattenbach, S. Zaehle, R. Hiederer, , R. J. A. Jones, L.Montanarella, M. D. A. Rounsevell, I.Reginster, and F. Ewert (2005), Projected changes in mineral soil carbon of European croplands and grasslands, 1990–2080, *Glob. Change Biol.*, 11, 2141–2152, DOI: 10.1111/j.1365-2486.2005.001075.x.

Smith, P, and D.S. Powlson (2000), Considering manure and carbon sequestration, *Science*, 287, 428-429, DOI: 10.1126/science.287.5452.427e.

Smith, P., J. Smith, M.Wattenbach, J.Meyer, M. Lindner, S.Zaehle, R.Hiederer, R. J. A. Jones, L.Montanarella, M. Rounsevell, I.Reginster, and S.Kankaanpaˆa (2006), Projected changes in mineral soil carbon of European forests, 1990–2100, *Canad. J. Soil Sci.*, 86, 159–169, DOI:10.4141/S05-078.

Smith, S. V., W. H. Renwick, R. W. Buddenmeier, and C. J. Crossland (2001), Budgets of soil erosion and deposition for sediments and sedimentary organic carbon across the conterminous United States. *Global Biogeochemical Cycles*15: 697–707, DOI: 10.1029/2000GB001341.

Soon, Y. K. and S. Abboud (1991), A comparison of some methods for soil organic carbon determination, *Communications in Soil Science & Plant Analysis*, 22 (9 & 10), 943–954, DOI:10.1080/00103629109368465.

Stallard, R. (1998), Terrestrial sedimentation and the carbon cycle: coupling weathering and erosion to carbon burial, *Global Biogeochem. Cycles*, 12, 231–257. DOI: 10.1029/98GB00741

State of Forest Report (SFR).(2009), Forest Survey of India, Dehra Dun.

Staub, B., and C. Rosenzweig (1992), Global Zoller Soil Type, Soil Texture, Surface Slope, and Other Properties, Digital raster data on a 1-degree geographic (lat/long) 180X360 grid, Global ecosystems database version 2.0. Seven independent spatial layers, 561,782 bytes in 16 files. NOAA National Geophysical Data Center: Boulder, CO.

Steege, A., and G. Govers (2001), Correction factors for estimating suspended sediment export from Loess catchments, *Earth Surface Processes and Landforms* 26, 441–449. DOI: 10.1002/esp.196.

Steege, A., G. Govers, L. Beuselinck, and K. Van Oost (2000), The use of phosphorus as a tracer in erosion/sedimentation studies. In: Stone, M. (Ed.), *The Role of Erosion and Sediment Transport in Nutrient and Contaminant Transfer*, Conference Proceedings of Symposium, Waterloo, Canada. International Association of Hydrological Sciences Press, Wallingford, U.K., pp. 59–66.

Takata, Y., S. Funakawa, K. Akshalov, N. Ishida and T. Kosaki (2007), Spatial prediction of soil organic matter in northern Kazakhstan based on topographic and vegetation information, *Soil Science & Plant Nutrition* 53,289-299. 10.1111/j.1747-0765.2007.00142.x

Terra, J.A., J.N. Shaw, D.W. Reeves, R.L. Raper, E. van Santen and P.L. Mask (2004), Soil carbon relationships with terrain attributes, electrical conductivity, and a soil survey in a coastal plain landscape, *Soil Science* 169,819-831.

Thapa, B.B., D.K. Cassel, and D.P. Garrity (2001), Animal powered on sloping land tillage translocated soil affects nutrient dynamics and soil properties at Claveria, Philippines, *J. Soil Water Conserv.* 56,14–21.

Theocharopoulos, S.P., H. Florou, D.E.Walling, H. Kalantzakos, M.Christou, P.Tountas, and T. Nikolaou (2003), Soil erosion and deposition rates in a cultivated catchment area in central Greece, estimated using the ¹³⁷Cs technique, *Soil Tillage Res.* 69, 153–162. [doi:10.1016/S0167-1987\(02\)00136-8](https://doi.org/10.1016/S0167-1987(02)00136-8).

Tisdall, J.M. and J.M.Oades (1982), Organic matter and water-stable aggregates in soils, *J. Soil Sci.* 62,141–163, DOI: 10.1111/j.1365-2389.1982.tb01755.x.

Tiwari, K.N., G. Sulewski, and S.Portch (2005), Challenges of meeting nutrient needs in organic farming, *Fertilizer News* 1(4), 51- 59.

Tiwari, K. N. (2007), Reassessing the role of fertilizers in maintaining food, nutrition and environmental security, *Indian J. Fert.* 3, 33–50.

Trumbore, S. (2009), Radiocarbon and soil carbon dynamics. *Annual Review of Earth and Planetary Sciences* 37,47-66, DOI: 10.1146/annurev.earth.36.031207.124300.

UK National Ecosystem Assessment, (2011), The UK National Ecosystem Assessment: Synthesis of the Key Findings. UNEP-WCMC, Cambridge, 87p

UNSCEAR, (1982), Ionizing Radiation: Sources and Biological Effects, United Nations Scientific Committee on the Effects of Atomic Radiation 1982 report.

Van Hemelryck, H., G. Govers, K. Van Oost, and R. Merckx (2011), Evaluating the impact of soil redistribution on the in situ mineralization of soil organic carbon, *Earth Surface Processes and Landforms*,36, 427–438 , <http://dx.doi.org/10.1002/esp.2055>.

Van Hemelryck, H., P. Fiener, K. Van Oost, and G. Govers (2010), The effect of soil redistribution on soil organic carbon: an experimental study, *Biogeoscience* 7,3971-3986.

Van Oost, K., G. Govers, T. A. Quine, G. Heckarth, J. E. Olesen, S. De Gryze, and R. Merckx (2005a), Landscape-scale modeling of carbon cycling under the impact of soil

redistribution: The role of tillage erosion, *Global Biogeochemical Cycles* 19, GB4014.
DOI: 10.1029/2005GB002471

Van Oost, K., G.Govers, T. A. Quine, and G. Heckrath (2004), Comment on “Managing soil carbon” (I), *Science*, 305, 1567b. DOI: 10.1126/science.1100273.

Van Oost, K., G. Govers, and P. Desmet (2000), Evaluating the effects of changes in landscape structure on soil erosion by water and tillage, *Landscape Ecology*, 15, 577–589.

Van Oost, K., T. A. Quine, G. Govers, S. De Gryze, J. Six, J.W. Harden, J.C.Ritchie, G.W.McCarty, G.Heckrath, C.Kosmas, J.V. Giraldez, J.R.Marques Da Silva, and R.Merckx (2007), The impact of agricultural soil erosion on the global carbon cycle, *Science* 318, 626–629. DOI: 10.1126/science.1145724.

Van Oost, K., T. A. Quine, G. Govers, and G. Heckrath (2005b), Modeling soil erosion induced carbon fluxes between soil and atmosphere on agricultural land using SPEROS-C. In E.J. Roose, R. Lal, C. Feller, B. Barthes, and B.A. Stewart (Eds.). *Advances in soil science. Soil erosion and carbon dynamics*. CRC Press, Boca Raton. pp. 37-51.

Van Oost, K., G. Verstraeten, B. Doetterl, F. Wiaux, N. Broothaerts, and J. Six (2012), Legacy of human-induced C erosion and burial on soil–atmosphere C exchange, *Proc. Natl. Acad. Sci.* 109, 19492–19497, doi: 10.1073/pnas.1211162109.

Vandenbygaart, A. J., E. G. Gregorich, and B. L. Helgason (2015), Cropland C erosion and burial: Is buried soil organic matter biodegradable?, *Geoderma*, 239, 240–249, doi:10.1016/j.geoderma.2014.10.011.

Vandenbygaart, A. J., D. Kroetsch, E. G. Gregorich, and D. Lobb (2012), Soil C erosion and burial in cropland, *Glob. Change Biol.*, 18, 1441–1452, DOI: 10.1111/j.1365-2486.2011.02604.x.

Verardo, D.J., P.N. Froelich, and A.McIntyre (1990), Determination of organic carbon and nitrogen in marine sediments using the Carlo Erba NA-1500 Analyzer, *Deep Sea Res.* 37 (1), 157–165, doi:10.1016/0198-0149(90)90034-S.

Verity, G. E. and D. W. Anderson (1990), Soil erosion effects on soil quality and yield, *Can. J. Soil Sci.* 70, 471-484, 10.4141/cjss90-046.

Vitousek, P. M., O. Chadwick, P. Matson, S. Allison, L. Derry, L. Kettley, A. Luers, E. Mecking, V. Monastera, and S. Porder, (2003), Erosion and the rejuvenation of Oweathering derived nutrient supply in an old tropical landscape, *Eco systems* 6,762-772, <http://dx.doi.org/10.1007%2Fs10021-003-0199-8>.

von Lu'tzow, M., I. Ko'gel-Knabner, K. Ekschmitt, H. Flessa, G. Guggenberger, E. Matzner, B. Marschner (2007), SOM fractionation methods: relevance to functional pools and to stabilization mechanisms, *Soil Biol. Biochem.*, 39, 2183–2207, [doi:10.1016/j.soilbio.2007.03.007](https://doi.org/10.1016/j.soilbio.2007.03.007).

Walker, T.W. and A.F.R. Adams (1958), Studies on soil organic matter, 1. Influence of phosphorus content of parent materials on accumulation of carbon, nitrogen, sulfur and organic phosphorus in grassland soils, *Soil Sci.*, 85, 307--318.

Wallbrink, P.J., J.M. Olley, and A.S. Murray (1994), Measuring soil movement using ¹³⁷Cs: implications of reference site variability. In: Proceedings of the Canberra Symposium on Variability in Stream Erosion and Sediment Transport. IAHS Publication, pp. 95-102.

Walling, D. E. and T. A. Quine (1990), Use of caesium- 137 to investigate patterns and rates of soil erosion on arable fields, In *Soil Erosion on Agricultural Land* (eds J. Boardman, I.D.L. Foster & J.A. Dearing), pp. 33-53. Wiley, Chichester.

Walling, D. E. and T. A. Quine (1991), The use of caesium-137 measurements to investigate soil erosion on arable fields in the UK: potential applications and limitations, *Journal of Soil Science* 42, 147–165, DOI: 10.1111/j.1365-2389.1991.tb00099.x.

Walthert, L., U. Graf, A. Kammer, J. Luster, D. Pezzotta, S. Zimmerman, and F. Hagedorn (2010), Determination of organic and inorganic carbon, δ¹³C, and nitrogen in soils containing carbonates after acid fumigation with HCl, *J. Plant Nutr. Soil Sci.* 173, 207-216.

Wang, X., L. H. Cammeraat, Z. Wang, J. Zhou, G. Govers, and K. Kalbitz (2013), Stability of organic matter in soils of the Belgian Loess Belt upon erosion and deposition, *European Journal of Soil Science*, 64, 219–228., doi: 10.1111/ejss.12018.

Wang, Z., K. Van Oost, A. Lang, T. Quine, W. Clymans, R. Merckx, B. Notebaert, and G. Govers (2014), The fate of buried organic carbon in colluvial soils: A long-term perspective, *Biogeosciences*, 11(3), 873–883, doi:10.5194/bg-11-873-2014.

Wang, Z., K. Van Oost, and G. Govers (2015), Predicting the long-term fate of buried organic carbon in colluvial soils, *Global Biogeochem. Cycles*, 29, 65–79, doi:10.1002/2014GB004912.

Wang, Z., S. Doetterl, M. Vanclooster, B. van Wesemael, and K. Van Oost (2015), Constraining a coupled erosion and soil organic carbon model using hillslope-scale patterns of carbon stocks and pool composition, *J. Geophys. Res. Biogeosci.*, 120, 452–465. doi: [10.1002/2014JG002768](https://doi.org/10.1002/2014JG002768).

WHRC: <http://www.whrc.org/global/carbon/index.html>

Wiaux, F., J. T. Cornelis, W. Cao, M. Vanclooster, and K. Van Oost (2014), Combined effect of geomorphic and pedogenic processes on the distribution of soil organic carbon quality along an eroding hillslope on loess soil, *Geoderma*, 216, 36–47, doi:10.1016/j.geoderma.2013.10.013.

Williamjs., D. H., J. K. Syers, W. Walkert, and R. W. Rex (1970), A comparison of methods for the determination of soil organic phosphorus, *Soil Sci.* 110, 13-18.

Yoo, K., R. Amundson, A. M. Heimsath, and W. E. Dietrich (2005), Erosion of upland hill slope soil organic carbon: Coupling field measurements with a sediment transport model, *Global Biogeochemical Cycles* 19, GB3003. DOI: 10.1029/2004GB002271.

Zhang, X., D.L. Higgitt, and D.E. Walling (1990), A preliminary assessment of the potential for using cesium-137 to estimate rates of soil-erosion in the Loess Plateau of China, *Hydrological Sciences Journal*, 35, 243–252.

Zhang J. H., Y. Wang , and F. C. Li (2015), Soil organic carbon and nitrogen losses due to soil erosion and cropping in a sloping terrace landscape. *Soil Research* 53, 87–96, <http://dx.doi.org/10.1071/SR14151>.

Zhang, J. H., X. J.Nie, and Z. A. Su (2008), Soil properties in relation to soil redistribution by intense tillage on a steep hillslope, *Soil Sci. Soc. Am. J.* 72, 1767–1773.

Zhang, J. N., T. A. Quine, S. Ni, and F. Ge (2006), Stocks and dynamics of SOC in relation to soil redistribution by water and tillage erosion, *Global Change Biology* 12,1834-1841. DOI: 10.1111/j.1365-2486.2006.01206.x.

Zhang, X., Y. Long, X. He, J. Fu, and Y. Zhang (2008), A simplified ¹³⁷Cs transport model for estimating erosion rates in undisturbed soil, *J. Environ. Radioact.* 99, 1242-1246, [doi:10.1016/j.jenvrad.2008.03.001](https://doi.org/10.1016/j.jenvrad.2008.03.001).

Zupanc, V., L. Mabit (2010), Nuclear techniques support to assess erosion and sedimentation processes: A preliminary step in investigating the use of ¹³⁷Cs as soil tracer in Slovenia, *Dela* 33 ,21–36.